Aus dem Institut für Molekularbiologie und Tumorforschung
Geschäftsführender Direktor: Prof. Dr. Rolf Müller
des Fachbereichs Medizin der Philipps-Universität Marburg

Functional characterization of ATP-dependent chromatin remodelers of the CHD family of *Drosophila*

Inaugural-Dissertation
zur Erlangung des Doktorgrades der Naturwissenschaften
(Dr. rer. nat.)

dem Fachbereich Medizin der Philipps-Universität Marburg
vorgelegt von

Magdalena Murawska
aus Wolomin, Polen

Marburg, 2011

Angenommen vom Fachbereich Medizin der Philipps-Universität Marburg am:
02.09.2011

Gedruckt mit Genehmigung des Fachbereichs

Dekan: Prof. Dr. Matthias Rothmund
Referent: Prof. Dr. Alexander Brehm
Korreferent: Prof. Dr. Renate Renkawitz-Pohl

To my parents

"Do not go where the path may lead,
go instead where there is no path and leave a trail."
— Ralph Waldo Emerson

Table of contents

1. Summary

Members of the CHD family (Chromodomain-Helicase-DNA binding) of ATP-dependent chromatin remodelers play key roles at different steps of the transcription cycle. They are essential in regulation of developmental and differentiation programs in multicellular organisms. However, the complexity of these remodelers makes it difficult to study them in higher eukaryotes. In this study, advantage was taken of *Drosophila melanogaster* as a model organism, which possesses only four CHD family members.

In the first part of this study, a novel chromatin remodeler, dCHD3, has been characterized biochemically and functionally. dCHD3 is highly similar to dMi-2 and consequently it possesses similar enzymatic activities *in vitro*. dCHD3 is a highly active, nucleosome stimulated ATP-dependent chromatin remodeler which slides mononucleosomes *in vitro*. The chromodomains of dCHD3 seem to be important for substrate recognition and for the remodeling activity of this enzyme. Despite the similarities, dCHD3 and dMi-2 differ significantly in other aspects. In contrast to dMi-2, dCHD3 exists as a monomer *in vivo* and it is not associated with deacetylase activity. Moreover, dCHD3 expression is restricted to early developmental stages and certain tissues. Finally, dCHD3 cannot compensate for the loss of dMi-2 which suggests that they are not functionally redundant.

In the second part of this work, a role of dMi-2 in active transcription has been studied. dMi-2 has been implicated in transcriptional repression as a part of dNuRD or dMec complexes. This study shows that dMi-2 colocalizes with active regions on polytene chromosomes and it is recruited to heat shock genes. Both, reduction of dMi-2 expression in flies or ectopic expression of a catalytically inactive mutant, impair heat shock gene response. Interestingly, 3' end processing and splicing of some of these genes is affected. In agreement with this, dMi-2 binds to nascent *hsp* gene transcripts upon heat shock induction. Consequently, these results suggest a role of dMi-2 catalytic activity in co-transcriptional RNA processing. Study of the recruitment mechanism of dMi-2 to heat shock genes suggests that it occurs in a poly(ADP-ribose) dependent manner. Several results support this hypothesis. First, dMi-2 recruitment to *hsp70* gene is reduced upon PARP inhibition. Second, dMi-2 binds PAR polymers directly *in vitro* and several dMi-2 regions, which bind PAR independently *in vitro*, have been identified. Third, a dMi-2 mutant unable to bind PAR does not localise to active heat shock loci *in vivo*. Moreover,

RNA and PAR compete for dMi-2 binding *in vitro* suggesting a two-step process for dMi-2 association with active heat shock genes. First, dMi-2 is recruited to the locus via PAR binding followed by association with nascent RNA transcripts. Collectively, these studies suggest, that stress-induced chromatin modification by PARP serves as a scaffold for rapid recruitment of factors that are required for quick and efficient transcriptional response.

Zusammenfassung

Mitglieder der CHD Familie (Chromodomain-Helicase-DNA binding) chromatin-modifizierender Proteine spielen eine zentrale Rolle in unterschiedlichen Schritten des Transkriptionszyklus. Sie sind für die Regulation von Entwicklungs- und Differenzierungsprogrammen in mehrzelligen Organismen essentiell. Die Komplexität dieser Proteine erschwert allerdings ihre genauere Untersuchung in höheren Eukaryoten. In der vorliegenden Arbeit wurde daher auf den Modellorganismus Drosophila melanogaster zurückgegriffen, der lediglich über vier Mitglieder der CHD Familie verfügt.

Im ersten Teil der Arbeit wurde dCHD3, ein neuentdecktes Mitglied der CHD Familie, biochemisch und funktionell charakterisiert. dCHD3 ist dMi-2, einem anderen CHD Familienmitglied, sehr ähnlich und besitzt folglich ähnliche enzymatische Aktivitäten *in vitro*. dCHD3 ist ein hochgradig aktives, durch Nukleosomen stimuliertes ATP-abhängiges Chromatin-modifizeirendes Enzym, das Mononukleosomen *in vitro* verschiebt. Die Chromo-Domänen von dCHD3 scheinen für Substraterkennung und die Aktivität dieses Enzyms wichtig zu sein. Trotz der Ähnlichkeiten in diesen Belangen, unterscheiden sich dCHD3 und dMi-2 in anderer Hinsicht deutlich. Im Gegensatz zu dMi-2 liegt dCHD3 in vivo als Monomer vor und ist mit keiner Deazetylierungsaktivität assoziiert. Darüberhinaus ist die Expression von dCHD3 auf frühe Entwicklungsstadien und bestimmte Gewebe beschränkt. dCHD3 ist zudem nicht in der Lage, einen Verlust von dMi-2 zu kompensieren, was dafür spricht, dass beide Proteine funktionell nicht redundant sind.

Im zweiten Teil dieser Arbeit wurde die Beteiligung von dMi-2 in aktiver Transkription untersucht. dMi-2 spielt als Bestandteil der dNuRD und dMec-Komplexe bekanntermaßen bei der transkriptionellen Repression von Genen eine Rolle. Diese Arbeit zeigt hingegen, dass dMi-2 mit transkriptionell-aktiven Bereichen auf Polytänchromosomen kolokalisiert und zu Hitzeschock-Genen rekrutiert wird. Sowohl die Verringerung der Expression von dMi-2 als auch Überexpression einer katalytisch-inaktiven Mutante verringern die Hitzeschockantwort in Fliegen. Interessanterweise ist bei einigen dieser Gene die 3‘-Prozessierung und das Spleissen beeinträchtigt. In Übereinstimmung mit diesen Beobachtungen bindet dMi-2 im Verlauf der Hitzeschockinduktion an hsp Transkripte, die im Entstehen begriffen sind. Insgesamt deuten diese Resultate auf eine Funktion von dMi-

2 bei der kotranskriptionellen RNA-Prozessierung hin. Die Untersuchung der Rekrutierung von dMi-2 zu Hitzeschock-Genen deutet darauf hin, dass sie in einer Poly-(ADP-Ribose)-abhängigen Weise stattfindet. Mehrere Ergebnisse unterstützen diese Hypothese. Erstens ist die Rekrutierung von dMi-2 zum hsp70 Gen verringert, wenn PARP inhibiert wird. Zweitens bindet dMi-2 PAR Polymere *in vitro* und mehrere Regionen, die PAR *in vitro* unabhängig binden, wurden identifiziert. Drittens ist eine dMi-2 Mutante, deren PAR-Binderegionen entfernt wurden, nicht in der Lage, in vivo zu aktiven Hitzeschockloci zu lokalisieren. Weiterhin konkurrieren RNA und PAR um Bindung an dMi-2. Insgesamt deuten die Ergebnisse auf einen zweischrittigen Mechanismus hin, der zur Assoziierung von dMi-2 mit aktiven Hitzeschock-Genen führt. Zuerst wird dMi-2 mittels Bindung an PAR zum Locus rekrutiert, bindet daraufhin aber an neuentstandene Transkripte. Insgesamt deuten die vorliegenden Ergebnisse daraufhin, dass die stress-induzierte Modifikation von Chromatin durch PARP als Gerüst für die Rekrutierung von Faktoren dient, die ihrerseits für eine schnelle und effiziente transkriptionelle Antwort notwendig sind.

2. Introduction

2.1 General aspects of chromatin structure regulation

The genetic information is encoded in a long, negatively charged DNA polymer. Eukaryotic DNA is hundred thousands times longer than the diameter of a typical cell nucleus, making it difficult to fit within the small dimension of this sub-cellular compartment. A solution to this has evolved in the form of highly basic histone proteins that bind tightly to the acidic DNA and provide the electrostatic surface that allows for the hierarchical folding of DNA. A complex of DNA, histones, and nonhistone proteins called chromatin comprises a sophisticated system of genome packaging. Core histones form octamers wrapped with DNA constituting the fundamental unit of chromatin, named nucleosomes. Furthermore, nucleosomes are arranged as a linear array along the DNA as 'beads on a string'. This structure can be further compacted by histone H1 into higher-order 30 nm fibers. This allows the DNA to be folded to a greater extent of DNA compaction eventually creating metaphase chromosomes. Thus, DNA can be compacted by as much as a factor of 10,000 (reviewed in (Woodcock 2006)). The packaging of DNA into chromatin allows the cell to overcome the nuclear space constraints, however, it creates major obstacles for all DNA based processes, such as transcription, DNA repair, replication, and recombination. Chromatin has to be, therefore, a stable but yet highly dynamic structure which provides the condensed state of DNA and also permits its accessibility for different factors regulating chromosomal processes. Eukaryotic cells overcome this problem by utilizing a number of enzymatic activities, which control the access to DNA.

2.1.1 The nucleosome structure

The fundamental repeating unit and building block of chromatin is the nucleosome. Over 35 years ago the first electron microscopic images of the eukaryotic genome that clearly showed the existence of a uniformly sized particles along DNA were published (Olins and Wright 1973; Kornberg 1974; Oudet et al. 1975). A detailed structure of a nucleosome core particle was provided by X-ray crystallography in 1997 (Luger et al. 1997) (Fig. 2.1). The structure revealed that the nucleosome core particle consists of 147 bp of DNA wrapped 1.65 times around the histone octamer in a left-handed toroid (Luger et al. 1997). The histone core comprises two copies each of the histone proteins H2A, H2B, H3 and H4.

Each histone contains a three helix core domain, the histone fold. These domains form "handshake" arrangements to give rise to H2A-H2B and H3-H4 dimers (Arents and Moudrianakis 1995; Khorasanizadeh 2004). Apart from the structured histone fold core, each histone forms extensions consisting of unstructured N-terminal and C-terminal tails that protrude from the nucleosome. The tails provide surfaces for covalent post-translational modifications by different histone modifying enzymes and are important for higher order chromatin structure formation (Fischle et al. 2003).

Positively charged residues in the histones contact the phosphate backbone of the DNA every 10.4 bp, providing 14 histone-DNA contacts in the nucleosome, called superhelical locations (SHL) (Fig. 2.1). The central base pair, where the major groove faces the octamer at the particle pseudo-twofold axis (dyad), is labeled as SHL0. For each successive DNA turn, the location number increases up to SHL 7, and decreases down to SHL -7. In addition, each minor groove facing histone core is denoted as SHL 0,5, SHL 1,5, etc. (Luger et al. 1997; Luger and Richmond 1998).

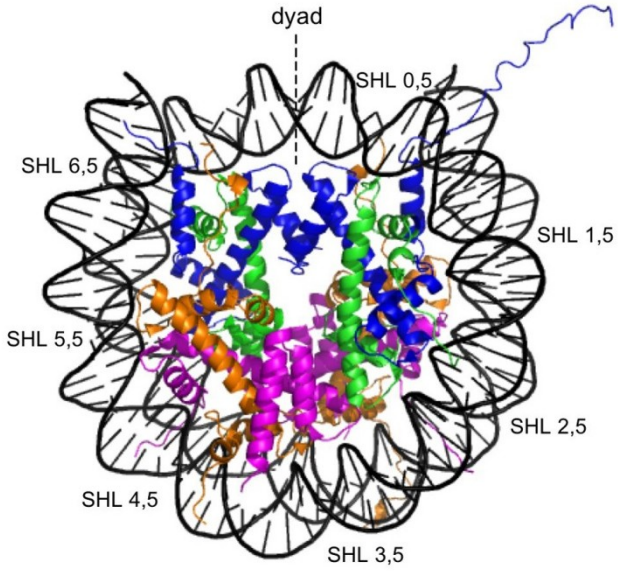

Figure 2.1 Structure of the nucleosome core particle
DNA depicted in black, eight histone protein main chains shown as ribbons (blue: H3, green: H4, orange: H2A, magenta: H2B). The axis of the histone core aligns with the major groove at the middle of the DNA fragment, and this region is called the dyad. DNA-histone interactions occur approximately every 10 bp on each DNA strand and they are called superhelical regions (SHL). The histone-DNA contact at the dyad is named SHL0 (not shown). Traveling along the DNA away from the SHL0 position, each minor groove facing histone core is denoted as SHL 0,5, SHL 1,5, etc. Note, for clarity, the SHLs at only one half of the DNA superhelix are labelled. The figure was prepared in PyMol, PDB code 1AOI using data from (Luger et al. 1997).

2.1.2 Enzymes that regulate chromatin structure

Eukaryotic cells utilize numerous enzymatic activities to regulate the access of DNA for factors involved in transcription, replication, repair or recombination. In general the enzymes belong to three main groups: histone modifying enzymes, DNA methyltransferases and ATP-dependent chromatin remodelers. The main substrates for these enzymes constitute histone tails, DNA and nucleosomes, respectively.

Histone tails are extensively posttranslationally modified. The most common modifications reported so far include lysine acetylation, serine or threonine phosphorylation, lysine methylation (mono-, di- and tri-) and arginine methylation (mono-, asymmetrical- and symmetrical dimethylation), lysine monoubiquitination, sumoylation, and ADP-ribosylation (Workman and Kingston 1998; Shilatifard 2006; Berger 2007; Bernstein et al. 2007; Kouzarides 2007; Weake and Workman 2008; Campos and Reinberg 2009). Histone modifications possess a variety of functions. They change the charge of a residue to modulate protein-DNA, protein-protein and nucleosome-nucleosome interactions. Some histone modifications are only transient, for example, histone H2B monoubiquitination is added and then quickly removed during the process of gene activation (Henry et al. 2003). Others, like H3K9me3 is part of the process of stable maintenance of heterochromatic silencing (Li et al. 2002; Krauss 2008).

Enzymes responsible for the removal of certain histone marks have also evolved. For instance, histone acetylation is removed by various histone deacetylases (HDACs) (Li et al. 2002). Histone lysine methylation considered for many years to be a stable mark, recently turned out to be also reversible, and it is removed by two families of enzymes, amine oxidases such as LSD1 and hydroxylases of the JmjC family (Klose et al. 2006; Shi 2007).

Other enzymes regulating chromatin structure belong to the family of DNA methyltransferases (DNMTs). In higher eukaryotes, DNA methylation takes place at the 5-carbon position of cytosine in CpG dinucleotides (Bird 2002; Fatemi et al. 2002). The catalytic reaction involves the transfer of a methylgroup from S-adenosyl-L-methionine to the C5 position of cytosine. DNA methylation is the most prevalent epigenetic modification of DNA in mammalian genomes and it is associated with transcriptional repression. Discrete regions in the genome, including most repetitive DNA and promoters of inactive genes are hypermethylated. By contrast, CpG islands often associated with the regulatory regions of housekeeping genes are hypomethylated (Yoder et al. 1997). CpG

methylation functions in many processes, including transcriptional regulation, genomic stability, chromatin structure modulation, X chromosome inactivation, and the silencing of parasitic DNA elements (Jones and Laird 1999; Baylin et al. 2001; Robertson 2001). In these contexts, DNA methylation promotes genomic integrity and ensures proper temporal and spatial gene expression during development.

The third family of enzymes which regulate chromatin structure are ATP-dependent chromatin remodelers. These enzymes utilize energy from ATP hydrolysis to alter histone-DNA interactions within the nucleosome. All known ATP-dependent chromatin remodeling enzymes belong to the helicase superfamily 2 (SF2), so named because their ATPase domain harbors motifs that are characteristic of helicases (Eisen et al. 1995) (for details see chapter 2.2).

All these different enzymes very often work in concert to trigger the proper chromatin structure changes and thus regulate the temporal access for DNA acting factors. Moreover, a multitude of non-enzymatic activities, such as histone chaperones, histone variants and noncoding RNAs, are involved in chromatin structure maintenance (for recent reviews see (Talbert and Henikoff 2010; Avvakumov et al. 2011; Beisel and Paro 2011)).

2.2 ATP-dependent chromatin remodelers

2.2.1 Families of chromatin remodelers

The pioneering work originally identified an ATP-dependent chromatin remodeler, Snf2 in yeast, after which the SNF2 family of ATP-dependent chromatin remodelers has been named (Carlson et al. 1984; Eisen et al. 1995). The common feature of all SNF2 family members is a region of sequence similarity that includes seven helicase-related sequence motifs that are also found in DExx box helicases. Helicase-related proteins are classified into several superfamilies with respect to the sequence similarity and spacing of these motifs. Based on these criteria, SNF2 family members have been assigned to the SF2 superfamily of helicases (Eisen et al. 1995).

A phylogenetic analysis of a subset of proteins similar to yeast Snf2 revealed several functionally and evolutionally distinct groups of SNF2 proteins. Additional motifs characteristic for each subfamily were also identified (Eisen, 1995). The most common classification of ATP-dependent chromatin remodelers distinguishes four distinct families: SWI/SNF (switch/sucrose-non-fermenting), ISWI (imitation switch), CHD

(chromodomain-helicase-DNA binding) and INO80 (inositol requiring 80). All remodeler families contain a SNF2-family ATPase domain which is split in two parts: DExx and HELICc. Remodelers of the SWI/SNF, ISWI, and CHD families possess a short insertion within the ATPase domain, whereas remodelers of the INO80 family contain a long insertion (Fig. 2.2). The unique domains reside adjacent to the ATPase domain. SWI/SNF remodelers contain bromodomains; ISWI remodelers - SANT-SLIDE modules; CHD remodelers - tandem chromodomains and INO80 family members possess HAS (helicase-SANT) domains (Fig. 2.2). Each of these domains play roles in remodeler recruitment to chromatin or binding to certain histone modifications and/or they are involved in the regulation of the ATPase activity of the remodeler (Clapier and Cairns 2009).

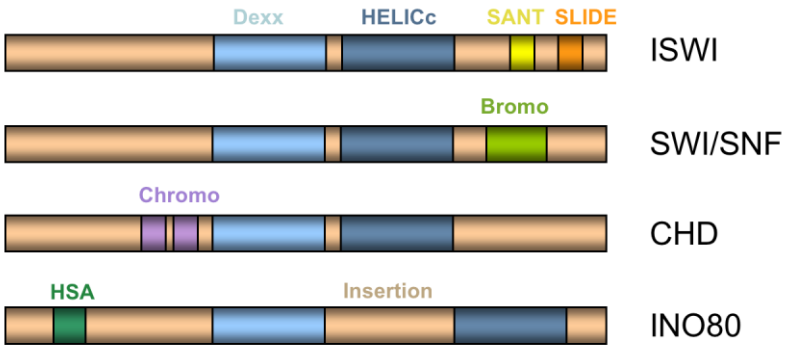

Figure 2.2 ATP-dependent chromatin remodeler families
Schematic representation of ATP-dependent chromatin remodeler families. The two conserved parts of the ATPase domain are shown as light blue (Dexx) and dark blue (HELICc) boxes. Bromo, bromodomain; Chromo, chromodomains; SANT, SANT domain; SLIDE, SLIDE domain, HSA, helicase-SANT domain. Modified after (Clapier and Cairns 2009).

There are other helicases that share homology with SNF2 through their ATPase domain, but lack these additional signature motifs. A recent comprehensive analysis of SNF2 proteins identified over 1300 family members which can be divided into 24 distinct subfamilies based on the alignments of helicase-related regions. This analysis also revealed a good correlation between biological and biochemical functions of these proteins, suggesting that SNF2 family ATPase domains are adapted for specific tasks (Flaus et al. 2006).

2.2.2 SWI/SNF

The yeast SWI/SNF complex was the first ATP-dependent chromatin remodeler to be described. The genes encoding various subunits of SWI/SNF complex were found in two independent genetic screens for altered gene expression involved in regulating mating type switching (SWI) and sucrose fermentation in yeast (Sucrose Non-Fermenting) (Carlson et al. 1984; Stern et al. 1984). The function of these genes was initially linked to chromatin structure by isolation of suppressors of *swi*/*snf* mutations in genes encoding histones and other putative chromatin components (Sudarsanam and Winston 2000). Biochemical purification of SWI/SNF complexes revealed that they are large, multi-subunit complexes containing eight or more proteins (Peterson and Herskowitz 1992). SWI/SNF ATPases possess a bromodomain which might target them to acetylated histone tails (Marmorstein and Berger 2001). Another characteristic of SWI/SNF complexes is the presence of actin and/or actin related proteins (Arps). It has been proposed that actin and Arps modulate binding of the remodeling complex to chromatin, stimulate the DNA-dependent ATPase activity, promote complex assembly and stability, histone binding, or remodeling and translocation (Olave et al. 2002; Rando et al. 2002; Shen et al. 2003; Szerlong et al. 2003).
In yeast there are two SWI/SNF ATPases, Swi2/Snf2 and Sth1, which are part of two complexes, ySWI/SNF and RSC, respectively. They share two identical and at least four similar subunits (Cairns et al. 1994; Cairns et al. 1999). Despite these similarities, only RSC is essential for yeast viability (Cairns et al. 1996). *Drosophila* contains only a single protein corresponding to yeast Swi2/Snf2, called Brahma (BRM), which is found in two complexes – BAP and PBAP (Dingwall et al. 1995; Crosby et al. 1999). Human cells contain two distinct Swi2/Snf2-like ATPase subunits, named hBRM (human Brahma) and BRG1 (Brahma-Related Gene 1), which constitute subunits of BAF and PBAF complexes (Kwon et al. 1994; Wang et al. 1996). Human SWI/SNF complexes have been found in many different cell lines from a wide range of tissues, and the complexes containing them might have slightly different subunit composition (Mohrmann and Verrijzer 2005). Mammalian BAF complexes have been found recently to possess unique compositions in embryonic stem cells, and during developmental transitions which suggests that they help guide cell fate decisions (Ho and Crabtree 2010).
SWI/SNF-like complexes possess diverse functions. Many studies have shown a positive role for SWI/SNF complexes in transcriptional regulation via its interaction with activator

proteins. In addition, ySWI/SNF often cooperates with histone acetytransferase complexes to activate transcription (Roberts and Winston 1997; Krebs et al. 1999). However, some studies also suggested a role of the SWI/SNF complexes in gene repression (Trouche et al. 1997). Mammalian BAF complexes can both activate and repress the transcription of a single gene depending on the developmental context (Chi et al. 2002; Wan et al. 2009).

In *Drosophila* BRM was shown to be involved in transcription regulation of most genes. BRM marks nearly all transcriptionally active sites on polytene chromosomes which suggests that it could be required for most gene activation in salivary gland nuclei. However, BRM is absent from activated heat-shock genes and their expression is not affected by *brm* gene loss-of-function (Armstrong et al. 2002).

Although, most of SWI/SNF-family functions are related to transcription, they also have a direct role in other processes such as DNA replication or DNA repair. ySWI/SNF was shown to promote replication initiation in a minichromosome assay in yeast (Flanagan and Peterson 1999). ySWI/SNF complex can stimulate the nucleotide excision repair on reconstituted nucleosomal substrates *in vitro* (Hara and Sancar 2002; Gaillard et al. 2003). Moreover, mammalian SWI/SNF complexes facilitate double strand brake (DSB) repair, at least in part, by promoting H2AX phosphorylation by directly acting on chromatin (Park et al. 2006).

yRSC is implicated in chromosome segregation. It was shown to be constitutively present at the centromeres and promote proper kinetochore function. Although the molecular mechanisms remain unclear, recent genetic studies suggest that RSC is required for the loading of cohesin onto chromosomes (Hsu et al. 2003; Baetz et al. 2004; Huang et al. 2004).

Mammalian SWI/SNF complexes play a role in cell cycle progression (Khavari et al. 1993; Cao et al. 1997). hBRG1 was shown to interact with Retinoblastoma (Rb), inducing the formation of growth-arrested cells in an Rb-dependent manner (Dunaief et al. 1994).

2.2.3 ISWI

The gene coding for ISWI ATPase was first identified in *Drosophila* as a gene with homology to yeast Swi2/Snf2 exclusively over the region of the ATPase domain and thus it was called imitation switch (ISWI) (Elfring et al. 1994). Chromatin remodeling complexes containing the ISWI ATPase were first identified using *in vitro* biochemical assays for

nucleosome-remodeling activities in *Drosophila* embryo extracts (Tsukiyama et al. 1995; Tsukiyama and Wu 1995; Ito et al. 1997; Varga-Weisz et al. 1997). ISWI-containing complexes were subsequently identified in many other organisms, including yeast, *C. elegans*, *Xenopus* and humans, highlighting the conserved function of this ATPase in chromatin remodeling. In contrast to SWI/SNF remodelers, ISWI complexes are relatively small and they possess between two and four subunits. All of these complexes contain the nucleosome-dependent ATPase ISWI. Yeast possess two ISWI ATPases – Isw1 and Isw2, which exist in four different complexes. *Drosophila* has only one ISWI ATPase, which is a component of three complexes: dNURF (Nucleosome Remodeling Factor), dACF (ATP-utilizing chromatin assembly and remodeling factor) and dCHRAC (chromatin accessibility complex) (Tsukiyama et al. 1995; Ito et al. 1997; Varga-Weisz et al. 1997). In mammals there are two ISWI ATPases: SNF2H and SNF2L which reside in at least eight different complexes (for precise complex composition see (Yadon and Tsukiyama 2011)).

The hallmark of ISWI complexes is the presence of a SANT domain (structurally related to the c-Myb DNA-binding domains) which binds unmodified histone tails, a SLIDE (SANT-like ISWI domain) domain which binds nucleosomal DNA near the dyad axis, and a HAND domain implicated in both histone and DNA binding/recognition (Clapier and Cairns 2009). Specialized subunits deliver additional domains to the complexes, including DNA-binding histone fold motifs (in hCHRAC), plant homeodomain zinc fingers (PHD fingers), bromodomains (hBPTF and hACF1), and additional DNA-binding motifs (HMGI(Y), for dNURF301) (Clapier and Cairns 2009).

Many ISWI family complexes optimize nucleosome spacing to promote chromatin assembly and the repression of transcription. However, certain complexes randomize spacing, and thus they can assist RNAP II activation. One of the first evidence of ISWI´s role in transcription activation came from an experiment that showed that dNURF directly facilitated GAL4-mediated transcription from chromatin templates *in vitro* (Mizuguchi et al. 1997). Subsequently, it was shown to interact with many sequence-specific transcriptional regulators, including dGAF and dHSF *in vivo*, helping to drive gene expression (Badenhorst et al. 2002).

Insights into the repressive role of ISWI remodelers in transcription come from studies on yeast, which showed that Isw2 represses transcription of yeast meiotic genes during mitotic growth. Isw2 complex establishes nuclease-inaccessible chromatin structure near the promoters of these genes as judged by nuclease digestion analysis (Goldmark et al. 2000).

Interestingly, recent nucleosome mapping on a genome wide scale in Isw2 mutants showed, that Isw2 helps prevent antisense transcription from intergenic region and from cryptic initiation sites (Whitehouse et al. 2007).

In line with ISWI´s role in nucleosome assembly, ISWI containing complexes are involved in the maintenance of higher order chromatin structure. Perhaps one of the most striking examples comes from studies on polytene chromosomes from 3rd instar *Drosophila* larvae. The loss of zygotic ISWI function in larval salivary glands leads to broad decondensation of the X chromosome (Deuring et al. 2000). Moreover, human hSNF2h complex was shown to interact with cohesins (Hakimi et al. 2002). Human ISWI complexes were also implicated in nucleosome positioning over several kilobases and thus regulate chromatin folding into loop domains (Yasui et al. 2002).

ISWI remodelers have also extensive connections to replication initiation timing and firing. For example, Isw2 is enriched at the sites of active replication and helps promote replication fork progression (Vincent et al. 2008). In human cells, hSNF2h, in concert with ACF1, is required for facilitating DNA replication through highly condensed heterochromatin (Collins et al. 2002).

2.2.4 INO80

The INO80 family was named by the yeast *ino80* gene product which is responsible for regulation of inositol-responsive gene expression (Ebbert et al. 1999). ATPase orthologues and homologues of INO80 have been identified subsequently in flies, plants and mammals. The chromatin remodeling enzymes of the INO80 family are: Ino80 and Swr1 in *S. cerevisiae*; INO80, and p400 in *Drosophila melanogaster* and Snf2-related CBP activator protein (SRCAP) and p400 in mammals. The complexes contain 14 to 15 subunits and the composition of individual complexes is highly conserved. They all possess Arps and actin components, similarly to SWI-SNF complexes (Clapier and Cairns 2009). Proteins, which are unique for INO80 and SWR1 complexes, are RuvB-like helicases. They are functionally related to the bacterial RuvB helicase, which has a role in DNA repair (Qiu et al. 1998; Kanemaki et al. 1999). *Drosophila* and mammalian INO80 complexes have been shown to contain a YY1 subunit, which is a zinc finger containing Polycomb group transcription factor involved in regulation of genes essential for growth and development (Klymenko et al. 2006; Cai et al. 2007; Wu et al. 2007).

The ATPase subunits of the INO80 family are distinguished from other ATPases in the SNF2 helicases by the presence of a long spacer region that splits the conserved ATPase domain. This region was shown to be bound by RuVB-like subunits and Arps (Jónsson et al. 2004). The motor subunits of INO80 protein also contain a HAS domain (Helicase-Sant domain) which is required for Arps and actin components binding (Szerlong et al. 2008).

Interestingly, complexes of the INO80 family possess a striking and specific affinity for histone variants H2AZ and the phosphorylated form of H2AX (γ-H2AX) (Krogan et al. 2003; Kobor et al. 2004; Mizuguchi et al. 2004). *In vivo* INO80 complex influences nucleosome eviction, whereas SWR1 complex catalyses the replacement of a canonical H2A-H2B dimer with an H2AZ-H2B variant dimer (Krogan et al. 2003; Mizuguchi et al. 2004; Tsukuda et al. 2005; van Attikum et al. 2007). The substitution of core histones by the corresponding histone variants can generate a structurally and functionally distinct nucleosome.

INO80 complexes are involved both in transcription activation and repression (Mizuguchi et al. 2004). SWR1 complex deposits H2A.Z which flanks nucleosome free regions around the transcription start sites (Raisner et al. 2005)**.** This may change both nucleosome stability and dynamics near transcription start sites and facilitate or inhibit recruitment of other factors. Hence, the incorporation of H2A.Z may regulate transcription both positively and negatively. In addition, SWR1 complex deposits H2A.Z at the boundary of euchromatin and heterochromatin which can prevent heterochromatin spreading (Meneghini et al. 2003; Zhou et al. 2010).

The presence of RuvB-like helicases in INO80 complexes suggested an involvement in DNA repair. Indeed, INO80 complex associates with γ-H2AX at sites of DSB and participates in eviction of nucleosomes surrounding DSBs (Morrison et al. 2004; van Attikum et al. 2004; Tsukuda et al. 2005). Conversely, it was suggested that SWR1 complex can exchange γ-H2AX for H2A.Z around DSBs (Papamichos-Chronakis et al. 2006). Ultimately, deletion of histone H2A.Z (*HTZ1*) in yeast, results in changes in chromatin structure at DSBs which consequently leads to reduced association of DNA repair and check point factors (Kalocsay et al. 2009). It has been proposed, that both complexes function antagonistically at chromatin surrounding a DSB, and that they regulate the incorporation of different histone H2A variants that subsequently can either promote or block cell cycle checkpoint adaptation (Papamichos-Chronakis et al. 2006).

In addition, both complexes have been shown in genetic screens in yeast to be involved in telomere regulation and proper chromosome segregation (Krogan et al. 2004; Yu et al. 2007).

2.2.5 CHD

The CHD family (Chromodomain - Helicase - DNA binding) is characterized by the presence of two signature sequence motifs: tandem chromodomains located in the N-terminal region, and the SNF2-like ATPase domain located in the central region of the protein (Fig. 2.2). The cloning of the first chromodomain helicase DNA binding protein, mouse CHD1, was reported in 1993 (Delmas et al. 1993). Subsequently, many proteins belonging to this highly conserved family have been identified in *Drosophila*, yeast and other species (Stokes et al. 1996; Woodage et al. 1997). Currently, the CHD family constitutes a large group of ATP-dependent chromatin remodelers which can be divided into three subfamilies according to the presence or absence of additional domains. As the CHD chromatin remodelers comprise the main objective of this PhD thesis, a detailed description of this family can be found in a separate chapter (chapter 2.5).

2.3 Mechanisms of chromatin remodeling

2.3.1 ATPase domain structure

As mentioned in chapter 2.2.1 the common feature of all ATP-dependent chromatin remodelers is the presence of a highly conserved SNF2-like helicase domain that is responsible for ATP hydrolysis required for nucleosome remodeling. The ATPase domain includes seven helicase-related sequence motifs also found in DExx box helicases. However, SNF2 family enzymes do not show the DNA unwinding activity specific for helicases. A number of biochemical and structural analyses suggest that instead of duplex unwinding, SNF2 family enzymes utilize the energy of ATP-hydrolysis to translocate on duplex DNA by a mechanism that does not require strand separation (Ristic et al. 2001; Saha et al. 2002; Whitehouse et al. 2003; Lia et al. 2006).

The first insights into the structure of SNF2 like ATPase domain came from two crystallographic structures of the ATPase domains of zebrafish Rad54 and archeal *Sulfolobus solfataricus* SSO1653, both in the complex with dsDNA. These structures

revealed that the SNF2-like ATPase domain possess two N- and C-terminal lobes, often referred to as DExx and HELICc domains (Figures 2.2 and 2.3). These two modules form a cleft that binds and hydrolyses ATP and drives translocation of the protein on DNA (Dürr et al. 2005; Thomä et al. 2005). Only very recently the first structure of the ATPase domain of ATP-dependent chromatin remodeler, yChd1, has been resolved (Fig. 2.3). The structure of yChd1 ATPase domain together with tandem chromodomains revealed the regulatory role of the latter domains in the motor activity (Hauk et al. 2010).

The conserved ATPase domain of ATP-dependent chromatin remodelers is not just a generic motor that hydrolyses ATP to obtain energy but it also can determine how to convert this energy into specific remodeling function. One of the most stunning observations comes from a domain swapping experiment, where the ATPase domain of human SNF2h (ISWI) and BRG1 (SWI/SNF) were exchanged. The resulting chimeric SNF2h exhibited BRG1 remodeling properties *in vitro*. Conversely, chimeric BRG1 behaved like SNF2h in the same set of experiments (Fan et al. 2005). These experiments suggest that the region containing the ATPase domain can specify the outcome of the remodeling reaction.

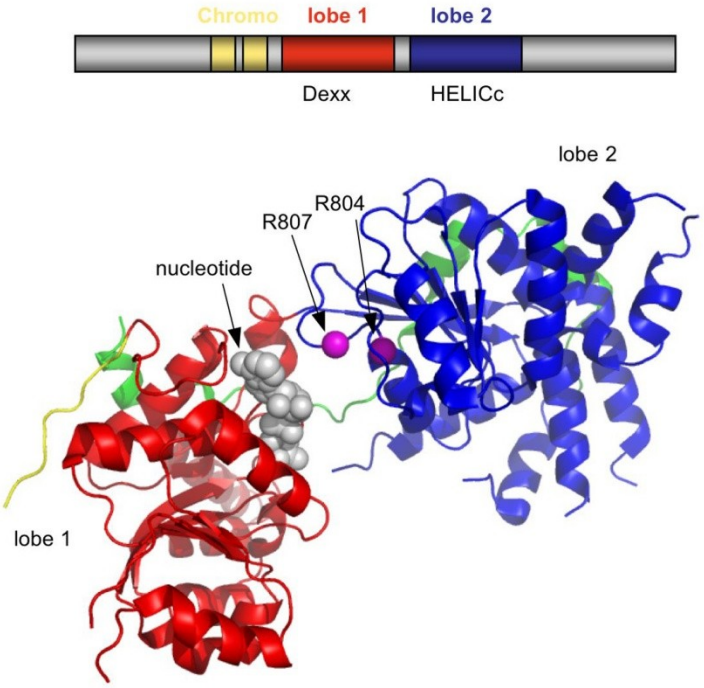

Figure 2.3 Crystal structure of the ATPase domain of yChd1
Upper panel: schematic of yChd1 domain organization. Chromo, chromodomains; lobe 1 and 2 represent two parts of the ATPase domain. Lower panel: crystal structure of the ATPase domain of yChd1. Two ATPase lobes are coloured with red and blue, yellow represents a linker from chromodomain, green is the extended C-terminal region of the ATPase domain. The bound ATP

analog (ATPγS) is represented as gray spheres, the Cα positions of two arginine residues important for ATP hydrolysis are shown as magenta spheres. The figure was prepared in PyMol, PDB code 3MWY. Picture colouring and representation adapted from (Hauk et al. 2010).

2.3.2 Different outcomes of chromatin remodeling

Although all chromatin remodelers share common properties, they are highly specialized for particular tasks. Consequently, the outcome of chromatin remodeling can be very different. Remodelers can slide or evict nucleosomes, thus transiently exposing the regulatory elements on DNA. Others assist in chromatin assembly by moving already deposited histone octamers to evenly spaced nucleosomal arrays and generating room for additional deposition. Finally, some specialized remodelers are involved in histone variant exchange (see Table 2.1 and Fig. 2.4) (Clapier and Cairns 2009). In the following chapter different outcomes of chromatin remodeling identified mostly by *in vitro* studies are described.

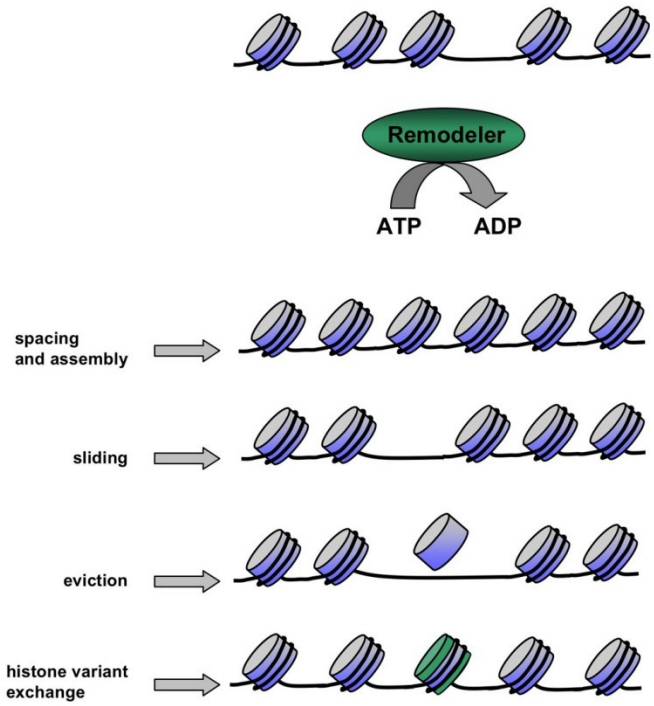

Figure 2.4 Outcomes of ATP-dependent chromatin remodeling
An ATP-dependent remodeler (green oval) action on nucleosomal arrays results in various products. The remodeler activity can result in generation of regularly spaced nucleosomes often associated with additional nucleosome assembly by assembly factors, nucleosome sliding, eviction of the whole histone octamer or histone variant exchange (for details see text).

2.3.2.1 Nucleosome sliding

Most of the remodelers are able to induce the movement of intact histone octamers on DNA fragments, which is often referred to as nucleosome sliding. The ATP-dependent sliding of nucleosomes over distances of up to 100 bp in nucleosomal arrays was first observed during characterization of *in vitro* reconstituted chromatin in *Drosophila* embryo extracts (Varga-Weisz et al. 1995). Most of the current view of nucleosome sliding comes from *in vitro* nucleosome mobility assays, where mononucleosomes assembled at different positions on different DNA fragments were used and the migration of remodeling products was analysed on native polyacrylamide gels (Hamiche et al. 1999; Längst et al. 1999; Brehm et al. 2000; Guschin et al. 2000; Jaskelioff et al. 2000). These type of studies showed that different remodelers can create different products of the remodeling reaction. For instance, ISWI ATPase alone preferentially slides mononucleosomes positioned in the centre of the DNA fragment, towards the end. By contrast, the same ATPase in dCHRAC and dACF complexes moves octamers that are positioned at the end, towards the centre (Längst et al. 1999). SWI/SNF complex generates numerous nucleosome products in these types of assays (Whitehouse et al. 1999). However, a most prominent nucleosome product is a nucleosome particle where histone octamer is moved up to 50 bp beyond the DNA end, creating a corresponding bare histone surface (Kassabov et al. 2003). It has been also suggested that the underlying DNA sequence may influence the outcome of the remodeling reaction (Rippe et al. 2007). Although it is not clear how the results of such experiments correlate with the *in vivo* situation, where mononucleosomes do not exist, they undeniably contributed to the current knowledge of the mechanism of chromatin remodeling (chapter 2.3.3).

2.3.2.2 Nucleosome spacing

ISWI complexes have been implicated in equal spacing of DNA between each nucleosome on the DNA template (Ito et al. 1997; Varga-Weisz et al. 1997). Such evenly spaced nucleosomal arrays correlate with condensed chromatin and gene silencing which is in agreement with the biological functions of ISWI complexes. The mechanism of generation of such arrays has emerged from studies, which showed that ACF complex generates a dynamic equilibrium in which nucleosomes with equal flanking DNA on either site accumulate. It has been suggested, that the dynamic equilibrium is achieved by constant sampling by ACF either side of nucleosomes by moving them back and forth. Indeed, ACF

was shown to sense the length of the flanking DNA by moving the nucleosome towards longer flanking DNA (Yang et al. 2006; Narlikar 2010). In line with this model, previous studies showed that shortening the flanking DNA reduces the activity but not the nucleosome binding of ISWI complexes (Zofall et al. 2004; Dang et al. 2006; Stockdale et al. 2006; Yang et al. 2006). Recently, the explanation for moving nucleosomes back and forth between two sides of the nucleosome was given. ACF remodeler functions as a dimer in which the two ATPases work in a coordinated manner, taking turns to engage either side of a nucleosome, consequently allowing processive bidirectional movement (Racki et al. 2009). It remains to be determined, whether bidirectional movement via dimerization of the motor ATPase is a general feature of enzymes that space nucleosomes.

2.3.2.3 Histone octamer eviction

Apart from nucleosome sliding, the access to DNA can be obtained by histone octamer eviction. Indeed, the SWI/SNF remodelers have been implicated in ejection of histone octamers at promoters of several genes (Owen-Hughes et al. 1996; Lorch et al. 1999). RSC complex efficiently disassembles histone octamers from nucleosomes in the presence of a histone chaperone Nap1 (Lorch et al. 2006). Histone octamer removal by SWI/SNF was demonstrated to be enhanced by the chimeric transcription factor Gal4-VP6 and is dependent on the presence of the activation domain of the transcription factor (Gutiérrez et al. 2007). SWI/SNF is also displacing H2A-H2B dimer from the nucleosome and it has been suggested that dimer removal maybe the first step in octamer eviction (Bruno et al. 2003; Flaus and Owen-Hughes 2003). The H2A-H2B dimer removal by SWI/SNF can explain why the depletion of H2A and H2B is capable to suppress the requirement for the SWI/SNF complex at the *SUC2* promoter *in vivo* (Hirschhorn et al. 1992). Screens for supressors of SWI/SNF function have identified a number of SWI/SNF-independent (sin) mutations in the genes encoding yeast histones. Several of them would be expected to reduce the stability of H2A-H2B dimers (Hirschhorn et al. 1995; Flaus and Owen-Hughes 2003; Muthurajan et al. 2003).

2.3.2.4 Histone variant replacement

The most specialized function of chromatin remodelers involves a histone variant exchange. So far only SWR1 complex was shown to replace H2A-H2B dimer with H2A.Z-H2B *in vitro* (Mizuguchi et al. 2004). Recently the replacement reaction by SWR1 has

been characterized in detail. It was shown, that the ATPase activity of SWR1 is specifically stimulated by canonical nucleosomes without histone H2A eviction. Interestingly, addition of free H2A.Z-H2B dimer to the reaction leads to hyperstimulation of ATPase activity, eviction of nucleosomal H2A-H2B, and deposition of H2A.Z-H2B (Luk et al. 2010). These results indicate that the combination of H2A-containing nucleosome and free H2A.Z-H2B dimer determines the specificity and outcome of the replacement reaction.

Table 2.1 Summary of ATPase activation and outcome of the remodeling of different families of ATP-dependent chromatin remodelers

Chromatin remodeler	Activation of ATPase	Outcome of remodeling	References
SWI/SNF	DNA	nucleosome sliding, octamer eviction, octamer transfer from donor to acceptor DNA	(Lorch et al. 1999; Whitehouse et al. 1999; Reinke et al. 2001; Saha et al. 2002; Lorch et al. 2006; Zofall et al. 2006)
ISWI	nucleosomes, histone H4 tails required	nucleosome sliding, equal nucleosome spacing (CHRAC, ACF)	(Hamiche et al. 1999; Clapier et al. 2001; Clapier et al. 2002; Gangaraju et al. 2009)
INO80	INO80 - nucleosomes, DNA SWR1- canonical nucleosomes, hyperactivation in the presence of H2A.Z-H2B dimers and canonical nucleosomes	nucleosome sliding (INO80), H2A-H2B dimmer replacement with H2A.Z-H2B dimmer (SWR1)	(Mizuguchi et al. 2004; Jin et al. 2005; Papamichos-Chronakis et al. 2006; Luk et al. 2010)
CHD	nucleosomes, histone tails not important (dMi-2), nucleosomes histone H4 tails important (yChd1)	nucleosome sliding, nucleosome spacing (dCHD1)	(Brehm et al. 2000; Bouazoune et al. 2002; Lusser et al. 2005; Ferreira et al. 2007)

2.3.3 Mechanisms underlying nucleosome remodeling

2.3.3.1 Substrate recognition and activation of the ATPase

Although all ATP-dependent chromatin remodelers utilize nucleosomes as substrates of their reactions, they require different chromatin components for the stimulation of their ATPase activity. For example, SWI/SNF remodelers are activated in the presence of DNA, whereas others need nucleosomes for their ATPase activity. Moreover, remodelers, like ISWI or yChd1, need the histone H4 tails for full ATPase activation (for details and references see table 2.1). These differences might reflect, at least in some cases, the way in which chromatin remodelers recognize their substrates.

It has been shown that the presence of additional domains in the ATPase motor subunit can affect substrate specificity. This view comes from the recent crystal structure of the yChd1 chromodomains and ATPase domain (Hauk et al. 2010). The structure revealed that the double chromodomains lie across the central cleft of the ATPase motor. The two lobes of the ATPase domain are arranged in a way that the arginine residues, critical for ATP hydrolysis (Fig. 2.3) are too far from the bound nucleotide, thus, the ATPase domain is kept in inactive state. yChd1 ATPase activity is stimulated by nucleosomes but only very little with DNA. Mutations in the interface between the chromodomains and the ATPase domain or removal of the chromodomains impaired nucleosome recognition and consequently DNA was stimulating ATPase activity to the level of nucleosome stimulation. Furthermore, the same mutations brought about yChd1 DNA binding ability. Moreover, chromodomains are important for efficient nucleosome sliding by yChd1 as the deletion of chromodomains strongly impaired nucleosome remodeling. These experiments suggest that chromodomains of yChd1 bias this remodeler towards nucleosomes by inhibiting DNA binding and blocking ATPase activity in the context of inappropriate substrate (Hauk et al. 2010). The structure also suggests that some conformational rearrangements have to occur upon nucleosome binding in order to bring the ATPase domain to an active state.

Studies on another CHD family remodeler, dMi-2, have suggested that the C-terminus of this protein may regulate substrate recognition. The mutant lacking the entire C-terminal domain is stimulated by free DNA as well as by nucleosomes, in striking contrast to the wild-type protein, which is stimulated only by nucleosomes. In the case of dMi-2, chromodomains were shown to be important for ATP-dependent nucleosome mobilization, and binding the nucleosome via interactions with nucleosomal DNA. A chromodomain deletion mutant that no longer interacts with the nucleosome is compromised for ATPase activity and fails to mobilize mononucleosomes. It has been suggested that the dMi-2 chromodomains function at an early step of the chromatin remodeling process by mediating the interaction between the enzyme and its nucleosome substrate (Bouazoune et al. 2002).

The results of the studies described above indicate that different domains of the ATPase subunit of chromatin remodeling complexes may influence substrate determination and thus regulate the ATPase activity of the enzyme in the presence of the correct substrate. More crystallographic and biochemical studies will be required in the future to elucidate

whether substrate determination by additional SNF2 ATPase domains is a more broad phenomenon.

ATPase activity of a chromatin remodeler can be also activated by specific histone tails. A basic patch on the histone H4 tail is important for the catalytic activity of ISWI (Clapier et al. 2001). Removal of this histone part significantly decreases ATPase activity of ISWI without affecting the nucleosome binding of the remodeler, which indicates that the H4 tail is critical for a step subsequent to substrate binding (Clapier et al. 2001; Clapier et al. 2002; Gangaraju et al. 2009).

Non-enzymatic subunits of chromatin remodeling complexes can be also involved in the ATPase regulation of the motor. For instance, the presence of Arps in the INO80 complex is critical for the complex ATPase activity. The deletion of Arps revealed that although the complex remains intact, it is compromised for ATPase activity, DNA binding and nucleosome mobility (Wu C. Mol Cell, 2003). Collectively, these results indicate that chromatin remodelers utilize a wide range of modes to activate the ATPase in the presence of the correct nucleosomal substrate.

2.3.3.2 Role of histone-DNA contacts in the nucleosome remodeling process

In order to remodel chromatin, ATP-dependent chromatin remodelers have to disturb histone-DNA contacts within the nucleosome. Recent single molecule experiments have revealed that histone-DNA contacts vary greatly in strength. The strongest contacts locate around the dyad of the nucleosome (SHL0) (Hall et al. 2009) (Fig. 2.1.). Several studies have mapped the region on the nucleosome, from which the remodeler initiates the remodeling reaction. The presence of DNA gaps at different position in the nucleosomes inhibited the sliding reaction only when the gap was located at position SHL2, close to the dyad (Schwanbeck et al. 2004; Saha et al. 2005; Zofall et al. 2006). Crosslinking experiments have revealed that several ATP-dependent chromatin remodelers contact the nucleosome at this position (Dang and Bartholomew 2007; Dechassa et al. 2008). Interestingly, this side is flanked by an energetically weak histone-DNA contact and suggests that the ATPase motor could disrupt this contact at an early step of the remodeling reaction (Bowman 2010). Despite the fact, that not all histone-DNA contacts are energetically equivalent, it is conceivable that disruption of only some histone-DNA contacts is sufficient to generate a force required for nucleosome remodeling. Indeed, the force measurements by single molecule experiments showed that remodelers impart

sufficient force to disrupt several histone-DNA contacts, but not a "rip force" that can disrupt all the contacts at once (Lia et al. 2006). In agreement with this, in the current models for nucleosome mobility not all histone-DNA interactions are broken simultaneously (see below).

2.3.3.3 Current model for ATP-dependent nuclesome remodeling

One of the biggest challenges in the field of chromatin remodeling is to gain a mechanistic view of how ATP hydrolysis is coupled to disruption of histone-DNA contacts and subsequent nucleosome redeposition. Nucleosome sliding was first explained by the "twist diffusion model" which suggested that thermal energy fluctuations would be sufficient to twist the DNA helix at the edge of the nucleosomes, replacing histone-DNA interactions by neighboring DNA base pairs. Propagation of this twist around the histone octamer surface would change the translational position of the nucleosome (Widom 2001; Längst and Becker 2004). An alternative model, called "loop recapture" was also proposed (Studitsky et al. 1994; Widom 1998; Schiessel et al. 2001). Thermal energy would lead to the detachment of a segment of DNA at the entry site of the nucleosome and would lead to the formation of a DNA loop on the histone octamer (Brower-Toland et al. 2002; Li et al. 2005). Subsequent propagation of the DNA loop over the histone octamer would change the position of the nucleosome, corresponding to the size of the DNA loop. Initial studies on chromatin remodeling have shown that remodeling complexes can introduce superhelical torsion into nucleosomal DNA, suggesting a twisting mechanism (Havas et al. 2000). However, nicked nucleosomal DNA or DNA extrusions, which should inhibit nucleosome mobility according to the DNA twisting mechanism, did not affect the chromatin remodeling enzymes (Längst and Becker 2001; Aoyagi and Hayes 2002; Schwanbeck et al. 2004). Moreover, other studies indicate that different classes of ATPases move nucleosomes in steps that are multiples of around 10 bp (Flaus and Owen-Hughes 2003; Kassabov et al. 2003). In these experiments nucleosome movements in single base pair steps were not observed, which would be expected for a mechanism that involves DNA twisting. These observations suggest that remodeling occurs via propagation of a loop of detached DNA.

A main change in the view of the mechanism of chromatin remodelers came from studies which showed that ATP-dependent chromatin remodelers can translocate on DNA (Ristic et al. 2001; Saha et al. 2002; Whitehouse et al. 2003; Lia et al. 2006). A model for

nucleosome remodeling, based on a number of biochemical and single molecule experiments on chromatin remodelers as well as the structural insights from the DNA translocase field, has been suggested. According to this, the ATPase motor of the remodeler binds nucleosome in two positions: a DNA binding domain contacts the linker DNA, whereas the ATPase domain (translocation domain) binds to SHL2 on the nucleosomal DNA. DNA is pumped into the nucleosome by coordinated, ATP-dependent conformational changes between the translocation domain and the DNA binding domain of the motor protein. This conformational change would result in a helicase-typical typical "inch–worm" like movement of the remodeler and it would facilitate the disruption of histone-DNA contacts and the formation of a loop (Fig. 2.5). Indeed, recent footprinting and crosslinking experiments have revealed large changes in the interactions of Isw2 with nucleosomal DNA that occur upon ATP hydrolysis and a channel-like organization of the protein around the nucleosomal DNA (Gangaraju et al. 2009). DNA release by the translocation domain would enable the passage and subsequent propagation of the loop resulting in the change of the nucleosome position around 10 bp away from the initial one. This model was based on studies made mostly on the ISWI ATPase, which was shown to contact two sites of the nucleosome, but it could be probably adjusted with some changes to other chromatin remodelers (Cairns 2007; Gangaraju et al. 2009).

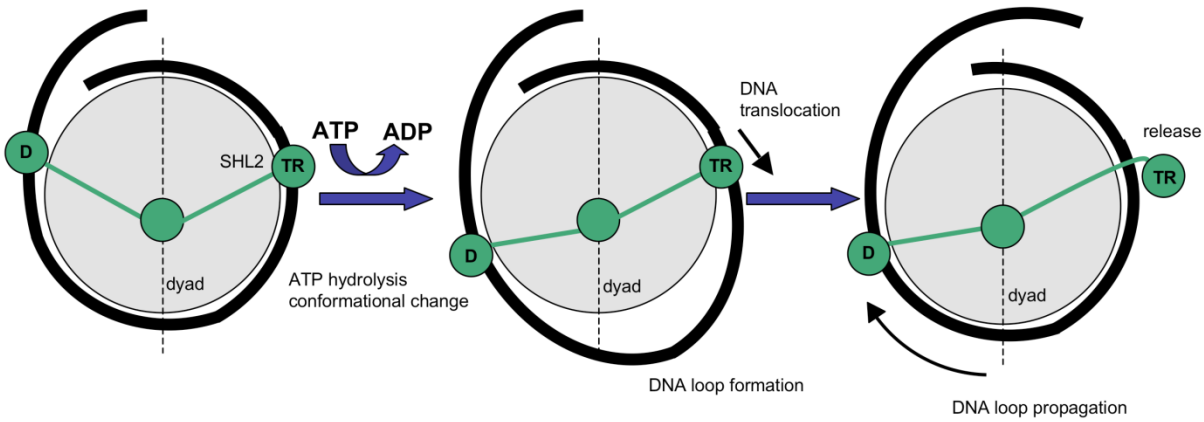

Figure 2.5 Model for nucleosome remodeling
The model for nucleosome sliding by ISWI. A DNA loop is formed on the nucleosome surface by the coordinated action of a DNA translocase (Tr) domain located at SHL2 position and a DNA binding domain (D) located close to the linker DNA. Top view of the nucleosome is shown (grey circle), DNA is depicted in black, nucleosome dyad is shown as dashed line. For details see text. The model is based on (Cairns 2007; Gangaraju et al. 2009).

2.4 Recruitment mechanisms of chromatin remodelers

In order to regulate chromatin structure *in vivo*, ATP-dependent chromatin remodelers have to be targeted to their sites of action in the nucleus. Studies on recruitment mechanisms of these complexes strongly contributed to our current knowledge on functions of chromatin remodelers *in vivo*. Various recruitment mechanisms include binding to sequence specific transcription factors, recognition of specific histone marks, binding to methylated DNA and interaction with poly(ADP-ribose) or noncoding RNAs (Fig. 2.6). In the following chapter I will summarize mechanisms which are utilized by chromatin remodelers for their targeting to chromatin.

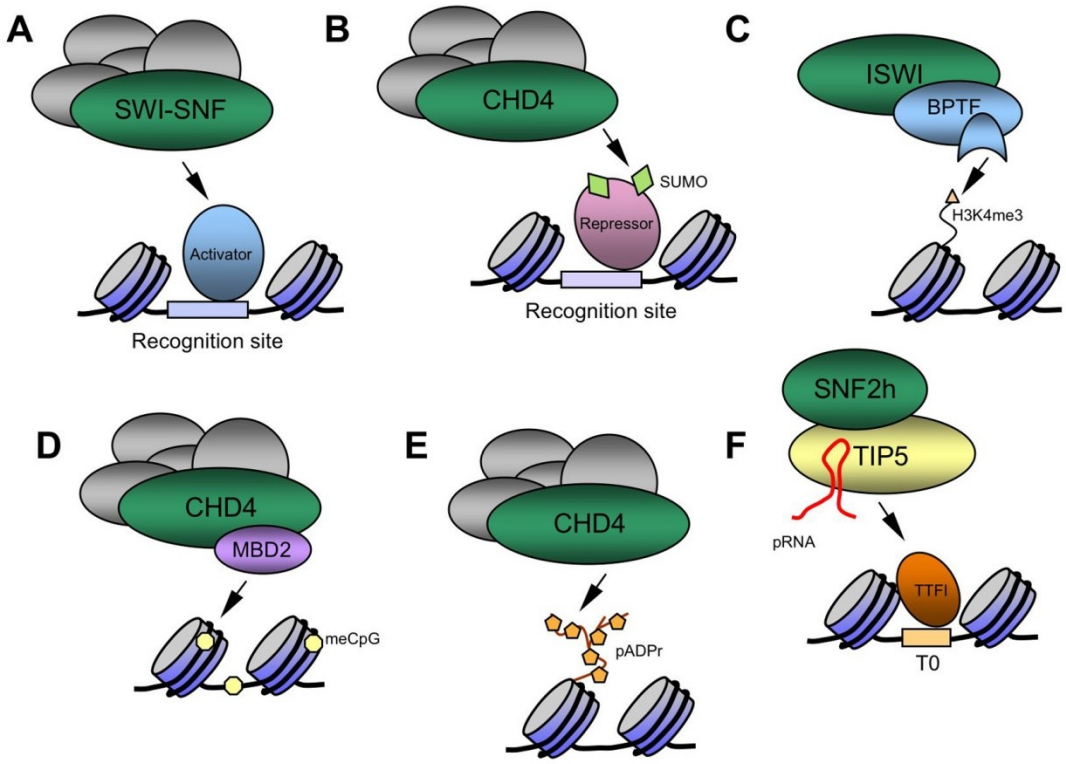

Figure 2.6 Mechanisms of recruitment of chromatin remodeling complexes to chromatin
Different targeting mechanisms are summarized (for detail see text). (**A**) Chromatin remodeling complexes can be targeted to chromatin by sequence specific transcription factors (activator or repressors). (**B**) SUMOylation of some transcription factors targets repressor complexes. (**C**) Various histone tail modifications are recognized by specific structural modules within remodeling complexes. (**D**) DNA methylation is recognized by methyl-binding proteins which constitute subunits of certain remodeling complexes. (**E**) Poly(ADP-ribosylation) of chromatin associated proteins (for example histones) is recognized by CHD4 remodeler at sites of DNA damage. (**F**) ncRNA (pRNA) targets NoRC complex to the promoter of rDNA genes.

2.4.1 Sequence specific transcription factors

Chromatin remodeling complexes bind DNA and nucleosomes in a sequence independent manner. Still, they regulate expression of only a subset of genes genome wide (Holstege et al. 1998). Early studies on SWI/SNF in yeast revealed that the complex can interact with the mammalian glucocorticoid receptor in yeast whole-cell extracts (Yoshinaga et al. 1992).

These initial observations led to the hypothesis that SWI/SNF activity must be targeted to specific loci *in vivo*. One way to recruit a complex to specific genes would be an interaction with sequence specific transcription regulators. Indeed, a number of studies have shown that SWI/SNF associates with a plethora of sequence specific transcription factors in yeast, *Drosophila* and human. Moreover, this mechanism is utilized by other families of chromatin remodelers, such as ISWI, CHD and INO80 which were shown to bind to various transcriptional activators or repressors (for examples and references see table 2.2).

Studies on SWI/SNF have revealed that the recruitment of the complex to promoters requires the activation domain of various transcriptional activators (Neely et al. 1999; Yudkovsky et al. 1999). These interactions seem to be functional, as the association of SWI/SNF with activators recruits the complex to nucleosomal arrays *in vitro* and consequently stimulates RNAP II transcription from these templates (Neely et al. 1999; Yudkovsky et al. 1999).

Often, the enzymatic activity of one chromatin remodeling enzyme is required for the subsequent, activator-dependent targeting of a second type of enzymatic activities. One prominent example of such orchestrated events is the Swi5 activator, which potentiates transcription of the yeast *HO* gene by recruitment of ySWI/SNF (Cosma et al. 1999). Chromatin remodeling by ySWI/SNF is required for subsequent recruitment of Gcn5 histone acetyltransferase (HAT) complex, called SAGA. Acetylation of the nucleosomes upstream of the transcription start site is required for binding of a second gene-specific activator, SBF, which in turn drives expression of the *HO* gene in late mitosis by recruiting components of the general transcription machinery (Cosma et al. 1999; Krebs et al. 1999). These studies indicate that not only transcription factors recruit chromatin remodelers, but also the binding of some transcription factors can be facilitated by the activity of chromatin remodelers. It has been suggested that this can depend on the context of specific promoters.

For example, activators whose binding sites are not occluded by nucleosomes (for example Swi5) can recruit ySWI/SNF complex. Conversely, activators that have difficulty accessing a nucleosomal site (for example SBF) may require SWI/SNF and HATs activities for binding (Cosma et al. 1999; Krebs et al. 1999; Peterson and Workman 2000).

Table 2.2 Chromatin remodeling complex recruitment by transcription factors and the influence on gene activity

Remodeler	Recruiting factor	Remarks	References
ySwi-Snf	Swi5	*H0* gene activation in late mitosis	(Cosma et al. 1999; Krebs et al. 1999)
	Gal4	Activation of *Gal* genes upon galactose induction	(Bryant et al. 2008)
	Gcn4p	Activation of amino acid biosynthetic genes in response to amino acid starvation	(Natarajan et al. 1999)
	Hir1/Hir2	Recruitment by transcriptional repressors, required for histone gene locus activation	(Dimova et al. 1999)
dBrm	Zeste	Zeste binding to specific Brahma complex subunits, Moira (MOR) and OSA recruits the complex for active chromatin state inheritance at *Fab-7* region	(Kal et al. 2000)
BRG1, Brm (mammalian)	ER (estrogen receptor)	Ligand dependent interaction, enhancement of transcription by the ER	(Ichinose et al. 1997; DiRenzo et al. 2000)
	GR (glucocorticoid receptor)	Ligand dependent interaction, enhancement of transcription by the GR	(Ostlund Farrants et al. 1997; Fryer and Archer 1998)
	c-Myc	c-Myc interaction with hSNF5 subunit of hSWI-SNF complex required for c-Myc transactivation functions	(Cheng et al. 1999)
	C/EBPβ	Myeloid gene activation	(Kowenz-Leutz and Leutz 1999)
	MyoD	Muscle-specific gene expression	(de la Serna et al. 2005)
	EKLF	β-globin gene expression	(Armstrong et al. 1998)
	HSF1	Heat shock gene activation	(Corey et al. 2003)
	β-catenin	β-catenin responsive gene activation	(Barker et al. 2001)
	Rest	Rest-mediated gene repression	(Ooi et al. 2006)
Isw2	Ume6	Repression of early meiotic genes during mitotic growth in yeast	(Goldmark et al. 2000)
dNURF	EcR (ecdysone receptor)	Ligand dependent interaction, required for ecdysone regulated gene	(Badenhorst et al. 2002)

		expression	
	GAF factor and HSF (heat shock factor)	Interaction with Nurf301, suggests role in recruitment, though not formally shown	(Badenhorst et al. 2005)
dNuRD	Ttk69	Repression of neuronal specific genes	(Murawsky et al. 2001; Reddy et al. 2010)
	Hunchback	Repression of *HOX* genes	(Kehle et al. 1998)
NuRD (mammalian)	Ikaros	Gene repression during lymphocyte differentiation	(Kim et al. 1999; Koipally et al. 1999)
	FOG-1	Gene repression in lineage commitment during erythropoiesis	(Gao et al. 2010; Gregory et al. 2010)
	KAP-1	KAP-1 co-repressor interacts with Mi-2α and targets NuRD complex for gene repression	(Schultz et al. 2001b)
	ER (estrogen receptor)	ER interacts with MTA1 subunit of NuRD and mediates NuRD recruitment to pS2 and c-*myc* promoters	(Mazumdar et al. 2001)
	Oct1	NuRD recruitment to the *Il2* promoter in naive CD4 T cells to mediate gene repression	(Shakya et al. 2011)
	EKLF	SUMO-dependent interaction with Mi-2β mediates transcriptional repression during erythropoiesis	(Siatecka et al. 2007)
	BCL11B	Recruitment of NuRD for repression of HIV-1 long terminal repeats in T cells	(Cismasiu et al. 2008)
INO80 (human)	YY1 (Yin-Yang-1)	YY1-dependent gene activation	(Cai et al. 2007)

2.4.2 SUMOylation of transcription regulators

An additional layer of regulation of chromatin remodeling complexes recruitment comprises SUMOylation of certain transcription factors. Small ubiquitin-like modifiers (SUMOs) are attached postranslationally to lysine residues of a myriad of proteins through a series of enzymatic reactions (for review see (Gill 2004; Johnson 2004; Hay 2005)). Transcriptional regulators constitute a large group of SUMO-modified proteins. These include transcription factors, cofactors and chromatin modifying enzymes. SUMOylation has mostly been linked to transcriptional repression. It has been suggested that SUMO-modified transcriptional regulators can recruit corepressors to promote transcriptional repression (Nishida and Yasuda 2002; Holmstrom et al. 2003). Several studies have

recently linked recruitment of chromatin remodelers via SUMOylated transcription factors (Ivanov et al. 2007; Stielow et al. 2008; Ogawa et al. 2009). A high-throughput screen performed in *Drosophila* cells to identify factors required for SUMO-dependent repression by transcription factor Sp3, revealed a number of chromatin regulators. Among them, a CHD family member of ATP-dependent chromatin remodelers, dMi-2, was found. dMi-2 is a catalytic subunit of at least two repressive chromatin remodeling complexes in *Drosophila*, called dNuRD and dMec (for details see chapter 2.5.3). dMi-2 was shown to bind SUMO and SUMOylated Sp3 *in vitro*. Moreover, dMi-2 knockdown relieved transcriptional suppression by SUMO-modified Sp3. Finally, dMi-2 was shown to be recruited to the promoter of a reporter gene in a SUMO dependent manner. In addition, the recruitment of mouse Mi-2 to *DHFR* promoter was abrogated in Sp3 deficient MEFs (Stielow et al. 2008).

Another study revealed that KAP1, a well characterized transcriptional co-repressor recruited to target genes by the KRAB-zinc finger sequence specific transcription factors, is also SUMOylated (Ivanov et al. 2007). Previous studies showed that Kap1 recruits CHD3 (Mi-2α) complex for repression of target genes (Schultz et al. 2001). SUMOylation of the Kap1 bromodomain has been subsequently shown to be critical for this recruitment event (Ivanov et al. 2007). Altogether these results suggest that recruitment via SUMOylated transcription factors may be a more general mechanism for Mi-2-like chromatin remodeling complexes.

There is also some evidence showing that SUMOylated transcription factors can stimulate ATPase activity of certain chromatin remodelers (Ogawa et al. 2009). Thus, it is plausible that in addition to recruitment, SUMOylation of transcription factors can play a regulatory role by enhancing the repressive activity of recruited chromatin remodeling complexes.

2.4.3 Histone modifications

Recognition of specific histone modifications has been also shown to play a role in chromatin remodeler recruitment. Several ATP-dependent chromatin remodelers have been reported to interact with H3K4me2/3. This modification is associated with transcription start sites of active genes and can be recognized by certain proteins resulting in recruitment of downstream effectors (Kouzarides 2007, Sims et al. 2007). It has been shown that H3K4me3 can recruit ISWI containing complexes (human NURF complex) via a PHD

finger of its largest subunit, BPTF. Histone peptide pulldown assays demonstrated that NURF preferentially associates with H3K4me3 tails. The crystal structure revealed the molecular basis of this specific recognition. BPTF interacts with the methyllysine through an anti-parallel beta-sheet formation on the surface of the PHD finger, with the side chains of R2 and K4me3 fitting in adjacent surface pockets, and bracketing an invariant tryptophan (Li et al. 2006). This binding seems to play a role in NURF complex recruitment *in vivo*. Depletion of H3K4me3 causes partial release of BPTF from chromatin and as a result, defective recruitment of the associated ATPase, SNF2L, to the *Hox8* gene promoter. Moreover, loss of BPTF in *Xenopus* embryos impairs *Hox* gene expression patterns during development (Wysocka et al. 2006). Collectively, these results suggest a role of H3K4me3 in direct recruitment of NURF complex to target genes. Another ISWI ATPase, yeast Isw1, was shown to require H3K4me2/3 for chromatin association *in vivo*, although the molecular basis of this interaction is not known (Santos-Rosa et al. 2003). Altogether, these experiments suggest that recruitment of some ISWI containing complexes via H3K4me3 binding is conserved throughout the evolution.

However, recognition of H3K4me3 by some chromatin remodelers seems to play a role only in higher eukaryotes. Human, but not yeast, CHD1 was shown to bind H3K4me2/3 via its chromodomains. The crystal structure revealed that hCHD1 requires tandem chromodomains, but the methyllysine is exclusively caged by the first chromodomain by two aromatic tryptophan residues (Flanagan et al. 2005). It has been suggested that hCHD1 recognition of H3K4me3 functions to recruit factors involved in pre-mRNA splicing (Sims et al. 2007). In concert with studies which showed hCHD1 binding to H3K4me2/3 peptides, it is plausible that this modification plays a role in hCHD1 recruitment to transcribed genes but it is also possible that it stabilizes hCHD1 on chromatin. Further experiments need to be done in order to distinguish between these two possibilities.

Studies on *Drosophila* CHD1 revealed that deletion of chromodomains of this remodeler had no impact on its localization to polytene chromosomes *in vivo* (Morettini et al. 2011). Moreover, though chromodomains of dCHD1 possess conserved aromatic residues, they were shown to bind H3K4 peptides independent of their methylation status (Morettini et al. 2011). Thus, it is currently unknown whether dCHD1 recognizes H3K4me3 *in vivo* and what is the chromatin recruitment mechanism of this remodeler. Chromodomains of yChd1 lack one of the conserved residues which can explain why they do not bind H3K4me3 (Sims et al. 2005). It has been suggested, that yChd1 can be recruited to transcribed genes

via its interaction with transcription machinery. Indeed, it was shown that yChd1 binds to PAF complex that associates with RNAP II and regulates transcription elongation (Simic et al. 2003).

The H3K4me3 mark might also block binding of certain chromatin remodelers to chromatin. For instance, it has been demonstrated that H3K4 methylation by Set9 reduces the association of the NuRD complex with H3 tail (Nishioka et al. 2002; Zegerman et al. 2002). Thus, by displacing this repressive chromatin remodeling complex, H3K4me3 might help to stimulate transcriptional activation.

Another prominent histone modification, which has been shown to play a role in chromatin remodeler recruitment, is histone acetylation. This modification can be recognized by bromodomains, and SWI/SNF and several subunits of other remodeling complexes possess this structural module. A number of studies in yeast and mammals demonstrated that histone acetylation facilitates SWI/SNF binding to different promoters *in vivo* (Reinke et al. 2001; Huang et al. 2003; Geng and Laurent 2004; Henderson et al. 2004). In some cases recruitment of SWI/SNF coincides with binding of histone acetyltransferases. For example Gcn5 is recruited simultaneously with SWI/SNF to the *SUC2* promoter in yeast (Geng and Laurent 2004). In other cases, histone acetylation precedes SWI/SNF binding. In the human system it was shown that transcriptional activation of interferon beta gene (IFN-β) begins with histone acetylation which in turn facilitates SWI/SNF recruitment and nucleosome remodeling at the promoter of this gene (Agalioti et al. 2002). Using an *in vitro* system with reconstituted nucleosomal arrays, it was demonstrated that H4K8 acetylation was required for BRG1 recruitment in a bromodomain dependent manner. It was suggested that at this promoter, histone acetylation by Gcn5 is followed by SWI/SNF recruitment during IFN-β gene activation (Agalioti et al. 2002).

As discussed above (chapter 2.4.1), binding to transcription activators constitutes the main mode of SWI/SNF recruitment to promoters and subsequent chromatin remodeling may facilitate binding of histone acetyltransferases (Cosma et al. 1999; Krebs et al. 1999). However, it was also suggested that histone acetylation may be involved in stabilization of the remodeler interaction with chromatin upon recruitment by transcription factor. This assumption comes from chromatin immunoprecipitation experiments which showed SWI/SNF binding to the *HO* promoter while the activator, Swi5, was not longer detected (Cosma et al. 1999). Subsequent *in vitro* studies have revealed that SWI/SNF retention on nucleosomal arrays was stabilized by acetylation after dissociation of the activator from the

template (Hassan et al. 2001). These studies clearly show that SWI-SNF chromatin remodelers work in concert with histone acetyltransferases, and often they rely on their enzymatic activities for recruitment and/or stabilization on the promoters of target genes.
Finally, histone modifications have been also implied in recruitment of ATP-dependent chromatin remodelers during DNA damage response. One of the first events in DNA DSB repair is phosphorylation of histone H2A in yeast and H2AX variant in mammals by PI3K kinases, like ATM and ATR (Burma et al. 2001). This phosphorylation functions to recruit a number of protein complexes involved in DNA repair. Several studies have shown that recruitment of INO80 chromatin remodeling complex relies on histone H2A phosphorylation. First, recruitment of INO80 is impaired in yeast strains lacking ATM and ATR homologs as well as in a H2A phospho-acceptor mutant (van Attikum et al. 2004). Secondly, Arp4 and Nhp10, subunits of INO80 complex were shown to bind to phospho-H2A peptide and contribute to INO80 recruitment *in vivo* (Downs et al. 2004; Morrison et al. 2004). Altogether, these experiments strongly suggest a role of H2A phosphorylation in INO80 recruitment to sites of DNA damage.

2.4.4 DNA methylation

Methylation of cytosine of CpG islands is an epigenetic modification implicated in transcriptional silencing (chapter 2.1.2). A number of studies indicated that methyl-CpG-binding proteins (MBPs) recruit corepressor complexes to silence gene expression (Nan et al. 1998; Wade 2001; Yoon et al. 2003; Sarraf and Stancheva 2004). One of the ATP-dependent chromatin remodeling complexes, which was shown to be targeted to chromatin via a methyl-CpG-binding protein, is the NuRD complex. The vertebrate NuRD complexes constitute a heterogeneous group of complexes which harbour both nucleosome remodeling and histone deacetylase activities, due to the presence of CHD3/4 (Mi-2) ATPases and HDAC1/2 deacetylases, respectively (for details see table 2.3). Various biochemical purification strategies revealed that NuRD complexes contain subunits which belong to the methyl-CpG-binding family of proteins, such as MBD2 or MBD3 (Zhang et al. 1999; Feng and Zhang 2001; Le Guezennec et al. 2006). While MBD3 cannot bind methylated DNA, MBD2 was shown to tether NuRD complex to free methylated DNA as well as nucleosomal arrays assembled on methylated DNA *in vitro* (Zhang et al. 1998; Zhang et al. 1999; Feng and Zhang 2001). Moreover, overexpression of Mi-2 enhanced

MBD2-dependent transcriptional repression in a luciferase assay (Feng and Zhang 2001). Collectively, these results strongly suggest that MBD2 recruits NuRD complex to methylated promoters contributing to their transcriptional repression.

In *Drosophila*, a functional link between dMi-2 and MBD2/3 has also been suggested. dMi-2 and MBD2/3 cofractionate in SL2 cells and interact genetically in flies (Ballestar et al. 2001; Marhold et al. 2004b). Moreover, both proteins partially colocalize in embryo nuclei and a fraction of dMi-2 is displaced from nuclear foci in *MBD* mutants (Marhold et al. 2004b). These results suggest that MBD2/3 might target some dMi-2 molecules to methylated DNA. However, given the low and transient levels of DNA methylation in *Drosophila*, this is unlikely to be a major recruitment mechanism for the dMi-2 complexes.

2.4.5 Poly(ADP-ribosylation)

Recently, a novel mode of recruitment of a chromatin remodeler to sites of DNA-damage has emerged. In response to DNA damage, poly(ADP-ribose) polymerase (PARP) enzymes are activated. PARP modifies itself and target proteins with poly(ADP-ribose) chains (PAR) at DNA damage sites. This modification has been linked to regulation of activity of various DNA repair factors, regulation of protein interactions with other proteins or nucleic acids as well as recruitment events to damaged chromatin (for review see (Malanga and Althaus 2005; Hakmé et al. 2008)). The connection between chromatin remodeler recruitment and poly(ADP-ribosylation) has been shown for the NuRD complex, which in addition to its role in transcription repression, plays a role in DNA damage response (chapter 2.5.5.2). The ATPase subunit of the complex, CHD4 has been shown to be recruited to laser-induced DNA damage sites in various human cells (Chou et al. 2010; Larsen et al. 2010; Polo et al. 2010; Smeenk et al. 2010). The measurement of recruitment kinetics revealed that CHD4 recruitment was rapid (it occurred within a few minutes), but transient (it declined within 30 minutes upon DNA damage induction). Other components of the complex, MTA2 and HDAC1, have been shown to be recruited in a CHD4 dependent manner. Interestingly, CHD4 recruitment was not impaired in H2AX or ATM deficient cells which indicates that phosphorylation of H2AX does not play a role in CHD4 targeting. By contrast, pharmacological inhibition of PARP1/2 enzymatic activity as well as PARP1/2 depletion by RNA interference, abrogated CHD4 recruitment to DNA damage sites. Biochemical experiments revealed direct CHD4 binding to PAR and the N-

terminal part of CHD4 was shown to bind PAR *in vitro* and to be important for CHD4 targeting *in vivo* (Polo et al. 2010). Altogether, these results suggest that CHD4 recruitment to chromatin at sites of DNA damage likely involves its binding to PARylated proteins present at these sites. Currently it is not known whether automodified PARP itself, histones or other PARylated factors are responsible for CHD4 targeting.

2.4.6 Noncoding RNA

Recent transcriptome analysis of many organisms has revealed that a large part of the genomes are transcribed into noncoding RNAs (ncRNAs). Several ncRNAs have been implicated in recruitment of chromatin modifying complexes, such as polycomb complex, PCR2 (Khalil et al. 2009; Tsai et al. 2010). A specific ncRNA has been also shown to be important for recruitment of ISWI containing chromatin remodeling complex, called NoRC (nucleolar remodeling complex) (Strohner et al. 2001). This complex silences a fraction of ribosomal RNA genes (rDNA) by nucleosome remodeling and recruitment of histone-modifying enzymes and DNA methyltransferases (Strohner et al. 2001; Santoro et al. 2002; Zhou et al. 2002). Two factors were shown to be involved in targeting of NoRC complex to the promoter of rDNA genes. First, TTF-I, a transcription termination factor bound to the promoter-proximal terminator T0, recruits NoRC to rDNA genes (Németh et al. 2004; Strohner et al. 2004; Santoro and Grummt 2005). Secondly, ncRNA called pRNA, which originates from the promoter located in the intergenic spacer separating rDNA genes, has been involved in NoRC recruitment and rDNA gene silencing (Moss et al. 1980; Mayer et al. 2006). Several experiments suggest a role of pRNA in NoRC targeting to chromatin. First, treatment of permeabilised cells with RNAse A abolished localization of NoRC to nucleoli. Secondly, pRNA was mapped to bind to TIP5, the large subunit of NoRC. Third, mutations in TIP5 which abrogate its binding to pRNA impaired NoRC binding to chromatin and prevented heterochromatin formation. Moreover, specific depletion of pRNA led to displacement of NoRC from nucleoli (Mayer et al. 2006). pRNA was shown to fold into a conserved stem-loop structure and mutations which disrupted this structure also impaired NoRC targeting to rDNA genes. Thus, it has been suggested that NoRC recognizes a secondary or tertiary RNA structure rather than a specific sequence within pRNA (Mayer et al. 2008). This is in line with recent studies on long ncRNAs which suggest that complex targeting may not necessarily imply linear base pairing with

target sequences, but instead the tertiary structure of the RNA may be key to specific target gene recognition (Margueron and Reinberg 2011). It remains to be determined whether other chromatin remodeling complexes utilize ncRNA for gene targeting.

2.5 CHD family of chromatin remodelers

Since the characterization of members of the CHD family of ATP-dependent chromatin remodelers in *Drosophila* constitutes the main aim of this PhD thesis, below, I will summarize the current knowledge on CHD proteins emphasizing their domain structure, complex composition and biological functions.

2.5.1 Family of CHD remodelers

As mentioned in chapter 2.2.5, the CHD family of ATP-dependent chromatin remodelers is characterized by the presence of tandem chromodomains located in the N-terminal region, and the SNF2-like ATPase domain located in the middle of the protein. The CHD family is further divided into three subfamilies according to the presence of additional structural modules (reviewed in (Woodage et al. 1997; Hall and Georgel 2007; Marfella and Imbalzano 2007)) (Fig. 2.7).

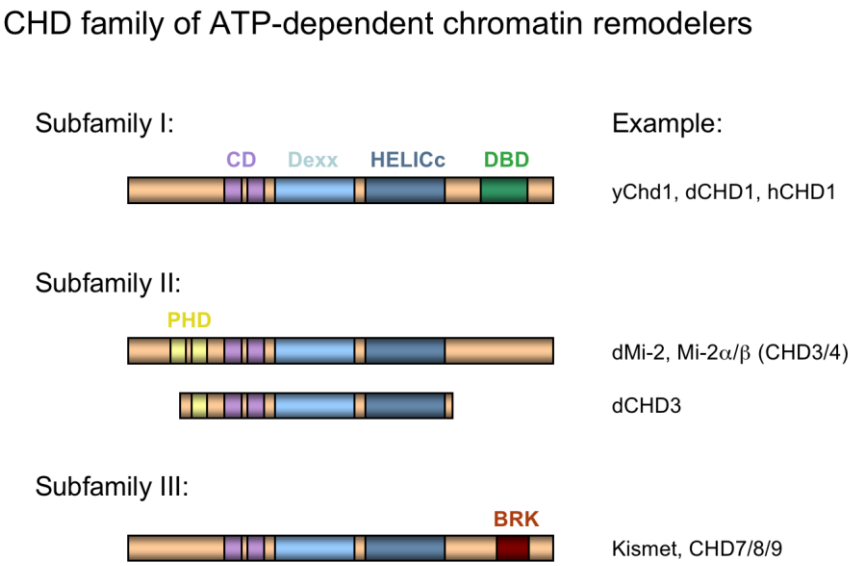

Figure 2.7 CHD family of ATP-dependent chromatin remodelers
Schematic representation of protein domains found in different subfamilies of CHD remodelers. CD, chromodomains; Dexx, HELICc, ATPase domain; DBD, DNA binding domain; PHD, Plant

Homeo Domain Zn-fingers; BRK, Brahma and Kismet domain. Protein examples are listed on the right. Note that the protein and domain sizes are not in scale.

The first subfamily contains yeast Chd1 (yChd1) which is the only CHD family member present in *S. cerevisiae*, Hrp1 and Hrp3 in *S. pombe* and the Chd1 and Chd2 proteins from higher eukaryotes. The Chd1 and Chd2 proteins contain a DNA-binding domain located in the C-terminal region. The DNA-binding domain preferentially binds to AT-rich DNA motifs *in vitro*, however the function of this interaction *in vivo* is elusive (Delmas et al. 1993; Stokes and Perry 1995).

The second subfamily includes CHD3 and CHD4 (called also Mi-2α and Mi-2β respectively) proteins from higher eukaryotes. They lack the standard DNA binding domain in the C-terminus but they harbour a pair of PHD Zn-finger-like domains at the N-terminal part.

The third subfamily contains proteins numbered from CHD6 to CHD9. This subfamily is most variable as it is defined by additional functional motifs in the C-terminal region, like SANT domain or BRK domains (Hall and Georgel 2007; Marfella and Imbalzano 2007). There is a discrepancy concerning CHD5 protein classification. The presence of both PHD fingers and a SANT domain places CHD5 between subfamily II and III.

2.5.2 Structural motifs of CHD family

2.5.2.1 Tandem chromodomains

Tandem chromodomains are the signature motifs that define CHD family. The chromodomain initially was named for its function as a chromatin organization modifier (Eissenberg 2001). It was originally characterized in *Drosophila* HP1 and Polycomb proteins, in which it contributes to binding to methylated histone marks, H3K9me3 and H3K27me3, respectively (Paro and Hogness 1991; Pearce et al. 1992; Brehm et al. 2004). The standard chromodomain module was refined to encompass ~50 amino acids and it folds into 3-stranded anti-parallel β-sheets and one α-helice (Ball et al. 1997). Chromodomains of CHD family members have been implicated in recognition of methylated histone tails, DNA binding as well as in regulation of the ATPase activity of the enzymes. As already discussed in chapter 2.4.3, chromodomains of human, but not yeast, CHD1 have been shown to bind H3K4me2/3 (Flanagan et al. 2005). Whether other CHD remodelers can bind to H3K4me2/3 or other histone modifications remains to be

determined. By contrast, dMi-2 chromodomains have been shown to be a DNA binding module (Bouazoune et al. 2002). Both chromodomains of yChd1 and dMi-2 have been implicated in regulation of the remodeling activity of these enzymes (chapter 2.3.3.1, (Bouazoune et al. 2002; Hauk et al. 2010). Altogether, the analysis of sequences of various CHD chromodomains in concert with available biochemical and structural data strongly suggest the evolutionary functional specialization of CHD double chromodomains (Flanagan et al. 2005).

2.5.2.2 PHD fingers

The PHD Zn-finger-like domains are ~50-residue modules characterized by a conserved Cys4HisCys3 motif that coordinates two zinc ions. They are found in a number of nuclear proteins involved in chromatin-based transcriptional regulation (reviewed in (Mellor 2006; Champagne and Kutateladze 2009)). The precise function of PHD fingers in CHD proteins is so far unknown. It has been described that PHD fingers of CHD3 and CHD4 interact with histone deacetylase HDAC1 within NuRD (Xue et al. 1998b). It was also shown that second PHD finger of CHD4 recognizes the N-terminus of histone H3 and that this interaction is facilitated by acetylation or methylation of Lys9 (H3K9ac and H3K9me respectively) but is inhibited by methylation of Lys4 (H3K4me) (Musselman et al. 2009; Mansfield et al. 2011). Interestingly, this suggests a possible regulation of CHD3/4 association with chromatin. Indeed, it was previously shown, that methylation of histone H3K4 by Set9 displaces the association of NuRD with the histone H3 tail (Nishioka et al. 2002; Zegerman et al. 2002). However, functional link between PHD fingers for these interactions has not been addressed.

2.5.2.3 Other domains

Additional domains were mapped in the sequences of CHD remodelers. SANT domains, involved in histone tail binding, were found in several CHD subfamily III members (for example CHD5). The BRK domain (Brahma and Kismet domain) present in several SWI/SNF complexes, was found in Kismet, CHD7, CHD8 and CHD9. However, their exact function remains unknown (Daubresse et al. 1999; Hall and Georgel 2007; Marfella and Imbalzano 2007).

2.5.3 CHD complexes in *Drosophila*

The CHD family is a highly heterogeneous group of ATP-dependent chromatin remodelers. Some members exist as monomers *in vivo*, whereas others are subunits of multiprotein complexes. Many of the complexes have not yet been purified or characterized well. There are also discrepancies in the literature concerning subunits composition of some complexes that likely reflect the heterogeneity of these complexes or the differences in purification procedures (Table 2.3). In this chapter I will describe the composition of *Drosophila* CHD complexes. CHD complexes from other species are included in Table 2.3.

In *Drosophila* there are four CHD remodelers, dCHD1, dMi-2, Kismet and dCHD3. Glycerol gradient fractionation experiment from *Drosophila* embryo nuclear extract revealed that dCHD1 is a monomer *in vivo* (Lusser et al. 2005). This is reminiscent of yeast where yChd1 has been shown to exist mainly in a monomeric state (Tran et al. 2000).

The best characterized member of the *Drosophila* CHD family is dMi-2. Mi-2 was initially identified in human as a dermatomyositis-specific antigen recognized by the patient Mitchell autoimmune antibodies (Seelig et al. 1995). Subsequently several groups purified Mi-2 complexes from *Xenopus* and human cells (Wade et al. 1998; Zhang et al. 1998; Wade et al. 1999; Zhang et al. 1999; Feng and Zhang 2001). Despite of some variability in subunit composition, these complexes are unique in coupling nucleosome remodeling with histone deacetylase activity, therefore they were named NuRD (nucleosome remodeling and histone deacetylation) (Xue et al. 1998b; Zhang et al. 1998). Several studies indicated that *Drosophila* Mi-2 exists in a similar NuRD complex. dMi-2 immunoprecipitates from a cell line with the histone deacetylase dRPD3, CAF1/p55 (homolog of human RbAp46/48), dMTA (metastasis associated protein), MBD2/3 (DNA-methyl binding) and dp66 (Bouazoune and Brehm unpublished and (Reddy et al. 2010)). The precise roles of different non enzymatic subunits within the complex are not known. The CAF1/p55 protein is a common subunit of many chromatin modifying complexes (Smith and Stillman 1989; Tyler et al. 1996; Verreault et al. 1996). It comprises seven WD repeat motifs and was shown to bind to histones (Verreault et al. 1998). Based on its structure, it has been suggested that CAF1/p55 may serve as a multifunctional protein interaction platform for the complexes (Song et al. 2008). MTA proteins have been shown to be highly expressed in metastatic tumour cell lines (Toh et al. 1994). It was reported that MTA directs

assembly of an active histone deacetylase within NuRD complex *in vitro*, however its exact function is unknown (Zhang et al. 1999). DNA-methyl binding protein, MBD2/3, is present in *Drosophila* as a long and a short isoform and both of them have been shown to be associated with dNuRD complex via dMi-2 and CAF1/p55 (Marhold et al. 2004a). Given that DNA methylation in *Drosophila* is restricted temporally during development and occurs at a significantly lower frequency than in mammals, it is conceivable that MBD2/3 plays different role in flies. Indeed, dMBD2/3 was shown to be unable to bind methylated DNA (Ballestar et al. 2001). However, dMBD2/3 has been suggested to function as a transcriptional corepressor through recruitment of histone deacetylase activity within dNuRD complex (Ballestar et al. 2001). Finally, the dp66 subunit is a highly conserved nuclear zinc-finger protein that is required for fly development (Kon et al. 2005). In the human system, dp66 homologs were shown to interact with MBD2 and histones (Brackertz et al. 2002; Brackertz et al. 2006). In addition, SUMOylation of human p66α/β was shown to be important for interactions with HDAC1 and RbAp46 and to enhance the repressive activity of NuRD complex (Gong et al. 2006). It is currently not known whether the same applies to the *Drosophila* NuRD complex.

Recently, a novel dMi-2 containing complex, called dMec (*Drosophila* Mep-1 containing complex) was purified from the Kc cell line (Kunert et al. 2009). This complex comprises only two subunits, dMi-2 and dMep1 and turned out to be the major dMi-2 complex in *Drosophila* cell line. dMec seems to be distinct from dNuRD, as dMep1 was shown not to precipitate with dRPD3 or dp66 in Kc nuclear extracts (Kunert et al. 2009). dMep1 is a zinc finger protein, previously shown to interact with the *C. elegans* Mi-2 homolog, Let-418 and be required for maintenance of somatic differentiation in *C. elegans* (Unhavaithaya et al. 2002). The dMec complex was shown, similarly to dNuRD complex, to be a nucleosome stimulated ATPase (Kunert et al. 2009).

It has been also suggested that dMep1 can be a subunit of dNuRD complex as immunoaffinity precipitation of dMep1 from embryo nuclear extracts revealed association of all dNuRD subunits (Reddy et al. 2010). These discrepancies could be due to the differences in purification procedures or due to the different material used for the complex purification (embryo nuclear extract versus cell line nuclear extract).

Another *Drosophila* CHD family member, Kismet (KisL) has been shown to exist in a large complex in embryo nuclear extracts, however the associated subunits have not been

identified so far (Srinivasan et al. 2005). dCHD3 is the only member of CHD family in *Drosophila* that has not been studied to date (chapter 5.1).

Table 2.3 Composition of CHD complexes in different species

ATPase (Complex)	Complex subunits	Method of purification	References
yChd1	monomer or dimmer	Myc-tagged yChd1 purification by anion exchange and size-exlusion chromatography	(Tran et al. 2000)
	yChd1, subunits of SLIK (Saga like) and Saga (Spt-ada-Gcn5 acetyltransferase) complexes	Tap-tagged yChd1 IP followed by anion exchange and size-exlusion chromatography	(Pray-Grant et al. 2005)
Hrp1	Hrp1, Hrp3, Nap1 (nucleosome assembly factor 1), CkII kinase	Fllag-tagged Hrp1 IP, followed by mass spectrometry (MS) analysis	(Walfridsson et al. 2007)
	Med15 (component of Mediator complex)	Flag-Med15 IP, followed by MS analysis	(Khorosjutina et al. 2010)
dCHD1	monomer	Glycerol gradient sedimentation from crude *Drosophila* embryo nuclear extracts	(Lusser et al. 2005)
hCHD1	hCHD1, SSRP1 (subunit of FACT complex)	Yeast 2 hybrid, size-exclusion chromatography in HeLa cells	(Kelley et al. 1999)
	hCHD1, PAF complex subunits, SNF2h, SF3A (subcomplex of the U2-snRNP)	Ion exchange chromatography from HeLa nuclear extracts, followed by size-exclusion chromatography and immunoprecipitation with CHD1 specific antibodies	(Sims et al. 2007)
xMi-2 (NuRD)	Mi-2, HDAC1/2, RbAp46/48, MTA1, p66/68, MBD3	Ion exchange chromatography and sucrose gradient sedimentation from *Xenopus* egg extracts	(Wade et al. 1998; Wade et al. 1999)
Mi-2β (NuRD)	Mi-2β, HDAC1/2, RpAp46/48, MTA1/2, MBD3	Immunoaffinity purification from HeLa nuclear extracts followed by MS, also conventional ion exchange chromatography	(Zhang et al. 1998; Zhang et al. 1999)
Mi-2 (MeCP1)	Mi-2, HDAC1/2, RbAp46/48, MTA2, p66/p68, MBD2and MBD3	Ion exchange chromatography from HeLa nuclear extracts	(Feng and Zhang 2001)
Mi2α/β (MBD2/NuRD) (MBD3/NuRD)	Mi-2 α/β, HDAC1/2, RpAp46/48, MTA1/2 MBD2, PRMT5, MEP50, DOC1, importin or Mi-2 α/β, HDAC1/2, RpAp46/48, MTA1/2 MBD3, DOC1	HEK 293 cell (human embryonic cells) lines stably expressing Tap-tagged MBD2 or MBD3, Tap-purification followed by MS	(Le Guezennec et al. 2006)
Mi2α/β (NuRD)	Mi-2 α/β, HDAC1/2, RpAp46/48, MTA2, MBD2, MBD3, LSD1, BRCA2	Immunoaffinity purification of Flag-tagged MTA2 from HeLa cells, followed by MS analysis	(Wang et al. 2009)

dMi-2 (dNuRD)	dMi-2, dRPD3, CAF1/p55, dMBD2/3, dMTA, p66	Immunoaffinity purification from *Drosophila* SL2 cell line	(Brehm et al. 2000; Ballestar et al. 2001; Bouazoune et al. 2002; Marhold et al. 2004a) and unpublished data (Bouazoune, Brehm)
dMi-2 (dMec)	dMi-2, dMep1	*Drosophila* Kc cell nuclear extract fractionation by ion exchange chromatography, followed by immunoaffinity purification and MS analysis	(Kunert et al. 2009)
dMi-2 (dNuRD)	dMi-2, dMep1, dRPD3, CAF1/p55, dMBD2/3, dMTA, p66, DOC1, Ttk69	Immunoaffinity purification from 0-12 hr embryo nuclear extracts with dMi-2 or dMep1 antibodies, followed by MS analysis	(Reddy et al. 2010)
Let-418 CHD3	Let-418 (CHD4), HDA-1 (HDAC1), Mep1 Let-418, HDA-1, Lin53 (RpAp46/48), Lin40 (MTA1) CHD3, HDA-1, Lin53, Lin40	Various immunoprecipitations from protein extracts from mixed-staged *C. elegans* worms (Tap-tag and GFP-tag purifications), followed by Western blot analysis	(Passannante et al. 2010)
Kismet	High molecular complex (1 MDa)	Size-exclusion chromatography of *Drosophila* embryo nuclear extract, complex composition not determined	(Srinivasan et al. 2005)
CHD7	CHD7, BAF/PBAF subunits, PARP1	Immunopurification with CHD7 antibodies from hNCLCs cells (human neuronal crest cells) followed by MS analysis	(Bajpai et al. 2010)
	CHD7, SETDB1, PPARγ, NLK	Immunaffinity purification of Flag-tagged NLK followed by MS analysis	Takada (Takada et al. 2007)
CHD8	CHD8, WDR5, Ash2L, RbBP5	Ion exchange chromatography from HeLa nuclear extracts followed by MS, complex reconstitution by subunit coexpression in SF9 cells	(Thompson et al. 2008; Yates et al. 2010)

2.5.4 Functions of CHD chromatin remodelers in transcription

Most of the CHD chromatin remodelers have been implicated in transcriptional regulation, both repression and activation. It is especially noticeable that different CHD chromatin remodelers play roles in different stages of the transcriptional cycle, such as transcription initiation, elongation and termination (Fig. 2.9). Moreover, they have been also reported to participate in cotranscriptional events, such as pre-mRNA splicing. In the following chapter, transcriptional functions of the CHD family will be described.

2.5.4.1 Transcription repression

NuRD is the only so far purified chromatin remodeling complex which couples ATP-dependent nucleosome remodeling with histone deacetylation. These two activities of the complex have been shown to be involved in transcriptional repression of various genes during differentiation and development in *C. elegans*, *D. melanogaster* and mammals (reviewed in (Ahringer 2000; Ramírez and Hagman 2009)). NuRD can accomplish these tasks by being recruited to the promoters of target genes via interaction with a plethora of transcription factors and co-regulators (Table 2.2). Despite of all these studies, relatively little is known about the mechanism of gene repression by NuRD. It has been suggested that the net result of the combined enzymatic activities of ATP-dependent nucleosome remodeling and histone deacetylation would be the generation of densely packed, hypoacetylated nucleosomes (Denslow and Wade 2007). Purified NuRD disrupts nucleosomes and recombinant Mi-2 slides mononucleosomes *in vitro* in the presence of ATP (Xue et al. 1998b; Zhang et al. 1998; Brehm et al. 2000). It has been demonstrated that inhibition of histone deacetylase activity of NuRD complex has no effect on its nucleosome remodeling activity. By contrast, ATP was shown to stimulate the histone deacetylase activity of NuRD on nucleosomal arrays (Tong et al. 1998; Xue et al. 1998; Zhang et al. 1998). Thus, it has been suggested, that ATP-dependent nucleosome remodeling may help a histone deacetylase to get access to the histone substrate. In addition, RbAp46 and RbAp48, histone binding subunits of the NuRD complex, are not able to bind to nucleosomes and may require the remodeled nucleosome structure to get access to histones (Verreault et al. 1996; Zhang et al. 1998). Based on these results a model for NuRD transcriptional repression was suggested (Fig. 2.8). According to it, NuRD is recruited to the promoters of target genes via interaction with various sequence specific transcription factors or cofactors (chapter 2.4.1). Upon recruitment, the complex remodels adjacent nucleosomes, allowing histone tails to be accessible for deacetylation. Consequently, a more compacted chromatin structure is generated, leading to gene repression (Zhang et al. 1998). The formation of the compacted, less accessible chromatin is regulated by a series of coordinated enzymatic activities. For example, SUMOylated Kap1 (chapter 2.4.2) was shown to recruit not only NuRD, but also Lys9 specific histone methyltransferase, SETDB1, leading to subsequent HP1 binding to a regulated transgene locus in mammalian cells. Increased DNA-methylation was also detected in this silenced chromatin region and it has been suggested that NuRD binding to methylated DNA via

MBD2 subunit can maintain the HDAC activity at the locus (Schultz et al. 2001a; Ayyanathan et al. 2003). Given that NuRD interacts with a growing number of transcription factors and cofactors in different cell and developmental contexts, it is plausible that gene repression by this complex might be promoter or gene specific. Certainly, more detailed studies remain to be done to elucidate the mechanism of gene repression by NuRD complex.

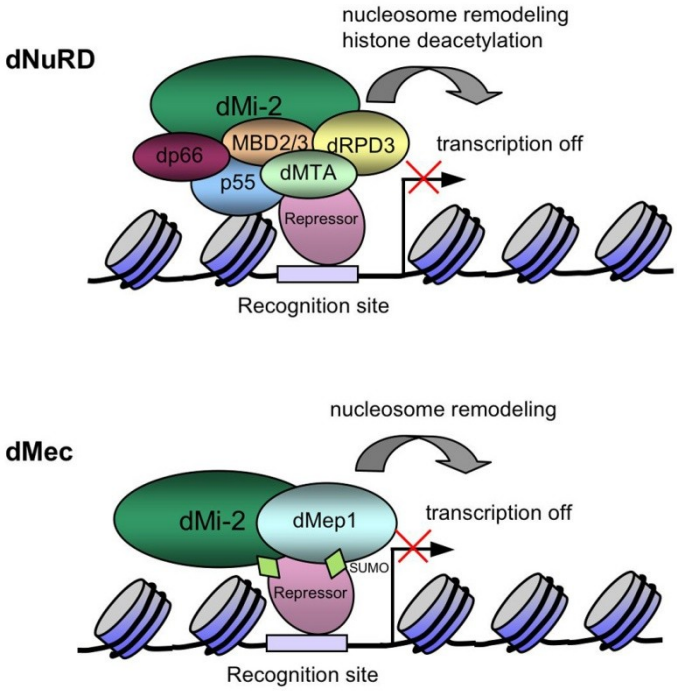

Figure 2.8 Models for gene repression by dNuRD and dMec complexes
Repression of a putative target gene by dNuRD or dMec is represented. As an example *Drosophila* NuRD is shown but the same model applies to vertebrate NuRD complex. See text for details.

In addition to the NuRD complex, the presence of dMec repressive complex, which lacks histone deacetylase activity, raises the question about its role in transcriptional repression. It was shown that depletion of dMep1 from SL2 cells results in derepression of a set of proneuronal genes in HDAC independent manner (Kunert et al. 2009). In the RNAi screen performed to identify factors required for SUMO-dependent repression by a transcription factor Sp3 (chapter 2.4.2), in addition to dMi-2, dMep1 was found. Depletion of dMep1 but not other subunits of the dNuRD complex resulted in derepression of SUMOylated Sp3 target gene and dMep1 was shown to bind SUMO directly (Stielow et al. 2008). These results suggest that dMec might be recruited via SUMOylated transcription factors to its

target genes and use its ATPase activity to promote gene repression (Kunert and Brehm 2009). This model has to be tested but there are several pieces of evidence which are in agreement with it. First, SUMOylation of Lin1 transcription factor in *C. elegans* was shown to promote Mep1 association and repression of genes involved in vulval cell fate (Leight et al. 2005). Second, a SUMOylated transcription factor, tramtrack69 (Ttk69), was shown to associate with dMi-2 and dMep1 biochemically and genetically. Third, dMi-2 and Ttk69 co-localize at a number of discrete sites on polytene chromosomes, showing that they bind common target loci. Indeed, recent genome-wide expression analysis has revealed that they share an overlapping set of target genes (Murawsky et al. 2001; Reddy et al. 2010). Hence, dMi-2 may mediate SUMO-dependent transcriptional repression as part of the dMec complex. However, in the human system, SUMO-dependent repression by the NuRD complex has been shown in the context of several transcription cofactors, like Kap-1 or EKLF (Ivanov et al. 2007; Siatecka et al. 2007) (chapter 2.4.2). Therefore, it is currently unknown how the specificity of dMec complex towards SUMOylated transcription factors would be achieved. Also, nothing is known about the mechanism of gene repression and repressive chromatin formation by dMec. More experiments have to be done in order to clarify these issues.

2.5.4.2 Transcription initiation

The role of ATP-dependent chromatin remodelers at promoters has been extensively studied in the context of SWI/SNF complexes, which help to generate an open chromatin providing access to transcription factors and subsequent transcription machinery assembly and transcription initiation (chapter 2.4.1). However, far less is known about possible functions of CHD remodelers in transcription initiation. Recent genome-wide studies on *S. pombe* homologs of CHD1, Hpr1 and Hpr3, have revealed their function in nucleosome disassembly at gene promoters (Walfridsson et al. 2007). Both ATPases have been shown to copurify with a histone chaperone Nap1, which was previously linked to nucleosome assembly and disassembly in concert with remodeling complexes (Lusser et al. 2005; Lorch et al. 2006). Hpr1 and Hpr3 localize at the promoters and to a lesser extent in the ORFs of many *S. pombe* genes. Moreover, Hpr1/3 display a clear preference to nucleosome dense promoters. Depletion of these remodelers results in a genome-wide increase in histone H3 density at the promoters suggesting a role in nucleosome

disassembly, which in turn may facilitate transcription of these genes. In agreement with this, many genes are downregulated in *hpr1/3* double mutant (Walfridsson et al. 2007).

In addition to regulation of chromatin structure at the promoters, transcription activation *in vivo* is influenced by more distal sequences, called enhancers. Binding of an activator to an enhancer is thought to influence transcription via nucleosome displacement and recruitment of histone-modifying enzymes that generate a local access to chromatin and subsequent targeting of the basal transcription machinery to the core promoter. The interaction between promoter and activator bound enhancer is mediated by loop formation (reviewed in (Szutorisz et al. 2005)). Several studies have implicated CHD remodelers in facilitating transcription activation via binding to enhancers. Recently, human CHD7 has been shown to occupy enhancer elements genome-wide. It was found to bind to DNAse I hypersensitive sites enriched in H3K4me1, a hallmark of enhancers. CHD7 was shown to bind H3K4me1/2/3 peptides via its chromodomains which may stabilize its binding at enhancers. Moreover, CHD7 binding strongly correlates with active transcription, which suggests its role in gene activation (Schnetz et al. 2009). Indeed, another study showed that CHD7 directly regulates transcription of core neural crest transcription factors in *Xenopus*. In addition, it was shown to interact with BRG1-like complexes, BAF/PBAF and both CHD7 and BRG1 occupy distal regulatory elements of their target genes (Bajpai et al. 2010). Currently it is not known, what is the mechanism of gene activation by CHD7. Weak signals of CHD7 are also detected nearby promoters, thus a looping mechanism has been suggested (Schnetz et al. 2009).

CHD8 was shown to bind to an enhancer element of an androgen receptor (AR) responsive gene in prostate cancer cells, in an induction independent manner. CHD8 might be involved in the remodeling of chromatin structure at this enhancer as recruitment of AR and consequently the gene activation were strongly abrogated upon CHD8 knockdown (Menon et al. 2010).

Mi-2β (CHD4) was also implicated in enhancer element binding at the *CD4* gene during T-cell development. Interestingly, Mi-2β was shown to facilitate recruitment of transcription factor HEB and a histone acetyltransferase, p300, to the *CD4* enhancer element, leading to open chromatin formation and transcription activation. Mi-2β was shown to interact with both factors in an HDAC independent manner, which suggests that this remodeler may be involved in active transcription outside of the NuRD complex (Naito et al. 2007).

2.5.4.3 Transcription elongation

A growing number of recent studies indicate that chromatin structure is highly controlled during transcription elongation. Nucleosomes ahead of RNAP II are partially disassembled or displaced and then reassembled behind the passage of RNAP II (reviewed in (Armstrong 2007)). To a large extent, the phosphorylation status of the C-terminal domain of the largest subunit of RNAP II (CTD) defines the state of transcription elongation (reviewed in (Phatnani and Greenleaf 2006)). The CTD of RNAP II has a heptapeptide repeat that is conserved from yeast to humans and contains the consensus amino acid sequence YSPTSPS. The second and fifth serines of each repeated unit are major sites of phosphorylation. Hypophosporylated form of RNAP II is recruited to the promoters. Next, at 5' of genes, CTD is phosphorylated at Ser5 by the Cdk7 subunit of TFIIH. RNAP II becomes phosphorylated at Ser2 in the body and towards the end of genes by the Cdk9 subunit of P-TEFb. This modification serves as a platform for recruitment of various transcription elongation and RNA processing factors (Saunders et al. 2006).

One CHD remodeler suggested to be involved in an early elongation step is Kismet (KisL). It was originally identified in a genetic screen for supressors of polycomb (Pc) repressors in *Drosophila* suggesting that it antagonizes Pc to activate homeotic gene expression (Kennison et al. 1998; Daubresse et al. 1999). It was shown that KisL localizes to transcriptionally active sites on polytetene chromosomes as its binding pattern highly overalapped with RNAP II phosphorylated at Ser5 and Ser2, Brahma and dCHD1. However, no interaction with any of these factors was detected in coimmunoprecipitation experiments. Interestingly, the levels of elongating RNAP II (Ser2) in *kis* mutants were strongly reduced, whereas RNAP II phosphorylation at Ser5 was not affected. Accordingly, chromatin association of other elongation factors Spt6 and dCHD1 was significantly reduced (Srinivasan et al. 2005). The reduction of CTD Ser2 phosphorylation in *kis* mutants suggested that P-TEFb recruitment could be affected. However, polytene chromosome staining with P-TEFb subunit, Cdk9, was not affected in these flies, which suggests that KisL acts downstream of P-TEFb recruitment to stimulate elongation by RNAP II. Further investigations have revealed that association of H3K4 methyltransferases, ASH1 and TRX, with chromosomes was decreased in *kis* mutants. In addition, H3K27me3 methylation, a modification required for Pc function, was significantly increased both in *kis* as well as *ash1* and *trx* mutants (Srinivasan et al. 2008). These results suggest that KisL counteracts Pc repression by facilitating recruitment of

ASH1 and TRX to chromatin. In agreement with this, the human homolog of KisL, CHD8, has been found to be associated with subunits of MLL, a histone H3K4 methyltransferase Ash2L containing complex. CHD8 was implicated in ASH2 recruitment to the promoter of the *HOXA2* gene, however the role of CHD8 in early transcription elongation at this gene is not clear as depletion of CHD8 was shown to enhance *HOXA2* expression under activating conditions (Yates et al. 2010). Another study on CHD8 has revealed its function in early transcription elongation or activation of cyclin E2 gene in G1/S cell cycle transition. CHD8 was shown to be associated with promoter and 5' end of this gene during the entire cell cycle and to interact with elongating forms of RNAP II. It is noteworthy that CHD8 depleted cells displayed sensitivity to transcription elongation inhibitors, like DRB and flavopiridol. Thus, it has been suggested that CHD8 might act in the same process that is affected by these drugs (Rodríguez-Paredes et al. 2009). More studies have to be done in order to elucidate the precise functions of CHD8-like remodelers in transcription elongation.

CHD1 remodeler has also been implicated in transcription elongation. Initial studies in flies showed that dCHD1 is located in active sites of transcription on polytene chromosomes (Stokes et al. 1996). Subsequent studies in yeast revealed that yChd1 interacts with Spt4-Spt5 and Spt16-Pob3 (FACT) and PAF complexes involved in transcription elongation (Krogan et al. 2002; Simic et al. 2003; Warner et al. 2007). Chromatin immunoprecipitation experiments revealed yChd1 association with transcribed regions but not promoters of active genes. Moreover, this association was decreased in Rtf1 mutants (a subunit of the PAF complex), which suggests a mode of recruitment of yChd1 to active genes (Simic et al. 2003). Several studies suggested that yChd1 might be involved in establishment and maintenance of chromatin structure over transcribed regions. First, in *chd1* mutants, processivity or elongation of RNAP II were not affected. Secondly, the same mutants displayed internal transcription initiation from a reporter gene and weak cryptic initiation defect from an endogenous gene. The cryptic transcription initiation was much stronger in *chd1* and *isw1* double mutants, as these two remodelers may act redundantly (Cheung et al. 2008; Quan and Hartzog 2010). Third, *chd1* mutant strains displayed alterations in the chromatin structure and nucleosome spacing in the coding and termination regions of the *ADH2* gene (Xella et al. 2006). Finally, yeast extracts made from *chd1* mutant strains failed to assemble chromatin *in vitro* (Robinson and Schultz 2003). In addition to this, dCHD1 was shown to assemble and generate regularly spaced

nucleosomes *in vitro* and deposit histone variant H3.3 into chromatin *in vivo* (Lusser et al. 2005). Altogether, these experiments suggest a role of CHD1 in reassembly of nucleosomes in the wake of elongating RNAP II and in re-establishing of a repressive chromatin structure. However, given that in *chd1* mutant strains expression of only a small fraction of genes is affected, and given that *chd1* deletion has only a minor effect on cryptic initiation (Tran et al. 2000; Cheung et al. 2008), the role of CHD1 in chromatin assembly might be gene specific or it might be redundant with other chromatin remodelers and histone chaperones. Thus, the function of CHD1 in transcription dependent chromatin assembly demands further investigation.

2.5.4.4 Transcription termination

The last step of the transcription cycle is transcription termination, which involves release of the RNA transcript and the dissociation of the transcription complex from the DNA template (reviewed in (Buratowski 2005)). A genetic screen designed to isolate factors involved in transcription termination by RNAP II in *S. pombe*, identified Hrp1, a homolog of yChd1 (Alén et al. 2002). Both *hrp1* and *chd1* deletion strains have been shown to fail to terminate transcription of several genes in run on assays, giving high levels of transcription reading through the 3' gene end. Analysis of chromatin structure of these genes revealed alterations in their termination region, which spanned around 800 bp region extending beyond the 3' end of the gene (Alén et al. 2002). These changes were detected in both induced and uninduced gene states which suggests a role of yChd1 in establishment of chromatin structure in the termination regions of yeast ORFs. The function of yChd1 in some gene termination might be redundant with other remodelers, like Isw1 and Isw2. It has been suggested that chromatin structure at 3' end of the gene may enhance RNAP II pausing in order to allow to switch its mode from elongation to termination (Alén et al. 2002). Furthermore, yChd1 together with Isw1/2 was also shown to be important for transcription termination of RNA Pol I at rDNA genes (Jones et al. 2007). Importantly, the steady-state levels of ribosomal RNA was not affected in these mutants, which indicates that the observed termination defects were not due to transcription elongation defects (Jones et al. 2007). These results suggest that yChd1 function in transcription termination might be more general and not restricted to RNAP II genes.

2.5.4.5 pre-mRNA splicing

A number of recent studies have revealed that transcription, co-transcriptional RNA processing and modulation of chromatin structure are tightly interlinked processes (reviewed in (Luco and Misteli 2011)). Noteworthy, CHD1 has been linked to regulation of splicing in human cells (Tai et al. 2003). In an H3K4me3 pulldown experiment designed to identify factors binding to this modification, CHD1 was copurified with elongation factors (FACT, PAF) and SF3A, a subunit of spliceosomal U2snRNP complex. Partial purification of the complex revealed that CHD1 exists in a complex with U2snRNP subunits but not U1snRNP components. Moreover, this association is functionally significant, as depletion of CHD1 decreased splicing rate *in vitro* and *in vivo* and led to the impaired SF3A recruitment to the transcribed genes. Collectively, these results suggest, that CHD1 regulates pre-mRNA splicing by recruiting components of the splicing machinery to the transcribed RNA via recognition of the H3K4me3 mark (Fig. 2.9) (Sims et al. 2007). Currently it is not known whether the ATPase activity of CHD1 is involved in splicing regulation.

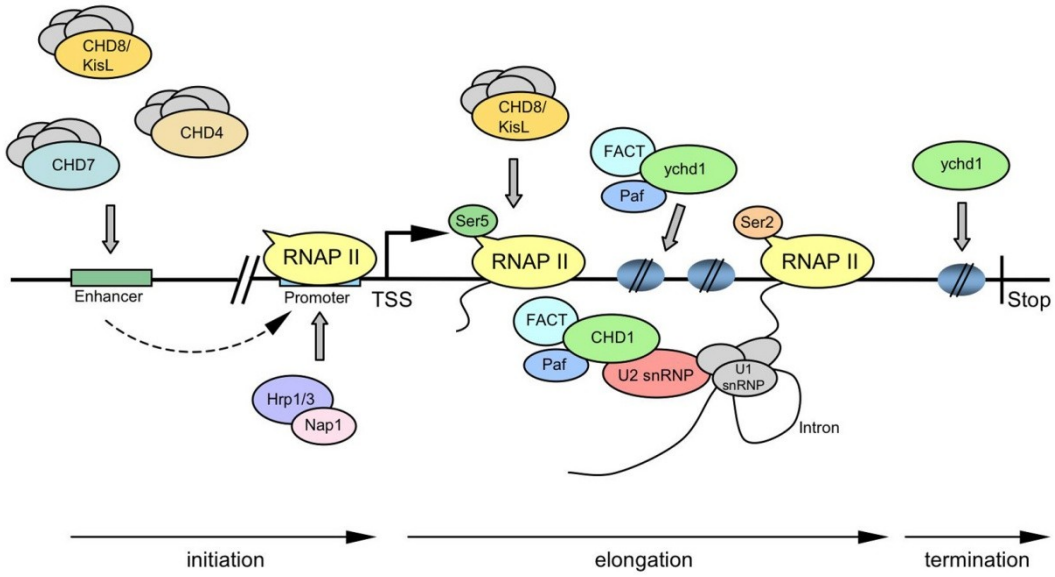

Fig. 2.9 CHD remodelers at various steps of transcription cycle
Involvement of CHD remodelers at different stages of active transcription (initiation, elongation, termination). Grey ovals represent additional subunits of CHD complexes or spliceosome subunits. TSS, transcription start site; Stop; transcription stop signal (see text for details).

2.5.5 CHD chromatin remodeler roles outside of transcription

In addition to their role in transcription regulation, recent studies have revealed that CHD chromatin remodelers are also involved in other cellular processes, such as histone variant deposition, DNA repair and global chromatin maintenance.

2.5.5.1 Histone variant deposition

Histone proteins exist in different variants providing specialized functions in addition to their fundamental role in DNA packaging, such as DNA repair, sperm chromatin regulation and the definition of centromer identity (reviewed in (Talbert and Henikoff 2010)). The metazoan histone H3.3 has been mostly associated with active transcription and it has been suggested that H3.3 variant deposition and nucleosome assembly during transcription elongation might be accomplished by CHD1 (chapter 2.5.4.3). However, recently H3.3 deposition has been shown to also occur outside of transcription, during early *Drosophila* development. Upon fertilization and sperm nuclear envelop breakdown, the compacted sperm chromatin is decondensed leading to replacement of sperm protamines with maternal histones in early *Drosophila* embryogenesis. During sperm decondensation, histone variant H3.3 is deposited in the paternal pronucleus in a replication independent manner (Loppin et al. 2005). In this respect, dCHD1 has been shown to be involved in histone variant H3.3 deposition in the paternal pronucleus at early stages of *Drosophila* embryo development (Konev et al. 2007). In dCHD1 mutant embryos H3.3 histone variant deposition was heavily impaired, leading eventually to the loss of paternal DNA and embryo haploidy. In addition, a fraction of dCHD1 was associated with a histone H3.3 chaperone HIRA, which suggests that they might cooperate in H3.3 deposition (Konev et al. 2007).

Another function of CHD remodelers associated with histone variant deposition is linked to centromere identity. Despite differences in the structure, centromeres contain a highly conserved histone H3 variant, called CENP-A (also known as CID, Cnp1, Cse4). In *S. pombe hpr1* mutant strains display silencing defects of the centromeric region, increased H4 acetylation levels at centromeres and defects in chromosome segregation. Moreover, Hpr1 is enriched at centromeric chromatin regions in early S-phase, when centromers are replicated. Thus, Hpr1 plays a role in Cnp1 deposition in fission yeast (Walfridsson et al. 2007).

Similarly, CHD1 has been suggested to be involved in centromere function in mammalian cell lines. CHD1 has been shown to associate with centromeres throughout the cell cycle and this association seems to depend on FACT complex. Furthermore, CHD1 knockdown resulted in significant decrease of CENP-A binding to centromers, which suggests that CHD1 can be involved in centromeric histone variant deposition also in higher eukaryotes (Okada et al. 2009). However, this function of CHD1 is not necessarily conserved, as in *Drosophila* this remodeler is not required for CENP-A deposition (Podhraski et al. 2010).

2.5.5.2 DNA repair

Despite a well established role of INO80 complexes in DNA break repair in yeast (chapter 2.2.4), much less is known about ATP-dependent chromatin remodeling at damaged sites in the human genome. CHD4 has been previously shown to interact with ATR kinase and it was found to be a target of the ATM/ATR pathway in a proteomic screen, which suggested its possible role in DNA repair (Schmidt and Schreiber 1999; Matsuoka et al. 2007). Notably, several recent studies have revealed a link between DNA repair and CHD4 remodeler in human cells (Chou et al. 2010; Larsen et al. 2010; Polo et al. 2010; Smeenk et al. 2010). CHD4 and some other NuRD subunits have been shown to be recruited to laser induced DNA-damage sites in a PARP dependent manner (chapter 2.4.5). The role of CHD4 phosporylation by ATM is not clear at the moment but it does not seem to be important for the recruitment step. The function of CHD4 remodeler at sites of DNA-damage has also been investigated. Despite some differences in the results of these studies, they clearly show that CHD4 depleted cells are hypersensitive to ionizing radiation, deficient in DSB repair and they display prolonged persistence of the phosphorylated form of H2AX histone variant (γH2AX) (Larsen et al. 2010; Smeenk et al. 2010). Moreover, CHD4 knockdown results in cell cycle delays and activation of apoptosis via the p53/p21 pathway. It has been suggested, that CHD4 might play a role in regulating p53 deacetylation status and thus controlling G1/S cell cycle transition (Polo et al. 2010). The association of NuRD complex with p53 deacetylation has been proposed previously (Luo et al. 2000).

The effect of CHD4 on chromatin at DNA breaks is far less understood. The lack of nascent transcripts and elongating RNAP II at sites of DSB has suggested that NuRD complex could be involved in inhibition of transcription at sites of DNA breaks (Chou et al. 2010). However, currently there is no direct evidence for this. Interestingly, two studies

have shown decreased accumulation of ubiquitination at the DSB sites in CHD4 depleted cells. Histone ubiquitination by ubiquitin ligases, RNF8 and RNF168, is an important step in recruitment of downstream repair and check point factors, such as BRCA1, 53BP1 and RAD18 (reviewed in (van Attikum and Gasser 2005)). Notably, CHD4 knockdown leads to a significant decrease in RNF168 and BRCA1 accumulation at the DSB sites (Larsen et al. 2010; Smeenk et al. 2010). Thus, chromatin remodeling by CHD4 might help ubiquitin ligases to get substrate access at DNA-damage sites. Altogether, these results indicate complex and probably mutually dependent roles of CHD4 in DNA damage response and cell cycle progression. Further studies are needed to elucidate the function of CHD4 in DNA repair.

2.5.5.3 Global chromatin maintenance

Several recent studies have suggested a role of CHD remodelers in global chromatin regulation. It has been proposed that the local events at the DSB sites cannot account for the complex defects in chromatin and cell cycle observed in CHD4 depleted cells (Larsen et al. 2010). Consequently, a more widespread role of CHD4 in chromatin maintenance has been suggested. Several observations support this idea. First, CHD4 depleted cells display increased levels of spontaneous DNA breaks (Larsen et al. 2010). Second, ATM/ATR signalling in these cells is elevated, leading to increased levels of γH2AX, which indicates permanent DNA breaks (Larsen et al. 2010). Finally, the loss of NuRD subunits has been recently linked to increased DNA damage and a decrease of heterochromatin marks, like H3K9me3 and HP1, in a premature aging disorder and physiological aging (Pegoraro et al. 2009). These results, argue that CHD4 might contribute to genome maintenance by protecting heterochromatic regions from susceptibility to DNA damage.

Another study has suggested that CHD1 might also have a broader role in chromatin maintenance at least in mouse embryonic stem cells (ES). One hallmark of ES cells is a more open chromatin status, which is believed to be important for keeping the pluripotent state of these cells. It has been demonstrated that CHD1 knockdown increases the number of heterochromatic foci, monitored by the elevated levels of H3K9me3 and HP1 (Gaspar-Maia et al. 2009). Moreover, CHD1 is associated with euchromatin in ES cells and it is required for pluripotency of these cells (Gaspar-Maia et al. 2009). The authors have argued that CHD1 may act to counter heterochromatin spreading in pluripotent cells. To this end, CHD1 could mediate incorporation of the H3.3 variant, which is specifically enriched

within actively transcribed genes and is less prone to H3K9 methylation (Ahmad and Henikoff 2002; Schwartz and Ahmad 2005). Whether CHD1 maintains the euchromatin state of ES cells by this mode remains to be determined.

2.6 *Drosophila melanogaster* as a model organism to study the role of chromatin remodeling in transcription

Drosophila melanogaster constitutes a well established model organism that provides many unique tools to study chromatin regulation and transcription. In the following chapter, two major systems, polytene chromosome and heat shock genes, will be presented as they are utilized extensively in many experiments of this doctoral thesis

2.6.1 Polytene chromosomes

Drosophila 3rd instar larvae offer an unusual possibility to study the *in vivo* distribution of chromatin associated proteins by indirect immunofluorescence (Schwartz et al. 2004). During development of 3rd instar larvae the genome of salivary gland cells undergoes repeated rounds of endoreplication. As a result, polytene chromosomes that consist of one thousand synapsed sister chromatids are produced. The centromeric regions remain underreplicated, bundle together and form the so called chromocentre. Staining of polytene chromosomes with DNA-binding dyes allows the visualisation of heterochromatin and euchromatin. Heterochromatin is concentrated at the chromocentre, the telomeres and covers most of the fourth chromosome. In addition, densely stained (heterochromatic) bands are clearly visible along the chromosome arms. Heterochromatic bands are divided by weakly stained (euchromatic) interbands which contain actively transcribed genes (Murawska M. and Brehm A., Methods Mol Biol, submitted). Indirect immunofluorescence staining of polytene chromosomes with factor specific antibodies may therefore deliver important information about its chromatin localization. Since the 1960s, imaging of polytene chromosomes has provided a plethora of data for gene and chromatin regulation *in vivo* (Lis 2007). For instance, using specific antibodies it has been shown that HP1 binds to heterochromatin in the chromocentre (James and Elgin 1986). By contrast, RNAP II staining gives many bands in euchromatic regions, consistent with ongoing transcription (Jamrich et al. 1977). Colocalization with RNAP II delivers an important view into possible role of a chromatin associated protein in transcription. Many

factors involved in active transcription, like elongation factors (for instance Spt5, Spt6, ELL) highly colocalize with RNAP II (Kaplan et al. 2000; Gerber et al. 2001). In addition, many proteins, like exosome or nucleoporins, previously not associated with transcription, have been revealed to be involved in gene regulation by RNAP II polytene colocalization studies (Andrulis et al. 2002; Capelson et al. 2010). Moreover, chromosomal colocalization of two factors, which interact with each other in solution, provides additional information about their functional interactions on chromatin and regulation of common target genes (Reddy et al. 2010).

In addition, polytene chromosome staining combined with pharmacological treatment with different inhibitors or RNAse A may shed light onto chromatin recruitment mechanism or the binding mechanism of a given factor. In this regard, it has been shown that a fraction of HP1 is binding to euchromatic regions in an RNA dependent manner (Piacentini et al. 2003).

Finally, ectopic expression of tagged variants of proteins allows to combine structural and functional analysis, for example by mapping factor domains important for chromatin binding (Bao et al. 2008; Morettini et al. 2011).

2.6.2 Inducible heat shock genes

Heat shock genes comprise a well established system to investigate gene activation and the accompanying chromatin alterations. Upon environmental stimuli, such as elevated temperature, heat shock genes are rapidly activated which results in chromatin decondensation and formation of so-called transcriptional puffs. These puffs provide a cytological landmark of actively transcribed genes. The most prominent heat shock loci, 87A and 87C, constitute a cluster of two and four *hsp70* genes, respectively, easily visible on polytene chromosomes as puffs (Fig. 2.10). These genes code for protein chaperones, which assist protein folding processes preventing their denaturation and aggregation during cellular stress (reviewed in (Mayer and Bukau 2005)).

Initial polytene chromosome staining with RNAP II antibodies revealed a rapid relocalization of the enzyme to only few sites on polytene chromosomes which represent primarily heat shock loci (Jamrich et al. 1977) (Fig. 2.10). Much has been learnt about active transcription regulation based on *hsp70* genes. Briefly, before heat shock a transcription factor, called GAF (GAGA factor) and RNAP II are bound to the promoter of

hsp70. The Cdk7 subunit of TFIIH phosphorylates the CTD of RNAP II at Ser5 which leads RNAP II to initiate transcription into the first 20-40 bases of the gene, where it pauses. RNAP II is held there by the negative elongation factor (NELF) and DRB sensitivity-inducing factor (DSIF). Upon heat shock, heat shock factor (HSF) trimerises and binds to heat shock elements (HSE) in the promoter. In turn, HSF recruits additional co-activators and mediator, that lead to PTEFb kinase recruitment, which causes phosphorylation and dissociation of NELF complex, Ser2 phosphorylation at CTD and subsequent release of paused RNAP II into productive elongation (reviewed in (Lis 2007; Weake and Workman 2010)).

In addition to transcription regulation, heat shock genes provide an excellent system to investigate chromatin alterations associated with active transcription. Rapid heat shock gene induction is accompanied by a dramatic change in the chromatin structure upon gene activation. It has been recently shown that nucleosomes are rapidly removed from the *hsp70* locus in a transcription independent manner and this removal requires HSF, GAF and PARP activity. It has been suggested that poly(ADP-ribosylation) of histones might destabilize nucleosomes resulting in their removal from DNA at heat shock genes (Petesch and Lis 2008). However, much less is known about roles of ATP-dependent chromatin remodelers in regulation of heat shock gene transcription. It has been demonstrated, that ISWI containing complex, NURF, is important for heat shock gene activation. In the mutants of NURF301, the biggest subunit of the NURF complex, HSF binding to *hsp70* loci was heavily impaired. Consequently, expression of these genes was strongly reduced (Badenhorst et al. 2002). These results suggest that nucleosome remodeling by NURF might provide the access to DNA for HSF. Indeed, it has been shown that NURF cooperates with the GAF factor to mobilize nucleosomes on the promoter of the heat shock genes, establishing a nucleosome-free domain over the promoter (Tsukiyama et al. 1994). A second chromatin remodeler important for maximal expression of heat shock genes is dCHD1. It has been shown to be recruited to heat shock puffs on polytene chromosomes and depletion of dCHD1 significantly decreases heat shock gene activation. The function of dCHD1 in the context of heat shock genes it not well understood, however it has been suggested that it might be involved in the remodeling of the first positioned nucleosome downstream of the transcription start site (Morettini et al. 2011).

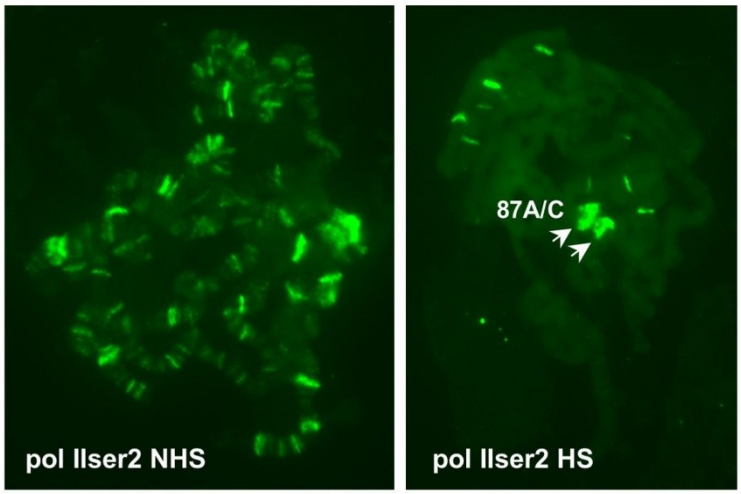

Figure 2.10 Relocalization of RNAP II on polytene chromosomes upon heat shock
Immunofluorescence staining of polytene chromosomes with RNAP II (pol IIser2) antibodies and as indicated. Polytene chromosomes were isolated from 3rd instar larvae which were heat shocked at 37°C for 20 min. Arrows indicate the *hsp70* loci 87A and 87C.

3. Material and Methods

3.1 Material

3.1.1 Material sources

All common material, chemicals, reagents and instruments used in this study, were ordered from the following companies: Abcam, Alexis Biochemicals, AppliChem, Amersham Bioscience/GE Healthcare, Beckmann, BioRad, Calbiochem, Camag, Eppendorf, Fermentas, Fisher Scientific, Fugifilm, Gibco, Gilson, Greiner, Hareus, Invitrogen, Kobe, Leica, Millipore, Merc, PAA, MWG Biotech, New England Bioloabs, PeqLab, Polysciences, Promega, Qiagen, Roche, Roth, Santa Cruz Biotechnology, Sarstedt, Sigma, Stratagene, Whatman, Zeiss. Radioactive material was ordered from Amersham Bioscience/GE Healthcare and PerkinElmer.

3.1.1.1 Enzymes

Restriction endonucleases	Fermentas, New England Biolabs, Promega
Klenow enzyme	Fermentas
T4 DNA ligase	Fermentas
Calf intestine alkaline phospatase (CIAP)	Fermentas
DNAse I (RNAse-free)	Fermentas, Peqlab
Benzonase	
RNAse A (DNAse-free)	Qiagen
Proteinase K	Roth
Trypsin	Sigma
Micrococcal nuclease (MNase)	Roche
Taq DNA polymerase	Fermentas
M-MLV Reverse Transcriptase	Invitrogen

3.1.1.2 Enzyme inhibitors

RNAsin	Promega, Fermentas
Trypsin Inhibitor (Soybean)	Sigma
PMSF (phenylmethanesulfonylfluoride)	Roth
Leupeptin	Roth
Pepstatin	Roth
Aprotinin	Roth
DRB (5,6-Dichloro-1-β-D-ribofuranosylbenzimidazole)	Sigma

PJ34 (*N*-(5,6-Dihydro-6-oxo-2-phenanthridinyl)-2-acetamide hydrochloride)	Alexis Biochemicals

3.1.1.3 Chromatographic material

Hydroxyl apatite resin	BioRad
Gelfiltration column (Superose 6)	Amersham
Chromatography system (ÄKTA, FPLC & HPLC)	Amersham
TLC PEI Cellulose F25 20x20	Merc
StrataClean Resin	Stratagene

3.1.1.4 Affinity purification material

Protein A Sepharose 4 FF	Amersham
Protein G Sepharose 4 FF	Amersham
M2 Agarose (Flag-beads)	Sigma
SulfoLink Coupling Gel	Pierce

3.1.1.5 Dialysis and filtration material

Centriprep YM-10	Millipore
Dialysis membranes	Spectra/Por
Sterile syringe filters	VWR

3.1.1.6 Consumable material

6x DNA Loading Dye	Fermentas
GeneRuler 1 kb DNA Ladder Plus	Fermentas
PageRuler Prestained Protein Ladder	Fermentas
Roti Load1	Roth
PageBlue	Fermentas
NuPAGE Novex 4-12% Bis-Tris Gels	Invitrogen
NuPAGE MES-running buffer	Invitrogen
Roti-PVDF	Roth
Whatman-3MM Paper	Whatman
Nitrocelulose	Whatman
Rotilabo-Blottingpaper	Roth
Protein Assay (Bradford solution)	Bio-Rad
Super RX (Fuji Medical X-Ray Film)	Fujifilm
Fluoromount - G	SouthernBiotech

SlowFade antifade Kit	Invitrogen
DAPI (4',6-diamidino-2-phenylindole)	Invitrogen
Normal Goat Serum	Sigma
Liquid scintillation cocktail	PerkinElmer

3.1.1.7 Kits

Table 3.1 Kits with corresponding application and company

Kit name	**Application**	**Company**
QIAquick Gel Extraction Kit	Extraction of DNA from agarose gels after restriction digestion	Qiagen
Qiagen Plasmid Midi Kit	DNA isolation for cell transfection and cloning	Qiagen
peqGOLD Cycle-Pure Kit	DNA isolation after ChIP	Peqlab
DNAzol Reagent	Genomic DNA isolation	Invitrogen
peqGOLD Total RNA Kit	RNA isolation from cell lines and larvae	Peqlab
Megascript T7 Kit	*In vitro* transcription	Ambion
ABsolute SybrGreen Mix	QPCR	Thermo Fisher
QuickChange Site-directed Mutagenesis Kit	Site directed mutagenesis	Agilent Technologies
Expand High FidelityPLUS PCR System	PCR for cloning	Roche
Bac-N-Blue Transfection Kit	SF9 cells transfection for baculovirus generation	Invitrogen
Immobilon Western HRP Chemiluminescent Substrate	Western blot detection system	Millipore

3.1.2 Standard solutions

Stock solutions and buffers were prepared according to standard protocols (Sambrook and Russel 2001). The most standard solutions are listed below.

Phosphate Buffered Saline (PBS)	140 mM NaCl 2,7 mM KCl 8,1 mM Na_2HP 1,5 mM KH_2PO_4 pH adjusted to 7,4 with HCl
TAE Buffer	40 mM Tris-Acetate 1 mM EDTA

TBE Buffer	90 mM Tris 90 mM Boric Acid 2 mM EDTA
SDS-PAGE Running buffer	192 mM Glycin 25 mM Tris 0,1% (w/v) SDS
Stacking buffer (4x)	0,5 M Tris-HCl, pH 6,8 0,4% (w/v) SDS
Resolving buffer (4x)	1,5 M Tris-HCl, pH 8,8 0,4% (w/v) SDS
5x SDS-Page loading buffer	250 mM Tris-HCl, pH 6,8 10% (w/v) SDS 50% (v/v) Glicerol 0,5% (w/v) Bromophenol blue 500 mM Dithiothreitol (DTT)

Additional buffers are described in the individual method sections.

3.1.3 Antibodies

3.1.3.1 Primary antibodies

Table 3.2 Primary antibodies with corresponding dilutions or amounts used

Antibody	Species and type	Dilution or amount	Type of experiment	Source
α-dCHD3(#5)	Rabbit, polyclonal	1:10000 1 µl	Western blot IP	Peptide Speciality Laboratories (PSL), Heidelberg
α-dCHD3(7A11)	Rat, Monoclonal	1:10 1:2	Western blot Immunofluorescence	E. Kremmer
α-dMi-2(N)	Rabbit, polyclonal	1:10000 1:200 2 µl	Western blot Immunofluorescence RIP	Kehle et al, 1998
α-dMi-2(C)	Rabbit, polyclonal	2 µl 2 µl	ChIP RIP	Kehle et al, 1998
α-Pol II(8WG16)	Mouse, monoclonal	8 µl	ChIP	Santa Cruz

α-Pol II (H5)	Mouse, monoclonal	1:50	Immunofluorescence	Covance
α-Pol II (H14)	Mouse, monoclonal	1:50	Immunofluorescence	Covance
α-Spt5	Guinea pig	1:250	Immunofluorescence	F. Winston
α-Mep1	Guinea pig	1:20 4 µl	Immunofluorescence ChIP	P. Verrijzer
α-RPD3	Rabbit, plyclonal	1:1000	Western Blot	J. Müller
α-PARP1	Rabbit, polyclonal	1:20000	Western Blot	A. Ladurner
α-PAR (10H)	Mouse, monoclonal	1:500	Western Blot	A. Ladurner
α-tubulin	Mouse, monoclonal	1:15000	Western Blot	Millipore
α-H3	Rabbit, polyclonal	1 µg	ChIP	Abcam
α-ISWI	Rabbit, polyclonal	1:200	Immunofluorescence	C. Wu
α-Brahma	Rabbit, polyclonal	1:200	Immunofluorescence	C. Wu
α-HSF	Rabbit, polyclonal	2 µl	ChIP	J. Tamkun
α-IgG	Rabbit, polyclonal	1 µg	ChIP	Cell signaling
α-Flag	Mouse, monoclonal	1:4000	Western Blot	Sigma

3.1.3.2 Secondary antibodies

Table 3.3 Secondary antibodies with corresponding dilutions

Antibody	**Species and type**	**Dilution**	**Experiment**	**Source**
α-rabbit HRP	Donkey, polyclonal	1:25000	Western blot	GE Healthcare
α-mouse HRP	Sheep, monoclonal	1:20000	Western blot	GE Healthcare
α-rat HRP	Goat, polyclonal	1:10000	Western blot	Jackson Immuno-Research
α-guinea pig HRP	Donkey, polyclonal	1:20000	Western blot	Santa Cruz
α- rabbit Alexa488	Goat, polyclonal	1:200	Immunofluorescence	Invitrogen
α-mouse Alexa546	Goat, polyclonal	1:200	Immunofluorescence	Invitrogen

α-mouse Alexa488	Goat, polyclonal	1:200	Immunofluorescence	Invitrogen
α-guinea pig Alexa546	Goat, polyclonal	1:200	Immunofluorescence	Invitrogen
α-rat Alexa546	Goat, polyclonal	1:200	Immunofluorescence	Invitrogen

3.1.4 Plasmids

Table 3.4 Plasmids used for baculovirus generation and protein expression in SF9 cells

Construct name	Description	Source
pVL1392-dCHD3FlagWT	cDNA encoding for full length dCHD3 with C-terminal Flag-tag, PCR-cloned via NotI and EcoRI with primer pairs: dCHD3_NotI_f, dCHD3_BamHI_r.	This study
pVL1392-ΔPHD-dCHD3Flag	cDNA encoding for a short dCHD3 form (81-892 aa) with C-terminal Flag-tag, PCR-cloned via NotI and EcoRI with primer pairs: dCHD3ΔPHD_NotI_f, dCHD3_EcoRI_r.	This study
pVL1393-ΔPHD/Chromo-dCHD3Flag	cDNA encoding for a short dCHD3 form (241-892 aa) with C-terminal Flag-tag, PCR-cloned via NotI and EcoRI with primer pairs: dCHD3ΔPHD/Chromo_NotI_f, dCHD3_EcoRI_r.	This study
pVL1392-ΔC-dCHD3Flag	cDNA encoding for a short dCHD3 form (1-800 aa) with C-terminal Flag-tag, PCR-cloned via NotI and EcoRI with primer pairs: dCHD3_NotI_f, dCHD3ΔC_EcoRI_r.	This study
pVL1392-dCHD3_K298RFlag	cDNA encoding for a catalytically inactive mutant of dCHD3 carrying a point mutation changing lysine 298 to arginine. This mutant was generated using a site directed mutagenesis with an appropriate primer and pBlueScriptII-SK(+)dCHD3Flag as a template, followed by subcloning with EcoRI and NotI into pVL1392 vector.	This study
pVL1392-dMi-2_K761RFlag	cDNA encoding for a catalytically inactive mutant of dMi-2 carrying a point mutation changing lysine 761 to arginine. This mutant was generated using a site directed mutagenesis with an appropriate primer and pBlueScriptII-SK(+)dM-2SacI as a template, followed by subcloning dMi-2SacI fragment into pVL1392-dMi-2FlagWT_ΔSacI vector.	This study
pVL1392-dMi-2N	cDNA encoding for a short dMi-2 form (1-691 aa) with C-terminal Flag-tag, PCR-cloned via NotI and XbaI with primer pairs: dMi-2_NotI_f, dMi-2N_XbaI_r	This study
pVL1392-dMi-2(1-485)	cDNA encoding for a short dMi-2 form (1-485 aa) with C-terminal Flag-tag, PCR-cloned via NotI and XbaI with primer pairs: dMi-2_NotI_f, dMi-2(1-485)_XbaI_r	This study

Table 3.5 Plasmids used for protein overexpression in bacteria

Construct name	Description	Source
pGEX4T1GST-hCHD1_CD1+2	cDNA encoding for hCHD1 chromodomains (250-467 aa) fused with GST, PCR-cloned via EcoRI and NotI using HeLa cell	This study

	cDNA as a template, with primer pairs: hCHD1CDs_EcoRI_f, hCHD1CDs_NotI_r.	
pGEX4T1GST-dCHD3_CD1+2	cDNA encoding for dCHD3 chromodomains (50-254 aa) fused with GST, PCR-cloned via EcoRI and NotI using pVL1392-dCHD3FlagWT as a template, with primer pairs: dCHD3CDs_EcoRI_f, dCHD3CDs_NotI_r.	This study
pGEX4t1GST-dMi-2_CD1+2	cDNA encoding for dMi-2 chromodomains (452-716 aa) fused with GST, PCR-cloned via EcoRI and NotI using pVL1392-dMi-2FlagWT as a template, with primer pairs: dMi-2CDs_EcoRI_f, dMi-2CDs_NotI_r.	This study
pGEX4t1GST-dMi-2_(2-690)	cDNA encoding for dMi-2 fragment (2-690 aa) fused with GST, PCR-cloned via SalI and NotI using pVL1392-dMi-2FlagWT as a template, with primer pairs: (2-690)_f and (2-690)_r	This study
pGEX4t1GST-dMi-2_(2-483)	cDNA encoding for dMi-2 fragment (2-483 aa) fused with GST, PCR-cloned via SalI and NotI with primer pairs: (2-690)_f and (2-483)_r	This study
pGEX4t1GST-dMi-2_(2-376)	cDNA encoding for dMi-2 fragment (2-376 aa) fused with GST, PCR-cloned via SalI and NotI with primer pairs: (2-690)_f and (2-376)_r	This study
pGEX4t1GST-dMi-2_(2-117)	cDNA encoding for dMi-2 fragment (2-117 aa) fused with GST, PCR-cloned via SalI and NotI with primer pairs: (2-690)_f and (2-117)_r	This study
pGEX4t1GST-dMi-2_(118-238)	cDNA encoding for dMi-2 fragment (118-238 aa) fused with GST, PCR-cloned via SalI and NotI with primer pairs: (118-238)_f and (118-238)_r	This study
pGEX4t1GST-dMi-2_(239-376)	cDNA encoding for dMi-2 fragment (239-376 aa) fused with GST, PCR-cloned via SalI and NotI with primer pairs: (239-376)_f and (2-376)_r	This study
pGEX4t1GST-dMi-2_(2-50)	cDNA encoding for dMi-2 fragment (2-50 aa) fused with GST, PCR-cloned via SalI and NotI with primer pairs: (2-690)_f and (2-50)_r	This study
pGEX4t1GST-dMi-2_(46-76)	cDNA encoding for dMi-2 fragment (46-76 aa) fused with GST, PCR-cloned via SalI and NotI with primer pairs: (46-76)_f and (46-76)_r	This study
pGEX4t1GST-dMi-2_(77-98)	cDNA encoding for dMi-2 fragment (77-98 aa) fused with GST, PCR-cloned via SalII and NotI with primer pairs: (77-98)_f and (77-98)_r	This study
pGEX4t1GST-dMi-2_(99-117)	cDNA encoding for dMi-2 fragment (99-117 aa) fused with GST, PCR-cloned via SalI and NotI with primer pairs: (99-117)_f and (2-117)_r	This study
pGEX4t1GST-dMi-2_(249-282)	cDNA encoding for dMi-2 fragment (249-282 aa) fused with GST, PCR-cloned via SalI and NotI with primer pairs: (249-282)_f and (249-282)_r	This study
pGEX4t1GST-dMi-2_(283-342)	cDNA encoding for dMi-2 fragment (283-342 aa) fused with GST, PCR-cloned via SalI and NotI with primer pairs: (283-342)_f and (283-342)_r	This study
pGEX4t1GST-dMi-2_(343-376)	cDNA encoding for dMi-2 fragment (343-376 aa) fused with GST, PCR-cloned via SalI and NotI with primer pairs: (343-376)_f and (2-376)_r	This study

Table 3.6 Plasmids used for generation of transgenic flies

Construct name	Description	Source
pUASTattB-dCHD3FlagWT	cDNA encoding for full length dCHD3 with C-terminal Flag-tag in pUASTattB vector, subcloned from pVL1392-dCHD3FlagWT with XbaI and NotI restriction sites.	This study
pUASTattB-dCHD3_K298RFlag	cDNA encoding for a catalytically inactive mutant of dCHD3 with C-terminal Flag-tag, subcloned from pVL1392-dCHD3_K298RFlag with XbaI and NotI restriction sites.	This study
pUASTattB-dMi-2 FlagWT	cDNA encoding for a full length dMi-2 with C-terminal Flag-tag in pUASTattB vector, subcloned from pVL1392-dMi-2FlagWT with XbaI and NotI restriction sites.	This study
pUASTattB-dMi-2_K761RFlag	cDNA encoding for a catalytically inactive mutant of dMi-2 with C-terminal Flag-tag, subcloned from pVL1392-dMi-2_K761RFlag with XbaI and NotI restriction sites.	This study
pUASTattBeGFP	eGFP cDNA with NLS in pUASTattB vector, PCR-cloned via EcoRI and XhoI using pNLS-eGFP-C1 as a template, with primer pairs: eGFP_EcoRI_f, eGFP(+NotI)_ XhoI _r.	This study
pUASTattBeGFP-dMi-2WT	cDNA encoding for a full length dMi-2 with N-terminal eGFP-tag, PCR-cloned via NotI and XbaI using pVL1392-dMi-2WTFlag as a template, with primer pairs: eGFPdMi-2WT_NotI_f, eGFPdMi2WT_XbaI_r.	This study
pUASTattBeGFP-dMi2ΔN	cDNA encoding for a short dMi-2 form (691-1982 aa) with N-terminal eGFP-tag, PCR-cloned via NotI and XbaI using pVL1392-dMi-2WTFlag as a template, with primer pairs: eGFPdMi-2ΔN_NotI_f, eGFPdMi2WT_XbaI_r.	This study
pUASTattBeGFP-dMi2ΔCD	cDNA encoding for a short dMi-2 form (Δ485-690 aa) with N-terminal eGFP-tag and C-terminal Flag-tag, subcloned from pVL1392-dMi-2ΔCD with NotI and XbaI restriction sites.	This study

Table 3.7 Plasmids described previously

Construct name	Description	Source
pFLCI-dCHD3cDNA	cDNA encoding for dCHD3. The pFLC-I vector is a derivative of the ampicillin-resistant plasmid pBlueScriptII-SK(+). cDNA sequences were inserted into the vector with the XhoI the BamHI sites. A premature stop codon was repaired by PCR with primer pairs: dCHD3_BamHI_f, dCHD3_BamHIr_r.	BDGP (Berkeley Drosohila Genome Project), clone no. RE55932
pUASTattB	An integration vector for Gal4/UAS mediated expressing of transgenes. Contains an attachment *attB* site which is recognized by the φC31 integrase, which integrates the construct into the *attP* site in a transgenic fly genome. It is a pUAST plasmid derivate which carries a *lacZ* reporter and a *white*$^{+}$ marker gene and ampicillin resistance.	H. Jäckle, Generated by Basler lab (Bischof et al. 2007)
pNLS-eGFP-C1	A pEGFP-C1 (Clontech) derivate which encodes a red-shifted variant of wild-type GFP which has been optimized for brighter fluorescence and higher expression in mammalian cells. It contains N-terminal Nuclear Localization Signal (NLS) and kanamycin resistance.	H. Leonhardt
pVL1392	A baculovirus transfer vector. Contains recombination	Invitrogen

	sequences which are homologous to sequences in the baculovirus genome, AcMNPV polyhedrin enhancer-promoter sequences to drive high protein expression and ampicillin resistance.	
pVL1392-dMi-2FlagWT	cDNA encoding for full length dM-2 with C-terminal Flag-tag, used as a template for PCR for generation of following constructs: pUASTattB-dMi-2FlagWT, pUASTattBeGFP-dMi-2WT, pUASTattBeGFP-dMi2ΔN.	(Bouazoune et al. 2002)
pVL1392-dMi-2ΔCDFlag	cDNA encoding for a short dMi-2 form (Δ485-690 aa) with C-terminal Flag-tag, used as a template for PCR for generation of a following construct: pUASTattBeGFP-dMi2ΔCD.	(Bouazoune et al. 2002)
pUC12x601	A vector containing 12 nucleosome positioning sequences (601). Used for assembly of mononucleosomes for a nucleosome sliding assay.	G. Längst

3.1.5 Oligonucleotides

All oligonucleotides were purchased from Eurofins MWG Operon and diluted to a final solution of 100 µM with MilliQ-water.

3.1.5.1 Primers for cloning

Table 3.8 Primers used for cloning of constructs listed in chapter 3.1.4

Oligoname	**Sequence (from 5' to 3')**
dCHD3_BamHI_f	CGGGATCCTGAGCAAGTACCGCATCG
dCHD3_BamHI_r	CGGGATCCTCACATTAATACTATACTGC
dCHD3_NotI_f	AAAGCGGCCGCTTATGTCGTCTAAGAGAG
dCHD3_EcoRI_r	CCGGAATTCCTACTTGTCATCGTCGTCCTTGTAGTCCATTAATACTATACTG
dCHD3ΔPHD_NotI_f	AAAGCGGCCGCTTATGCCCTTGCCCGGAAAAG
dCHD3ΔPHD/Chromo_NotI_f	AAAGCGGCCGCTTATGGATAGACCTGCACCCAC
dCHD3ΔC_EcoRI_r	CCGGAATTCCTACTTGTCATCGTCCTTGTAGTCCTTAAAGGACGAAAG
dMi-2_NotI_f	AAAGCGGCCGCATGGCATCGGAGGAAGAG
dMi-2N_XbaI_r	CCGTCTAGACTACTTGTCATCGTCGTCCTTGTAGTCGCAGCTGCAACGAGGACAG
dMi-2(1-485)_XbaI_r	CCGTCTAGACTACTTGTCATCGTCGTCCTTGTAGTCGACCTTGAGCTTGGACTTG
eGFP_EcoRI_f	AGCGAATTCATGGCACCAAAGAAGAAG3´
eGFP(+NotI)_ XhoI_ r	ATTCTCGAGCTAGCGGCCGCTGAGTCCGGACTTGTACAG
eGFPdMi2WT_NotI_f	ATAGCGGCCGCGCATCGGAGGAAGAGAATG
eGFPdMi2WT_XbaI_r	AGGTCTAGACTAGACGCCGGAATTATTCG
eGFPdMi-2ΔN_NotI_f	ATAGCGGCCGCGAGGACGACGAGGATCG
dCHD3CDs_EcoRI_f	TGAGAATTCGATTCCTGCCCTTCCGTTTAC
dCHD3CDs_NotI_r	ATAGCGGCCGCCTAGTACTTCTTATTCAGGTC

dMi-2CDs_EcoRI_f	TGTGAATTCGACTCATGTCCCTCCGCCTATC
dMi-2CDs_NotI_r	ATAGCGGCCGCCTAATACTTCTTCTTCAGATC
hCHD1CDs_EcoRI_f	CGGGAATTCGATTCTGATGACCTACTGG
hCHD1CDs_NotI_r	ATAGCGGCCGCCTACTTCAGGGCTACAAACC
(2-690)_f	ATAGTCGACTTGCATCGGAGGAAGAGAATG
(2-690)_r	ATAGCGGCCGCCTAGACCTTGAGCTTGGACTTGC
(2-483)_r	ATAGCGGCCGCCTAGCAGCTGCAACGAGGACAG
(2-376)_r	ATAGCGGCCGCCTAGTGCTCATGCTCGCCATC
(2-117)_f	ATAGCGGCCGCCTATGCCGACTCCTTCTCCTTG
(118-238)_f	ATAGTCGACTTTCATCCGGAATGCCATCTG
(118-238)_r	ATAGCGGCCGCCTAGACGGCCTCCTCGTAAATG
(239-376)_f	ATAGCGGCCGCCTAGACGGCCTCCTCGTAAATG

3.1.5.2 Primers for QPCR for transcript expression analysis

Table 3.9 Primers for gene expression analysis

Oligoname	**Sequence (from 5' to 3')**	**References**
rp49_f	CGGATCGATATGCTAAGCTG	(Beisel et al. 2007)
rp49_r	GAACGCAGGCGACCGTTGGGG	
actin5C_f	AAGTTGCTGCTCTGGTTGTCG	(Marcillac et al. 2005)
actin5C_r	GCCACACGCAGCTCATTGTAG	
GAPDH_f	GAGCAAGGACTAAACTAGCCAAA	(Kunert et al. 2009)
GAPDH_r	CAACAGTGATTCCCGACCA	
hsp70_f	ATATCTGGGCGAGAGCATCACA	(Boehm et al. 2003)
hsp70_r	GTAGCCTGGCGCTGGGAGTC	
hsp70total_f	TTGGGCGGCGAGGACTTTG	(Kopytova et al. 2010)
hsp70total_r	GCTGTTCTGAGGCGTCGTAGG	
hsp70-3end_f	GTTGGCATCCCTATTAAACAGC	
hsp70-3end_r	CAGGACTCACTTAGCGGGG	
hsp26_f	CACCGTCAGTATTCCCAAGC	This study
hsp26_r	GTTCTCCTTGCCCTTCACC	This study
hsp26-3end_f	TACCCGCTGGAGCTTTTCTA	This study
hsp26-3end_r	TCTCTACTCTTTCCTTTTTCTGTCA	This study
hsp83_f	TCTGTGAATAGAACGAAAAATACA	This study
hsp83_r	TGATGATCAGGGACATCAGC	This study
hsp83total_f	GGGTTTCTACTCCGCCTACC	This study
hsp83total_r	CACGTACTGCTCGTCATCGT	This study
hsp83-3end_f	GATGACCCGATCGATGATAAA	This study
hsp83-3end_r	CCCCCAATAAATACTCGCTCA	This study
hsp83-intr_f	TCCTTAGTGTTGAACCCACAGA	This study
hsp83-intr_r	TCTCTGCTTCTTCTGGCATC	This study

Random hexamer primers were purchased from Invitrogen, and oligo-dT primers were purchased from Eurofins MWG/Operon

3.1.5.3 Primers for QPCR for ChIP analysis

Table 3.10 Primers for ChIP analysis
Numbers in primer names indicate the position where the amplicons were centred.

Oligoname	Sequence (from 5' to 3')	References or source
hsp70-350_f	TGGGTGTCTACCAACATGGCAA	(Petesch and Lis 2008)
hsp70-350_r	ATGAGGCGTTCCGAATCTGTGA	
hsp70-154_f	TGCCAGAAAGAAAACTCGAGAAA	(Boehm et al. 2003)
hsp70-154_r	GACAGAGTGAGAGAGCAATAGTACAGAGA	
hsp70+58_f	CAATTCAAACAAGCAAAGTGAACAC	
hsp70+58_r	TGATTCACTTTAACTTGCACTTTA	
hsp70+681_f	CACCACGCCGTCCTACGT	
hsp70+681_r	GGTTCATGGCCACCTGGTT	
hsp70+1427_f	CTGTGCAGGCCGCTATCC	
hsp70+1427_r	GCGCTCGATCAGCTTGGT	
hsp70+1702_f	GGGTGTGCCCCAGATAGAAG	
hsp70+1702_f	TGTCGTTCTTGATCGTGATGTTC	
hsp70+2065_f	AGGAGCTCACCCGCCACT	(Petesch and Lis 2008)
hsp70+2065_r	CTGCTGGCCGCAGTTTGCT	
hsp70+2549_f	GTTGGCATCCCTATTAAACAGC	(Kopytova et al. 2010)
hsp70+2549_r	CAGGACTCACTTAGCGGGG	
intergenic_f	TGCTGACTGCCATCAAATTC	Karin Meier
intergenic_r	TACTGCTGTGACGGCTTTG	

3.1.5.4 Primers for site-directed mutagenesis

Table 3.11 Primers used for site-directed mutagenesis
The mutated DNA base is highlighted in bold. Numbers in the primer name indicate the mutated amino acid position.

Oligoname	Sequence (from 5' to 3')
dCHD3_K298R_f	GATGGGTCTGGGCA**G**GACCATTCAGACCG
dCHD3_K298R_r	CGGTCTGAATGGTC**C**TGCCCAGACCCATC
dMi2_K761R_f	GATGGGTCTGGGTA**G**GACCATTCAGACGG
dMi2_K761R_r	CCGTCTGAATGGTC**C**TACCCAGACCCATC

3.1.5.5 Primers for dsRNA and ssRNA generation by *in vitro* transcription

Table 3.12 Primers for *in vitro* transcription
Sequence in lowercase letters indicates T7 promoter.

Oligoname	Sequence (from 5' to 3')	Source
T7-dCHD3_f (a)	taatacgactcactatagggGATTTACGTCAGAAGGCCATTGAC	This study
T7-dCHD3_r (a)	taatacgactcactatagggAGCGACCTTAAAGGACGAAAGAC	
T7-dCHD3_f (b)	taatacgactcactatagggAGTTGTCTTATAACGATAGCAG	
T7-dCHD3_r (b)	taatacgactcactatagggGTTTTCGCGCATGGTTTTG	
T7-dMi-2_f(a)	taatacgactcactatagggACCCATTCGCAATGCCAG	GenomeRNAi
T7-dMi-2_r(a)	taatacgactcactatagggCGGAGGGCGAAGATGG	(HFA11222)

T7-dMi-2_f(b)	taatacgactcactatagggTTAACTCGCTGACCAAGGCT	G. Suske
T7-dMi-2_r(b)	taatacgactcactatagggATATCGTTGTGGGGATTCCA	
T7-Luc_f	taatacgactcactatagggGGAAGAACGCCAAAAAC	G. Suske
T7-Luc_r	taatacgactcactatagggCTCTGGCACAAAATCG	
T7-EGFP_f	taatacgactcactatagggGAGCTGGACGGCGACGTAA	G. Suske
T7-EGFP_r	taatacgactcactatagggACTTGTACAGCTCGTCCATG	
T7-hsp70_f	taatacgactcactatagggCCTACGGACTGGACAAGAAC	This study
hsp70_r	AGGGTTGGAGCGCAGATCCTTCTTGTAC	

3.1.6 Baculoviruses

Table 3.13 Baculoviruses used for protein expression in SF9 cells

Name	Expressed protein	Source
dCHD3WT	Full length Flag-tagged dCHD3	This study
dCHD3ΔPHD	Flag-tagged dCHD3 (81-892 aa)	This study
dCHD3ΔPHD/ Chromo	Flag-tagged dCHD3 (241-892 aa)	This study
dCHD3ΔC	Flag-tagged dCHD3 (1-800 aa)	This study
dCHD3K298R	Flag-tagged catalytically inactive mutant of dCHD3	This study
dMi-2K761R	Flag-tagged catalytically inactive mutant of dMi-2	This study
dMi-2WT	Full length Flag-tagged dMi-2	(Bouazoune et al. 2002)
dMi-2ΔCD	Flag-tagged dMi-2 (Δ485-690 aa)	
dMi-2ΔN	Flag-tagged dMi-2 (691-1982 aa)	
dMi-2ΔC	Flag-tagged dMi-2 (1-1271 aa)	
dMi-2-CD+ATPase	Flag-tagged dMi-2 (484-1271 aa)	
dMi-2-ATPase	Flag-tagged dMi-2 (691-1271 aa)	
dMi-2N	Flag-tagged dMi-2 (1-691 aa)	This study
dMi-2(1-485)	Flag-tagged dMi-2 (1-485 aa)	This study

3.1.7 Bacteria strains and culture media

Chemical competent *E. coli* strain XL1-Blue was used for plasmid DNA amplification and cloning. *E. coli* strain BL21 was used for GST-fusion protein expression.

XL1-Blue *supE*44 *hsdR*17 *recA*1 *endA*1 *gyrA*46 *thi relA*1 *lac*$^-$ F' [*proAB*$^+$ *lacI*^{q} *lacZ* ΔM15 Tn*10* (*tet*^{r})]

BL21 *hsdS gal* (λcI*ts*857 *ind1 Sam7 nin5* lacUV5-T7 gene 1)

LB-Medium (Luria-Bertani-Medium)	1% (w/v) Tryptone 0,5% (w/v) Yeast extract 171 mM NaCl
LB-Agarplates	1,5% (w/v) Agar LB-Medium 100 µg/ml Ampicillin or 30 µg/ml Kanamycin

3.1.8 Cell lines and tissue culture media

3.1.8.1 Insect cell lines

Kc_{167} - *Drosophila melanogaster* embryonic cell line isolated from 6-12 hr old *Drosophila* embryos (Echalier and Ohanessian 1970).

SL2 - *Drosophila melanogaster* cell line derived from a primary culture of late stage (20-24 hours old) embryos (Schneider 1972).

SL2-dRPD3Flag - SL2 cells stably transfected with a plasmid constitutively expressing Flag-tagged full length dRPD3 (Czermin et al. 2001).

SF9 - a clonal isolate, derived from *Spodoptera frugiperda* (Fall Armyworm), used for transient or stable expression of recombinant proteins in Baculovirus system (Vaughn et al. 1977).

3.1.8.2 Tissue culture media

Schneider's Drosophila Medium: medium (with L-Glutamine) for *Drosophila* cell culture, supplemented with 10% Fetal Bovine Serum and 1% Penicilin/Streptomycin.

Sf-900 II SFM: medium for SF9 cells, supplemented with 10% Fetal Bovine Serum and 0,1% Gentamycin.

Cell culture material	**Company**
Schneider's Drosophila Medium	Gibco
Sf-900 II SFM	Gibco
Fetal Bovine Serum (FBS)	HyClone
Penicilin/ Streptomycin (10 mg/ml)	PAA
Gentamycin (10 mg/ml)	PAA

3.1.9 Fly strains

All fly stocks were maintained at room temperature and all crosses were kept at 26°C in a fly incubator. Fly stocks were sustained on standard food as described in (Kunert and Brehm 2008).

Table 3.14 Fly strains used in this study

Name	Description and Genotype	Source
OrR	Oregon R wild-type fly strain	P. Becker
w[1118] isogenic	w[1118] isogenic fly strain, isogenized chromosomes 1,2,3	Bloomington (BL#5905)
J5	attP-zh86Fb/vas-phi-zh102D, microingection fly strain, integration site at 3rd chromosome	K. Basler
daughterless-Gal4	P{da-Gal4}, expresses Gal4 in *da* pattern	R. Renkawitz-Pohl
sgs-58AB-Gal4	Gal4 driver strain, salivary gland specific	R. Renkawitz-Pohl
14.2-Gal4	Strong Gal4 driver, salivary gland specific	H. Saumweber
eyeless-Gal4	P{eye-Gal4}, expresses Gal4 in *eye* pattern	R. Renkawitz
GMR-Gal4	P{GMR-Gal4}, expresses Gal4 in *GMR* pattern	R. Renkawitz
dMi-2 RNAi strain	Transgenic line carrying UAS –RNAi construct against dMi-2, inserted at 2nd chromosome	VDRC library, ID #107204
dCHD3 RNAi strain	Transgenic line carrying UAS –RNAi construct against dCHD3, inserted at 2nd chromosome	VDRC library, ID # 102689
dMi-2WT	Transgenic line carrying UAS dMi-2FlagWT, inserted at 3rd chromosome	This study
dMi-2K761R	Transgenic line carrying UAS dMi-2FlagK761R, inserted at 3rd chromosome	This study
dCHD3WT	Transgenic line carrying UAS dCHD3FlagWT, inserted at 3rd chromosome	This study
dCHD3K298R	Transgenic line carrying UAS dCHD3FlagK298R, inserted at 3rd chromosome	This study
eGFP	Transgenic line carrying UAS eGFP, inserted at 3rd chromosome	This study
eGFPMi2WT	Transgenic line carrying UAS eGFPMi2WT inserted at 3rd chromosome	This study
eGFPMi-2ΔN	Transgenic line carrying UAS eGFPMi-2ΔN, inserted at 3rd chromosome	This study
eGFPdMi-2ΔCD	Transgenic line carrying UAS eGFPdMi-2ΔCD, inserted at 3rd chromosome	This study

3.2 Methods

3.2.1 Analysis of DNA

3.2.1.1 Basic molecular biology methods

Standard procedures in molecular biology, including preparation of chemically-competent bacteria, transformation of chemically-competent bacteria with plasmid DNA, amplification of plasmid DNA in bacteria, DNA purification from bacteria, determination of DNA concentration, restriction enzyme digestion, ligation of DNA fragments, analysis of DNA on agarose gels and amplification of DNA by polymerase chain reaction (PCR), were performed according to standard protocols (Sambrook and Russel 2001).

Site-directed mutagenesis was done using QuickChange Site-directed Mutagenesis Kit (Agilent Technologies) according to the manufacturer's instructions. Primers used for mutagenesis were designed with PrimerX tool and are listed in Table 3.11.

Plasmid DNA was routinely prepared with plasmid purification kits (Qiagen). Isolation of DNA fragments from agarose gels was done with Qiagen Gel Extraction Kit according to the manufacturer's instructions.

3.2.1.2 Genomic DNA isolation from flies

Fly genomic DNA was isolated from 50 g of wild type flies with DNAzol Reagent (Invitrogen) following the manufacturer's instructions. For checking the transgene presence in generated transgenic flies, single fly was homogenized in 50 µl of Squishing buffer with a pipette tip followed by 30 min Proteinase K (0,2 mg/ml) digestion at 37°C. The enzyme was stopped by 10 min incubation at 85°C. Solution was spun down at 13000 rpm (Haraeus Biofuge Pico) at RT, supernatant was transferred to a fresh tube. Genomic DNA was stored at -20°C.

Squishing buffer	10 mM Tris-HCl, pH 8,0
	25 mM NaCl
	1 mM EDTA

3.2.2 Analysis of RNA

3.2.2.1 RNA isolation from cells and larvae

RNA was isolated using the peqGOLD Total RNA Kit, according to the manufacturer's instructions. RNA was isolated from approximately $1x10^7$ Kc cells. For RNA isolation from *Drosophila* larvae, 10-20 third instar larvae were collected, heat shock treated (as described in chapter 3.2.9.1) or directly frozen down in liquid nitrogen and then pestled in cell lysis buffer (TRK) provided by the manufacturer. A DNAse I digestion step on the RNA binding column was included as suggested by the manual. RNA was eluted with 50 µl of nuclease free water, and RNA concentrations were determined by 260 nm absorption measurements using NanoDrop spectrophotometer. RNA was aliquoted and stored at -20°C for several months.

3.2.2.2 Reverse transcription for cDNA synthesis

For the analysis of gene expression levels, RNA was transcribed to cDNA (complementary DNA) using either unspecific oligo-dT primers or random primers, and recombinant Moloney Murine Leukemia Virus Reverse Transcriptase (MMLV-RT). cDNA synthesis was performed with M-MLV Reverse Transcriptase Kit (Invitrogen) with 1 µg of isolated total RNA according to the manufacturer's instructions. 1 µl of 50 µM oligo-dT or 0,5 µl of 0,3 µg/µl random primers (Invitrogen) were used for 20 µl cDNA reaction. For QPCR analysis cDNA was diluted 1:20 or 1:50 when oligo-dT or random primers were used, respectively.

3.2.2.3 Quantitative real-time PCR (QPCR)

Quantitative real-time PCR was used to analyse gene expression levels and to determine the genome binding sites in ChIP experiments (chapter 3.2.5.3).

Quantitative real-time PCR combines the DNA amplification of a common PCR reaction with the detection of a fluorescent dye after each amplification cycle, to monitor the accumulation of PCR product in "real-time". When an amplification reaction is in the log phase, the fluorescence is directly proportional to the amount of the PCR product.

For all experiments SYBR Green dye was used. It intercalates to the double stranded, but not single stranded DNA. The fluorescence is strongly increased when intercalated and therefore allows a quantification of the PCR product. When a certain amount of DNA has

been synthesized, the fluorescence is strong enough to be distinguished from the background signals. For each sample the software measures the cycle number at which the fluorescence crosses the arbitrary line, the threshold. This crossing point is the Ct (cycle threshold) value. Hence, the lowest Ct values, the highest amount of DNA starting material.

For comparison of the relative amount of cDNA in two different samples, ΔΔCt quantification method was used (Livak and Schmittgen 2001). This method involves comparing the Ct values of the samples of interest with a calibrator such as a non-treated sample or RNA from normal tissue. The Ct values of both the calibrator and the samples of interest are normalized to an appropriate endogenous reference gene with constant expression levels under different experimental conditions. All experiments were calculated with *rp49* as a reference, which is a housekeeping gene encoding a ribosomal protein.

First, a ΔCt value for both, the sample of interest and the calibrator was calculated:

$\Delta Ct_{sample} = Ct_{sample} - Ct_{rp49}$ and $\Delta Ct_{calibrator} = Ct_{calibrator} - Ct_{rp49}$

The comparison of the two samples results in a $\Delta\Delta Ct$ value:

$\Delta\Delta Ct = \Delta Ct_{sample} - \Delta Ct_{calibrator}$

As the DNA amount per amplification cycle increases exponentially, the difference in expression levels was calculated as $x = 2^{-\Delta\Delta Ct}$. For gene induction analysis, the x -value was set to 1 for the calibrator and all other samples were normalized and displayed as fold induction. All samples were measured in technical triplicates and standard deviations s were determined, resulting in a standard deviation for ΔCt value of:

$$s_{\Delta Ct} = \sqrt{s_{rp49}^{\ 2} + s_{sample}^{\ 2}}$$

and a standard deviation for the normalized fold expression of :

$$s_{norm} = \sqrt{\left(x \times \ln(2)\right)^2 \times 2 \times s_{\Delta Ct}^{\ 2}}$$

For QPCR calculations for chromatin immunoprecipitation (ChIP) see chapter 3.2.5.3.

QPCR was performed in 96 well plates using ABsolute SybrGreen Mix (Theromo Fisher), which contains the enzyme, nucleotides, buffer and the SYBR Green dye. For each QPCR reaction, 6 µl of DNA solution were used. 1 µl of 10 µM primer mix (including forward and reverse primer), 8 µl of nuclease free H_2O and 12 µl of SYBR Green master mix were combined and 19 µl were added to the DNA in each well, resulting in the reaction volume

of 25 µl. QPCR was run using Mx300P QPCR System (Agilent) and the data was collected with MxPro software.

All QPCR runs were performed using the same PCR program:

Initial denaturation and enzyme activation	95°C, 15 min	
Denaturation	95°C, 15 sec	45 cycles
Primer annealing	55°C, 30 sec	
Elongation	72°C, 30sec	
Dissociation curve	95°C, 1 min	
	55°C, 30s	
	95°C, 30s	

3.2.2.4 dsRNA and ssRNA synthesis and purification

dsRNA (double stranded DNA) for knockdown experiments was synthesized using *in vitro* transcription. For this, Megascript T7 Kit (Ambion) was applied. T7-promoter containing DNA template was amplified on appropriate plasmid templates by PCR with primers listed in Table 3.12. For each reaction, 1 µg of DNA template was used, 8 µl of NTPs mix (30 mM final concentration) and 2 µl of reaction buffer (10x) in a volume of 20 µl. The *in vitro* transcription reaction was conducted for 16 hrs at 37°C. Template DNA was then removed by incubation of the sample with 1 µl of Turbo DNAse (Ambion) for 15 min at 37°C. For RNA precipitation, 20 µl of 5M NH_4OAc and 100 µl of 100% ethanol were added and sample was incubated for 30 min at -20°C followed by centrifugation for 5 min at 13000 rpm at RT (Haraeus Biofuge Pico). RNA pellet was washed in 70% ethanol, dried in a speed vac for 2 min and dissolved in 40 µl of nuclease free H_2O followed by incubation for 50 min at 37°C. In order to obtain dsRNA, the complementary RNA strands were hybridized by incubation of the sample for 30 min at 65°C followed by slow cooling down to room temperature for about 1 hr. Concentration of dsRNA was determined by 260 nm absorption measurements using NanoDrop spectrophotometer and analysed on 1% agarose gel.

ssRNA for electrophoretic mobility shift assays was synthesized by the same method with the difference that the hybridization step was omitted.

3.2.3 Protein biochemistry methods

Protein analysis was performed according to standard protocols. In general, proteins were kept on ice (4°C), in the presence of proteinase inhibitors – a mix of Leupeptin, Pepstatin, Aprotinin (each at 1µg/ml), PMSF (0,2 mM), and the reducing reagent DTT (1 mM), which were added freshly to the buffers.

3.2.3.1 Nuclear extracts from Kc or SL2 cells

Cells from one 6 well plate, 10 cm plate or 75 cm^3 flask were spun down at 1000 rpm for 5 min at 4°C (Heraeus Laborfuge 400R). Cells were washed twice with ice cold PBS and resuspended in 50 µl (6 well plate), 100 µl (10 cm plate) or 500 µl (75 cm^3 flask) of hypotonic Buffer B and incubated on ice for 10 min. Cells were spun down at 13000 rpm for 1 min at RT (Heraeus Biofuge Pico) and the supernatant (cytoplasmic fraction) was discarded. Pellet was resuspended in 250 µl of high salt Buffer C and incubated on ice for 20 min. Then cells were spun down at 13000 rpm for 10 min at 4°C (Heraeus Biofuge Pico), supernatant (nuclear extract) was transferred to a fresh tube and protein concentration was measured by Bradford assay. Extracts were frozen down in liquid nitrogen and stored at - 80°C.

Buffer B	10 mM Hepes/KOH, pH 7,9 10 mM KCl 1,5 mM $MgCl_2$ 0,1 mM DTT proteinase inhibitors added freshly
Buffer C	20 mM Hepes/KOH, pH 7,9 420 mM NaCl 1,5 mM $MgCl_2$ 0,2 mM EDTA 25% (v/v) glycerol 0,1 mM DTT proteinase inhibitors added freshly

3.2.3.2 Whole cell extracts from *Drosophila* brains

Whole cell extract was prepared from Drosophila 3rd instar larvae brains for checking ectopic expression of Gal4-driven transgenes. 20 brains from 3rd instar larvae were dissected in PBS and collected in 20 µl of IP Buffer. Roti Load1 SDS-Page loading buffer

was added, brains were boiled for 5 min at 95°C and directly loaded on SDS-Page gel. Expression of proteins was analysed by Western blot using appropriate antibodies.

IP Buffer	50 mM Tris, pH 8,0 150 mM NaCl 2,5 mM EDTA 2,5 mM EGTA 1% (v/v) NP-40 protease inhibitors added freshly

3.2.3.3 *Drosophila* stage-specific whole cell extracts

Different developmental stages of *Drosophila melanogaster* were collected from small chambers, washed or dechorionized, dried, weighted, froze down at liquid nitrogen and kept at -80°C. For each gram of material, 1 ml of Homogenising Buffer was added and material was disrupted with a mini glass dounce homogenizer for 3 minutes on ice. The homogenate was passed through a single layer of miracloth to remove debris and spun down at 2000 rpm for 3 min at 4°C (Heraeus Biofuge Pico). The supernatant was carefully transferred to a fresh tube and spun down at 13000 rpm for 30 min at 4°C (Heraeus Biofuge Pico). Supernatant was transferred again to a fresh tube and protein concentration was measured by Bradford assay. Extracts were frozen down in liquid nitrogen and stored at - 80°C.

Homogenizing Buffer	50 mM Hepes, pH 7,4 100 mM NaCl 0,5 mM EDTA 0,05% (v/v) NP-40 protease inhibitors added freshly

3.2.3.4 Determination of protein concentration

Protein concentration in extracts was determined using the colorimetric assay described by Bradford (Bradford 1976). The concentration of purified recombinant proteins was estimated according to a protein standard with a known concentration (BSA) run on the same SDS-PAGE gel, followed by Coomassie blue staining.

3.2.3.5 Co-immunoprecipitation

Protein G beads were equilibrated by washing 3 times in PBS. For one IP, appropriate antibodies (Table 3.2) were coupled to protein G beads by incubation with 10 µl of protein G beads in 300 µl of PBS for 30 min on a rotating wheel at RT. Subsequently the beads were washed 3 times with PBS and once with HEMG-100 KCl buffer. Proper amount of protein nuclear extracts (usually 50-100 µl) were added, filled up with 100 KCl/HEMG up to 350 µl and incubated for 3 hrs at 4°C on a rotating wheel. Beads were washed once with HEMG-100 KCl and two times with HEMG-100 NaCl, resuspended in 2xSDS-Page loading buffer and analysed by Western blot.

Alternatively, co-immunoprecipitations were carried out in PBS. For this, protein G beads were equilibrated by washing 3 times in PBS. Nuclear extracts were filled up with PBS up to 350 µl and incubated with the appropriate antibody for 2 hrs at 4°C on a rotating wheel and after addition of 10 µl of Protein G beads (1:1 slurry) for an additional hour. The beads were washed three times with PBS, resuspended in 2xSDS-Page loading buffer and analysed by Western blot.

For each IP, samples without antibody and without extract were included as background controls. 10-20% of nuclear extracts were taken as an input control.

HEMG-X buffer	25 mM Hepes, pH 7,6
	X mM KCl or NaCl
	12,5 mM $MgCl_2$
	0,1 mM EDTA pH 8,0
	10% (v/v) glycerol
	0,1 mM DTT
	proteinase inhibitors added freshly

3.2.3.6 SDS-polyacrylamide gel electrophoresis

Pouring and electrophoresis of SDS-polyacrylamide gels was performed using the Novex system (pre-assembled gel cassettes). Resolving and stacking gels were prepared according to standard protocols (chapter 3.1.2) using ready-to-use polyacrylamide solutions from Roth (Rotiphorese Gel 30; 37.5:1). Gels were run using standard SDS-PAGE Running buffer. For PARP/PAR pulldowns gradient NuPAGE Novex 4-12% Bis-Tris Gels were used. These gels were run in NuPAGE MES-running buffer.

For electrophoresis protein samples were mixed with SDS-Page Loading buffer, heat-denatured for 5 min at 95°C and directly loaded onto the gel. Electrophoresis was run initially at 100V until the dye front had reached the resolving gel and then at 160V until the dye front had reached the end of the gel. The molecular weight of proteins was estimated by running pre-stained protein ladder. Following electrophoresis, proteins were either stained with PageBlue according to the manufacturer's instructions, Coomassie Briliant Blue or subjected to Western blotting.

3.2.3.7 Coomassie Blue staining of protein gels

Polyacrylamid gels were stained overnight on a horizontal shaker with a ready-to-use PageBlue Protein Stain Solution (Fermentas) according to the manufacturer's instructions. For histone visualization gels were stained with a traditional Coomassie blue staining solution for 60 min to overnight and then destained in a destaining solution. After documentation, gels were dried on a Whatman paper at 80°C for 2 hrs using a gel drier (BioRad).

Coomassie blue staining solution	10% (v/v) acetic acid 50% (v/v) methanol 0,025% (w/v) Coomassie Brilliant Blue R250
Destaining solution	10% (v/v) acetic acid 50% (v/v) methanol

3.2.3.8 Western blot analysis

Protein were separated by SDS-Page and transferred to polyvinylidene fluoride (PVDF) membrane. Before blotting, PVDF membrane was activated shortly in methanol. The gel was placed onto the membrane and sandwiched between four gel-sized Whatman-3MM Paper soaked in the transfer buffer. Proteins were transferred onto the membrane for 1 hour at 400 mA constant current using the BioRad Wet Blotting System. The blotting chamber was cooled with an ice block and kept on ice. After transfer, to reduce a non-specific antibody binding, membranes were incubated in a blocking solution for 1 hr at RT. Then, membranes were incubated with an appropriate dilution of the primary antibody (Table 3.2) diluted in the blocking solution for 2 hours at RT, on a horizontal shaker. Alternatively, membranes were incubated overnight in the coldroom. To remove unbound

antibodies, membranes were washed three times with PBST for 5 minutes and incubated for one additional hour with horseradish peroxidase-coupled secondary antibody diluted in blocking solution, at RT. After three washes (with PBST, 5 minutes each), antigen-antibody bound complexes were detected using Immobilon Western HRP Chemiluminescent Substrate and autoradiography according to the manufacturer's instructions. Different exposure times were chosen for different antibodies.

For stripping, membranes were incubated in a stripping buffer for 30 minutes at 65°C in a water bath. This strips the bound antibodies from the membrane, thus it can be re-probed with different primary antibodies. After stripping, membranes were washed three times for 10 minutes with PBST and then blocked and immunoblotted as described above.

Transfer buffer	192 mM Glycin 24 mM Tris 20% methanol 0,02% SDS
PBST	PBS with 0,1% Tween-20
Blocking solution	PBST with 5% dried milk
Stripping buffer	62,5 mM Tris-HCl, pH 6,8 10% β-Mercaptoethanol 2% SDS

3.2.3.9 Antibody generation

Monoclonal antibodies against dCHD3 were generously generated by Elisabeth Kremmer. Briefly, Lou/C rats were immunized with a KLH-coupled (Keyhole Limpet Hemocyanin) peptide (CGKRIRKEIDYSNQYPSPNRAT, Peptide Speciality Laboratories) that is specific for the dCHD3protein. After an 8-week interval, a final boost was given three days before fusion of the rat spleen cells with the murine myeloma cell line P3X63-Ag8.653. Hybridoma supernatants were tested in ELISA using the same peptide coupled to ovalbumin. The specificity of antibodies was confirmed by monitoring the disappearance of protein signals on Western blot after protein knockdown with RNAi (Fig. 5.14). Antibodies were also tested for potential cross-reactivity with recombinant dMi-2 (Fig. 3.1). Lack of signal for dMi-2 in Western blot probed with α-dCHD3 antibodies, validated

their specificity. Based on these experiments hybridoma supernatant dCHD3 #7A11 (IgG1) was used for further experiments. Polyclonal dCHD3 antibody (#5) was generated by injecting rabbits with three dCHD3 derived peptides (Peptide Speciality Laboratories, KDKRPKTNAKKQKFRDEEYC, SQPKLPKKQKKQSQQSC, CGKRIRKEIDYSNQY PSPNRAT).

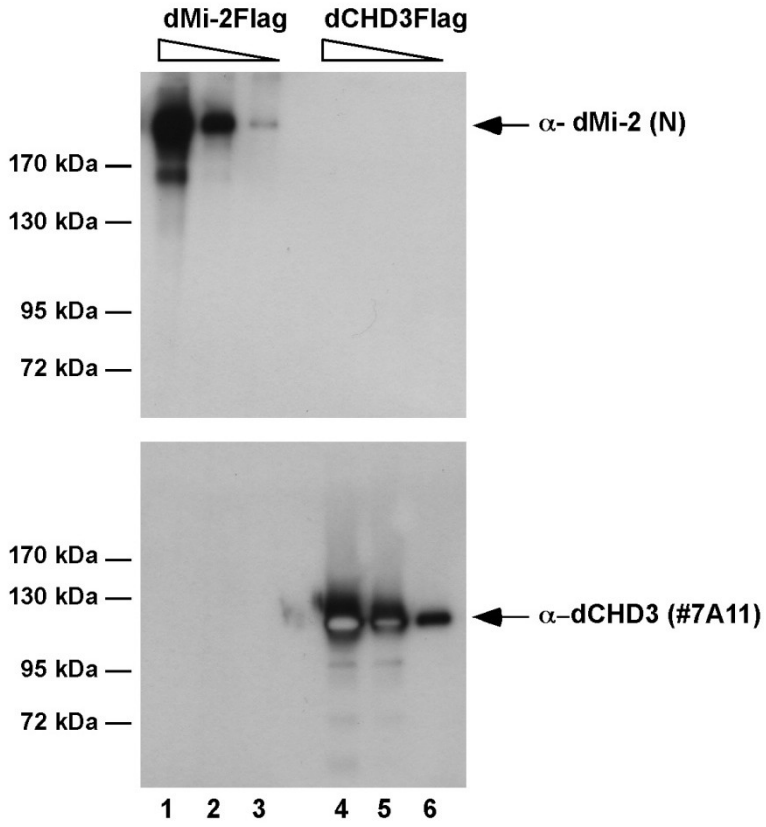

Figure 3.1 Specificity of dMi-2 and dCHD3 antibodies
Different amounts of recombinant dMi-2 and dCHD3 were subjected to Western blot analysis using dMi-2 (upper panel; polyclonal rabbit, α-dMi-2(N)) and dCHD3 (lower panel; rat monoclonal, (7A11)) antibodies. Lanes 1 and 4: 18 and 36 picomol; lanes 2 and 5: 4,5 and 9 picomol; lanes 3 and 6: 0,9 and 1,8 picomol recombinant protein. Molecular weights are indicated on the left, the position of dMi-2 and dCHD3 is shown by arrows on the right.

3.2.3.10 Antibody concentration

Cell culture supernatant containing monoclonal antibodies was concentrated on Protein G Sepharose FF beads. Protein G beads were equilibrated in 100 mM Tris/HCl, pH8.0. pH of the serum was adjusted by adding 1/10 volume of 1 M Tris/HCl, pH 8.0. For one concentration step, 8 ml of cell culture supernatant was incubated with 0,5 ml of Protein G beads on the wheel for 2 hrs at 4°C. Beads were applied on a small gravity flow column

and washed once with 5 ml of 100 mM Tris/HCl, pH 8.0, and once with 5 ml of 10 mM Tris/HCl, pH 8.0. Antibodies were eluted with 50 mM glycine pH 3.0, 10-12 fractions of 250 µl volume were collected and immediately neutralized with 50 µl of 1 M Tris/HCl to adjust pH to 8.0. All fractions were separated on 10% SDS-PAGE gel and analysed by Coomassie staining. Fractions containing most concentrated antibodies were pooled and stored at 4°C.

3.2.3.11 Baculovirus generation and protein expression in SF9 cells

Baculovirus generation

All protein-expressing vectors were cloned into pVL1392 vector (Table 3.7). SF9 cells were transfected using Bac-N-Blue Transfection Kit. $2x10^6$ of SF9 cells were split onto a 60 mm plate. For one transfection mixture, following reagents were used:

Bac-N-Blue DNA (0,5 µg)	10 µl
Recombinant transfer plasmid (1 µg/µl)	4 µl
Sf-900 II SFM medium (without supplements or FCS)	1 ml
Cellfectin Reagent	20 µl

The trasfection mixture was gently mixed for 10 sec and incubated for 15 min at RT. In the meantime the medium was carefully removed from cells and cells were washed with 2 ml of Sf-900 II SFM medium (without supplements or FCS). The medium was removed and the entire transfection mix was added dropwise onto the 60 mm dish. Cells were incubated for 4 hrs at RT on a side-to-side rocking platform with a lowest speed (~ 2 side to side motions per minute) followed by adding 1 ml of complete Sf-900 II SFM medium. Dishes were sealed and incubated for 6 days at 26°C in the incubator.

For second round of virus amplification, 6 days after transfection, SF9 cells were harvested by centrifugation at 800 rpm for 5 min at RT (Heraeus Megafuge 1.0), supernatant was collected. 7,5 $x10^6$ fresh SF9 cells were split onto a 10 cm plate. After cells settled down, medium was removed and 2,5 ml of fresh, complete Sf-900 II SFM medium were added. 1 ml of cell supernatant from first cell infection was added to the cells and plates were incubated for 1 hr at RT on a side-to-side rocking platform with a lowest speed. After that, 10 ml of complete Sf-900 II SFM medium were added to the cells. Cells were incubated for another 5-7 days at 26°C in the incubator. For third round of virus amplification, 12 $x10^6$ fresh SF9 cells were split onto a 15 cm plate. After cells settled down, medium was

removed and 5 ml of fresh, complete Sf-900 II SFM medium were added. 1 ml of cell supernatant from second amplification was added to the cells and plates were incubated for 1 hr on a side-to-side rocking platform as before followed by adding 15 ml of complete Sf-900 II SFM medium. Cells were incubated for another 5-7 days for 3rd amplification or for 48 hrs for test expression. The supernatant from 3rd virus amplification was collected as before and stored at 4°C.

Protein expression in SF9 cells

48 hours after virus infection, cells were scraped from a 15 cm plate and spun down at 800 rpm for 10 min at 4°C (Heraeus Laborfuge 400R). The supernatant was discarded and cells were resuspended in 5 ml of PBS and spun down again. Cell pellet was resuspended in 2 ml of Lybu 200 buffer, froze down in liquid nitrogen and slowly thawed at 26°C in a water bath. Freezing/thawing procedure was repeated two times. The extract was sonified twice with a big tip, for 15 sec with setting 30% output and 30 sec brake on ice. Extract was cleared by pelleting debris at 4500 rpm at 4°C. Protein extract was analysed by Western blot or used for Flag affinity purification.

Lybu 200	20 mM Hepes, pH 7,6 200 mM KCl 10% (v/v) glycerol 0,1% (v/v) NP-40 0,1 mM DTT proteinase inhibitors added freshly

Protein purification from baculovirus-infected SF9 cells

α-Flag M2 agarose beads were equilibrated in Lybu 200 buffer. Different amounts of whole cell extracts were used depending on the expression level of a particular protein. Typically, 150 µl beads (1:1 slurry) were added to 10 ml SF9 whole cell extract and incubated on the rotating wheel for 2-3 hrs at 4°C. Beads were spun down at 1000 rpm for 4 min at 4°C (Heraeus Laborfuge 400R) and washed 2 times for 5 min with 10 ml of Lybu 200 buffer, one time with 10 ml of Lybu 500 buffer. Then beads were transferred to a siliconized tube and washed once with 1 ml of Lybu 200. Proteins were eluted twice with 100 µl of Elution Buffer containing Flag peptide for 2 hrs and then overnight on the rotating wheel at 4°C. Eluted fractions were froze down in liquid nitrogen and stored at -

80°C. 7-15 µl of aliquots were taken and analysed on SDS-Page gels stained with Coomassie.

Lybu 500	20 mM Hepes, pH 7,6 500 mM KCl 10% (v/v) glycerol 0,1% (v/v) NP-40 0,1 mM DTT proteinase inhibitors added freshly
Flag Elution Buffer	20 mM Hepes, pH 7,6 100 mM KCl 10% (v/v) glycerol 0,05% (v/v) NP-40 0,1 mM DTT proteinase inhibitors added freshly

3.2.3.12 Protein expression in bacteria

For GST-tag protein fusion expression a starter culture of 100 ml was inoculated with freshly transformed BL21 bacteria and incubated overnight at 37°C at 200 rpm in a bacteria shaker (Inforst HT). The overnight culture was diluted with 800 ml of fresh LB-medium to the optical density (OD_{600}) of 0,07 and incubated for 1-2 hrs at 37°C until OD_{600} reached about 0,6-0,8. At this point protein expression was induced with 0,1 mM IPTG and cells were incubated overnight at 18°C at 200 rpm in a bacteria shaker.

Bacterial cells were pelleted at 4000 rpm (Haraeus Cryofuge 5000) for 30 min at 4°C. Cells were washed once in PBS, pelleted as before and resuspended in 15 ml of PBS/1% (v/v) Triton-X and the extract was sonified with a big tip, 6 times for 20 sec with setting 30% output and 1 min brake on ice. Extract was cleared by pelleting debris at 13000 rpm for 30 min at 4°C (Sorvall RC-5B).

300 µl of Glutathione Sepharose 4B Fastflow-Beads were equilibrated in PBS/1% (v/v) Triton-X, added to 15 ml of protein extract and incubated for 2 hrs on a rotating wheel at 4°C. Beads were spun down for 4 min at 2000 rpm at 4°C (Haraeus Labofuge 400R) and washed 2 times for 5 min with 10 ml of PBS/1% (v/v) Triton-X and twice with PBS. For PARP pulldown experiments, protein bound beads were resuspended in 80% (v/v) glycerol and stored at -20°C. For histone peptide pulldown experiments, beads were applied on a small gravity flow column in the cold room and bound proteins were eluted with fresh

GST elution buffer. Eight fractions of 350 µl volume were collected, all fractions were analysed on Coomassie stained SDS-PAGE gels.

GST elution buffer	50 mM Tris, pH 8,0 150 mM KCl 20 mM reduced Glutathione

3.2.3.13 Superose 6 filtration

200 µl of embryo or Kc cell nuclear extract or 0,5-1 µg of recombinant protein were applied to a Superose 6 HR 10/30 gel filtration column and resolved in EX-300 buffer on an Äkta purifier system according to the manufacturer's instructions. Eluted fractions (500 µl each) were subsequently precipitated by using StrataClean Resin, resuspended in 1x SDS-Page loading buffer and analysed by Western blot.

EX-300 buffer	10 mM Hepes, pH 7,6 300 mM KCl 1,5 mM $MgCl_2$ 0,5 mM EGTA 10% (v/v) glycerol 0,1 mM DTT 0,2 mM PMSF

3.2.4 Chromatin specific methods

3.2.4.1 Histone octamer isolation from embryos

0-12 hr embryos were collected, dechorionized, rinsed in sieves, dried and weighted. For one histone preparation around 100 g of dechorionated embryos were used. Embryos were resuspended in 150 ml of Glycine Buffer and homogenized with Yamato homogenisator (6 strokes, 1000 rpm at 4°C). The homogenate was then centrifuged in a Sorvall RC-5B centrifuge for 15 min at 8000 rpm at 4°C. Supernatant was discarded and nuclei phase was resuspended in 50 ml of Suc Buffer and spun down again at 8000 rpm for 10 min at 4°C. Nuclei were washed once more in Suc Buffer and spun down as before. Finally, nuclei were resuspended in 30 ml of Suc Buffer, $CaCl_2$ was adjusted to 3 mM with 1M $CaCl_2$ and solution was warm up to 26°C for 10 min in a water bath. 125 µl of MNase (50u/µl) was added to the nuclei and incubated for 10 min in a water bath at 26°C to digest the

internucleosomal DNA. Reaction was stopped by adding 600 µl of 0,5 M EDTA and spun immediately at 8000 rpm for 10 min at 4°C (Sorvall RC-5B). To extract nucleosomal particles, pellet was resuspended in TE buffer supplemented with DTT, PMSF and proteinase inhibitors and the sample was rotated on the wheel for 45 min at 4°C followed by centrifugation at 11 000 rpm for 35 min at 4°C (Sorvall RC-5B). Supernatant containing released nucleosomal particles was kept overnight on ice in the coldroom.

Histone octamer purification was performed using Chromatography Systems from Amersham (ÄKTA, FPLC & HPLC) on a hydroxylapatite column. The column material was washed several times with 0,63 M KCl/100 mM K-PO_4 to remove fines and the column was prepared according to the manufacturer's instructions. Before the sample was loaded on the column, salt was adjusted to 0,63 M KCl with the 2 M KCl/100 mM K-PO_4 solution, spun down at 13000 rpm for 15 min at 4°C (Heraeus Biofuge Pico), filtered with 0,45 µm and then 0,22 µm sterile filter. Histones were loaded on the 30 ml hydroxylapatite column, flowthrough (histone H1) was collected and the column was washed with 10 column volume (300 ml) with 0,63 M KCl/100 mM K-PO_4. Histones were eluted with 2 M KCl/100 mM K-PO_4. Presence of histones was monitored by OD at 215 nm, and fractions containing histone peak were concentrated with Centriprep YM-10 according to the manufacturer's instructions. Equal volume of glycerol was added to each concentrated fraction and histones were stored at -20°C for few months.

10-15 µl of glycerol diluted histones were separated on 15% SDS-Page gel and analysed by Coomassie blue staining (Fig. 3.2).

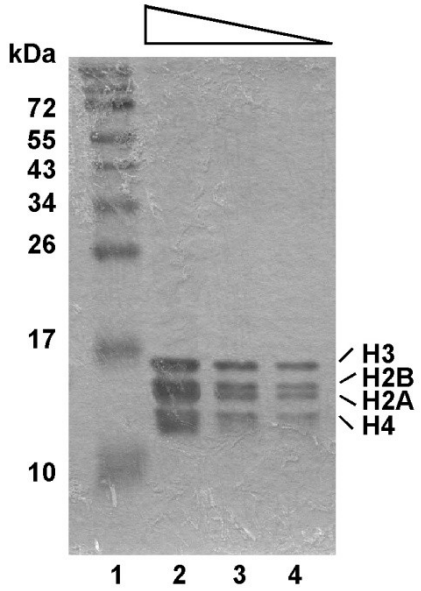

Figure 3.2 Core histone octamers from *Drosophila* embryos
Core histone octamers were isolated from *Drosophila* embryos (0-12 hr). Histones were resolved on 15% SDS-PAGE and stained with Coomassie blue. Different amounts of histones were loaded on the gel - lane 1: 5 µl, lane 2: 2 µl, lane 3: 1 µl. Lane 1: molecular weight standard. Different histone types are marked on the right.

Glycine Buffer	15 mM Hepes/KOH, pH 7,6
	10 mM KCl
	5 mM $MgCl_2$
	0,05 mM EDTA
	0,25 mM EGTA
	10% (v/v) glycerol
	1 mM DTT
	0,2 mM PMSF
Suc Buffer	15 mM Hepes/KOH, pH 7,6
	10 mM KCl
	5 mM $MgCl_2$
	0,05 mM EDTA
	0,25 mM EGTA
	30 mM Sucrose
	1 mM DTT
	0,2 mM PMSF
100 mM K-PO_4 (200 ml)	0,2 M KH_2PO_4 (28 ml)
	0,2 M K_2HPO_4 (72 ml)

3.2.4.2 Polynucleosome reconstitution by salt dialysis

Nucleosomes were assembled on the lid of siliconized 1,5 ml eppendorf tubes. The bottom of the tube was cut and a big hole was made into the lid with a heated metal scalpel. The dialysis membrane (1,5x1,5 cm/3,5 kDa, Spectra/Por) was equilibrated in Hi Buffer for 30 min, cut and fixed on the lid of the siliconized tube. Such prepared tubes were put into a Styrofoam floater and placed on 300 ml of Hi buffer in a beaker with a magnetic stirrer. Air bubbles below the membrane were removed with a bent Pasteur pipette. The assembly reaction was pipetted onto the dialysis membrane.

A typical test assembly reaction contained 4,4 µg of plasmid DNA with varying amounts of histone octamer in a 50 µl volume. To estimate the optimal histone to DNA ratio increasing amounts of histones were mixed with a fixed amount of DNA. The assembly was done in Hi Buffer, supplemented with BSA (200 ng/µl).

A big assembly reaction was done as the test assembly in a 400 µl volume. The final DNA concentration was increased to 150 ng/µl and the calculated histone amount was reduced by around 15%.

The salt gradient dialysis was done by continuous addition of Lo Buffer (3 liters in total) into the beaker with 300 ml of Hi Buffer with a peristaltic pomp over 30 hour period in the cold room. Polynucleosomes were checked then by MNase assay.

Hi Buffer	10 mM Tris/HCl, pH 7,6 2 M NaCl 1 mM EDTA 1 mM β-mercaptoethanol 0,05% (v/v) NP-40
Lo Buffer	10 mM Tris/HCl, pH 7,6 50 mM NaCl 1 mM EDTA 1 mM β-mercaptoethanol 0,05% (v/v) NP-40

3.2.4.3 Partial trypsinization of nucleosomes

To remove histone tails, polynucleosomes were partially digested by trypsin as described previously (Guyon et al. 1999). Polynucleosomes (0,05 µg/µl) were digested with trypsin (0,27 ng/µl, Sigma) in a final volume of 40 µl in buffer V for 10-30 min at RT. The

trypsinization reaction was stopped with 20-fold excess (w/w) of a soybean trypsin inhibitor (Sigma) and the reaction was monitored by SDS-PAGE electrophoresis and Coomassie staining.

Buffer V	10 mM Tris/HCl, pH 8,0 25 mM NaCl 1 mM EDTA

3.2.4.4 Micrococcal nuclease (MNase) assay

Polynucleosomes were analysed with a Micrococcal nuclease (MNase) digest. MNase induces double-strand breaks within nucleosome linker regions, but only single-strand nicks within the nucleosome itself. Therefore, at limiting concentrations it leads to generation of a characteristic nucleosomal ladder which can be used for the assessment of the quality of nucleosomal arrays (Axel 1975).

Polynucleosomes were partially digested with MNase. A new batch of MNase was always titrated as the activity of the enzyme is variable. Typically, 1 µg of assembled polynucleosomes was incubated with 5-200U of MNase in EX80 buffer (supplemented with 5 mM $CaCl_2$ and 200 ng/µl BSA) in a final volume of 37 µl. 12 µl of the reaction were transferred to a new tube after 10 sec, 40 sec and 4 min and the reaction was stopped with 6 µl of MNase stop mix. Proteinase K digestion was continued for 2 hrs at 45°C. For DNA precipitation, 45 µl of 100% ethanol, 9 µl of 7,5M NH_4Ac were added, samples were incubated on ice for 10 min spun down for 20 min at 13000 rpm at 4°C (Haraeus Biofuge Pico). Supernatant was discarded and pellets were washed once with 70% ethanol, air-dried and dissolved in 10 µl of TE buffer. Samples were analysed on 1,3% agarose gel.

MNase stop mix	4% (w/v) SDS 0,1 M EDTA Glycogen (3,6 µg/µl) Protenase K (0,85 µg/µl)

3.2.4.5 Nucleosome mobility assay

Mononucleosomes were assembled on 200 bp fragments containing the '601' positioning sequence at different positions. The '601' sequence was identified in a screen which sought to find a DNA sequence that binds the histone octamer with high affinity and with a unique

position (Lowary and Widom 1998). 200 bp DNA fragments were obtained by digestion with specific restriction enzymes from pUC12x601 vector. NotI digestion results in DNA fragments with '601' sequence at the edge for end positioned nucleosomes and AvaI digestion results in DNA fragments with '601' sequence at the centre for middle positioned nucleosomes. Digested DNA was used for mononucleosome assembly by salt gradient dialysis. Assembly was carried out in the presence of 5 µg of digested DNA with different amounts of histones in a final volume of 40 µl in Hi buffer, as for polynucleosome assembly (chapter 3.2.4.2). Assembly was verified by native gel electrophoresis in 6 % PAA and ethidium bromide staining (Fig. 3.3). Faster migrating mononucleosomes are positioned at the periphery of the DNA fragment, whereas slowly migrated mononucleosomes are located at the centre of the DNA fragment. Samples with best positioned nucleosomes were combined (usually histone:DNA ratio -1,2 and 1,4) and stored at 4°C for few weeks.

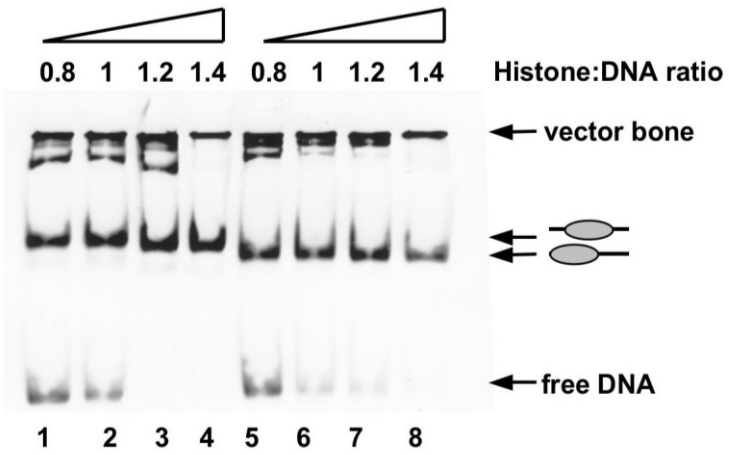

Figure 3.3 Mononucleosome assembly test for the mobilization assay
Mononucleosomes were assembled on a '601' positioning sequence. Different histone:DNA ratios were tested, as indicated. Lines: 1-4, middle positioned nucleosomes, lines: 5-8, end positioned nucleosomes. Positions of free DNA and vector bone are indicated on the right.

Standard nucleosome mobilisation reactions (10 µl) contained 200 ng of mononucleosomes in EX-40 buffer in the presence or absence of 1 mM ATP and different amounts of Flag-eluted baculovirus purified remodelers. Reactions were incubated at 26°C for 75 min and stopped by adding 1 µg of competitor DNA (pUC18). Products were analysed on 6 % native PAA gel and visualized with ethidium bromide (EtBr) staining.

EX-*X* buffer	10 mM Tris/HCl, pH 7,6 *X* mM KCl 1,5 mM $MgCl_2$ 0,5 mM EGTA 10% (v/v) glycerol BSA (200 ng/µl) 1 mM DTT

3.2.4.6 ATPase assay

ATPase assay was performed in the presence of [γ-^{32}P]-ATP (3000 Ci/mmol, 10 mCi/ml) using different substrates to analyse the specific activity of a chromatin remodeling enzyme. A typical reaction (14 µl) contained 100 ng of plasmid DNA or polynucleosomes in EX40 buffer in the presence of 10 µM cold ATP and 0,1 µl of [γ-^{32}P]-ATP. Different amounts of proteins were added and the reactions were incubated for 30 min at 26°C. Reactions were stopped by putting them on ice and 1 µl of each sample was spotted on a half-cut thin layer chromatography cellulose plate (PEI Cellulose F25) and air-dried. The hydrolysed phosphate was separated from unconsumed ATP in 0,5 M LiCl/1M formic acid buffer using thing layer chromatography. Samples were separated until the buffer reached one cm to the plate end. Plate was dried for 5 min at 60°C and exposed on X-ray film or Phosphorimager (Fugifilm FLA-3000) for quantification of ATP hydrolysis. ATP and hydrolyzed phosphate were quantified using Fugifilm Image Reader software. The percentage of hydrolysed ATP was determined using the following calculation:

$$(\gamma\text{-}^{32}P_{hydrolyzed})/(\gamma\text{-}^{32}P_{hydrolyzed} + \gamma\text{-}^{32}P_{unhydrolyzed})$$

3.2.4.7 Histone deacetylase (HDAC) assay

HDAC assay was done as described previously (Brehm et al. 2000). 50 µl of Kc nuclear extract were used for IPs with different antibodies. IPs were performed in PBS and after extensive washes (4x5 min) beads were subjected for HDAC assay.

Beads were incubated in 30 µl of HDAC buffer in the presence of 2 µl of ^{3}H-labelled *Drosophila* histones (kindly provided by Alexander Brehm) at 30°C for 1 hr in a thermomixer. Reactions were stopped by adding 65 µl of 1M HCl/0,16 M HAc and 220 µl of water followed by vortexing. 700 µl of ethylacetylate was added, samples were vortexed for 15 sec and cleared by centrifugation for 2 min at 13000 rpm at RT (Haraeus Biofuge Pico). 500 µl of upper water phase were transferred to a scintillation vial containing 5 ml of

scintillation cocktail and vortexed for 10 sec. Released ^{3}H was counted in a liquid scintillation counter.

HDAC buffer	10 mM Tris, pH 8,0 50 mM NaCl 1 mM $MgCl_2$ BSA (100 ng/µl)

3.2.4.8 Chromatin fractionation

Chromatin fractionation was carried out as described in (Wang et al. 2004) with few modifications. $150x10^6$ Kc cells were collected, washed twice in ice cold PBS and spun down at 1000 rpm (Heraeus Megafuge 1.0) for 5 min at RT. Cells were resuspended in 1 ml of hypotonic buffer and incubated on ice for 5 min followed by centrifugation at 4000 rpm for 5 min at 4°C (Heraeus Biofuge Pico). Supernatant (cytoplasmic) fraction was collected and kept on ice. The nuclear pellet was washed in isotonic sucrose buffer (STM) and spun down as before. The nuclear envelope was removed by addition of 1 ml of LS-buffer supplemented with 1% (v/v) Triton X-100. At this step, RNAse A (0,5 µg/µl) was added to cells and samples were incubated 10 min at 26°C in a thermomixer. The nuclear pellet was washed then twice with LS-buffer and further extracted with increasing concentrations of NaCl (0,3M and 0,5M) in the same buffer. For each extraction, cells were resuspended in 100 µl of the buffer and incubated on ice for 5 min followed by centrifugation at 13000 rpm for 5 min at 4°C (Hereus Biofuge Pico). The resulting supernatants were kept on ice, protein concentration was measured with Bradford assay and samples were loaded on SDS-PAGE gel and analysed by Western blot.

Hypotonic buffer	10 mM Hepes, pH 7,6 10 mM KCl 1,5 mM $MgCl_2$ Proteinase inhibitors (added freshly)
STM-buffer	50 mM Tris-HCl, pH 7,6 5 mM $MgCl_2$ 0,25 M Sucrose Proteinase inhibitors (added freshly)

SL-buffer	10 mM Tris-HCl, pH 7,6 0,2 mM $MgCl_2$

3.2.4.9 Histone peptide pulldowns

SulfoLink Coupling Resin is porous, crosslinked, 6% beaded agarose that has been activated with iodoacetyl groups. When incubated with a solution of peptide that contains reduced cysteine residues, the iodoacetyl groups react specifically and efficiently with the exposed sulfhydryls (-SH) to form covalent and irreversible thioether bonds that permanently attach the peptide to the resin.

Histone peptides were chemically synthesized by Peptide Speciality Labolatories (Heidelberg) and coupled to sulfolink-coupling gel (Pierce). All pulldown steps were done in siliconized tubes. Sulfolink-coupling gel was equilibrated in coupling buffer. 50 µg of peptide were added to 100 µl of 1:1 bead slurry of sulfolink-coupling gel. Coupling peptides to the beads took place at RT for 30 min with extensive shaking (14000 rpm) in a thermomixer followed by 1 hr incubation at RT without shaking. Beads were washed 4 times with 1 ml of coupling buffer. Then 50 mM L-cysteine in coupling buffer was added to the beads and they were incubated as before. During this step L-cysteine binds to all free iodoacetyl groups. Unbound L-cysteine was removed by washing 8 times with 1M NaCl and 4 times with dH_2O at RT. Beads were stored as 1:1 slurry in dH_2O (final peptide concentration - 0,5 µg/µl) for 2-3 months at 4°C.

Table 3.15 Histone peptide sequences
All histone peptides contain sulfhydryl groups at C-terminus which couple peptides to the Sulfolink beads. Numbers in parenthesis indicate amino acids at H3 N-terminal tail.

Peptide	Sequence
H3(1-15)	ARTKQTARKSTGGKA-C
H3K4me3 (1-15)	ART(Kme3)QRARKSTGGKA-C
H3 (1-30)	ARTKQTARKSTGGKAPRKQLATKAARKSAP-C
H3 (22-44)	TKAARKSAPATGGVKKPHRYRPG-C
H3K36me3 (22-44)	TKAARKSAPATGGV(Kme3)KPHRYRPG-C

For each pulldown 0,5 µg of peptide and 0,25 µg of recombinant protein were applied. To use this amount of peptide, 10 µl of bead-bound peptide was diluted with 90 µl of empty, L-cysteine blocked beads and 10 µl of this solution (1:1 bead slurry) were used for each

pulldown. Beads were washed 2 times with binding buffer and blocked with BSA (1 μg/μl) for 1 hr on a rotating wheel at 4°C. Then the blocking solution was removed and beads were incubated with recombinant proteins in binding buffer for 2 hrs. Beads were washed 4 times in binding buffer, resuspended in 15 μl of 2x SDS loading buffer and protein binding to the peptides was detected by Western blot.

Coupling buffer	50 mM Tris-HCl, pH 8,5 5 mM EDTA
Binding buffer	25 mM Tris-HCl, pH 8,0 150 mM NaCl 2 mM EDTA 0,5%(v/v) NP-40

3.2.5 Protein - nucleic acid interaction analysis

3.2.5.1 Electrophoretic mobility shift assay

A typical DNA or RNA binding reaction (25 μl) was performed in the presence of 0.2 μg of dMi-2F and 80 ng of nucleic acid (DNA or ssRNA) in 40 mM KCl, 20 mM Tris pH 7.6, 1.5 mM $MgCl_2$, 0.5 mM EGTA, 10 % glycerol, BSA (200 ng/μl), 1 mM DTT (supplemented with 0.4 units of RNAsin). For competition assays, samples were preincubated for 15 min at 26°C before the different amounts of competitor (PAR or DNA or RNA) were added. Reactions were further incubated at 26°C for 75 min. Products were analysed on 6 % native PAA gel and visualized with ethidium bromide (EtBr) staining. ssRNA was synthesized by *in vitro* transcription using a fragment of hsp70 DNA as a template. This template (also used for the DNA EMSA assays) was produced by PCR amplification of cDNA derived from heat shocked Kc cells using the following primers: T7-hsp70_f and hsp70_r (Table 3.12).

3.2.5.2 Native gel electrophoresis

For analysis of mononucleosome mobilization assay or EMSA products, native gel electrophoresis was conducted using the Novex system. Samples were separated on 6% native polyacrylamide gel in 0,4 TBE buffer (chapter 3.1.2). The gel was pre-run at constant current of 80V for 45 min before samples were loaded and then the

electrophoresis was continued for 2 hrs at RT. Samples were run without a dye in 10% glycerol. After electrophoresis, the gel was stained with ethidium bromide (0,5 μg/ml) in distilled water for 15 min on a horizontal rotating shaker at RT followed destaining by washing twice in water for 10 min. Gels were documented with the gel documentation system.

3.2.5.3 Chromatin immunoprecipitation (ChIP)

Method principle

Chromatin immunoprecipitation assay (ChIP) was developed to determine whether a protein of interest binds to a specific DNA sequence *in vivo* (Solomon et al. 1988; Dedon et al. 1991; Orlando et al. 1997). Proteins are reversibly crosslinked to target DNA with formaldehyde. Chromatin is subsequently fragmented by sonication to short fragments, with an average of 500 bp. Subsequently protein-DNA complexes are precipitated using antibodies specific to the protein of interest. After extensive washing, crosslinking reversal and protein removal, DNA associated with the precipitated protein can be identified by conventional PCR, QPCR, by labelling and hybridization to DNA microarrays (ChIP-chip), or by direct high-throughput deep sequencing (ChIP-seq) (Collas 2010).

ChIP in cell culture

Kc cells were grown to 4-7x10^6 cells/ml in Schneider's Drosophila medium, 1x10^8 cells were usually processed for ChIP. Heat shock treatment was performed as described in chapter 3.2.8.4. In order to obtain temperature comparable to untreated cells for the crosslinking reaction, heat shock was stopped by adding 1/3 volume of 4°C medium. Cells were immediately crosslinked with 1% formaldehyde for 10 min at RT with slow agitation on a horizontal shaker. Crosslinking was quenched by adding 2 M Glycine to a final concentration of 240 mM. Cells were pelleted by centrifugation (1000 rpm, 10 min, 4°C, Heraeus Biofuge Pico) and washed once with 10 ml of cold PBS. Cell pellet was resuspended in 1 ml of SDS-Lysis Buffer and incubated on ice for 10 min. Cells were sonicated for 18 minutes (30 sec on/off) at the high intensity setting with a Bioruptor sonication device (Diagenode). To keep the temperature constant, ice was added to the ultrasound water bath after 9 minutes of sonication. Average length of sonified DNA was below 500 bp. Chromatin was spun down at 13000 rpm for 10 min at 4°C (Heraeus Biofuge Pico) and the lysate was diluted 1:10 in Chip Dilution Buffer. To remove DNA

and proteins which unspecifically bind to beads, chromatin was precleared with 80 µl of 50% protein G-sepharose beads (in 10 mM Tris-HCl pH 8.0, 1 mM EDTA, 1 mg/ml BSA) and rotated on the wheel in the coldroom for 30 min.

1% of the diluted, precleared chromatin was taken as input sample. For each precipitation 1,3 ml of precleared chromatin was used and appropriate amounts of antibodies (Table 3.2) were added. As a negative control, α-IgG were added to chromatin. Immunoprecipitation was carried out in siliconized tubes, overnight at 4°C on the rotating wheel. For each IP, 35 µl of 50% protein G-sepharose beads were added and incubated for 2 hours at 4°C. The immunoprecipitates were washed 3 times with Low Salt Wash buffer, 3 times with High Salt Wash Buffer, once with LiCl Wash Buffer and twice with TE buffer. Before the last wash with TE buffer, beads were transferred to fresh siliconized tubes. Each washing step was carried out on a rotating wheel for 10 min at 4°C and samples were spun down at 2000 rpm for 3 min at 4°C (Heraeus Biofuge Pico).

Protein-DNA complexes were eluted from the beads with 250 µl of freshly prepared Elution Buffer for 30 minutes at RT on a rotating wheel. Beads were spun down and the supernatant was collected to a fresh tube. Elution was repeated and both supernatants were pooled. Appropriate amount of elution buffer was added to the input samples to adjust the volume to 500 µl. 20 µl of 5M NaCl were added to the eluates and input samples and decrosslinking was carried out at 65°C overnight in a thermomixer.

Proteins were removed from the samples by proteolytic digestion with Proteinase K. For this, 20 µl of 1M Tris-HCl pH 6.5, 10 µl of 0,5M EDTA and 2 µl of Proteinase K (10 mg/ml) were added and samples were incubated at 45°C for 1 hour. DNA was purified using PeqGold Cycle Pure DNA isolation kit according to the manufacturer's instructions. DNA was eluted from columns with 30 µl PeqLab elution buffer. The relative amount of DNA compared to the IP input was determined via QPCR, using 1 µl DNA per reaction and specific primer pairs (Table 3.10 and chapter 3.2.2.3).

SDS-Lysis Buffer	50 mM Tris-HCl, pH 8,0 1% (w/v) SDS 10 mM EDTA Proteinase inhibitors
Chip Dilution Buffer	16,7 mM Tris-HCl, pH 8,0 16,7 M NaCl

	1,2 mM EDTA 1,1% (v/v)Triton X-100 0,01% (v/w) SDS Proteinase inhibitors
Low Salt Wash Buffer	20 mM Tris-HCl, pH 8,0 150 mM NaCl 2 mM EDTA 1% (v/v) Trion X-100 0,1% (w/v) SDS
High Salt Wash Buffer	20 mM Tris-HCl, pH 8,0 500 mM NaCl 2 mM EDTA 1% (v/v) Trion X-100 0,1% (w/v) SDS
LiCl Wash Buffer	10 mM Tris-HCl, pH 8,0 0,25M LiCl 1 mM EDTA 1% (v/v) NP-40 1% (w/v) Sodium Deoxycholate
TE Buffer	10 mM Tris-HCl, pH 8,0 1 mM EDTA
Elution Buffer	0,1 M $NaHCO_3$ 1% (w/v) SDS

QPCR calculations for ChIP

For ChIPs, all samples were referenced to the respective IP-input:

$\Delta Ct_{sample} = Ct_{input} - Ct_{sample}$ and displayed as a percentage of input: $\%input = 2^{\Delta Ct\ sample}$

Standard deviations s from triplicate technical measurements were used to determine the error for input percentages:

$$s_{\%input} = \ln(2) \times \%input \times \sqrt{\left(s_{input}^{2} \times s_{sample}^{2}\right)}$$

3.2.5.4 RNA immunoprecipitation (RIP)

RNA immunoprecipitation method (RIP) is used to identify RNA-protein interactions which occur *in vivo*. In the immunoprecipitation methodology, an RNA binding protein is immunoprecipitated from a cell lysate, followed by reverse transcription of the immunoprecipitated RNA and PCR with primers targeting the interacting RNA (Peritz et al. 2006).

RNA immunoprecipitation was performed as described in (Gilbert and Svejstrup 2006). Kc cells were heat shocked and crosslinked as for ChIP with 1% formaldehyde for 10 min. Crosslinking was quenched by adding 2 M Glycine to a final concentration of 240 mM. Cells were pelleted by centrifugation (1000 rpm, 10 min, 4°C, Heraeus Megafuge 1.0) and washed once with 10 ml of cold PBS. $75x10^6$ cells were resuspended in 800 µl of FA Buffer and lysed on ice for 15 min. Cells were sonicated as for ChIP, spun down and chromatin was digested with DNAse I. For this, chromatin solution was adjusted to 25 mM $MgCl_2$ and 5 mM $CaCl_2$, 1 µl of DNAse I (Fermentas) was added and reaction was incubated for 10 min at RT and then stopped with 20 mM EDTA. Chromatin was spun down at 13000 rpm for 10 min at 4°C (Heraeus Biofuge Pico). 100 µl of chromatin were taken as input and froze down at -20°C. 300 µl of chromatin were used for each precipitation, filled up to 500 µl with FA buffer. Appropriate amounts of antibodies were added, in addition 2 µl of rabbit pre-immunoserum from unrelated antibody were used as a negative control. Samples were incubated in siliconized tubes overnight at 4°C on the rotating wheel.

RNA-protein complexes were precipitated with 30 µl of 50% protein G-sepharose beads (equilibrated in FA buffer and 1 mg/ml BSA) for 2 hrs at 4°C. IPs were washed 5 times in FA buffer and twice with TE buffer. Before the last wash with TE buffer, beads were transferred to fresh siliconized tubes. Each washing step was carried out on a rotating wheel for 10 min at 4°C and samples were spun down at 2000 rpm for 3 min at 4°C (Heraeus Biofuge Pico).

RNA-protein complexes were eluted twice with 100 µl of RIP Elution Buffer - first by incubation on the rotating wheel for 10 min at RT and second by incubation in a thermomixer at 1000 rpm at 65°C for 10 min.

100 µl of elution buffer were added to the input samples to adjust the volume to 200 µl. Eluates and input samples were digested with proteinase K (10 mg/ml) for 1 hr at 42°C and decrosslinking was performed at 65°C overnight. Immunoprecipitated RNA was purified

using PeqGold Total RNA Kit (PeqLab) according to the manufacturer's instructions. All samples were additionally digested with DNAse I on the columns and eluted with 30 µl of RNAse free dH_20. cDNA was synthesized with 10 µl of eluted RNA and 2 µl of input RNA with random hexamers and analysed by QPCR with appropriate primer pairs. Amount of precipitated RNA was calculated as for ChIP. For IP specificity, abundant transcripts of *rp49* and *actin5c* were detected.

FA Buffer	50 mM Hepes-KOH, pH 7,6 140 mM NaCl 1% (v/v) Triton X-100 0,1% (w/v) Sodium Deoxycholate RNAsin (100 U/ml) Proteinase inhibitors (added freshly)
RIP Elution Buffer	100 mM Tris-HCl, pH 8,0 10 mM EDTA 1% (w/v) SDS RNAsin (40 U/ml)

3.2.6 Poly(ADP-ribose) binding analysis

3.2.6.1 PARP pulldowns

PARP reaction

Non-radioactive PARP reaction was performed according to the standard protocol (Karras et al. 2005). PARP reactions were set up in a final volume of 0,5 ml: 2 µg of recombinant Parp1, 100 mM Tris-HCl, pH 7.5, 50 mM NaCl, 10 mM $MgCl_2$, 2 µg/ml DNA oligonucleotides , 1 mM NAD+, 1 mM DTT.

Reactions were incubated in a thermomixer at 500 rpm for 25 min at 37°C. All reactions were stopped with 5 µM PJ34. Subsequently, reactions were used for PARP pulldowns or for PAR polymer isolation.

PARP pulldown

For pulldowns, bead bound proteins (dMi-2WT and dMi-2 mutants or GST-fusions) were titrated on Coomassie stained SDS-Page gels. Control beads and beads with bound proteins (dMi-2, dMi-2 mutants and mH2A1.1 or GST fusions) were equilibrated in binding buffer. 10 µl of bead-bound proteins were used for each pulldown. Pulldowns were performed

with the whole PARP reaction (0,5 ml) and 500 µl of binding buffer (for baculovirus expressed proteins) or in 250 µl of PARP reaction and 250 µl of binding buffer (for GST fusions) for 1 hr at 4°C. The beads were extensively washed 5 times with 1 ml of Pulldown Binding Buffer, resuspended in 2xSDS-Page loading buffer, boiled, resolved on 4-12% gradient SDS-Page gel and analysed by Western Blot. For Western blot α-PAR and α-PARP1 antibodies were used. mH2A1.1 V5-tagged was used as a positive control for PAR/PARP binding (Kustatscher et al. 2005).
Radioactive pulldown reactions were performed in the same way, in addition 2 µl of radioactive NAD+ (PerkinElmer) was added to each PAR reaction. After washing, samples were resuspended in 30 µl of SDS-loading buffer and 10 µl were loaded on the gel. The gel was dried and exposed overnight on the X-Ray film.

Pulldown Binding Buffer	50 mM Tris, pH 8,0
	200 mM NaCl
	4 mM $MgCl_2$
	0,1% (v/v) NP-40
	0,2 mM DTT

3.2.6.2 Poly(ADP-ribose) purification

For PAR purification, ten PARP reactions were set up and the reactions were allowed to proceed in a thermomixer at 500 rpm for 25 min at 37°C. The reaction product was then precipitated with 0,5 ml of ice-cold 20% (w/v) TCA and incubated on ice for 30 minutes. The polymer was pelleted by centrifugation at 11000 rpm for 10 minutes at 4 °C (Heraeus Biofuge Pico). The supernatant was removed and the pellet was resuspended in 1 ml of ice-cold 100% ethanol and incubated on ice for 10 minutes. After centrifugation at 11000 rpm for 10 minutes at 4 °C (Heraeus Biofuge Pico), the supernatant was removed and the pellet was once again washed in 1 ml of ice-cold 100% ethanol, incubated on ice for another 10 minutes and centrifuged again as previously. After complete removal of the ethanol, the poly(ADP-ribose) pellet was air-dried and dissolved in 400 µl of 500 mM KOH/NaOH to detach polymer from proteins, and incubated in a thermomixer at 500 rpm for 30 min at 50 °C. 50 µl of 1 M Tris-HCl, pH 8.0 were added resulting in a final concentration of approx. 100 mM, and the alkaline conditions were carefully adjusted to pH 7.5 with 37% HCl. For DNA degradation, $MgCl_2$ to final concentration of 10 mM and 50 U of Benzonase were

added. Samples were incubated at 550 rpm in a thermomixer for 1 hour at 37°C. Protein degradation was accomplished by adding 5 µl of proteinase K (10 mg/ml) and 10 µl of 100 mM $CaCl_2$ and incubating samples for 2 hours at 37°C in a thermomixer. 300 µl phenol:chloroform:isoamyl alcohol (25:24:1 (v/v/v)) were added and samples were vortexed and centrifuged at 13000 rpm for 10 minutes at RT (Heraeus Biofuge Pico) to separate the aqueous from the organic phase. The aqueous (upper) phase was transferred to a new reaction tube and extraction was repeated. 300 µl of chloroform:isoamyl alcohol were added and samples were centrifuged again. Upper phase was transferred to a new tube. For ethanol precipitation, 100% ethanol was added to a final concentration of 70% (v/v). Samples were incubated overnight at -20 °C before precipitated polymers were pelleted by centrifugation for at 11000 rpm for 30 minutes at 4 °C (Heraeus Biofuge Pico). Pellets were air-dried and dissolved in 100 µl of Milli-Q water and the concentration was determined by measuring the absorbance at 258 nm. Concentrations were calculated according to Lambert-Beer with a relative spectral absorption coefficient of 13,500 M-1cm-1 for mono(ADP-ribose).

3.2.6.3 PAR binding assay

Recombinant Flag-tagged proteins were purified from SF9 cells and eluted with Flag peptide. Nitrocellulose membrane was equilibrated in TBS-T buffer. 0,2 µg of dMi-2WT or BSA were spotted on the membrane and air-dried. [P^{32}]-PAR (approx. 400 µl) was diluted in 10 ml TBS-T and the membrane was incubated with [P^{32}]-PAR for 2,5 hrs at RT with gentle agitation. The membrane was washed several times with TBS-T, air-dried and visualized with a phosphorimager after 2 hour exposure.

TBS-T buffer	10 mM Tris, pH 7,4
	150 mM NaCl
	0,05% (v/v) Tween20

3.2.7 Generation of transgenic flies

For fly transgenesis, a site-specific φC31 integrase system was used (Bischof et al. 2007). This system is based on the site-specific φC31 integrase ectopically expressed in germ-line cells. The integrase mediates sequence-directed recombination between a bacterial attachment site (*attB*) flanking the construct on the integration vector and a phage

attachment site (*attP*) in a transgenic fly genome. As a result all generated flies carry a transgene integrated at the same genomic site which circumvents many problems associated with traditional, random transgenesis and allows precise *in vivo* structure/function analysis of multiple transgenes.

All constructs used for transgenic flies generation are listed in Table 3.6. For injections, the J5 strain (attP-zh86Fb/vas-phi-zh102D) with an *attP* landing site on the third chromosome was used. This strain was shown to have the highest frequency of transgenesis (Bischof et al. 2007). Injection of embryos was performed with the collaboration of the laboratory of Prof. Renate Renkawitz-Pohl.

After injection with pUASTattB constructs, F0 flies were crossed to the w1118 isogenic strain (BL # 5905) and the F1 generation was screened for orange eyes and then crossed against each other to obtain homozygotic UAS strains. Transgene integration was confirmed by PCR on genomic DNA and transgene expression was verified by Western blot analysis.

All fly strains used in this study, their genotypes and sources are listed in Table 3.14.

3.2.8 Tissue cell culture methods

Tissue cell culture work was done under sterile conditions under the hood and according to S1 laboratory safety rules.

3.2.8.1 General cell culture conditions

Kc and SL2 cells were cultured at 26°C in the incubator in Schneider's Drosophila Medium. SF9 cells were cultured at 26°C in the incubator in Sf-900 II SFM medium. *Drosophila* Kc cells were grown in the suspension in 75 cm^2 flasks and they were split by diluting with fresh medium to the density of 2-3x10^6 cells/ml every 3-4 days. SF9 cells were grown adherently in 75 cm^2 flasks and they were removed from them by pipetting or with a cell scraper. SF9 cells were split as Kc cells. Cell number was determined using a hemacytometer.

3.2.8.2 Cell freezing and thawing

For freezing, Kc cells were growing to a density of 3-5x10^6 cells/ml. Cells were spun down for 5 min at 1000 rpm at RT (Haraeus Megafuge 1.0). Cell pellet was resuspended in Schneider's Drosophila Medium (with 10% FBS) to a final cell concentration 1x10^7

cells/ml. An equal volume of Schneider's Drosophila Medium supplemented with 10% FBS and 20% DMSO was added to the cells. 1 ml of cells was aliquoted to cryo-tubes and they were frozen for 1 hr at -20°C, followed by 24-48 hrs at -80°C, before they were stored in liquid nitrogen.

For thawing, the frozen cells were slowly resuspended in 10 ml of fresh, supplemented Schneider's Drosophila Medium, spun down routinely, medium contaning DMSO was removed and cells were resuspended in fresh medium (Kc cells). Alternatively, cells after thawing were resuspended in 15 ml of Sf-900 II SFM medium and 24 hours later the medium was exchanged (SF9 cells).

3.2.8.3 Cell transfection with dsRNA

For protein knockdown experiments, Kc cells were transfected with dsRNA. For this, exponentially growing Kc cells were spun down and resuspended in serum free Schneider's Drosophila Medium (supplemented with 1% Penicilin/Streptomycin) to the density of $1x10^6$ cells/ml. 15 μg of dsRNA per well were spotted to a 6 well plate followed by adding $1x10^6$ cells. Cells were mixed gently and incubated with dsRNA for 40 min at 26°C. 1 ml of medium (20% FCS, 1% Penicilin/Streptomycin) was added to the cells and they were incubated for 3-6 days before the knockdown of protein was analysed by Western blot.

3.2.8.4 Heat shock treatment of *Drosophila* cells

Cells for heat shock were treated as previously described (Boehm et al. 2003). An equal volume of preheated medium (48°C) was added to cells, cells were incubated at 37°C for 20 min or shorter time and immediately processed for either RNA isolation or ChIP. In the latter case, heat shock was stopped by adding 1/3 volume of 4°C medium prior to formaldehyde crosslinking.

3.2.8.5 Pharmacological treatment of *Drosophila* cells

Transcription elongation inhibitor, DRB (5,6-dichloro-1-beta-D-ribofuranosyl-benz-imidazole) was added to the cell culture to the final concentration of 125 μM. PARP1 inhibitor, PJ34 (*N*-(5,6-Dihydro-6-oxo-2-phenanthridinyl)-2-acetamide hydrochloride, Alexis) was added to the cell culture to the final concentration of 5 μM. Cells were incubated with the drugs for 20 min at RT before processing for ChIP or RNA isolation.

3.2.9 Immunocytochemistry methods

3.2.9.1 Immunofluorescence of polytene chromosomes

Drosophila larvae were cultured under standard conditions at 26°C. 3rd instar wandering larvae were selected for dissection. Larvae were washed and salivary glands were dissected in PBS. For heat shock experiment, 3rd instar larvae were washed in PBS and transferred into eppendorfs (5-6 larvae). The lids of the eppendorfs were pierced with a needle to ensure oxygen supply during heat shock. Larvae were incubated for 30 min in a water bath at 37°C. Next, larvae were taken out and immediately dissected in a drop of PBS.

Dissected glands were fixed for 5 minutes in Polytene Fixing Solution on a siliconized cover slip. A cover slip was taken up by a glass microscope slide and glands were broken by tapping with the eraser side of a pencil. While tapping, the coverslip was gently moved back and forth to squash chromosomes. The squashed chromosomes were quickly checked under the light microscope (phase contrast) at 40x magnification. Sufficiently spread-out chromosomes were flattened by applying strong pressure with the thumb onto the coverslip. Each glass slide was immediately frozen in liquid nitrogen, the coverslip was removed with a scalpel and the glass slide was collected into a Coplin jar with PBS.

Collected glass slides were washed with PBS for 10 min while rotating. PBS was replaced by blocking solution (5% milk in PBS) and gentle rotation was continued for 30 min. Subsequently, the slides were rinsed in PBS, placed in a humid chamber and the squashed polytene chromosomes were covered with 40 µl of primary antibodies dilution and a fresh cover slip. All antibodies were diluted in 5% milk in PBS and 2% normal goat serum (NGS) to reduce unspecific binding of antibodies. Primary antibodies were incubated overnight at 4°C.

Then, cover slips were removed, glass slides were rinsed in PBS and washed three times in 5% milk in PBS for 5 min. Polytene chromosomes were incubated with the appropriate secondary antibodies (Table 3.3) diluted in 5% milk/PBS /2% NGS for 1 hr at RT in the dark. Slides were washed twice for 10 min with Buffer A and B, rinsed in PBS and DNA was stained with DAPI (0,2 µg/ml in PBS) for 4-5 min. Slides were washed once for 10 min in PBS, mounted with Fluoromount, sailed with nail polish and kept at 4°C in the dark.

Polytene Fixing Solution	45% acetic acid 1% formaldehyde
Wash Buffer A	PBS 300 mM NaCl 0,2% (v/v) NP-40 0,2% (v/v) Tween20
Wash Buffer B	PBS 400 mM NaCl 0,2% (v/v) NP-40 0,2% (v/v) Tween20

3.2.9.2 Immunofluorescence of *Drosophila* embryos

Embryos were collected, washed and dechorionized by incubation for 3 min a bleaching solution (3% sodium-hypochlorite). After extensive washing with tap water, embryos were transferred to 2-ml eppendorf tubes and 750 µl n-heptane/750 µl fixative (3,5 % paraformaldefyde in PBS) were added. Embryos were rotated on the wheel for 20 min at RT. The fixative was taken off (bottom phase) and 750 µl of methanol was added. Embryos were shaken vigorously for 30 sec to devitellinize them. Devitellinized embryos should sink down. The top phase, interphase embryos and most of the methanol layer were removed. Embryos were washed 3 times with methanol and 3 times in PBS-Tx.

Before staining, embryos were blocked in PBS-Tx/2% NGS for 1 hr on the wheel at RT. Embryos were then incubated with the appropriate primary antibodies diluted in PBS-Tx/2% NGS overnight on the wheel at 4°C. Subsequently, embryos were rinsed 2 times, then washed 2 times for 30 min in PBS-Tx. Embryos were incubated with the appropriate secondary antibodies diluted in PBS-Tx/2% NGS for 2 hrs on the wheel at RT in the dark. Embryos were again washed as after primary antibodies, stained with DAPI (0,05 µg/ ml) for 10 min and washed 2 times for 5 min in PBS-Tx. Embryos were mounted with SlowFade antifade Kit according to the manufacturer's instructions, sealed with nail polish and kept at 4°C in the dark.

PBS-Tx	PBS 0,1% (v/v) Triton-X

3.2.9.3 Immunofluorescence of *Drosophila* ovaries

Wild type OrR virgins were collected, mated with males and kept under standard conditions at 26°C for 2-3 days. Females were collected and kept on ice while ovaries were dissected. Ovaries were dissected in PBS-Tx and ovarioles were separated with a needle. Ovaries were fixed in a fixing solution (1:1 mixture of n-heptane and 5 % paraformaldefyde in PBS) for 15 min on the wheel at RT. Ovaries were washed 3 times for 5 min in PBS-Tx and blocked in PBS-Tx/2% NGS for 1 hr on the wheel at RT. Ovaries were then incubated with the appropriate primary antibodies diluted in PBS-Tx/2% NGS overnight on the wheel at 4°C. Subsequently, ovaries were washed 4 times for 30 min in PBS-Tx followed by incubation with the appropriate secondary antibodies diluted in PBS-Tx/2% NGS for 2-4 hrs on the wheel at RT in the dark. Ovaries were washed 2 times for 10 min in PBS-Tx, then they were washed for 1 hr with RNAse A (20 µg/ml) in PBS-Tx. Ovaries were stained with DAPI in PBS-Tx for 10 min, rinsed and washed for 15 min in PBS-Tx. Ovaries were mounted with SlowFade antifade Kit according to the manufacturer's instructions, sealed with nail polish and kept at 4°C in the dark.

3.2.10 Bioinformatics tools and methods

DNA and protein sequences were obtained from Flybase (http://flybase.org), NCBI (http://www.ncbi.nlm.nih.gov) or Expasy Proteomics Server (http://www.expasy.ch).

DNA sequence analysis was performed using The Basic Local Alignment Search Tool (BLAST).

For multiple protein sequence alignments and phylogenetic tree generation ClustaW (http://www.ebi.ac.uk) was used, sequences were subsequently displayed using a multiple sequence alignment editor Jalview (Waterhouse et al. 2009). Protein domains were analysed using different family and domain databases like ScanProsite, Pfam or Smart (http://www.expasy.ch).

Protein structures were retrieved from PDB (http://www.rcsb.org/pdb/home) and protein figures were performed with PyMOL (http://www.pymol.org).

For cloning and site directed mutagenesis, primers were designed with the help of EnzymeX and tools from Sequence Manipulation Suit (http://www.bioinformatics.org/sms2). Primer3 (http://frodo.wi.mit.edu/primer3) was used for primer design for Chips. Primers for QPCR assays for gene expression analysis were designed with The

ProbeFinder software (Roche Universal Probe Library). Primers for knockdown experiments for dsRNA synthesis were obtained from GenomeRNAi (http://ranai.dkfz.de).

4. Objectives

Two main research objectives of this doctoral work have been defined:

I. Biochemical and functional characterization of a novel ATP-dependent chromatin remodeler, dCHD3.

II. Investigation of a potential role of dMi-2 in active gene transcription.

4.1 Biochemical and functional characterization of dCHD3

Drosophila melanogaster comprises four members of CHD remodelers: dMi-2, dCHD3, dCHD1 and Kismet. All CHD proteins in *Drosophila* studied to date have been implicated in transcription regulation. If and how they differ in their chromatin remodeling activities is not well understood. One objective of this PhD thesis is to characterize a novel chromatin remodeler, dCHD3, which has not been studied to date. Although, dCHD3 is highly similar to dMi-2, it lacks several domains important for regulation of dMi-2 enzyme activity. Given these differences, it is plausible that dCHD3 and dMi-2 differ in their mechanisms of nucleosome remodeling. To address this issue, both remodelers will be compared in various biochemical assays *in vitro*. Substrate recognition, ATPase activation and nucleosome remodeling by dCHD3 and dMi-2 will be analysed thoroughly. Furthermore, biological functions of dCHD3 will be investigated. Given the similarity of dCHD3 to dMi-2, it is possible that it exists in a similar, dNuRD-like complex. Thus, it will be tested whether dCHD3 is a part of dMi-2-like complexes or whether it exists in a new complex or alternatively, as a monomer *in vivo*. To this end, new antibodies against dCHD3 have been obtained which will be applied for various biochemical and cell biology assays in cell culture and in different tissues and developmental stages of *D. melanogaster*. A systematic comparison of dCHD3 and dMi-2 in biochemical and functional studies constitutes a first attempt of comprehensive analysis of CHD remodelers in a model organism, *D. melanogaster*.

4.2 dMi-2 in active gene transcription

The second main objective of this thesis is to investigate a possible novel role of dMi-2 in active transcription. Initial indirect immunofluorescence staining of dMi-2 at sites of euchromatin on polytene chromosomes has suggested that dMi-2 might be involved in

active transcription (Murawsky et al. 2001). In order to study dMi-2 role in active genes, heat shock genes will be applied as a model. Binding of dMi-2 to active genes will be analysed by using both immunofluorescence and chromatin immunoprecipitation methods. Another objective within this project is to determine a possible function of dMi-2 in transcription. To this end, RNAi technology as well as ectopic expression of dMi-2 catalytically inactive mutant will be applied in flies. Finally, a mechanism of recruitment of dMi-2 to active genes will be studied in detail using biochemical, genetic and pharmacological assays.

Given that dMi-2 has been mostly implicated in transcriptional repression, investigation of dMi-2 role on active genes could bring novel and exciting insights into our current knowledge about this remodeler.

5. Results

5.1 Biochemical characterization of *Drosophila* CHD3

The *Drosophila* genome encodes four CHD family members: dMi-2, dCHD1, Kismet and dCHD3. dCHD3 is the only member of this family which has not been studied to date. dCHD3 and dMi-2 possess the highest amino acid sequence similarity within the family (67% identity and 77% similarity) (Fig. 5.1 A). dCHD3 comprises one PHD finger, two chromodomains, an ATPase/helicase domain and a short C-terminal domain. In comparison to dMi-2, dCHD3 lacks several important domains: two N - terminal domains - a CHDNT domain with unknown function and one PHD finger. In addition, dCHD3 lacks most of the C-terminus which modulates the ATPase activity of dMi-2 (Fig. 5.1 A) (Bouazoune et al. 2002). The differences suggest that these two proteins may differ in their DNA/nucleosome binding, ATP-dependent remodeling and nucleosome-positioning activities. Given that dCHD3 and dMi-2 differ in protein domains known to regulate ATPase and nucleosome positioning activities, we were prompted to characterize for the first time dCHD3 enzyme both biochemically and functionally. Comparison of dCHD3 to the highly related dMi-2 allowed to gain insights into dCHD3's mechanism of action and contributed to our current knowledge of CHD enzymes.

5.1.1 Sequence analysis of dCHD3

The *dCHD3* gene is referred to in FlyBase by the symbol Chd3 (CG9594, FBgn0023395) and based on sequence similarity it encodes a putative ATP-dependent chromatin remodeler. It has one annotated transcript and one annotated polypeptide. Protein sequence alignment revealed highest sequence similarity to dMi-2 (Fig 5.1 A). dMi-2 is a highly conserved remodeler, found in all invertebrate and vertebrate species. To check whether the same applies to dCHD3, *Drosophila* genomes of all twelve sequenced species were search for the presence of dMi-2 and dCHD3 coding genes. As expected, dMi-2 was found in all genomes examined. Genes encoding dCHD3 protein were identified in *D. simulans*, *D. sechellia*, *D. yakuba*, and *D. erecta* (*D. melanogaster* subgroup). By contrast, no dCHD3 sequences were found in *D. ananassae* (*D. melanogaster* group) or in more distantly related *Drosophila* species (Fig. 5.1 B). The evolutionary relationship suggests that the *dCHD3* gene originated more than 10 million years ago most likely by a gene

duplication event (Fig. 5.1 B). The dCHD3 coding gene was not found in any other species. This indicates that it is specific for the *Drosophila melanogaster* subgroup.

As dCHD3 possesses a putative ATPase activity, it was important to determine whether it is an active enzyme. To address this issue, the protein sequences of the ATPase/helicase domains of dCHD3, dMi-2, dCHD1, Kismet, ISWI, and Brahma were aligned. This revealed the conservation of all important ATPase domain motifs in dCHD3 (Fig 5.1 C). Accordingly, this result indicates that the enzymatic activity of the putative ATP-dependent chromatin remodeler has been maintained through evolution.

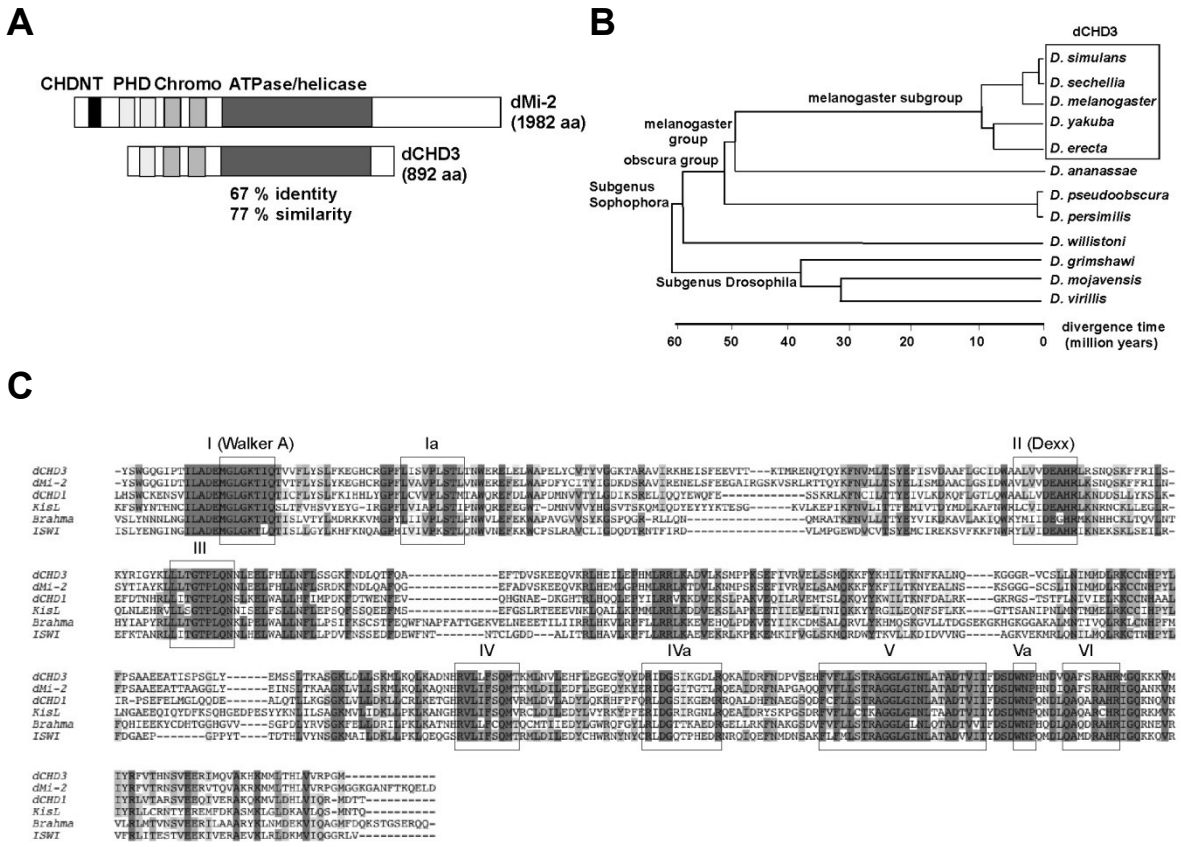

Figure 5.1 Sequence analysis of dMi-2 and dCHD3
(**A**) Schematic representation of dMi-2 and dCHD3. CHDNT; domain found in PHD/RING finger and chromo domain-associated helicases, belongs to HMG box-like domains (Pfam number: PF08073); PHD, PHD finger; Chromo, chromodomain; aa, amino acids. (**B**) Phylogenetic tree of *Drosophilae* (based on http://insects.eugenes.org/species/). Species with *dCHD3* genes are boxed. (**C**) Multiple sequence alignment of the ATPase/helicase domains of *D.melanogaster* CHD, Brahma and ISWI chromatin remodelers. Conserved regions are shaded in dark grey (strongly conserved) or light grey (moderately conserved). Helicase specific motifs are indicated with boxes. Figure taken from (Murawska et al. 2008).

5.1.2 Characterization of dCHD3 ATPase activity

Multiple sequence alignment of the ATPase/helicase domain of dCHD3 and other chromatin remodelers (Fig. 5.1 C) strongly suggests that dCHD3 possesses ATPase activity. In order to confirm this, a baculovirus expressing recombinant Flag-tagged dCHD3 was generated. dCHD3Flag and dMi-2Flag were affinity purified from extracts of baculovirus-infected SF9 cells (Fig. 5.2 A). The ATPase activity of both proteins was determined in the absence and in the presence of naked DNA or polynucleosomes assembled with native *Drosophila* histone octamers. dMi-2 had very low basic activity in the absence of any effector and in the presence of DNA. However, it displayed a strong activation in the presence of nucleosomes. These results are in agreement with previously published work (Brehm et al. 2000). dCHD3 had low basic ATPase activity. However, in the presence of DNA, it clearly displayed a modest activity (twofold) and a robust nucleosome stimulated ATPase activity (fivefold) (Fig. 5.2 B). Incubation of the reaction in the presence of increasing DNA amounts did not significantly change the stimulation of dMi-2 and dCHD3 ATPase activity, indicating that DNA was not limiting (Fig. 5.2 C). The ATPase assays clearly showed that dCHD3 is an ATPase which is stimulated preferentially by nucleosomes and to a lesser extent by DNA.

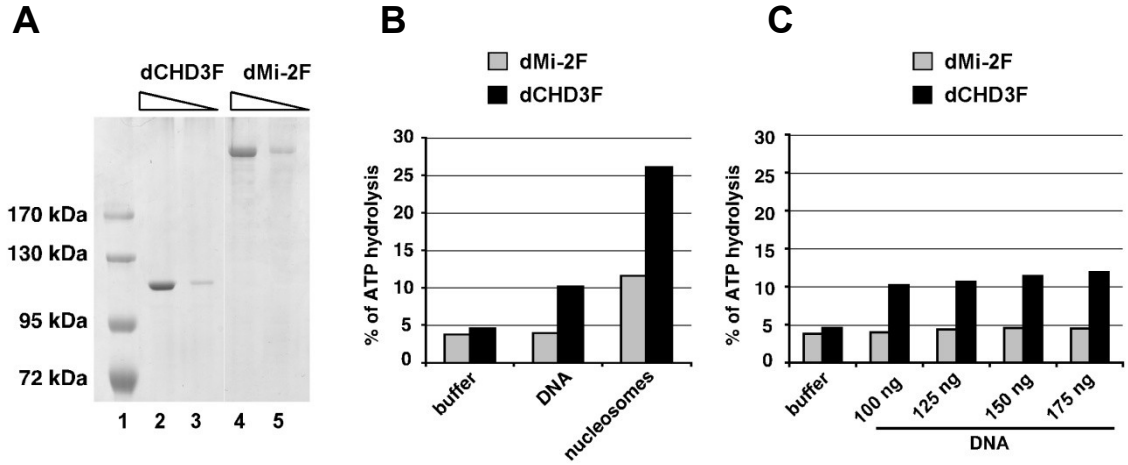

Figure 5.2 dCHD3 has DNA and nucleosome-stimulated ATPase activity *in vitro*
(**A**) Coomassie-stained gel showing recombinant proteins used for ATPase assays. Lane 1, molecular weight standard; lanes 2 and 3, Flag-tagged dCHD3 (36 and 9 pmol); lanes 4 and 5, Flag-tagged dMi-2 (36 and 9 pmol). (**B**) ATPase assay. 2.7 pmol of dMi-2 and dCHD3 were incubated in the absence or presence of 100 ng DNA or nucleosomes and [γ-^{32}P]ATP as indicated. (**C**) ATPase assay. 2.7 picomol of dMi-2 and dCHD3 were incubated in the absence or presence of increasing concentrations of DNA and [γ-^{32}P]ATP as indicated. Percentage of hydrolysed ATP was

determined by thin layer chromatography and quantified by phosphorimager analysis (**B** and **C**). Figure taken from (Murawska et al. 2008).

To investigate the ATPase activity of dCHD3 in more detail, the role of histone tails was investigated. The activity of some ATPases, like ISWI, depends on the presence of histone N-terminal tails (Clapier et al. 2001). By contrast, other remodelers, like dMi-2 or SWI/SNF, do not require histone tails for their activation (Whitehouse et al. 1999; Brehm et al. 2000). To examine the role of histone tails for dCHD3 ATPase stimulation, nucleosomes were subjected to a limited trypsin digestion. This treatment removed histone tails leading to faster migration of histones in an SDS-PAGE gel (Fig. 5.3 A). Incubation of dCHD3 with nucleosomes treated with trypsin did not impair the ATPase activity of the enzyme (Fig 5.3 B). This indicates that, similarly to dMi-2, activation of the dCHD3 ATPase does not require histone tails.

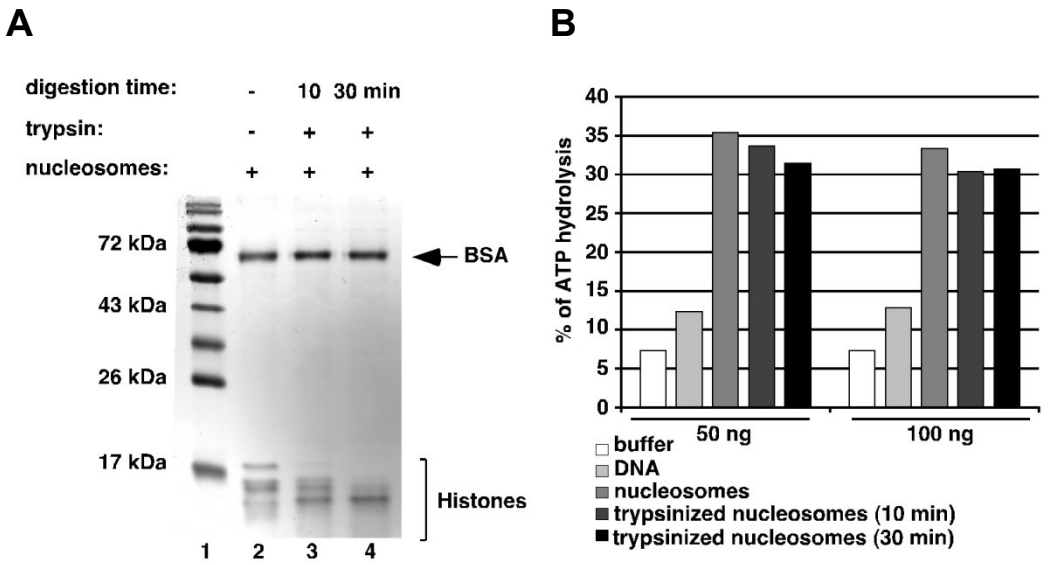

Figure 5.3 dCHD3 ATPase does not require histone tails
(**A**) Polynucleosomes were digested with trypsin for 10 (lane 3) or 30 min (lane 4) as indicated. Histones were visualized by Coomassie staining following SDS-PAGE gel electrophoresis. Positions of bovine serum albumin (BSA) and histones are indicated on the right. The presence or absence of trypsin is indicated on the top of the gel. (**B**) 50 and 100 ng of trypsinized nucleosomes were incubated with dCHD3 as indicated. Percentage of hydrolysed ATP was determined by thin layer chromatography and quantified by phosphorimager analysis. Figure taken from (Murawska et al. 2008).

5.1.3 dCHD3 binds DNA and mononucleosomes *in vitro*

The activation of dCHD3 by DNA and nucleosomes suggests that the remodeler could be able to recognize and bind to nucleosomal DNA. To test this possibility, dCHD3 and dMi-2 were compared in DNA and nucleosome binding mobility shift assays. Both remodelers displayed DNA binding to 200 bp DNA fragments. dCHD3 formed distinct complexes with DNA that were stable during electrophoresis through native polyacrylamide gels (Fig. 5.4 A, left panel, lanes 3 to 8). Increasing concentrations of dCHD3 led to the formation of up to four complexes with decreased mobility. This suggests that several dCHD3 molecules can simultaneously bind the DNA probe. As reported previously (Bouazoune et al. 2002), dMi-2/DNA complexes had a low mobility and did not enter the gel (Fig. 5.4 A, right panel, lanes 9 to 14).

To monitor nucleosome binding properties of dCHD3, two mononucleosomes that differ in the position of the octamer relative to the end of a 200 bp DNA fragment were used (Fig. 3.3). dCHD3 was binding to both types of mononucleosomes and again formed distinct complexes when the remodeler concentration was increased (Fig 5.4 B, left panel, lines 3 to 8). dMi-2 binding to mononucleosomes led to the formation of complexes with high molecular masses of low mobility (Fig 5.3 B, right panel, lines 9 to 14).

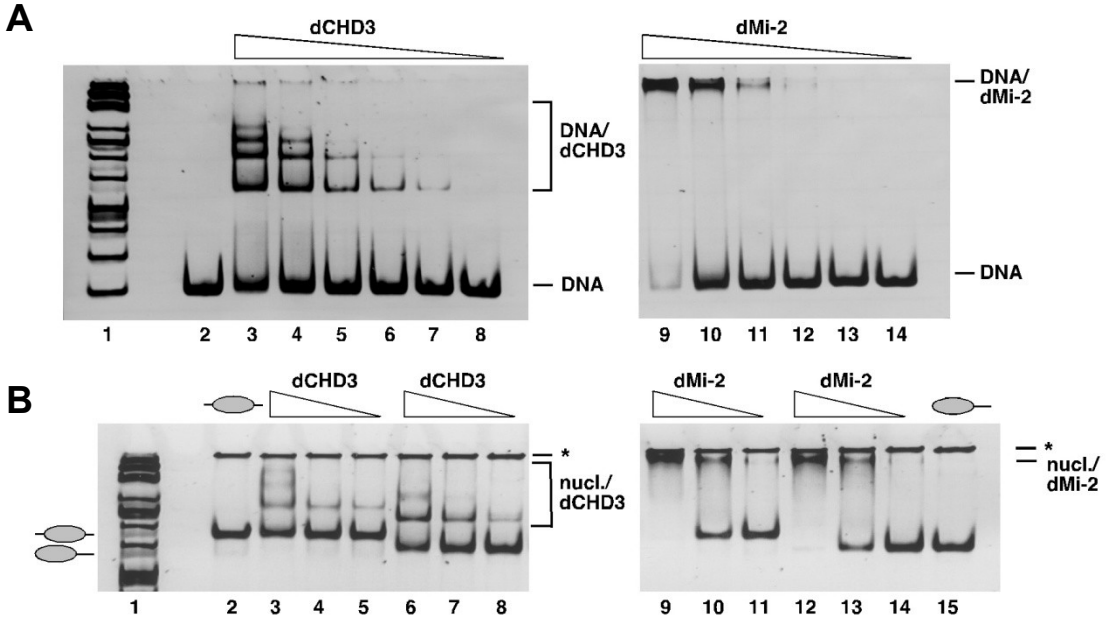

Figure 5.4 dCHD3 binds DNA and mononucleosomes *in vitro*

(**A**) Decreasing amounts of dCHD3 (lane 3, 18 pmol; lane 4, 9 pmol; lane 5, 3.6 pmol; lane 6, 1.8 pmol; lane 7, 0.9 pmol; and lane 8, 0.36 pmol) and dMi-2 (lane 9, 18 pmol; lane 10, 9 pmol; lane 11, 3.6 pmol; lane 12, 1.8 pmol; lane 13, 0.9 pmol; and lane 14, 0.36 pmol) were incubated with a 200 bp DNA fragment, and complexes were resolved by native agarose gel electrophoresis. The positions of DNA/protein complexes and unbound DNA are indicated on the right. (**B**) Decreasing amounts of dCHD3 (lanes 2 and 6, 18 pmol; lanes 3 and 7, 9 pmol; and lanes 4 and 8, 3.6 pmol) and dMi-2 (lanes 9 and 12, 18 pmol; lanes 10 and 13, 9 pmol; and lanes 11 and 14, 3.6 pmol) were incubated with centrally (lanes 2 to 5 and 9 to 11) or distally positioned (lanes 6 to 8 and 12 to 15) mononucleosomes. Complexes were resolved by native polyacrylamide gel electrophoresis. The positions of complexes are indicated on the right, and the positions of unbound mononucleosomes are indicated on the left. Asterisks denote assembled plasmid backbone that remains in the well. Nucl., nucleosome. Figure taken from (Murawska et al. 2008).

5.1.4 dCHD3 mobilizes mononucleosomes *in vitro*

It is conceivable that the nucleosome stimulated ATPase activity of dCHD3 as well as its ability to bind to mononucleosomes results in nucleosome remodeling. In order to address this issue directly, a mononucleosome mobilization assay was performed. Two 200 bp DNA fragments bearing the '601' nucleosome positioning sequence either in the centre or near the end were used for the assembly (Fig. 3.3). Assembly onto these DNA fragments produced two mononucleosomes that differ in the relative position of the histone octamer and in electrophoretic mobility on a native polyacrylamide gel (middle- and end-positioned nucleosomes) (Fig. 5.5, compare lanes 2 and 9).

As shown previously, dMi-2 mobilized mononucleosomes in an ATP-dependent manner. Furthermore, both types of nucleosomes were remodeled to the same extent (Fig 5.5 upper panels). Like dMi-2, dCHD3 also displayed nucleosome mobilization activities on both substrates (Fig 5.5 lower panels). In some reactions several bands were visible which probably reflects differently positioned nucleosomes (Fig. 5.5, upper panel, lane 5, and lower panel, lane 8). In some cases, a slightly faster migrating product than the end-positioned nucleosomes was generated (Fig. 5.5, lower left panel, compare lanes 8 and 9). This suggests that the histone octamer has been pushed over the edge and is no longer making contact with all 146 bp of DNA, consequently the migration of this particle is faster (Gutiérrez et al. 2007).

Despite of many similarities that dCHD3 and dMi-2 share in the remodeling activities, also some striking differences were observed. First, lower concentrations of dCHD3 than dMi-2 were required to show a nucleosome mobilization effect (compare upper with lower panels, line 8), which implies higher activity of dCHD3 enzyme. Second, dCHD3 produced a significant amount of free DNA when the centrally positioned

mononucleosome was used as a substrate (Fig. 5.5, left lower panel, lanes 5 and 6), suggesting that dCHD3 is capable of removing octamers from DNA.

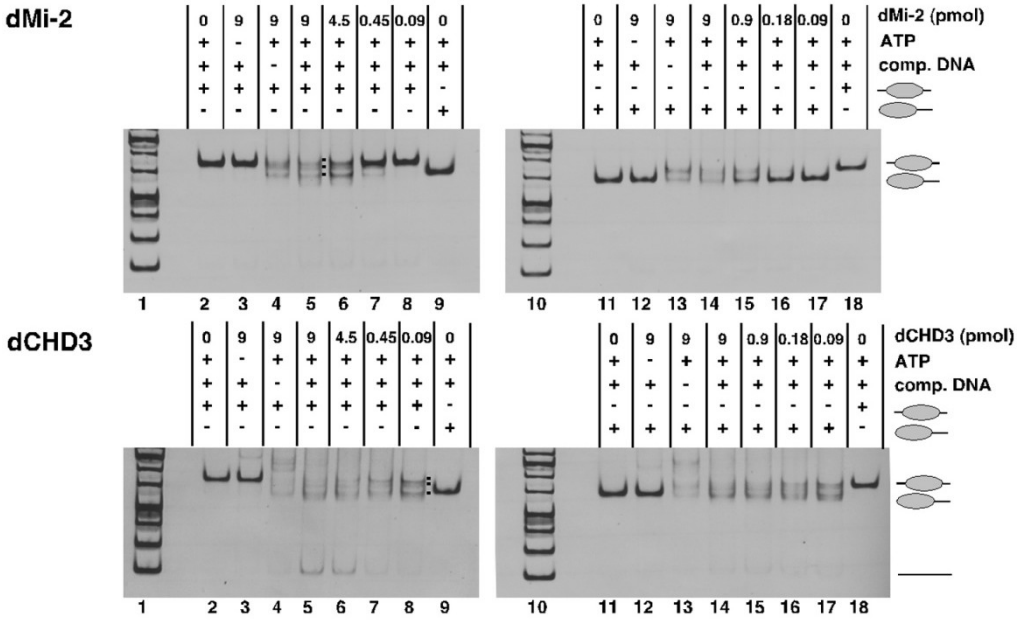

Figure 5.5 dCHD3 and dMi-2 remodel mononucleosomes *in vitro*.
dMi-2 (upper panels) and dCHD3 (lower panels) were incubated with positioned mononucleosomes (left panels -incubation with centrally positioned mononucleosomes, and right panels-incubation with distally positioned mononucleosomes) as indicated on top. Lanes 3 to 5 and 12 to 14, 9 pmol protein; lane 6, 4.5 pmol; lane 15, 0.9 pmol; lane 7, 0.45 pmol; lane 16, 0.18 pmol; lanes 8 and 17, 0.09 pmol; lanes 2, 9, 11, and 18, no protein. Nucleosome mobilization was visualized by ethidium bromide staining following native polyacrylamide gel electrophoresis. Positions of free DNA (straight line) and mononucleosomes (ovals) are indicated on the right. Comp. DNA, competitor DNA used to stop the reaction. Figure taken from (Murawska et al. 2008).

To assess possible differences in the mechanism of nucleosome remodeling by dCHD3 and dMi-2, a kinetic analysis using the middle positioned mononucleosome was performed. Remodeling reactions were stopped after various time points and the reaction products were analysed on native gels (Fig. 5.6). The analysis revealed that within 10 min, approximately 50% of nucleosomes have been mobilized by dMi-2 (Fig. 5.6, left panel). Longer incubation of the reaction did not change the position of nucleosomes significantly (Fig. 5.6, compare left panel, lines 8 and 9). By contrast, dCHD3 was capable to move 50% of middle positioned nucleosomes in as short a time as 5 seconds. dCHD3 continued to mobilize nucleosomes for 30 min, as at this time point most of them were repositioned (Fig. 5.6, right panel, compare lane 13 and 19). In addition, an increase in the amount of

free DNA became detectable only after 10 min. These results suggest that dMi-2 and dCHD3 differ in their reaction kinetics *in vitro*. Moreover, nucleosome mobilization and octamer removal by dCHD3 seem to be consecutive events, with nucleosome movement occurring earlier than octamer removal.

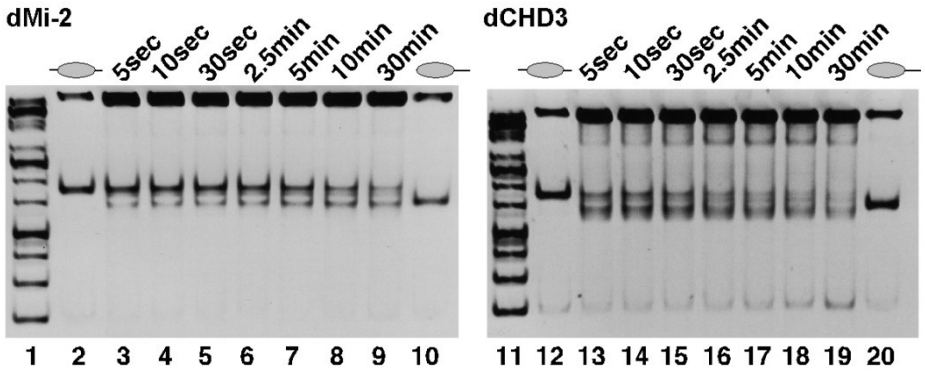

Figure 5.6 Kinetics analysis of mononucleosome remodeling by dMi-2 and dCHD3
dMi-2 (9 pmol; left panel) and dCHD3 (9 pmol; right panel) were incubated with centrally positioned mononucleosomes. Reactions were stopped at the times indicated at the top of the panels and directly analysed by native polyacrylamide gel electrophoresis. Figure taken from (Murawska et al. 2008).

5.1.5 Chromodomains are essential for dCHD3 remodeling activities

dCHD3 contains several protein domains that are potentially involved in the regulation of the remodeling reaction by the ATPase and/or the binding of the enzyme to the substrate. As reported previously, dMi-2 chromodomains are important for the remodeling activities (Bouazoune et al. 2002). In order to get insight into dCHD3 domain function, several truncated mutants of dCHD3 were generated and affinity purified from extracts of baculovirus-infected SF9 cells (Fig. 5.7).

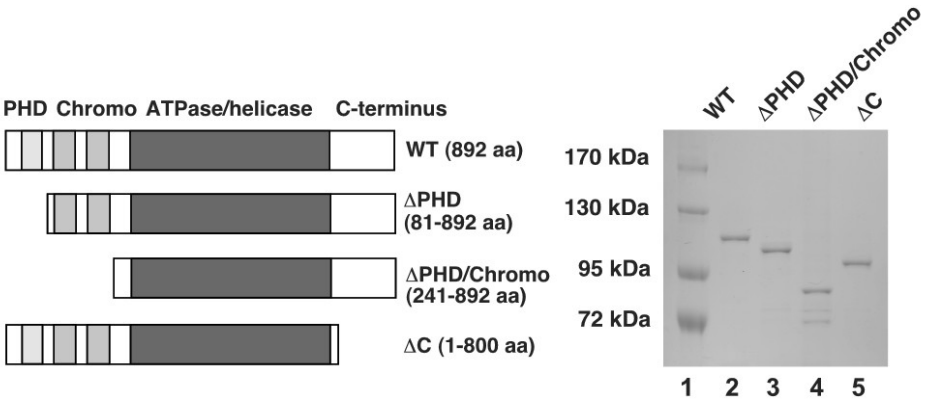

Figure 5.7 dCHD3 deletion mutants
Left panel, schematic representation of dCHD3 deletion mutants. Domains are indicated on top. PHD, PHD finger; Chromo, Chromodomains. Right panel, Coomassie Blue-stained gel showing recombinant Flag-tagged dCHD3 wild type (WT) (line 2) and indicated mutants (lines 3-5). 500 ng of each protein were loaded on the gel. Lane 1, molecular weight standard. Figure taken from (Murawska et al. 2008).

First, dCHD3 mutants were tested for ATPase activity in the absence and in the presence of DNA or nucleosomes. The deletion of the PHD finger (ΔPHD) did not abrogate ATPase activity and the enzyme was stimulated with DNA and nucleosomes to the similar extent as wild type dCHD3 (Fig. 5.8 A). However, the deletion of the C-terminus (ΔC) led to a noticeable increase of DNA-stimulated ATPase activity (from twofold to fourfold) (Fig. 5.8 A, compare samples with 100 ng of DNA). The activation by nucleosomes was modestly decreased in this mutant. The mutant lacking both PHD finger and chromodomains (ΔPHD/Chromo) retained basal ATPase activity but was no longer stimulated by DNA or nucleosomes.

Next, the same mutants were tested in DNA and nucleosome binding assays (Fig. 5.8 B).

The deletion of the PHD finger or the C-terminus did not abrogate DNA or nucleosome binding. However, the mutant lacking both PHD finger and chromodomains failed to bind DNA and nucleosomes (Fig 5.8 B upper and lower panel). These results indicate that dCHD3 chromodomains are essential for nucleosome-stimulated ATPase activity and DNA and nucleosome binding of dCHD3. Thus, it was plausible to test whether chromodomains have a role in nucleosome remodeling by dCHD3.

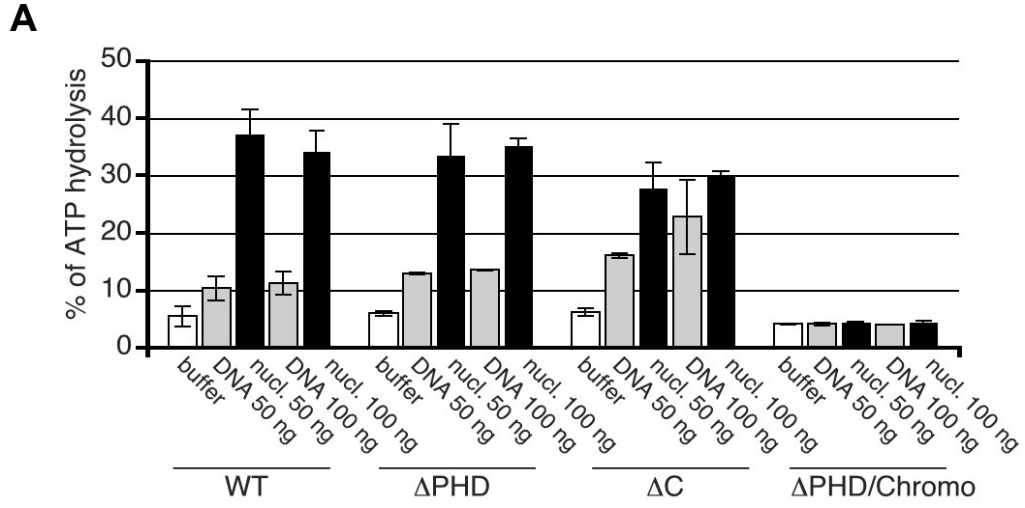

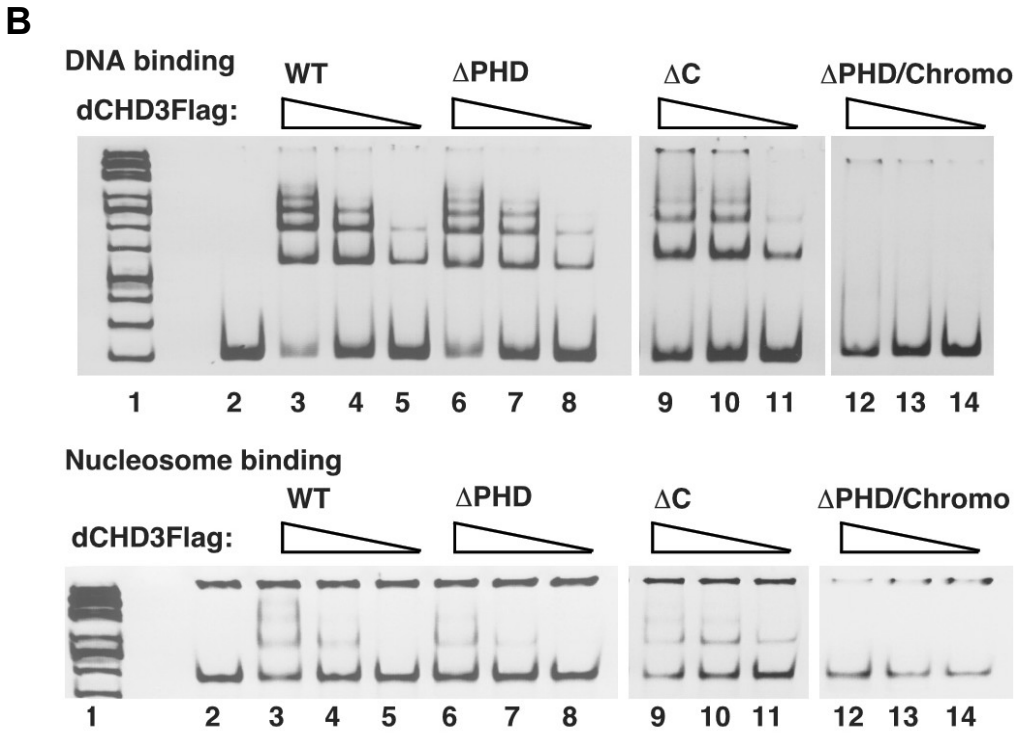

Figure 5.8 dCHD3 chromodomains are essential for ATPase, DNA and nucleosome binding activities of the remodeler
(**A**) Analysis of ATPase activity of dCHD3 mutants**.** Recombinant dCHD3 proteins (2.7 pmol) were incubated in the absence or presence of DNA or nucleosomes (nucl.) and [γ-32P]ATP as indicated. Percentage of hydrolysed ATP was determined by thin layer chromatography and quantified by phosphorimager analysis. Error bars indicate standard error of the mean (SEM) from 2-3 independent experiments.
(**B**) Eighteen picomoles (lanes 3, 6, 9 and 12), 9 pmol (lanes 4, 7, 10 and 13), or 1.8 pmol (lanes 5, 8, 11 and 14) of protein were incubated with DNA and middle-positioned mononucleosomes as indicated. Complexes were resolved by native polyacrylamide gel electrophoresis and visualized by ethidium bromide staining. Lanes 1, molecular weight marker; lanes 2, DNA (upper panel) and nucleosome (lower panel) binding. Figure taken from (Murawska et al. 2008).

dCHD3 mutants were subjected to mononucleosome mobilization assays with middle positioned nucleosomes as a substrate (Fig. 5.9). The activity of mutants retaining the chromodomains (ΔPHD and ΔC) was comparable to that of the wild type (compare left and right panel of Fig. 5.9 with Fig. 5.5, lower left panel). In addition, in reactions containing the C-terminal domain mutant (ΔC) less free DNA was detected which suggests that octamer removal may be slightly impaired in this mutant. This agrees with the ATPase assay (Fig. 5.8 A) where nucleosome stimulated ATPase activity of this mutant was also modestly decreased. By contrast, the mutant lacking the chromodomains (ΔPHD/Chromo) displayed no detectable nucleosome mobilization activities (Fig. 5.9, middle panel).

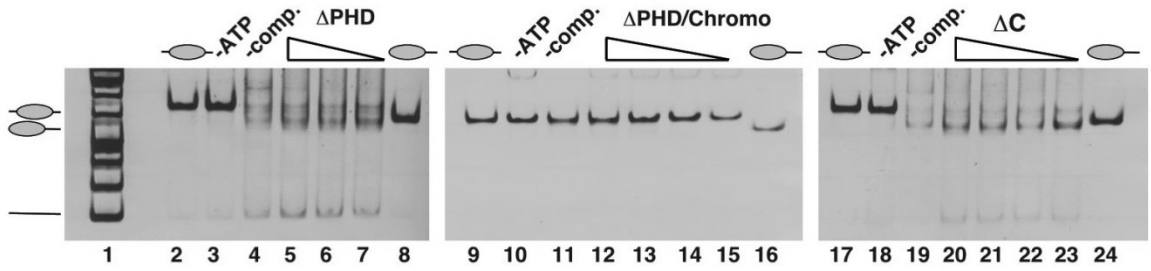

Figure 5.9 dCHD3 chromodomains are essential for nucleosome remodeling *in vitro*
Recombinant dCHD3 deletion mutants were incubated with centrally positioned mononucleosomes as indicated. Nucleosome mobilization was visualized by ethidium bromide staining following native acrylamide gel electrophoresis. Positions of free DNA (straight line) and mononucleosomes (ovals) are indicated on the left. Lanes 3 to 5, 10 to 12, and 18 to 20, 9 pmol of recombinant protein; lanes 6, 13, and 21, 4.5 pmol; lanes 7, 14, and 22, 2.25 pmol; lanes 15 and 23, 0.45 pmol; lanes 2, 9, 17, centrally positioned nucleosome; lanes 8, 16, and 24, distally positioned nucleosome. -ATP, ATP was omitted; -comp., no competitor DNA was used to stop the reaction. Figure taken from (Murawska et al. 2008).

Taken together, these results are in agreement with the view that the chromodomains of dCHD3 are essential for nucleosome stimulated ATPase, DNA/nucleosome binding and ATP-dependent nucleosome mobilization activities of this remodeler. In addition, the C-terminus seems to modulate the stimulation of ATP activity by DNA.

5.2 *In vivo* analysis of dCHD3

Biochemical characterization of dCHD3 revealed that it is a novel and potent ATPase *in vitro*. Despite of many similarities, dCHD3 differs from dMi-2 with regard to higher ATPase activity, stimulation by DNA and octamer removal from mononucleosomes. This raised the question whether and to which extent these remodelers differ in their functions *in vivo.*

5.2.1 Expression analysis of dCHD3 and dMi-2

In order to gain the first insight into the temporal expression profile of dCHD3, whole cell extracts were prepared from different developmental stages of *Drosophila*. Extracts were immunoprecipitated with specific antibodies raised against dCHD3 and dMi-2 followed by Western blot analysis (for antibody specificity tests see Fig. 3.1).

Anti-dCHD3 antibodies recognized a single band with an apparent molecular weight of above 100 kDa. This signal is consistent with the predicted molecular weight of dCHD3, which contains 892 amino acids and with the migration of recombinant dCHD3 (Fig. 5.2 A). In addition, this band disappeared after dCHD3 knockdown in a *Drosophila* cell line (Fig. 5.14 A) which strongly indicated that the observed band corresponds to endogenous dCHD3.

Analysis of extracts from different developmental stages revealed that dCHD3 was most strongly expressed in early embryos (0-3 hrs after egg deposition) (Fig. 5.10 A, lower panel, lane 1). Afterwards expression became weaker, until it dropped down in older embryos (9-24 hrs after egg deposition) (Fig. 5.10 A, lower panel, lanes 2-4). No dCHD3 was detected in larval and pupal stages (Fig. 5.10 A, lower panel, lanes 5-8). By contrast, dMi-2 was detected in all embryonic stages tested, with a peak around 6 to 9 hrs after egg deposition (Fig. 5.10 A, upper panel, lanes 1-4). dMi-2 levels declined sharply and became undetectable at larval stage, then weak dMi-2 expression was observed again at pupal stages (Fig. 5.10 A, upper panel, lanes 5-8).

Larvae extracts usually contain a lot of fat from fat tissue, which may interfere with immunoprecipitation or Western blot analysis. To exclude that this has adversely affected detection of dMi-2 and dCHD3, extracts as a control, were probed with an antibody recognizing an unrelated protein, RBF1. In agreement with published work, RBF1 levels remain relatively constant throughout embryonic and larval development (Stevaux et al. 2005) (Fig. 5.10 A).

dCHD3 and dMi-2 expression was also tested in adult flies. Female and male adult flies showed strong differences in dMi-2 and dCHD3 expression. No dCHD3 and only very little dMi-2 was detectable in extracts prepared from male flies, whereas strong expression of both proteins was apparent in extracts from female flies. This finding suggests that both remodelers are expressed in ovaries. To test this, ovaries dissected from adult female flies were stained with antibodies against dCHD3 and dMi-2 and indirect immunofluorescence was performed. As expected, both remodelers were detected in the nucleus of the oocyte as well as in the nuclei of follicle and nurse cells in ovaries (Fig. 5.10 B).

These results demonstrate that dMi-2 and dCHD3 expression is tightly regulated during development, is sex specific in adult flies, and suggest a significant maternal deposition of dMi-2 and dCHD3.

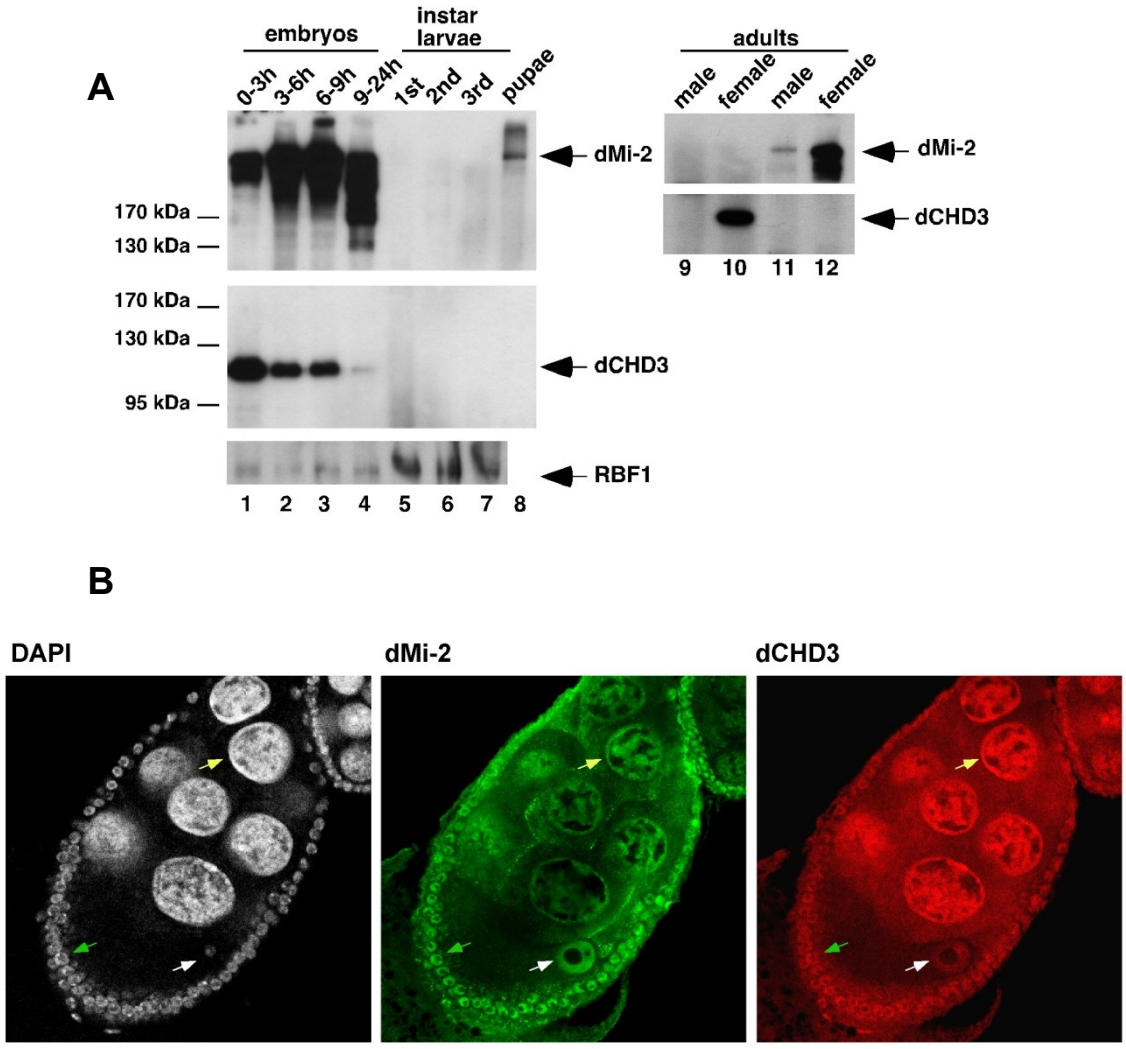

Figure 5.10 dCHD3 expression pattern in different developmental stages and ovaries
(**A**) Extracts derived from different developmental stages were immunoprecipitated and subjected to Western blot analysis as indicated using the following antibodies: for dMi-2, anti-dMi-2(N); for dCHD3, #5; and for RBF1, DX3. Antibodies used for immunoprecipitation were, for lanes 1 to 8, anti-dMi-2 (4D8, upper panel), anti-dCHD3 (7A11, middle panel), and anti-RBF1 (DX3, bottom panel); for lanes 9 and 10, anti-dCHD3 (7A11); and for lanes 11 and 12, anti-dMi-2 (4D8). Figure taken from (Murawska et al. 2008).
(**B**) Indirect immunofluorscence of *Drosophila* ovaries. Ovaries were stained with the following antibodies: anti-dCHD3 (7A11) and anti-dMi-2(N). DNA was counterstained with DAPI. Ovaries were analysed under confocal microscopy. White arrow: oocyte nucleus, green arrow: follicle cell nucleus, yellow arrow: nurse cell nucleus.

5.2.2 Subcellular localization analysis of dCHD3 and dMi-2 during *Drosophila* embryogenesis

As the analysis of dCHD3 expression showed the highest level of this protein in early embryos, it was possible to investigate its subcellular localization by direct comparison to dMi-2.

Drosophila embryo development provides a particularly useful system to study factor subcellular localization. The initial nuclear divisions in embryos are rapid, synchronous, and syncytial which allows to follow the protein behaviour during cell cycle progression. The embryo carries out 13 cycles of nuclear division and DNA replication until cellularization of the blastoderm. Between nuclear cycles four and ten, the majority of the nuclei migrate to the cortex where they form a syncytial blastoderm that undergoes four more rounds of nearly synchronous mitotic cycles. At this point, a large number of nuclei are clearly visible, and can be followed simultaneously. In addition, zygotic transcription commences (Sullivan et al. 2000).

To get insight into subcellular localization of dCHD3 and dMi-2 during embryogenesis, embryos at different stages were stained by indirect immunofluorescence with antibodies against dCHD3 and dMi-2 and analysed with a confocal microscope. Expression of dMi-2 and dCHD3 was detected in nuclei before their migration to the cortex of the preblastoderm embryo (Fig. 5.11 A) and both proteins remained nuclear after migration (Fig. 5.11 B). Interestingly, dCHD3 staining of mitotic nuclei resembled DNA staining with DAPI (Fig. 5.11 C). This indicates that dCHD3 stayed associated with condensed chromosomes in mitotic nuclei where dMi-2 displayed a more diffuse nuclear staining. Consequently, these two remodelers may differ in their affinity for condensed chromatin and perhaps play different roles in chromatin regulation in early embryogenesis.

At later stages, dMi-2 was still detectable in nuclei of the epidermis (Fig. 5.11 D). However, dCHD3 signals declined to background levels at this time point. These findings are consistent with the results of developmental Western blot, which showed a rapid drop of dCHD3 signal in postgastrulation embryos where dMi-2 was still present (Fig. 5.10 A).

Taken together, these results revealed that both, dCHD3 and dMi-2, localize to the nuclei of embryos, however dCHD3 stays associated with mitotic chromosomes during cell cycle progression. A sharp decrease of dCHD3 in later embryos suggests that the protein level of

dCHD3 remains under stringent control and points towards a role of this remodeler in early embryo development.

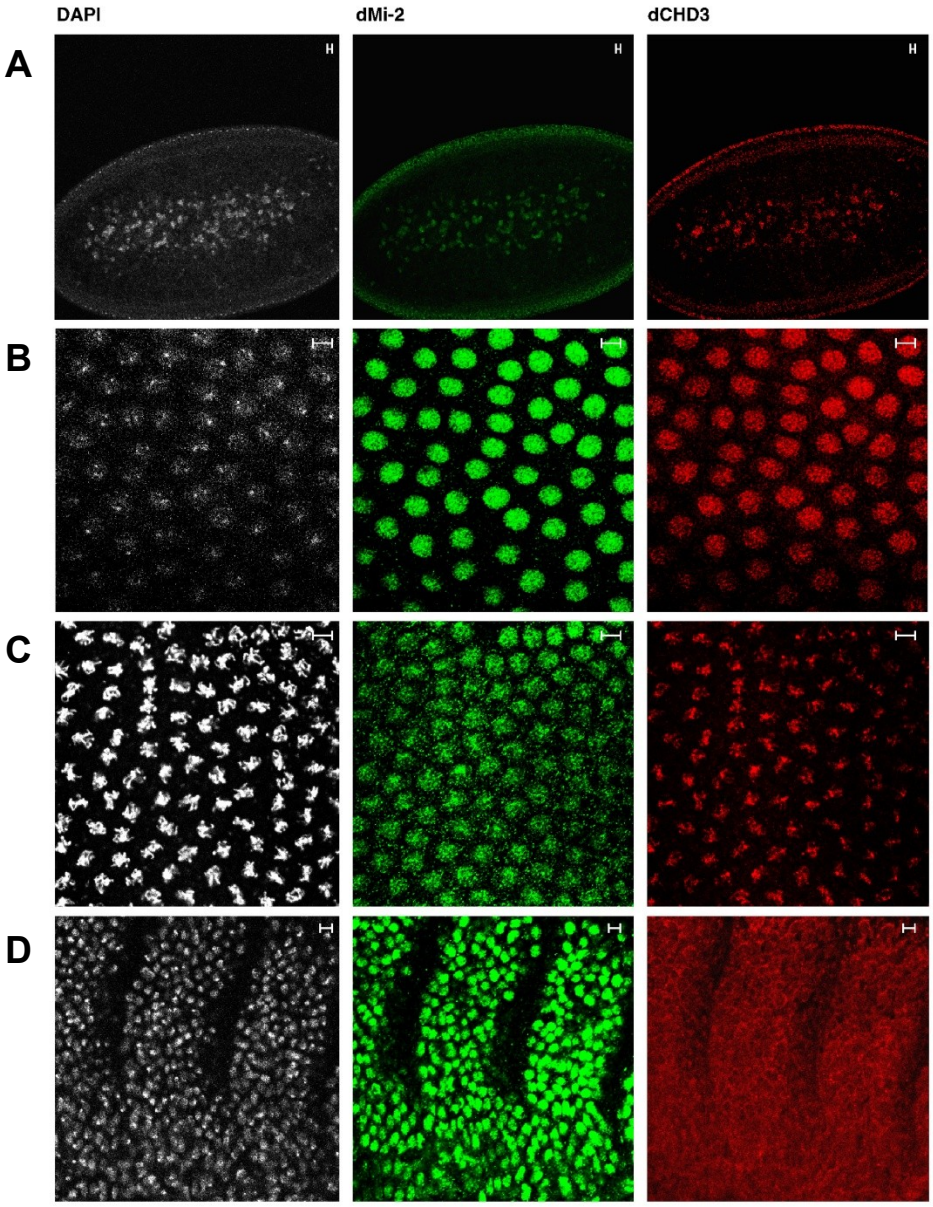

Figure 5.11 dCHD3 and dMi-2 expression in embryos
(**A**) Early preblastoderm; (**B, C**) late preblastoderm; (**D**) postgastrulation embryos were counterstained with DAPI (white; left panels), anti-dMi-2(N) (green; middle panels), and anti-dCHD3(7A11) antibody (red; right panels). Scale bars, 5 µm. Pictures were taken with confocal microscopy. Figure modified from (Murawska et al. 2008).

5.2.3 dCHD3 exists as a monomer *in vivo*

Most ATP-dependent chromatin remodelers exist in multiprotein complexes. Additional subunits could play a role in complex targeting to chromatin, regulation of enzymatic activity of the ATPase or carry additional enzymatic activities. Given the similarity between dCHD3 and dMi-2, it was conceivable that dCHD3 would interact with dNuRD complex subunits. To test this possibility, first dCHD3 was checked for immunoprecipitation with the histone deacetylase dRPD3, which is a hallmark of dNuRD complex. Immunoprecipitations were performed from nuclear extracts of a cell line stably expressing Flag-tagged dRPD3. As expected, immunoprecipitation of dMi-2 coprecipitated dRpd3 (Fig. 5.12 A, left panel, line 2). By contrast, no dRPD3 was detected in dCHD3 immunoprecipitates, although the dCHD3 specific antibody precipitates dCHD3 with good efficiency (Fig. 5.12 A, right panel, line 6). Moreover, in contrast to dMi-2, dCHD3 was not detectable in dRPD3 immunoprecipitates obtained from cells overexpressing Flag-tagged dRPD3 (data not shown).

Furthermore, to test whether dCHD3 interacts with a different histone deacetylase, an HDAC assay was carried out. dMi-2 and dCHD3 were precipitated from Kc cell nuclear extracts and the associated proteins were tested for histone deacetylase activity (Fig. 5.12 B). As shown previously, dMi-2 precipitates displayed robust HDAC activity. In contrast, dCHD3 was associated with low HDAC levels, comparable to background in a precipitation with control anti-GST antibodies. These results further strength the observation that dCHD3 is not associated with dRPD3 and thus is not associated with a dNuRD-like complex.

dMi-2 interacts also with dMep1 within the novel dMec complex (Kunert et al. 2009). However, the minimal region of dMi-2 (1308-1513 aa) required to bind dMep1, is not present in dCHD3, making it unlikely that these two proteins interact with each other (H. Klinker, unpublished data). In agreement with this, no interaction between recombinant dCHD3 and dMep1 overexpressed in baculovirus-infected SF9 cells was detected (data not shown).

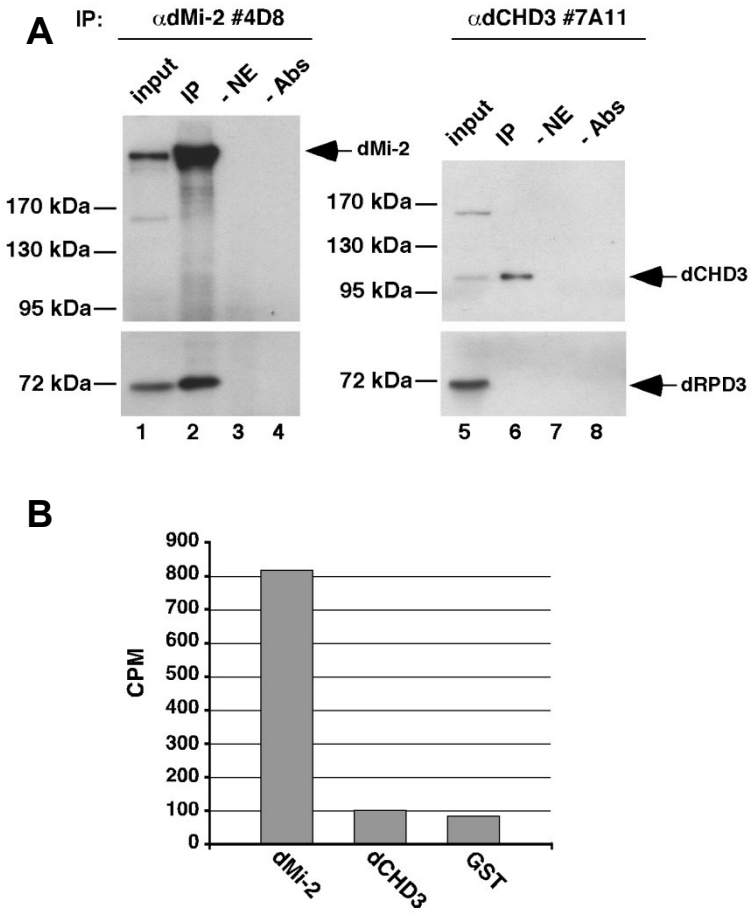

Figure 5.12 dCHD3 does not interact with dRPD3
(**A**) SL2 nuclear extracts from cells stably expressing Flag-tagged dRPD3 were immunoprecipitated with dMi-2(4D8) (left panels) and dCHD3(7A11) (right panels) antibodies, as indicated. Immunoprecipitates were analysed by Western blot using antibodies against dMi-2 (upper, left), dCHD3 (upper, right), and dRPD3 (lower panels). Lanes 1 and 5, 5% of input material; lines 2 and 6, immunoprecipitates (IP) with anti-dMi-2 and anti-dCHD3 antibodies, respectively; lanes 3 and 7, control immunoprecipitates without extracts (-NE); lanes 4 and 8, control mock precipitates without antibodies (-Abs). (**B**) Kc nuclear extracts were immunoprecipitated with dMi-2(4D8), dCHD3(7A11), and glutathione S- transferase (GST) antibodies, as indicated. Immunoprecipitates were subjected to histone deacetylase (HDAC) assay by using ^{3}H-labeled *Drosophila* histone octamers. Released ^{3}H was counted in a liquid scintillation counter. CPM, counts per minute. Figure taken from (Murawska et al. 2008).

Taken together, these results imply that dCHD3 does not interact with dNuRD or dMec subunits, suggesting that it may exist in a novel chromatin remodeling complex or it may act as a monomer *in vivo*. In order to distinguish between these possibilities, embryonic nuclear extracts were fractionated by size-exclusion chromatography on a Superpose 6 column and the fractions were assayed for the presence of dMi-2 and dCHD3. dMi-2 eluted with an apparent peak at the molecular mass of 670 kDa, confirming that dMi-2

exists in multisubunit complexes (Fig. 5.13, upper panel). By contrast, dCHD3 eluted with an apparent molecular mass of 120 kDa (Fig. 5.13, middle panel). dCHD3 eluted in similar fractions when Kc nuclear extracts were applied to the column (data not shown). Moreover, recombinant dCHD3, purified from SF9 cells, eluted in the same fractions as endogenous dCHD3 (Fig. 5.13, lower panel). As the size of 120 kDa corresponds to the predicted molecular mass of monomeric dCHD3, these data strongly suggest that, unlike dMi-2, dCHD3 exists as a monomer *in vivo*.

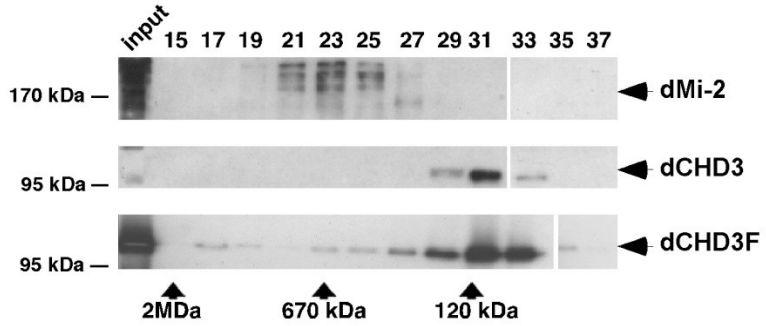

Figure 5.13 dCHD3 is a monomer *in vivo*
Embryo nuclear extracts (upper and middle panels) or recombinant Flag-tagged dCHD3 (bottom panel) were applied to a Superose 6 column. Odd fractions were analysed by Western blotting using appropriate antibodies as indicated. Gel filtration size markers are shown below (arrows); positions of dMi-2 and dCHD3 are shown on the right. Figure taken from (Murawska et al. 2008).

5.2.4 Nonredundant functions of dCHD3 and dMi-2 in embryonic cells

Coimmunoprecipitation experiments and gel filtration analysis revealed that in contrast to dMi-2, dCHD3 is a monomer in embryo cells and it does not interact with subunits of dNuRD or dMec complexes. Thus, it seemed plausible that these remodelers play different roles in early stages of *Drosophila* development and that their functions are not redundant.
It was reported previously, that dMi-2 is essential for the viability of germ cells (Kehle et al. 1998). Thus, it was tempting to determine whether this requirement also applied to embryonic Kc cells and to test for functional redundancy between dMi-2 and dCHD3. To do this, RNAi technology was applied and dMi-2 and dCHD3 were depleted from Kc cells. As judged by Western blot analysis (Fig. 5.14 A), the depletion of dMi-2 was specific and did not affect dCHD3 protein levels (Fig. 5.14 A, lines 3 and 4). The same applied to dCHD3 knockdown (Fig. 5.14 A, lines 5 and 6). Kc cells were then treated with dsRNA

against dMi-2 or dCHD3, and cell growth was monitored by counting cell number three, five, seven and nine days after dsRNA transfection. The depletion of dMi-2 had a significant effect on cell growth and viability, suggesting that dMi-2 is essential for Kc cell survival (Fig. 5.14 B). By contrast, the depletion of dCHD3 had no significant effect on cell growth.

If dMi-2 and dCHD3 function partially redundantly to regulate cell growth, then the co-depletion of both proteins would produce a more severe cell growth phenotype. However, the co-depletion of both factors affected cell growth to a degree similar to that of the depletion of dMi-2 alone. This result indicates that dCHD3 cannot substitute for the loss of dMi-2, and that dMi-2 and dCHD3 perform nonredundant functions in Kc cells.

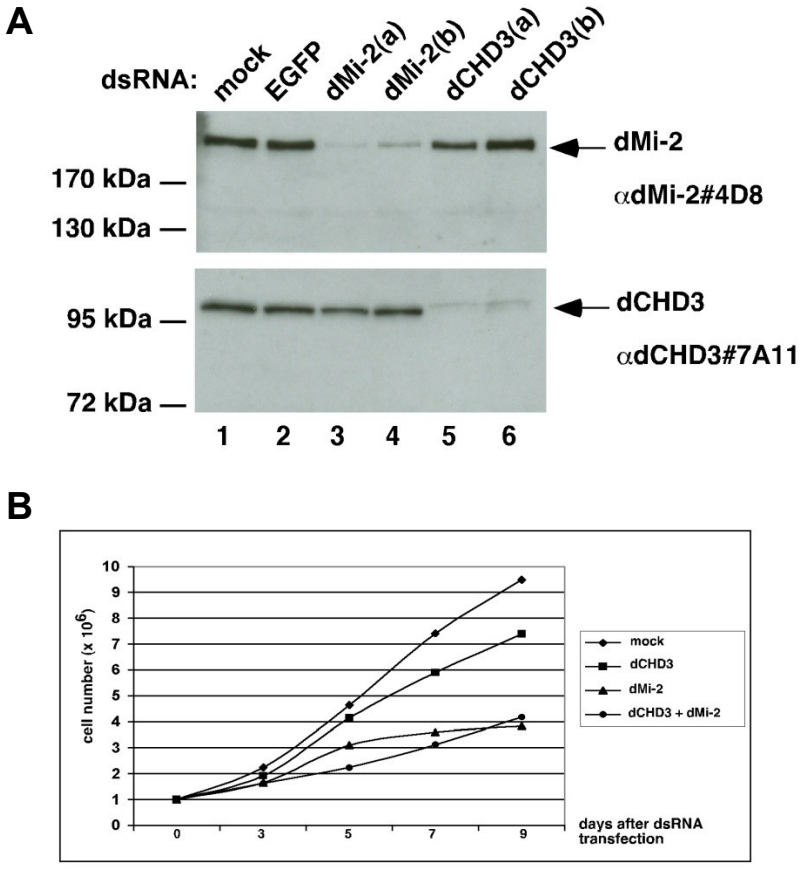

Figure 5.14 dCHD3 and dMi-2 are nonredundant *in vivo*
(**A**) Kc cells were treated with double-stranded RNAs (dsRNA) directed against enhanced green fluorescent protein (EGFP), two different dsRNA against dMi-2 [dMi-2(a) and dMi-2(b)], and dCHD3 [dCHD3(a) and dCHD3(b)]. Nuclear extracts were prepared 6 days after dsRNA treatment and 40 µg of protein from each extract were subjected to Western blot analysis using dMi-2 (upper panel) and dCHD3 antibodies (lower panel). Mock, nuclear extract derived from mock-treated cells. Positions of dMi-2 and dCHD3 are indicated on the right. (**B**) Kc cells were treated with

dsRNA directed against dCHD3, dMi-2, or a combination of the two. Cell numbers were determined after 3, 5, 7, and 9 days. Mock, treatment omitting dsRNA. Figure taken from (Murawska et al. 2008).

5.2.5 dCHD3 and dMi-2 colocalize on polytene chromosomes

Analysis of dCHD3 and dMi-2 in early embryos and embryonic cells revealed that they differ with respect to their spatial and temporal localization and expression. Moreover, they do not share binding partners and consequently have nonredundant functions at early stages of *Drosophila* development. In the light of these findings, dCHD3 and dMi-2 localization to genomic loci was compared and correlated to transcriptional activity. To do this, polytene chromosome staining from 3rd instar larvae was carried out. Although analysis of dCHD3 expression by Western blot (Fig. 5.10 A) showed no signals for this remodeler in whole cell extracts from larvae, it is still possible that it is expressed in certain larval tissues at low level. The same applies to dMi-2 which was previously shown to localize to many sites on polytene chromosomes (Murawsky et al. 2001). In accordance with this, dCHD3 expression in salivary glands from 3rd instar larvae was confirmed by Western blot analysis (data not shown, (Murawska et al. 2008)).

Next, polytene chromosomes from 3rd instar larvae were stained with dCHD3 and dMi-2 specific antibodies (Fig. 5.15). In agreement with previous work, dMi-2 localized to multiple bands on all chromosomes. dMi-2 staining was weak at the highly condensed chromocenter and the fourth chromosome (Fig. 5.15 A, middle panel). The dCHD3 antibody likewise revealed multiple bands and low staining of the chromocenter and the fourth chromosome (Fig. 5.15 A, right panel). Comparison of dCHD3 staining with DAPI showed that it localized mostly to interbands and was largely excluded from DAPI-dense regions (Fig. 5.15 B). This suggests that dCHD3 may be involved in active gene transcription in 3rd instar larvae.

Surprisingly, costaining with dMi-2 and dCHD3 antibodies revealed a remarkable overlap of their binding sites (Fig. 5.15 C, right panel). These data suggest that dMi-2 and dCHD3 are recruited to the same chromosomal regions on polytene chromosomes. Whether they play overlapping or distinct functions on these regions remains to be determined in the future.

Moreover, the unexpected observation of dMi-2 presence at interbands indicates that it may be involved not solely in gene repression but also play an unexplored role in active gene transcription.

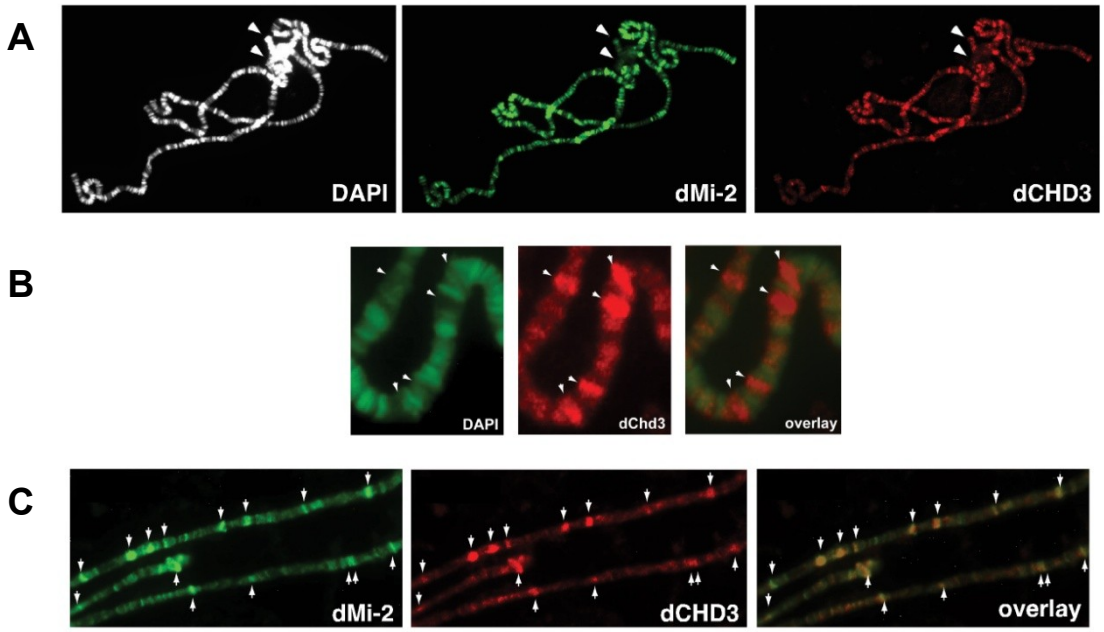

Figure 5.15 dCHD3 and dMi-2 colocalize on polytene chromosomes.
(**A**) Polytene chromosome squashes (right panels) were stained with DAPI (white; top), dMi-2(N) (green; middle), and dCHD3(7A11) antibody (red; bottom). Arrows indicate the chromocenter and the fourth chromosome. (**B**) Close-up of polytene chromosome stained with DAPI (green; left) and dCHD3 antibody (red; middle). An overlay of both signals is shown on the right. Arrows indicate bands of strong dCHD3 and weak DAPI staining. (**C**) Polytene chromosomes were stained with DAPI (white; top), dMi-2 (green; middle), and dCHD3 antibody (red; middle). An overlay of dMi-2 and dCHD3 signals is shown on the bottom. Arrows indicate overlapping dMi-2 and dCHD3 bands. Figure taken from (Murawska et al. 2008).

5.3 dMi-2 function in active gene transcription

5.3.1 dMi-2 localizes to active genes on polytene chromosomes

The unexpected staining of euchromatic regions on polytene chromosomes by dMi-2 antibody raises an intriguing possibility that besides its repressive functions, dMi-2 may be involved in regulation of active gene transcription.

To determine whether dMi-2 binding sites correspond to sites of active transcription, polytene chromosomes were costained with antibodies against dMi-2 and active forms of RNA polymerase II (RNAP II). As mentioned in the introduction, the hypophosphorylated form of RNAP II enters the preinitiation complex, whereas the hyperphosphorylated form is actively engaged in transcription elongation (Lu et al. 1991; Dahmus 1994). The C-terminal domain (CTD) of RNAP II is differentially phosphorylated as RNAP II progresses through the transcription cycle. Phosphorylation of Ser5 residues predominates near the 5' end of genes and correlates with transcription initiation and early elongation, whereas Ser2 residues are extensively phosphorylated towards the 3' end of the genes (Komarnitsky et al. 2000; Kim et al. 2010). Polytene chromosome staining with antibodies which specifically recognize elongating forms of RNAP II, clearly showed that dMi-2 colocalized on many sites with transcriptionally active forms of RNAP II (Fig. 5.16 A). Analysis of individual chromosome arms at higher magnification revealed that the binding pattern of dMi-2 was overlapping at many sites with both Ser5 and Ser2 phosphorylated RNAP II, suggesting that dMi-2 may be enriched throughout entire gene coding regions (Fig. 5.16 B, left and middle panel). Furthermore, dMi-2 and RNAP II binding was very similar but not identical, which implies that dMi-2 is recruited to only a subset of active genes. The regions stained by dMi-2 which do not overlap with RNAP II may represent genomic sites where dMi-2 plays a repressive role. A significant overlap with transcription elongation factor Spt5, further strengthened the idea that dMi-2 occupies actively transcribed genes (Fig. 5.16 B, right panel).

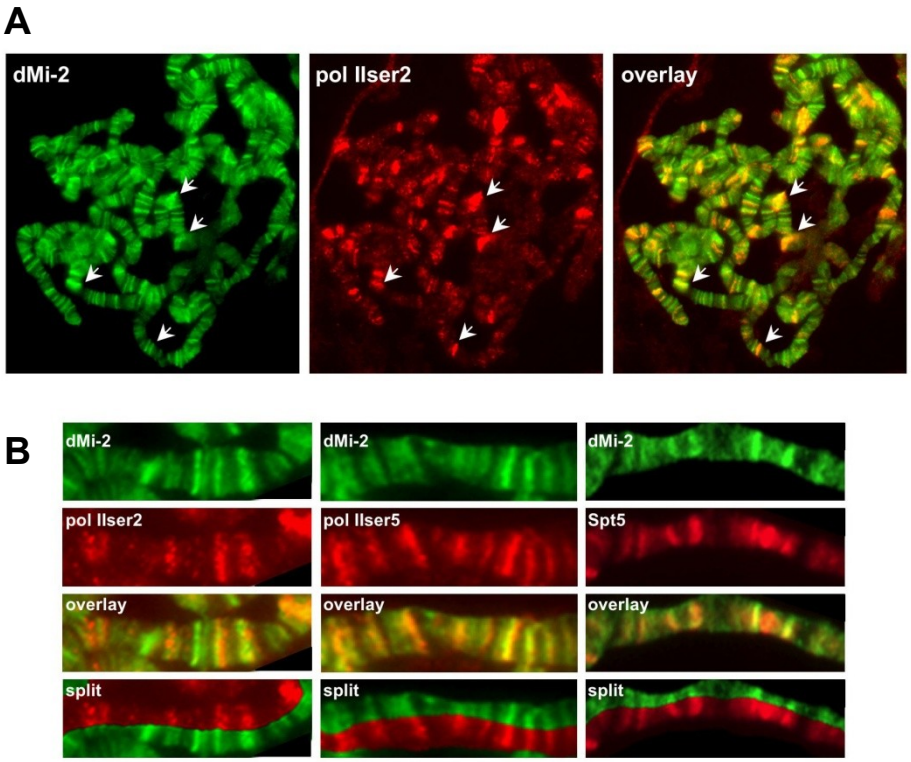

Figure 5.16 dMi-2 colocalizes with active genes
Immunofluorescence staining of polytene chromosomes with anti-dMi-2 (dMi-2(N)), anti-RNAP II (pol IIser2 and pol IIser5), anti-Spt5 antibodies and DAPI as indicated. (**A**) Whole chromosome squash. Arrows show prominent sites of colocalization between dMi-2 and elongating RNAP II. (**B**) Magnified sections of individual chromosome arms stained with antibodies as indicated.

To verify that dMi-2 is recruited to active sites of transcription, the recruitment of dMi-2 to induced heat shock genes was examined (Fig 5.17). Heat shock genes constitute one of the best known model system to study active gene transcription (chapter 2.6.2). Thus, it was plausible to test whether dMi-2 is recruited to these chromosomal loci. Polytene chromosome staining with dMi-2 antibodies after 20 min heat shock, showed clear localization of dMi-2 to the most prominent heat shock loci, 87A and 87C, which contain multiple copies of the *hsp70* gene. Similar binding to heat shock puffs was observed when independent polyclonal antibodies raised against dMi-2 were used (data not shown). These results further support a potential link between dMi-2 and active transcription.

RNAP II is rapidly recruited to heat shock loci upon heat shock and it disappears from other genes, which in turn are shut down (Fig. 2.10) (Jamrich et al. 1977). By contrast, dMi-2 was not significantly relocalized from other genomic sites (compare Fig. 5.16 A and

Fig. 5.17). This suggests that only a fraction of dMi-2 is recruited to induced heat shock genes.

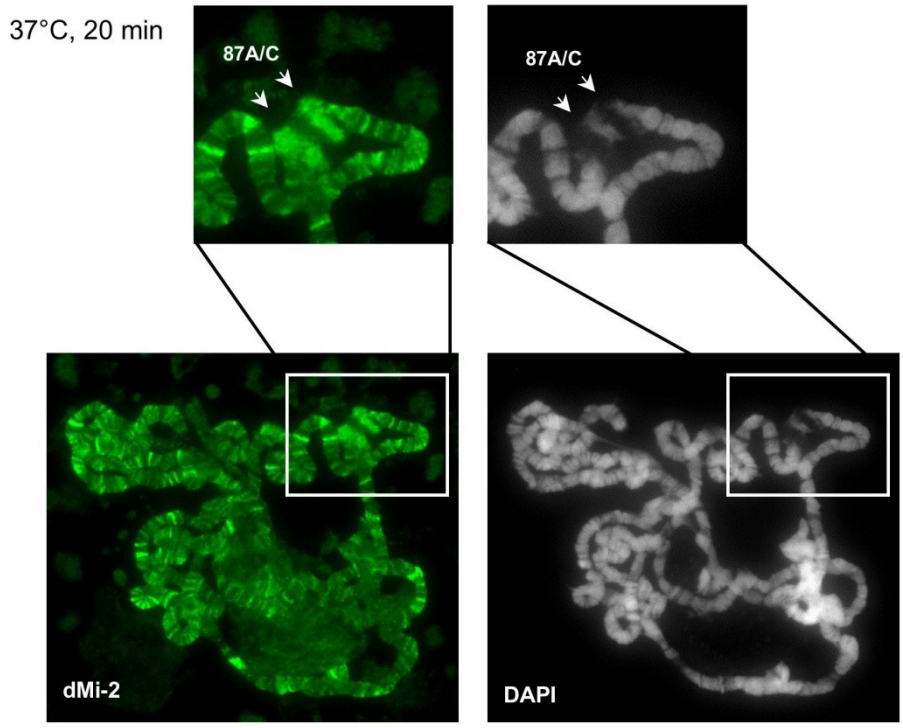

Figure 5.17 dMi-2 is recruited to heat shock genes.
Immunofluorescence staining of polytene chromosomes with anti-dMi-2 antibodies and DAPI as indicated. Polytene chromosomes were isolated from 3rd instar larvae which were heat shocked at 37°C for 20 min. Upper panels show magnified section containing the *hsp70* loci 87A and 87C (arrows).

The robust expression of heat hock genes results in dramatic changes of chromatin structure and nucleosome depletion (Petesch and Lis 2008). This raises the possibility that many chromatin remodelers are recruited there to facilitate transcription. To test this, polytene chromosomes were stained upon heat shock with antibodies against two different ATP-dependent chromatin remodelers, Brahma (SWI/SNF subfamily) and ISWI (ISWI subfamily). The staining of heat shock loci showed that Brahma signals were not above the background levels (Fig. 5.18, upper panel). This is in agreement with published work, which showed that Brahma is not recruited to heat shock loci, although it is generally involved in global transcription regulation by RNAP II (Armstrong et al. 2002). Polytene chromosome staining with ISWI antibodies also did not show any staining of *hsp70* loci, which points out that this remodeler is not recruited to heat shock genes (Fig. 5.18, lower

panel). However, ISWI containing complexes were shown to be important for heat shock gene transcription (Badenhorst et al. 2002). These results indicate that recruitment to heat shock loci is specific for dMi-2 and is not shared by other remodelers, like SWI/SNF or ISWI. Recruitment to HS puffs was demonstrated previously also for *Drosophila* CHD1 (Stokes et al. 1996; Morettini et al. 2011), which raises the possibility that members of CHD family of chromatin remodelers may play specific roles on these genomic loci.

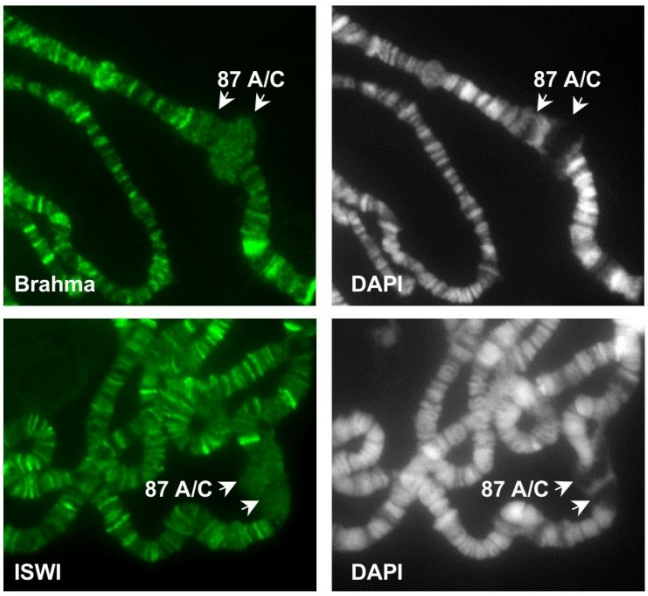

Figure 5.18 Brahma and ISWI are not recruited to *hsp* loci
Immunofluorescence staining of polytene chromosomes with anti-Brahma and anti-ISWI antibodies and DAPI as indicated. Polytene chromosomes were isolated from 3rd instar larvae which were heat shocked at 37°C for 20 min. Pictures show magnified chromosome sections containing the *hsp70* loci 87A and 87C (arrows).

5.3.2 dMi-2 is recruited to the transcribed region of *hsp70*

The indirect immunofluorescence staining of polytene chromosomes suggests that dMi-2 is recruited to heat shock genes upon their activation. However, polytene chromosome staining does not allow to determine the exact sites of factor binding, as this method provides only a view of genomic loci at low resolution. In order to define dMi-2 bound regions more accurately and confirm the polytene chromosome staining, chromatin immunoprecipitation (ChIP) in *Drosophila* cell culture was performed.

First, a chromatin immunoprecipitation protocol was established in Kc cells using heat shock factor (HSF) and RNA polymerase II as positive controls. Cells were treated for 20

min with heat shock, followed by immediate cell fixation and chromatin preparation. Binding of HSF and RNAP II was monitored with primer pairs designed to amplify heat shock elements (HSE) located in the promoter region of *hsp70* and downstream transcribed region respectively (Fig. 5.19 B). Transcript analysis of *hsp70* gene revealed that heat shock genes were rapidly and strongly activated in this system (Fig. 5.19 A). Analysis of HSF binding to the *hsp70* gene showed that low levels of HSF were associated with the *hsp70* promoter and transcribed region prior to heat shock (NHS). In agreement with previously published work, HSF levels increased significantly at the promoter upon heat shock (HS) with little change within the coding region (Fig. 5.19 B) (Boehm et al. 2003). By contrast, RNAP II ChIP with antibodies directed against phosphorylated Ser5, displayed heat shock-induced enrichment of the enzyme at both promoter and transcribed region, which correlates with RNAP II recruitment and its movement into the gene (Fig. 5.19 B). Altogether these results indicate that ChIP performed in Kc cells upon heat shock distinguishes between rapid recruitment of HSF to the promoter and RNAP II to both promoter and transcribed regions of the gene and can be used to follow the recruitment of other factors.

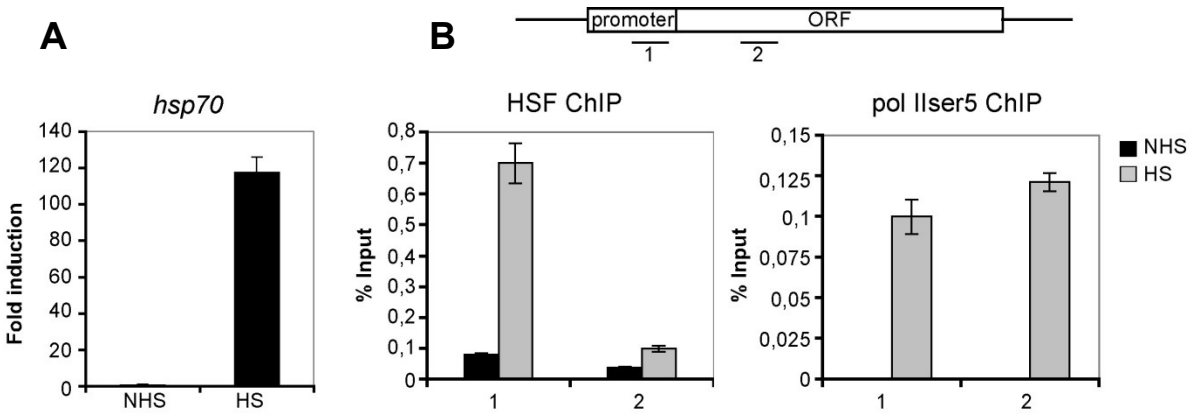

Figure 5.19 Induction of heat shock response in Kc cells
(**A**) RT-QPCR analysis of *hsp70* expression in Kc cells. Cells were incubated at 37°C for 20 min to induce heat shock response. Values are expressed relative to the value in NHS control cells. Error bars denote standard deviation. (**B**) ChIP analysis of heat shock factor (HSF) and RNAP II (Ser5P) recruitment to *hsp70* gene. Upper panel: *hsp70* gene and position of amplimers analysed (1: centred at -154, 2: +681). Lower panel: ChIP on control (NHS) and heat shocked treated Kc cells (HS). Cells were incubated at 37°C for 20 min followed by chromatin isolation and precipitation with indicated antibodies. Graphs represent enrichment of each amplimer shown as percentage input. Error bars denote standard deviation.

Next, the association of dMi-2 with the *hsp70* gene was investigated. As many antibodies tend to crosslink unspecifically to chromatin, protein knockdown by RNAi was applied to determine the specificity of dMi-2 antibodies used in this assay. As a negative control, cells were treated with dsRNA against lucyferase (Fig. 5.20 B). Surprisingly, ChIP analysis of dMi-2 revealed enrichment of the remodeler in the transcribed region upon heat shock, but not at the promoter. Upon efficient dMi-2 knockdown, the ChIP signal in the transcribed region of *hsp70* decreased significantly (Fig. 5.20 A). Similar results were obtained when independent polyclonal antibodies raised against dMi-2 were used (data not shown).

This result strongly indicates that dMi-2 is recruited to the transcribed region of *hsp70* upon gene activation. Moreover, this finding differs from a previous ChIP analysis of dMi-2 which showed recruitment to the promoters of genes repressed by dMi-2 (Kunert et al. 2009) and suggests that dMi-2 function and targeting may differ depending on the transcriptional status of the gene.

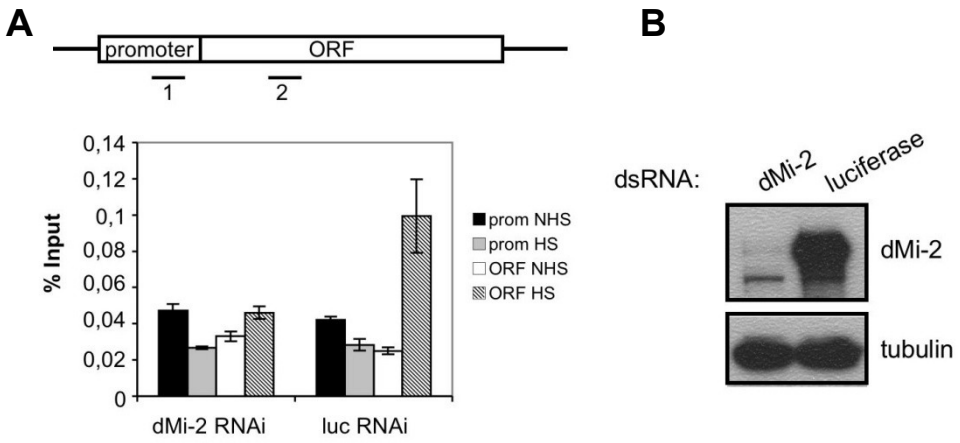

Figure 5.20 ChIP analysis of dMi-2 binding to the *hsp70* gene in Kc cells
(**A**) Upper panel: *hsp70* gene and position of amplimers analysed (1: centred at -154, 2: +681). Lower panel: dMi-2 ChIP from cells treated with dsRNA against luciferase or dMi-2 as indicated. prom (amplimer 1): promoter; ORF (amplimer 2): open reading frame; NHS: non heat shock; HS: heat shock. (**B**) Verification of RNAi knockdown by Western blot. 40 µg of Kc nuclear extracts were loaded on SDS-PAGE gel and analysed by Western blot with indicated antibodies.

5.3.3 dMi-2 is enriched over the entire transcribed region of *hsp70*

Factors associated with active genes can display differential accumulation over the transcribed regions. For instance, transcription elongation factor Spt5 was shown to be

enriched at 5' of *hsp70* gene, which is in agreement with its role in regulation of RNAP II stalling and elongation early in the transcription cycle and with its role in stimulating the 5'-capping machinery. By contrast, FACT and Spt6 were shown to accumulate towards the 3' end of *hsp70*, which reflects their role in controlling transcription elongation and modulation of chromatin structure upon RNAP II passage (Saunders et al. 2003).

To get more precise insight into the spatial distribution of dMi-2 on *hsp* genes, ChIP analysis was performed using primer pairs covering the entire transcribed region of *hsp70*. dMi-2 showed background binding to the gene before heat shock. However, upon gene activation, it was enriched over the entire transcribed region of *hsp70* (Fig. 5.21). Interestingly, dMi-2 was still detected at the very end of the gene, where the 3' end cleavage and processing occurs (Fig. 5.21, amplimer number 7). Overall, this result suggests that dMi-2 may be involved in regulation of heat shock genes transcription and point towards its role in co-transcriptional events such as chromatin structure modulation, elongation or RNA processing.

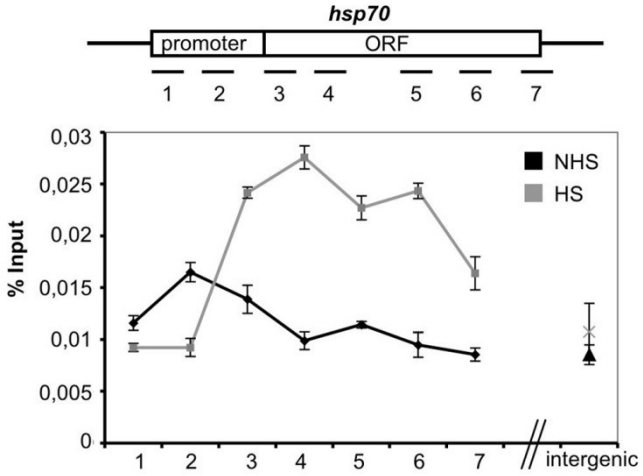

Figure 5.21 ChIP analysis of dMi-2 binding to the *hsp70* gene
Upper panel: *hsp70* gene and positions of analysed amplimers (1: centred at -350; 2: -154; 3: +58; 4: +681; 5: +1702; 6: +2065; 7: +2549). The intergenic region represents background binding of the antibody. Lower panel: dMi-2 ChIP from NHS (black graph) and HS (grey graph) Kc cells. ChIP was performed with anti-dMi-2(C) antibodies. Graph represents enrichment of each amplimer shown as percentage input. Error bars denote standard deviation.

5.3.4 dMi-2 is important for efficient *hsp* gene expression

Given that dMi-2 colocalizes with elongating forms of RNAP II on polytene chromosomes and given that dMi-2 is recruited to and enriched in the transcribed region of the *hsp70* gene, it was reasonable to test whether it contributes to heat shock gene transcription.

To investigate this, transgenic flies carrying an inducible UAS-RNAi construct targeting dMi-2 were used. In this system, expression of the transgene is controlled by the presence of the UAS element containing optimized GAL4 binding sites. To activate transgene transcription, flies that carry the transgene are mated to flies which express GAL4 in a particular pattern (driver strain). The resulting progeny express the transgene in a transcriptional pattern that reflects the GAL4 pattern of the respective driver (Duffy 2002).

To obtain dMi-2 depletion, a ubiquitous daughterless Gal4-driver was utilized. Due to significant maternal deposition of dMi-2 (Kehle et al. 1998), knockdown of the remodeler was obtained only at late 3rd instar larvae. Western blot analysis of whole cell extracts from larval brains confirmed efficient depletion of dMi-2 in these animals (Fig. 5.22 A). dMi-2 depleted animals arrested their development as 3rd instar larvae and they failed to develop to the pupal stage. This result confirmed that dMi-2 is indispensable for *Drosophila* development (Kehle et al. 1998).

To investigate the role of dMi-2 in heat shock gene transcription, dMi-2 depleted larvae were treated with heat shock at 37°C for 20 min. Heat shock gene response of dMi-2 depleted larvae was compared to control, wild type flies crossed with the same Gal4-diver strain. Several *hsp* genes were selected for RT-QPCR analysis. *hsp70*, *hsp26* and *hsp83* genes were all activated upon heat shock treatment in control flies. However, transcript levels of all *hsp* genes tested were severely reduced in dMi-2 depleted larvae compared to controls (Fig. 5.22 B). Importantly, transcription of a housekeeping gene (*actin5c*) was not significantly affected arguing that the observed effect on heat shock genes was specific. In conclusion, transcriptional analysis of the heat shock gene response in dMi-2 depleted larvae suggests that dMi-2 makes a positive contribution to transcription and is essential for full *hsp* gene activation in larvae.

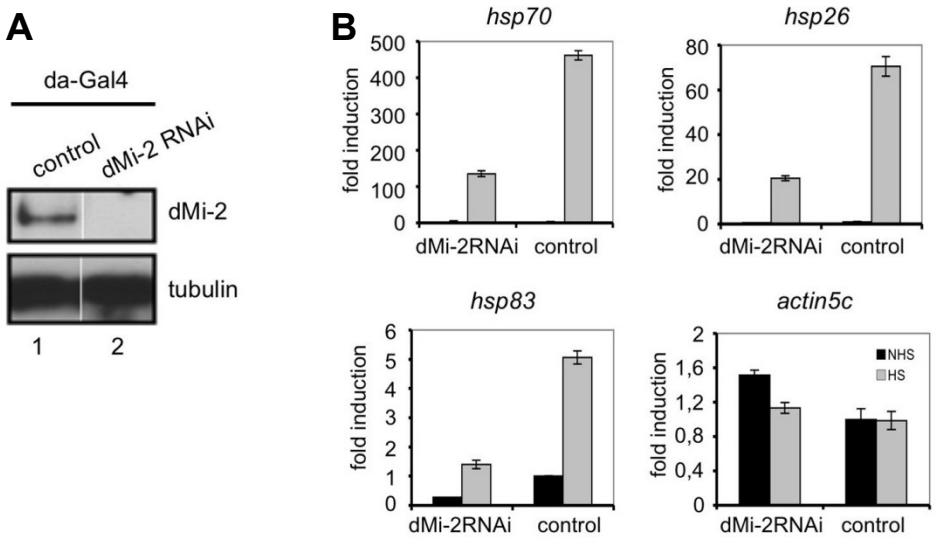

Figure 5.22 Heat shock gene expression is impaired in dMi-2 depleted larvae
(**A**) Verification of dMi-2 knockdown in control and dMi-2 RNAi larvae. Control flies and flies carrying a dMi-2 RNAi transgene under UAS control were crossed with a da-GAL4 driver strain. Extracts from third instar larvae were subjected to Western Blot. Antibodies used are indicated on the right. Tubulin was used as a loading control. (**B**) RT-QPCR analysis of *hsp70*, *hsp26*, *hsp83* and *actin5c* expression in control and dMi-2 RNAi larvae. Values are expressed relative to the value in NHS control larvae. Errors bars denote standard deviation. All graphs show representative of at least three independent fly crosses. NHS, no heat shock treatment; HS, heat shock treatment.

5.3.5 dMi2 catalytic activity is required for efficient *hsp* gene expression

Although, dMi-2 knockdown in larvae leads to inefficient expression of *hsp* genes, the RNAi approach can lead to effects which are indirectly associated with the observed phenotype. In addition, it was not clear whether enzymatic activity of dMi-2 is involved in *hsp* gene transcription regulation. To address this issue directly, an alternative approach to study dMi-2 function was utilized and a catalytically inactive mutant of dMi-2 was generated.

As previously reported, mutations in the ATP-binding site of ATP-dependent chromatin remodeling enzymes eliminate their activity without affecting their ability to interact with other proteins and thus the mutant proteins have dominant-negative effects on transcription when expressed in cells (Khavari et al. 1993; Côté et al. 1994; Armstrong et al. 2002).

First, a site-directed mutagenesis was carried out to create a mutation that replaces the conserved lysine (K761) in the ATP-binding site of the dMi-2 protein with an arginine (Fig. 5.23 A, upper panel). Second, the mutant dMi-2 was expressed and affinity purified

from SF9 cells (Fig. 5.23 A, lower panel). Both, dMi-2 mutant (dMi-2 K761R) and dMi-2 wild type (dMi-2WT) were then applied to ATPase assay in the presence of nucleosomes. In comparison to the wild type protein, dMi-2 mutant was completely inactive, confirming that the mutated residue is important for ATP binding and subsequent ATP hydrolysis (Fig. 5.23 B).

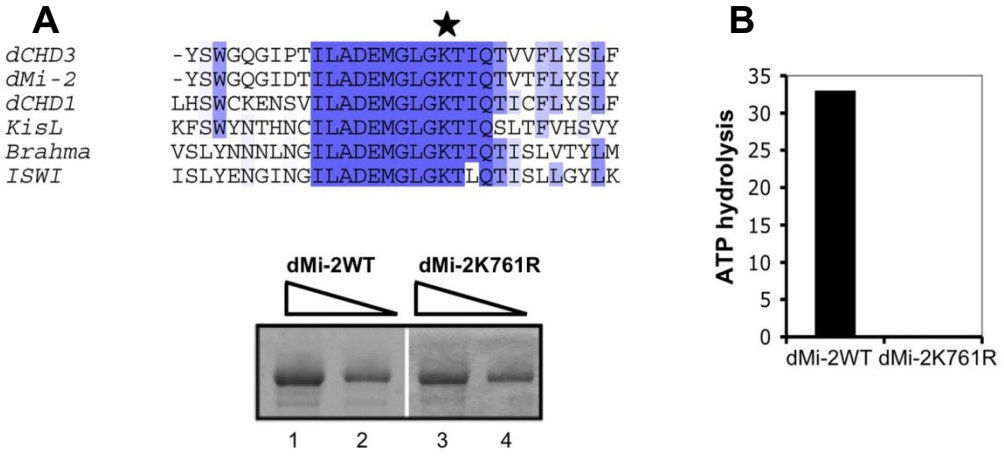

Figure 5.23 dMi-2 K761R mutant is catalytically inactive
(**A**) Upper panel: protein multiple alignment of a fragment of ATPase domain of *D. melanogaster* CHD, Brahma and ISWI chromatin remodelers. The mutated lysine is indicated by a black star. Conserved regions are shaded in dark blue (strongly conserved) or light blue (moderately conserved).
Lower panel: a Coomassie gel with dMi-2WT and dMi-2K761R mutant. 2 µg of protein (lanes 1 and 3) and 1 µg of protein (lanes 2 and 4) were loaded on the gel. (**B**) ATPase assay with wild type and mutant form of dMi-2 in the presence of nucleosomes. Percentage of hydrolysed ATP was determined by thin layer chromatography and quantified with phosphorimager.

Finally, flies carrying Flag-tagged dMi-2WT or dMi-2K761R transgenes under the control of the UAS promoter were generated. For this purpose, the site-specific φC31 integrase system was applied (for details see chapter 3.2.7). Hence, both transgenes were integrated at the same genomic site. To obtain dMi-2 expression, again a daughterless Gal4-driver was used. Western blot analysis of whole cell extracts from 3rd instar larval brains confirmed ectopic expression of both dMi-2WT and dMi-2K761R proteins (Fig. 5.24 A). Moreover, the expression of both transgenes was similar which allowed the direct comparison of their effect on *hsp* gene transcription. Animals expressing wild type dMi-2 did not show any apparent phenotype. However, expression of catalytically inactive dMi-2 mutant led to impaired animal development. These animals arrested at 3rd instar larvae and similarly to dMi-2 depleted larvae, failed to develop further to the pupal stage. This result

suggests that ectopic expression of catalytically inactive mutant of dMi-2 efficiently replaces the endogenous enzyme and results in a dominant-negative phenotype.

To determine effects on *hsp* gene transcription, 3rd instar larvae were subjected to heat shock as before. RT-QPCR analysis of *hsp70*, *hsp26* and *hsp83* genes revealed that whereas overexpression of wild type dMi-2 had little effect, levels of *hsp* gene transcripts were greatly reduced in larvae overexpressing the enzymatically inactive dMi-2 (Fig. 5.24 B). Expression of a housekeeping gene (*gapdh*) was not significantly affected in this system.

To assess possible effects on puff formation, polytene chromosome squashes from flies overexpressing a dominant-negative mutant of dMi-2, were prepared. Staining with antibodies specific for elongating RNAP II revealed that heat shock puffs were smaller, which is in line with the observed impaired transcription of *hsp* genes in these flies (Fig. 5.24 C). Altogether these results demonstrate that the enzymatic activity of dMi-2 is essential for full heat shock gene activation.

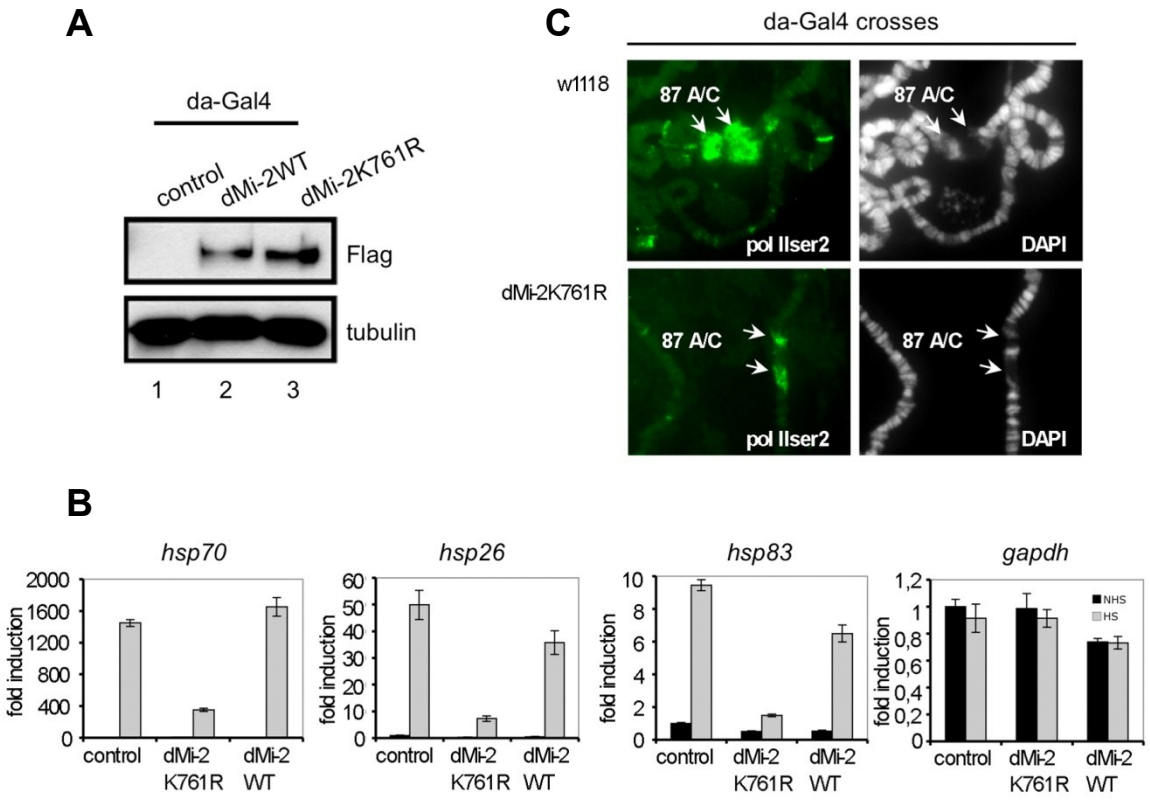

Figure 5.24 Catalytic activity of dMi-2 is important for full *hsp* gene expression
(**A**) Verification of dMi-2 transgene expression in larvae by anti-Flag Western blot. Control flies and flies carrying a dMi-2WT and dMi-2K761R transgene under UAS control were crossed with a da-GAL4 driver strain. (**B**) RT-QPCR analysis of *hsp70*, *hsp26*, *hsp83* and *gapdh* expression in control and transgenic larvae. Values are expressed relative to the value in NHS control larvae.

Errors bars denote standard deviation. All graphs show representative of at least three independent fly crosses. NHS, no heat shock treatment; HS, heat shock treatment. (**C**) Immunofluorescence staining of polytene chromosomes with RNAP II (Ser2P) and DAPI as indicated. Polytene chromosomes were isolated from control or dMi-2K761R mutant overexpressing 3rd instar larvae crossed to da-Gal4 driver. Larvae were heat shocked for 20 min at 37°C prior to polytene chromosome squashes preparation. Pictures show magnified chromosome sections containing the *hsp70* loci 87A and 87C (arrows).

5.3.6 dMi-2 catalytic activity is required for proper RNA processing and splicing of *hsp* genes

The inefficient expression of *hsp* genes may be a consequence of affecting several co-transcriptional processes in dMi-2 depleted or dMi-2 mutant overexpressing transgenic larvae. Heat shock genes undergo dramatic chromatin changes upon activation that are reflected by rapid nucleosome disruption across the entire gene (Petesch and Lis 2008). As dMi-2 is recruited to the entire transcribed region of *hsp70*, an attractive hypothesis was that dMi-2 could be involved in the regulation of nucleosome levels at *hsp* genes. In this context, dMi-2 would help to open the locus and thus alleviate the restrictive properties of chromatin to RNAP II. However, this seems not to be the case as no significant changes in histone H3 removal on *hsp* genes in dMi-2 knockdown flies were observed (data not shown). Another intriguing possibility is that dMi-2 can play a more direct role in transcription, for example by regulating co-transcriptional 3' end formation or splicing.

To test whether RNA 3' end processing is affected upon dMi-2 removal, the ratio of 3' unprocessed transcripts and total *hsp70* RNA in wild type and dMi-2 depleted or dMi-2 K761R mutant overexpressing larvae were determined (Fig. 5.25 A). For this, primer pairs were designed to distinguish between unprocessed and total transcripts. Primer pair 1 detected all *hsp70* transcripts whereas primer pair 2 detected only unprocessed *hsp70* transcripts with uncleaved 3' end (Fig. 5.25 A, upper panel). The ratio of 3' unprocessed transcripts to total *hsp70* RNA for the control cross was set to one and other ratios were displayed relative to this.

RT-QPCR analysis revealed a substantially higher ratio of unprocessed to total *hsp7*0 transcipts in dMi-2 depleted animals (4-fold, Fig. 5.25 A). Moreover, the observed defects were even more pronounced in flies overexpressing mutant form of dMi-2 (11-fold), whereas overexpression of wild type dMi-2 had little effect (2-fold). Similar defects were observed on the *hsp83* gene. The ratio of unprocessed to total *hsp83* transcripts in dMi-2

depleted animals was 2,7-fold with higher (3,5-fold) ratio in dMi-2K761R expressing flies and no changes in wild type dMi-2 expressing animals (Fig. 5.25 B, left graph).

Hsp83 is one of the few heat shock genes possessing an intron. In order to test whether splicing of this gene is impaired in transgenic larvae, primer pairs detecting unspliced and total *hsp83* transcripts were used (Fig. 5.25 B, amplimer 3 and 4, respectively) and the ratio of unspliced to total *hsp83* transcripts was determined. Again, a significant increase in the relative proportion of unspliced RNA in dMi-2-depleted larvae (2,8 fold) and in larvae overexpressing inactive enzyme (3,3 fold) in comparison to control and wild type dMi-2 expressing larvae, were observed. Altogether, these results suggest that dMi-2 activity is required for the efficient 3' end processing and splicing of heat shock genes.

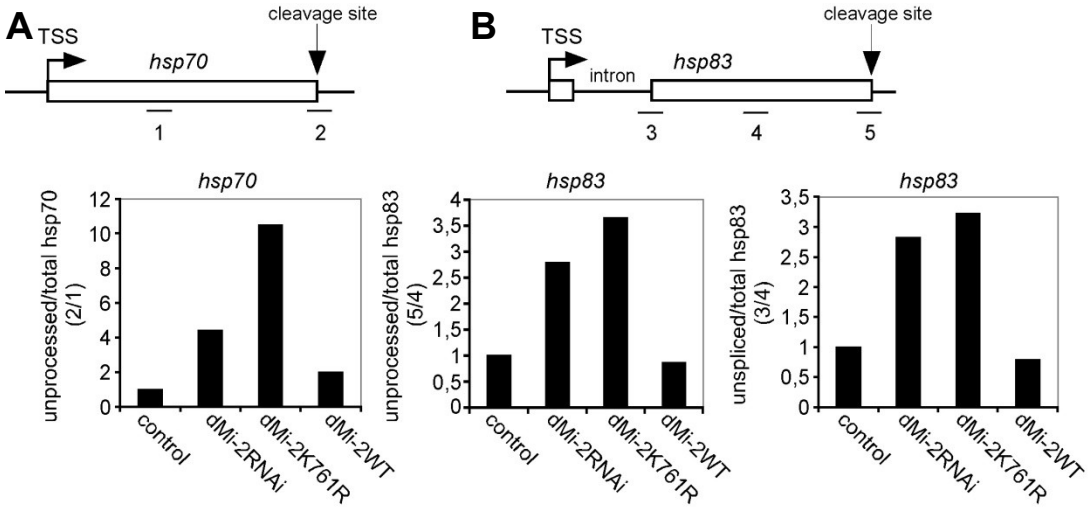

Figure 5.25 dMi-2 is required for efficient RNA processing.
(**A**) Upper panel: schematic representation of the *hsp70* gene. RT-QPCR amplimers, *hsp70* cleavage site, and transcriptional start site (TSS) are shown. Lower panel: RT-QPCR from control and transgenic larvae. The ratio between 3' unprocessed and total *hsp70* RNA was determined (amplimer 2 / amplimer 1). The ratio obtained for control larvae was set to 1, other ratios were expressed relative to this. (**B**) Upper panel: schematic representation of the *hsp83* gene. RT-QPCR amplimers, *hsp83* intron, and transcriptional start site (TSS) are shown. Lower panel: The ratio between unprocessed and total *hsp83* RNA (right graph, amplimer 5 / amplimer 4) or unspliced and total *hsp83* RNA (left graph, amplimer 3 / amplimer 4) were determined and plotted as in (**A**).

5.3.7 dMi-2 interacts with nascent *hsp* gene transcripts

Several chromatin factors involved in RNA processing were shown to interact with pre-mRNA directly. For instance, BRG1 and BRM are associated with pre-RNPs (Tyagi et al. 2009), the same applies to ENY2, THO and Xmas-2, proteins engaged in 3' end processing (Kopytova et al. 2010).

The involvement of dMi-2 in regulation of co-transcriptional RNA processing and splicing suggests that the remodeler may also bind to nascent transcripts. To address this issue, RNA immunoprecipitation from heat shocked Kc cells with two different antibodies against dMi-2 was performed. Upon extensive washes, RNA was recovered from immunoprecipitates and the presence of nascent transcripts was monitored by RT-QPCR with primer pairs designed to detect unprocessed or unspliced *hsp70* and *hsp83* transcripts, respectively. This analysis revealed an enrichment of nascent *hsp70* and *hsp83* transcripts in dMi-2 precipitates with two independent antibodies. In addition low presence of unrelated transcripts, like *actin5c* or *rp49*, in dMi-2 immunoprecipitates, demonstrates a specificity of this interaction (Fig. 5.26 A). To further support the hypothesis of dMi-2 binding to nascent RNA, cells were treated with RNase A followed by chromatin fractionation with increasing salt concentration. dMi-2 presence in different fractions was then determined by Western blot analysis (Fig. 5.26 B). This experiment showed that more dMi-2 was released from chromatin when cells were pretreated with RNAse A in comparison to the control (Fig. 5.26 B, right panel, compare lines 1 and 3). No changes upon RNAse A treatment of an unrelated nuclear protein, lamin, was observed, arguing for the specificity of this assay (Fig. 5.26 B, right panel). Accordingly, this demonstrates that at least a fraction of dMi-2 in cells is associated with chromatin in an RNA dependent manner.

Finally, to show a physical dMi-2/RNA interaction, an RNA electrophoretic mobility shift assay was carried out. A single-stranded, 250 bp fragment of *hsp70* RNA was generated by *in vitro* transcription. Then, recombinant dMi-2 was incubated with RNA followed by native gel electrophoresis. dMi-2 formed a distinct, slowly migrating protein-RNA complex that was stable during electrophoresis through the native polyacrylamide gel (Fig. 5.26 C). This result confirmed that dMi-2 binds single stranded RNA directly.

Altogether, these data suggest that dMi-2 interacts with heat shock pre-mRNA transcripts and further strength the evidence that it is involved in transcription regulation, at least in part, via RNA processing and splicing control.

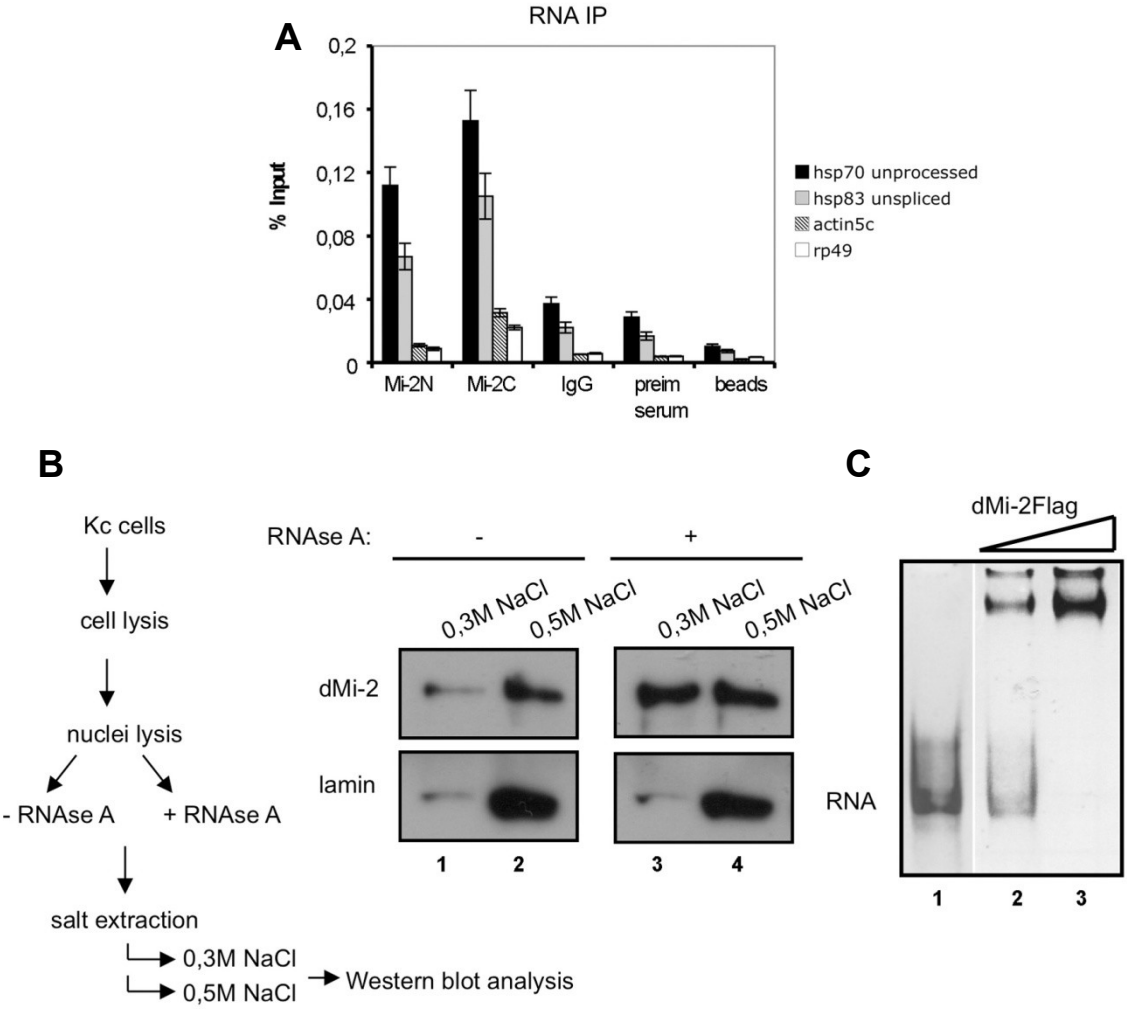

Figure 5.26 dMi-2 interacts with RNA *in vivo* and *in vitro*
(**A**) RNA immunoprecipitation (RIP) of *hsp70* and *hsp83* unprocessed transcripts from heat shocked Kc cells. RIP was performed with two independent dMi-2 antibodies (dMi-2(N) and dMi-2(C)), IgG, pre-immune serum and protein G beads as indicated. IgG, pre-immune serum and protein G beads were used as negative controls. Primer pairs that specifically amplify *actin5c*, *rp49* and unprocessed *hsp70* and *hsp83* transcripts (see Fig. 4.24) were used for RT-QPCR. (**B)** Chromatin fractionation. Left panel: experimental scheme. Right panel: Western blot analysis of protein fractions extracted with 0,3M (lanes 1, 3) and 0,5M NaCl (lanes 2, 4), treated (+) or not treated (-) with RNAse A, as indicated. Western blot was probed with anti-dMi-2 and anti-lamin antibodies as indicated on the left. The experiment was performed by Matthias Groh.
(**C**) RNA electrophoretic mobility shift assay. Single stranded hsp70 RNA (80 ng) was incubated with recombinant dMi-2. Lane 2: 0,2 µg dMi-2, lane 3: 0,5 µg, lane 1: no protein. RNA and RNA-protein complexes were resolved by electrophoresis and visualized with ethidium bromide. Position of unbound RNA probe is indicated on the left.

5.4 Recruitment mechanism of dMi-2 to active heat shock genes

The main recruitment mechanism of dMi-2 to the promoters of repressed genes involves interactions with several DNA binding transcription factors (chapter 2.4.1, Table 2.2). In addition, SUMOylation of transcription factors can increase their affinity for dMi-2 complexes (chapter 2.4.2). However, given that dMi-2 is recruited to the entire transcribed region of the *hsp70* gene but not to the promoter (Fig. 5.20 and 5.21), it is plausible that a different recruitment mode of dMi-2 to active genes exists.

5.4.1 dMi-2 does not bind to histone marks associated with active transcription

Chromatin carries numerous histone modifications which have been shown to be associated with transcription. The hallmarks of histone tail modifications on active genes comprise tri-methylation of lysine four on histone H3 (H3K4me3) and tri-methylation of lysine 36 on histone H3 (H3K36me3). The first modification is enriched near the transcription start sites of active genes, whereas the latter one increases towards the 3' end of the genes. These modifications serve as a recognition platform for chromatin remodeling and modifying factors, including human CHD1 and the yeast histone deacetylase containing complex Rpd3S (Carrozza et al. 2005; Sims et al. 2007), which are targeted to transcribed genes via binding to H3K4me3 and H3K36me3, respectively. Binding to methylated histone tails occurs via specific protein domains, such as chromodomains or PHD fingers. The tandem chromodomains of CHD1 have been shown to bind to H3K4me3, whereas Rpd3S recognizes H3K36me3 via the chromodomain of Eaf3, a specific subunit of the complex (Carrozza et al. 2005).

The involvement of chromodomains in recognizing histone methylation marks, raised the possibility that dMi-2 could be recruited to active genes in a similar manner. To test this hypothesis, the tandem chromodomains of dMi-2 (aa 452-716) were expressed as GST-fusion proteins in bacteria (Fig. 5.27 A) and their binding to modified histone tail-peptides, was determined. As a positive control, the human CHD1 chromodomains (aa 250-467) were purified from bacteria and used in the same assay. Protein binding to differentially modified histone tails was monitored by Western blot analysis (Fig. 5.27 B). This experiment confirmed that CHD1 was binding specifically to H3K4me3, but not to unmodified H3 or H3K36me3 (Fig. 5.27 B, upper panel). However, dMi-2 chromodomains were bound to all histone peptide used irrespective of their lysine methylation state (Fig.

5.27 B, lower panel). This result suggests that dMi-2 chromodomains do not possess any specificity towards methylated histone tails. The most probable explanation for this is the lack of an aromatic tryptophan residue (Fig. 5.27 C), which is indispensable for CHD1 chromodomain binding to H3K4me3 (Flanagan et al. 2005). It cannot be excluded that the substantial binding of dMi-2 chromodomains to all histone peptides is due to incorrect protein folding or aggregation. Similar problems were reported before for dCHD1 chromodomains (Morettini et al. 2011). This experiment does not eliminate the possibility that other domains of dMi-2 may recognize specific active histone marks. However, the full length dMi-2 displayed no specificity for methylated histone tails in histone peptide pulldowns (P. Steffen, unpublished data).

Altogether, these data strongly suggest that recognition of active histone marks, H3K4me3 and H3K36me3, is unlikely to be responsible for dMi-2 recruitment to active heat shock genes.

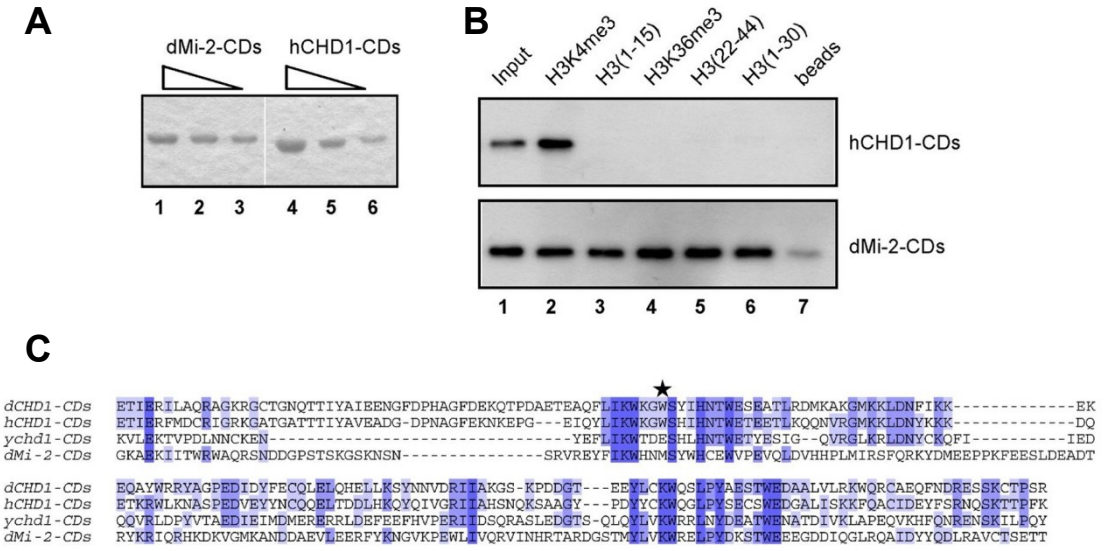

Figure 5.27 Chromodomains of dMi-2 do not possess specificity towards methylated histone tails *in vitro*.

(**A**) Coomassie-stained SDS-Page gel showing recombinant GST-tagged chromodomains of dMi-2 and hCHD1. Lanes 1 to 3, dMi-2 chromodomains (2, 1, and 0,5 µg), lanes 4 to 6, hCHD1 chromodomains (2, 1, and 0,5 µg). (**B**) Histone peptide pulldown. 0,25 µg of recombinant GST-tagged dMi-2 or hCHD1 chromodomains were incubated with different histone H3 peptides, as indicated. Binding was monitored by Western blot analysis with anti-GST antibodies. Bound proteins are labeled on the right. 5% of protein input was loaded on the gel. H3K4me3 peptide comprised 1-15 aa, H3K36me3 peptide comprised 22-44 aa of histone H3. H3, unmodified histone H3. Aminoacids of unmodified histone H3 are shown in parentheses.

(**C**) Multiple sequence alignment of the chromodomains of CHD remodelers from different species. Conserved regions are shaded in dark blue (strongly conserved) or light blue (moderately

conserved). Tryptophan residue responsible for hCHD1 binding to H3K4me3 is indicated with black star. dCHD1 (*Drosophila* CHD1), hCHD1 (human CHD1), yChd1 (yeast Chd1).

5.4.2 dMi-2 recruitment to *hsp* genes is independent of RNAP II interaction

Recruitment of different proteins to transcribed genes often involves interaction with RNAP II. Factors participating in transcription initiation, like the general transcription factor TBP and the multi-subunit Mediator complex, bind RNAP II through unphosphorylated CTD (Usheva et al. 1992; Myers et al. 1998). A number of elongation and RNA processing factors have been shown to be recruited to transcribed regions via binding to hyperphosphorylated CTD domain of RNAP II (Komarnitsky et al. 2000; Phatnani and Greenleaf 2006). Others, like PSF (Protein-associated Splicing Factor), recognize CTD independent of its phosphorylation status (Emili et al. 2002).

Given that dMi-2 is recruited to the entire transcribed region of *hsp70* (Fig. 5.21), it was conceivable that it could bind and travel with RNAP II or transcription elongation factors. To address this possibility, immunoprecipitation experiments from Kc cell nuclear extracts were performed. Immunoprecipitation of dMi-2 did not show any significant association with RNAP II, although the dMi-2 specific antibody precipitated dMi-2 with good efficiency (Fig. 5.28, upper left panels). The faint RNAP II signal in the dMi-2 immunoprecipitation was not stronger that the signal in the control precipitation, where antibodies were omitted (Fig. 5.28, upper left panels, compare line 2 and 3). In addition, immunoprecipitation with anti-RNAP II antibodies was carried out and the association of dMi-2 was tested. Again, no association of dMi-2 with RNAP II was observed (Fig. 5.28, upper right panels). The anti-RNAP II antibody (8WG16) used for precipitation recognizes mostly the hypophosphorylated form of RNAP II. It cannot be formally excluded that dMi-2 binds to hyperphosphorylated and thus transcriptionally engaged RNAP II. However, immunoprecipitation of dMi-2 followed by Western blot analysis with antibodies recognizing phosphorylated forms of RNAP II (Ser5 or Ser2), did not show any association with these RNAP II species (Fig. 5.28 lower left and right panels). Moreover, no interaction with transcription elongation factors Spt5 and Spt6 was detected (data no shown). The lack of association of dMi-2 with RNAP II or elongation factors, suggests that binding to the transcription machinery is not responsible for dMi-2 recruitment to active heat shock genes.

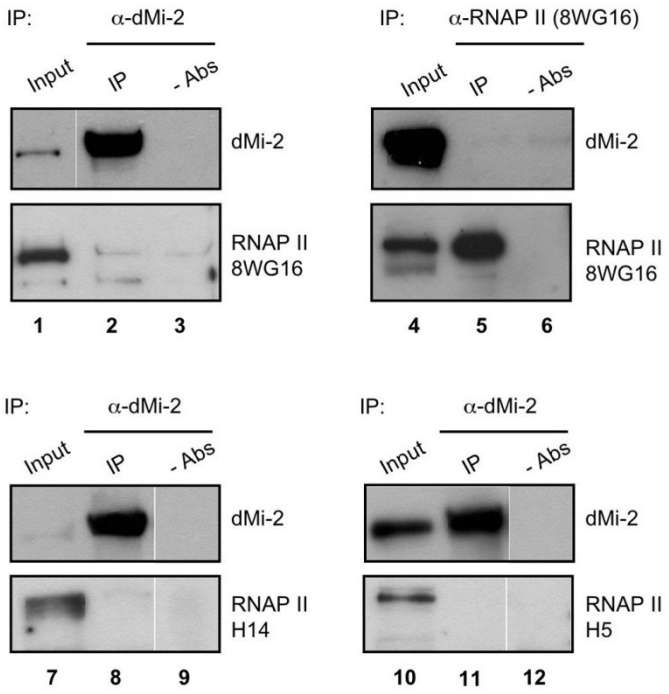

Figure 5.28 dMi-2 does not interact with RNAP II
Kc nuclear extracts were immunoprecipitated with dMi-2(4D8) (upper, left panels), dMi-2(N) (lower, left and right panels), and RNAP II (8WG16) (upper, right panels) antibodies, as indicated. Immunoprecipitates were analysed by Western blot using antibodies against dMi-2 and different forms of RNAP II, as indicated on the right. 8WG16 antibody recognizes hypophosphorylated forms of RNAP II, H14 antibody - Ser5 phosphorylated RNAP II, H5 antibody - Ser2 phosphorylated RNAP II. Lanes 1, 4, 7 and 10, 5% of input material; lines 2, 5, 8 and 11, immunoprecipitates (IP); lanes 3, 6, 9 and 12, control precipitates without antibodies (-Abs).

Recruitment of dMi-2 could precede, coincide or follow RNAP II binding to heat shock genes. It was not clear when dMi-2 is recruited to heat shock genes, as all ChIP experiments were carried out after 20 min of heat shock when transcription was already going on. To assess the kinetics of dMi-2 recruitment to heat shock genes, Kc cells were treated with heat shock for one, two, five and 20 minutes, followed by ChIP analysis with dMi-2 and RNAP II antibodies (Fig. 5.29). RNAP II was detected near the start site of transcription prior to heat shock, in agreement with previous studies showing that promoter-paused RNAP II is hypophosphorylated (Fig. 5.29, NHS, left graph). Recruitment of RNAP II near the start site was detected after 1 min, with the peak signal after 5 minutes, followed by small decrease after 20 min of the heat shock. Similar kinetics for RNAP II recruitment was reported previously (Boehm et al. 2003). As the anti-RNAP II antibody used for ChIP (8WG16) recognizes mostly hypophosphorylated forms of

RNAP II, the signal in the body of the gene detected with this antibody was low but above the signal before heat shock, which is in agreement with the observation that this antibody can still recognize RNAP II molecules that have some level of phosphorylation (Boehm et al. 2003). Conversely, dMi-2 ChIP showed that the remodeler was binding to the transcribed region of *hsp70* later than RNAP II, as it was detected earliest at 2 min after heat shock (Fig. 5.29, right graph). dMi-2 signal progressively increased with time, with the highest level reached at 20 min after heat shock. As observed previously (Fig. 5.21), dMi-2 was recruited to the entire transcribed region of *hsp70*. A significant signal for dMi-2 was still detected at the 3' prime end of the gene, suggesting that it extends beyond the transcribed region. Altogether, the time course ChIP revealed that dMi-2 differs from RNAP II with regard to its temporal patterns on transcribed *hsp70* gene. In addition, previously published ChIP patterns of different forms of RNAP II, with preferential detection of the enzyme at the 5' end of the transcribed *hsp70* gene, differ from the dMi-2 profile (Boehm et al. 2003). This further strengthens the hypothesis that dMi-2 is not recruited by the transcription machinery to heat shock genes.

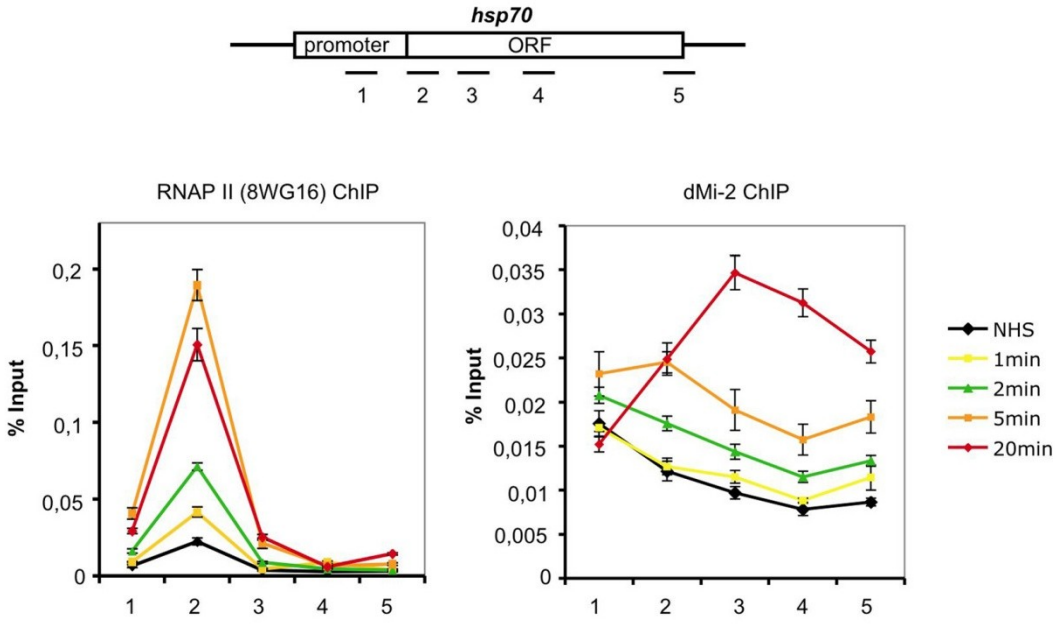

Figure 5.29 Kinetics analysis of RNAP II and dMi-2 binding to the *hsp70* gene
Upper panel: *hsp70* gene and position of amplimers analysed (1: centred at -154; 2: +58; 3: +681; 4: +1426; 5: +2549). Lower panel, left: RNAP II ChIP from non heat shocked and heat shocked Kc cells, as indicated. RNAP II ChIP was performed with 8WG16 antibodies. Lower panel, right: dMi-2 ChIP from Kc cells, as in left panel. ChIP was performed anti-dMi-2(C) antibodies. Graphs represent enrichment of each amplimer shown as percentage input. Error bars denote standard deviation.

5.4.3 dMi-2 recruitment to *hsp* genes is transcription independent

As dMi-2 binding to the *hsp70* gene takes place after RNAP II recruitment (Fig. 5.29), it is conceivable that dMi-2 recruitment depends on transcription elongation, rather than on transcription initiation. Although, in the light of the experiments described above, a direct association of dMi-2 with elongating RNAP II is rather improbable, it is still plausible that dMi-2 might be recruited to active genes via binding to nascent transcript during transcription elongation. To address this issue, a small molecule inhibitor DRB was used. DRB (5,6-Dichloro-1-β-D-ribofuranosylbenzimidazole) is a purine nucleoside analogue which inhibits transcriptional elongation, via specifically targeting P-TEFb kinase and thus blocking CTD phosphorylation at serine 2 (Bentley 1995; Yamaguchi et al. 1999). Kc cells were incubated with DRB for 20 min at RT, followed by heat shock treatment. RT-QPCR analysis revealed that *hsp70* transcript levels in cells treated with DRB were decreased to the basal levels, which confirmed the efficient inhibition of *hsp70* transcription in this system (Fig. 5.30 A). Next, dMi-2 ChIP was performed in the presence or absence of DRB. dMi-2 was recruited to the transcribed region of the *hsp70* in control, heat shock-treated cells, as shown previously. Surprisingly, in cells treated with DRB, the signal for dMi-2 binding was not significantly reduced, although transcription was completely abolished (Fig. 5.30 B). Consequently, this result demonstrates that dMi-2 recruitment to the active *hsp70* gene is transcription independent and strongly indicates that the remodeler recruiting signal is brought about by another mechanism.

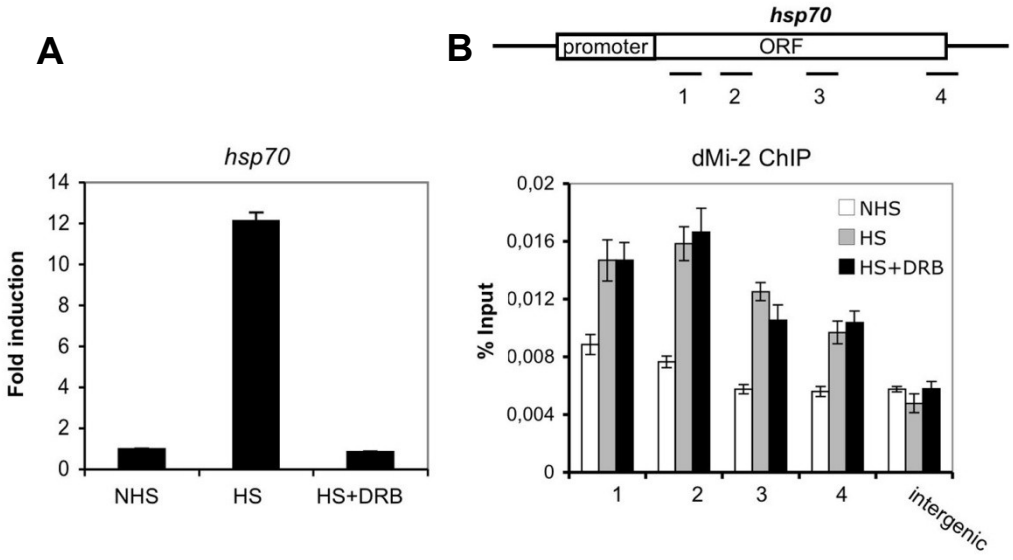

Figure 5.30 Transcription elongation inhibition by DRB has no effect on dMi-2 recruitment to the *hsp70* gene
(**A**) RT-QPCR analysis of *hsp70* expression in Kc cells. Cells were incubated in the presence or in the absence of DRB (125 μM) for 20 min followed by heat shock at 37°C for 20 min, as indicated. Values are expressed relative to the value in NHS control cells. Error bars denote standard deviation. (**B**) Upper panel: *hsp70* gene and position of amplimers analysed (1: centred +58; 2: +681; 3: +1426; 4: +2549). The intergenic region represents background binding of the antibody. Lower panel: dMi-2 ChIP from Kc cells was performed under non heat shock (NHS), heat shock (HS) or DRB treatment and heat shock conditions, as in (**A**). Graph represents enrichment of each amplimer shown as percentage input. Error bars denote standard deviation.

5.4.4 Inhibition of PARP impairs dMi-2 recruitment to *hsp* genes

It was reported previously, that formation of heat shock puffs on polytene chromosomes still occurs when transcription is blocked by actinomycin or by mutation of target gene promoters (Korge et al. 1990). This suggests that puff generation can be separated from transcription and that there must be a different cause of heat shock puff formation. Indeed, it was shown that heat shock genes are subjected to extensive poly(ADP-ribosylation) (PARylation) upon gene activation and it was suggested that this modification occurs independently of transcription (Tulin and Spradling 2003; Petesch and Lis 2008). Poly(ADP-ribosylation) is catalyzed by poly(ADP-ribose) polymerase (PARP), which utilizes nicotinamide adenine dinucleotide (NAD+) to add long chains of adenosine diphosphate-ribose residues to target proteins. Strikingly, in the presence of PARP mutations or an inhibitor of PARP activity, puffing does not occur and transcription of heat shock genes in response to a heat shock stimulus is strongly reduced in 3rd instar larvae (Tulin and Spradling 2003). Moreover, it has been recently reported, that the initial, rapid nucleosome loss from activated *hsp* genes requires PARP activity (Petesch and Lis 2008). Hence, one intriguing possibility was that dMi-2 could be recruited to heat shock genes in a PARP dependent manner.

To test this possibility, first the inhibition of PARP enzymatic activity was achieved by a specific PARP inhibitor, PJ34. Kc cells were treated with PJ34 for different time periods and subjected to Western blot analysis with anti-PAR antibodies. These antibodies recognize a specific epitope associated with poly(ADP-ribose) (PAR) polymer that is associated with numerous proteins within the cell. Thus, many Western blot signals were detected (Fig. 5.31 A, line 1). Upon PJ34 treatment, some of these signals disappeared or become reduced, which suggested partial PARP inhibition by PJ34 (Fig. 5.31 A, line 2). A substantial decrease of PAR signals was achieved already after 20 minutes of cell

treatment. As prolonged cell treatment with PJ34 did not result in stronger PAR signal decrease (data not shown), a 20 min treatment was chosen for a subsequent ChIP experiment. In addition, heat shock gene transcription was monitored after PJ34 treatment. RT-QPCR analysis revealed that transcription of the *hsp70* gene was not significantly affected upon PJ34 treatment (Fig. 5.31 B). Although it was reported that PARP is important for heat shock gene transcription in 3rd instar larvae, it is conceivable that the incomplete inhibition of PARP activity did not impair heat shock gene activation.

Next, dMi-2 ChIP was performed in the presence or absence of PJ34 and dMi-2 recruitment was followed through the entire *hsp70* transcribed region. As expected, dMi-2 was recruited to the activated *hsp70* gene in control, heat shock-treated cells. By contrast, in cells treated with PJ34, the signal for dMi-2 binding was significantly reduced despite the incomplete PARP inhibition (Fig. 5.31 C). Importantly, dMi-2 signal was not changed in the control, intergenic region, upon PJ34 treatment. Similar results were obtained for *hsp83* gene (data not shown). Thus, this experiment suggests that dMi-2 recruitment to heat shock genes depends on PARP enzymatic activity.

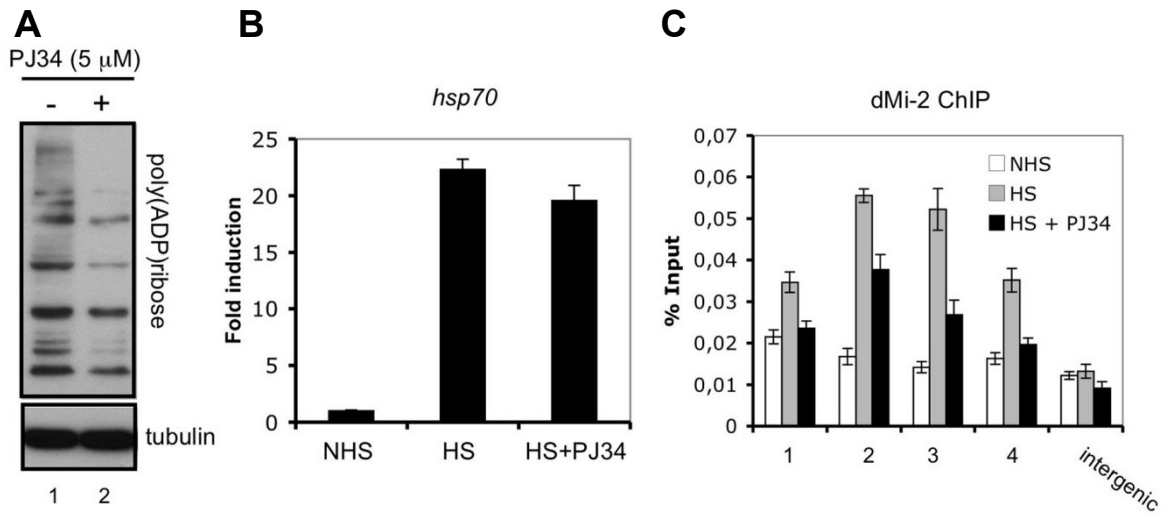

Figure 5.31 Inhibition of PARP activity decrease dMi-2 recruitment to the *hsp70* gene
(**A**) Western blot analysis for PARP inhibition efficiency. Kc cells were incubated without (-) or with (+) PJ34 (5 μM) for 20 min, followed by nuclear extract preparation and Western blot analysis with anti-PAR antibodies. 50 μg of protein were loaded on the gel, tubulin staining was used as a loading control. (**B**) RT-QPCR analysis of *hsp70* expression in Kc cells. Cells were incubated in the presence or in the absence of PJ34 (5 μM) for 20 min followed by heat shock at 37°C for 20 min, as indicated. Values are expressed relative to the value in NHS control cells. Error bars denote standard deviation. (**C**) dMi-2 ChIP from Kc cells was performed under non heat shock (NHS), heat shock (HS) or PJ34 treatment and heat shock conditions. Graph represents enrichment of each amplimer shown as percentage input (amplimer 1: centred +58; 2: +681; 3: +1426; 4: +2549). The

intergenic region represents background binding of the antibody. Error bars denote standard deviation.

5.4.5 dMi-2 binds to PAR polymers

As reported recently, the human homolog of dMi-2, CHD4 is recruited to laser induced DNA-damage sites in a PARP-dependent manner via binding to PAR chains (Polo et al. 2010). Given the conservation between CHD4 and dMi-2, it was conceivable that dMi-2 could bind to PAR polymers directly in the context of heat shock gene transcription. In order to test this idea, binding to auto-PARylated PARP1 *in vitro* was determined using PARP pulldown assays. First a PARP reaction was set up, where recombinant PARP1 enzyme was incubated with its substrate NAD+, to synthesize PAR chains. In this reaction PARP1 is the main substrate and is auto-PARylated. This results in a smear on Western blot which corresponds to PARP1 modified with PAR chains of different length (Fig. 5.32 A, lane 1). Purified and immobilised dMi-2 was subsequently incubated with PARP reactions and auto-modified PARP binding was detected by Western blot with anti-PAR antibodies (Fig. 5.32 A). In addition, mH2A1.1 which contains a macrodomain, known to interact with PAR, was used as a positive control in this assay. Western blot analysis revealed that dMi-2, like mH2A1.1, bound PARylated PARP1 efficiently (Fig. 5.32 A, lines 3 and 4).

To confirm that the observed Western blot signals correspond to auto-modified PARP1 and to exclude any unspecificity of antibodies, the same pulldown assay was carried out with radioactively labeled PARylated PARP1 and binding was detected by the exposure to X-ray film (5.32 B). This experiment verified dMi-2 binding to auto-PARylated PARP1. Interestingly, radioactive signals in mH2A1.1 were smeared until the end on the gel, whereas in dMi-2 pulldown they were detected in higher molecular weight range (Fig. 5.32 B). This suggests that dMi-2 may display some specificity towards longer PAR chains. Indeed, a role of PAR chain length for regulating PAR-protein interactions was reported previously (Fahrer et al. 2007).

As PARP pulldown assays are performed in the presence of auto-modified PARP1, it cannot be excluded that the interaction between dMi-2 and PAR is mediated, at least to some extent, via PARP1. To test whether dMi-2 binds PAR polymers directly, radioactive PAR was decoupled from PARP1 and purified. Next, recombinant dMi-2 was spotted on a nitrocellulose membrane, followed by incubation with radioactive PAR. After extensive

washing, the membrane was exposed to phosphorimager analysis. This revealed a significant radioactive PAR signal bound to dMi-2 but not to BSA spotted on the membrane which argues for the specificity of this assay (Fig. 5.32 C). Thus, similarly to human CHD4, dMi-2 displays PAR binding ability.

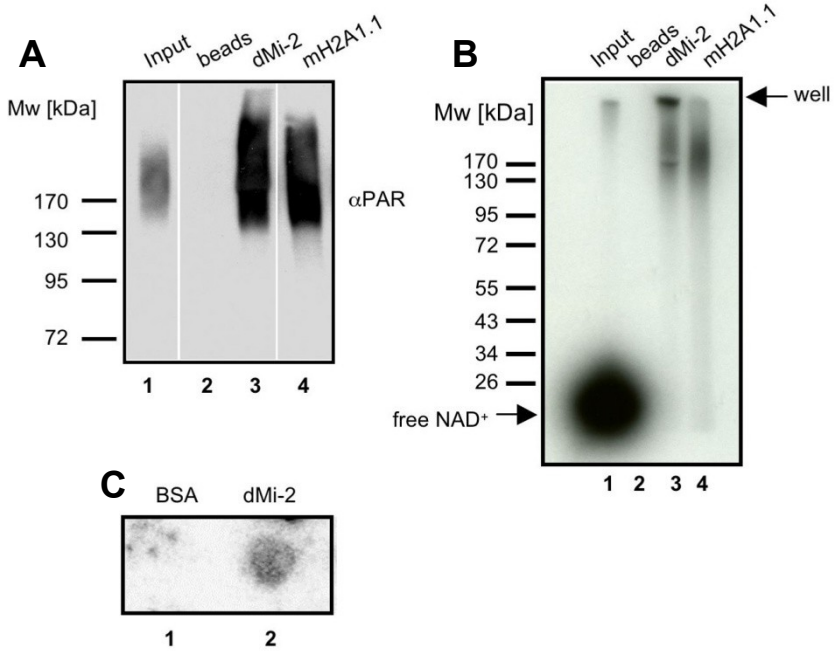

Fig. 5.32 dMi-2 binds PAR
(**A**) PAR was synthesized *in vitro* by recombinant PARP1. Reactions were incubated with control anti-Flag beads (beads) and beads with immobilized dMi-2 or mH2A1.1 as indicated on top. Bound material was analysed by Western blot using and anti-PAR antibodies. Lane1: input (3,5%). Molecular weight is depicted on the left. (**B**) Pulldown in the presence of radioactive auto-PARylated PARP1. Experiment was performed as in (**A**) with a difference that radioactive NAD+ was used for PAR synthesis. Samples were run on the gel, gel was dried and exposed overnight on the X-ray film. The gel well and free NAD+ are depicted with arrows. (**C**) PAR binding assay. Slot blot with radioactively labelled purified PAR. 0,2 μg of BSA or recombinant dMi-2 were spotted on the nitrocellulose and incubated with radioactive PAR. Upon extensive washes, membrane was dried and analysed by phosphorimager.

To get a better insight into the mode of dMi-2 binding to PAR, the pulldown assay was performed in the presence of the excess of free ADP-ribose (ADPr) followed by Western blot analysis. The macrodomain of mH2A1.1 was shown to bind free ADPr, thus its association with auto-PARylated PARP1 was abolished when the excess of ADPr was present in the pulldown reaction (Fig. 5.33, compare lines 4 and 5). By contrast, dMi-2 binding to auto-PARylated PARP1 was not abrogated in the presence of ADPr (Fig. 5.33, compare lines 2 and 3). This result suggests that in contrast to mH2A1.1, dMi-2 is not able

to bind free ADPr, it rather binds longer poly(ADP-ribose) chains. This also indicates that dMi-2 recognizes PAR polymers in a different manner that mH2A1.1, as it does not possess a macrodomain. As PAR polymer is negatively charged similarly to nucleic acids, it is plausible that PAR binding to dMi-2 reflects its general affinity for nucleic acids.

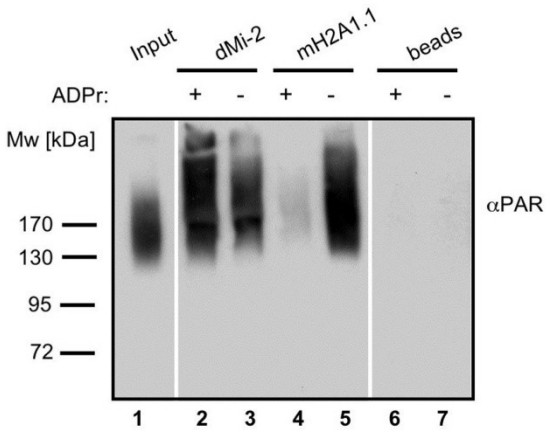

Fig. 5.33 Free ADPr does not compete with PAR for binding to dMi-2
(**A**) PAR was synthesized *in vitro* by recombinant PARP1 as in Fig. 5.32. Reactions were incubated with control anti-Flag beads (beads) and beads loaded with dMi-2 or mH2a1.1 in the absence or in the presence of free ADPr (final concentration: 200 μM), as indicated on top. Lane 1: input (3,5%). Bound material was analysed by Western blot using anti-PAR antibodies. Molecular weight is depicted on the left.

5.4.6 N-terminal domain of dMi-2 is responsible for PAR binding *in vitro* and recruitment to *hsp* loci *in vivo*

Several protein domains, such as the macrodomain and the PBZ domain, have been shown to interact with poly(ADP-ribose) specifically and directly (Karras et al. 2005; Ahel et al. 2008). However, dMi-2 lacks both of these domains. To map the dMi-2 part, which binds to PAR, pulldown assays with PARylated PARP1 were performed with a panel of dMi-2 truncation mutants (Fig. 5.34 A). dMi-2 mutants were purified from SF9 baculovirus-infected cells. All mutants were immobilized on the beads, titrated on a Coomassie stained SDS-Page gel and the same protein amount was used for each pulldown (Fig. 5.34 B, lower panel). Western blot analysis revealed strong binding of dMi-2WT, dMi-2ΔCD, dMi-2ΔC, dMi-2N and dMi-2(1-485) and weaker binding of the dMi-2-CD+ATPase mutant (Fig. 5.34 B, upper panel, lanes 3, 4, 6, 7, 9 and 10). However, the PAR binding of mutants lacking the N-terminal part or the isolated ATPase domain (dMi-2ΔN and dMi-2ATPase), was completely abolished (Fig. 5.34 B, upper panel, lanes 5 and 8). This

indicates that the N-terminal region of dMi-2 has a high affinity for PAR. Within this part of dMi-2, both the PHD finger containing region N-terminal of the chromodomains (aa 1-485) and (to a lesser extent) the chromodomains were independently capable of PAR binding. This suggests that dMi-2 possesses at least two PAR binding regions that can function independently from each other.

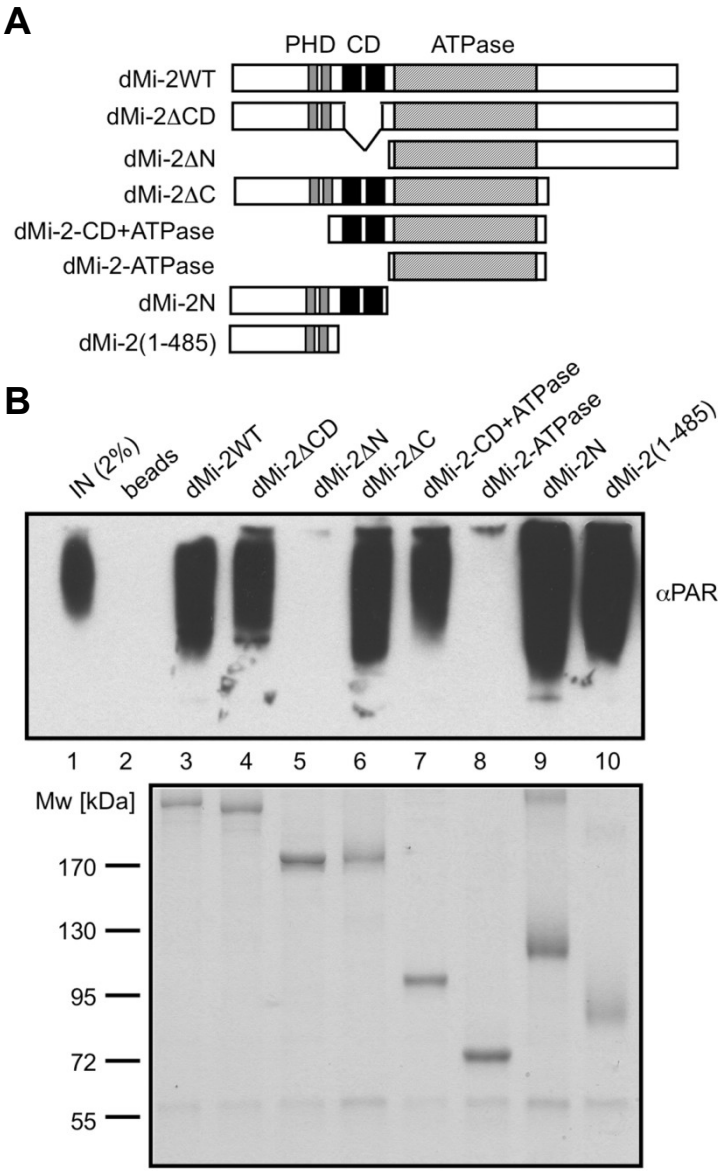

Figure 5.34 N-terminal region of dMi-2 binds PAR *in vitro*.
(**A**) Scheme of dMi-2WT and mutants used for PARP pulldown assay. PHD, PHD fingers; CD, chromodomains; ATPase, ATPase domain. (**B**) PAR was synthesised *in vitro* by recombinant PARP1 as in Fig. 5.32. Reactions were incubated with control anti-Flag beads (beads) and beads loaded with different dMi-2 mutants. Upper panel: Western blot analysis of PARP pulldowns performed with anti-PAR antibodies, as indicated. Lane 1 input (2%). dMi-2 mutants are shown on

top. Lower panel: Coomassie stained SDS-Page gel showing the dMi-2 constructs used, 1 μg of protein was loaded on each gel well.

Next the fine mapping of the PAR binding regions in the N-terminus of dMi-2 was performed. The N-terminal region of dMi-2 contains two highly conserved domains, a pair of PHD fingers (residues 377 to 484) and a tandem chromodomains (residues 488 to 673). The PARP pulldown experiment performed with baculovirus expressed proteins (Fig. 5.34) suggests that chromodomains might bind PAR. However, it was not clear whether PHD fingers bind this polymer as well. To resolve this issue, GST-fusions containing these domains were generated and tested for their ability to bind PAR in dot blot assays (data not shown). This confirmed that the chromomodomains bind PAR independently. However, the PHD fingers did not display PAR binding activity. Thus, other PAR binding regions close to the N-terminus of dMi-2 are responsible for PAR binding.

The N-terminal 375 residues of dMi-2 are characterized by a high content in charged residues (24% D/E, 21% R/K), a property that is conserved between dMi-2 and mammalian CHD4 proteins (Figure 5.35 A). In addition, these proteins share a region with high sequence similarity, the CHDNT domain (Pfam family PF08073) of unknown function. Several of diverse PAR binding motifs have been identified in number of proteins. A common feature of these motifs is that they all contain K/R rich motifs interspersed with residues with hydrophobic side chains (Pleschke J.M., JBC 2000, Gagne J.P. NAR 2008). To identify PAR binding regions, different dMi-2 fragments were expressed as GST-fusions, titrated and subjected to a PARP binding assay (Fig. 5.35 B). This analysis revealed strong PAR binding activity for three of the four K/R-rich fragments (K/R I, K/R III and K/R IV; Figure 5.35 B, lanes 10, 13 and 15). By contrast, K/R-rich fragment II and a fragment encompassing the CHDNT domain failed to interact with PAR (Fig. 5.35 B, lanes 6 and 12).

Altogether, these results suggest that dMi-2 contains multiple PAR binding regions in its N-terminus: three are characterised by a high content of basic amino acid residues (K/R I, K/R III and K/R IV) and one region containing the tandem chromodomains.

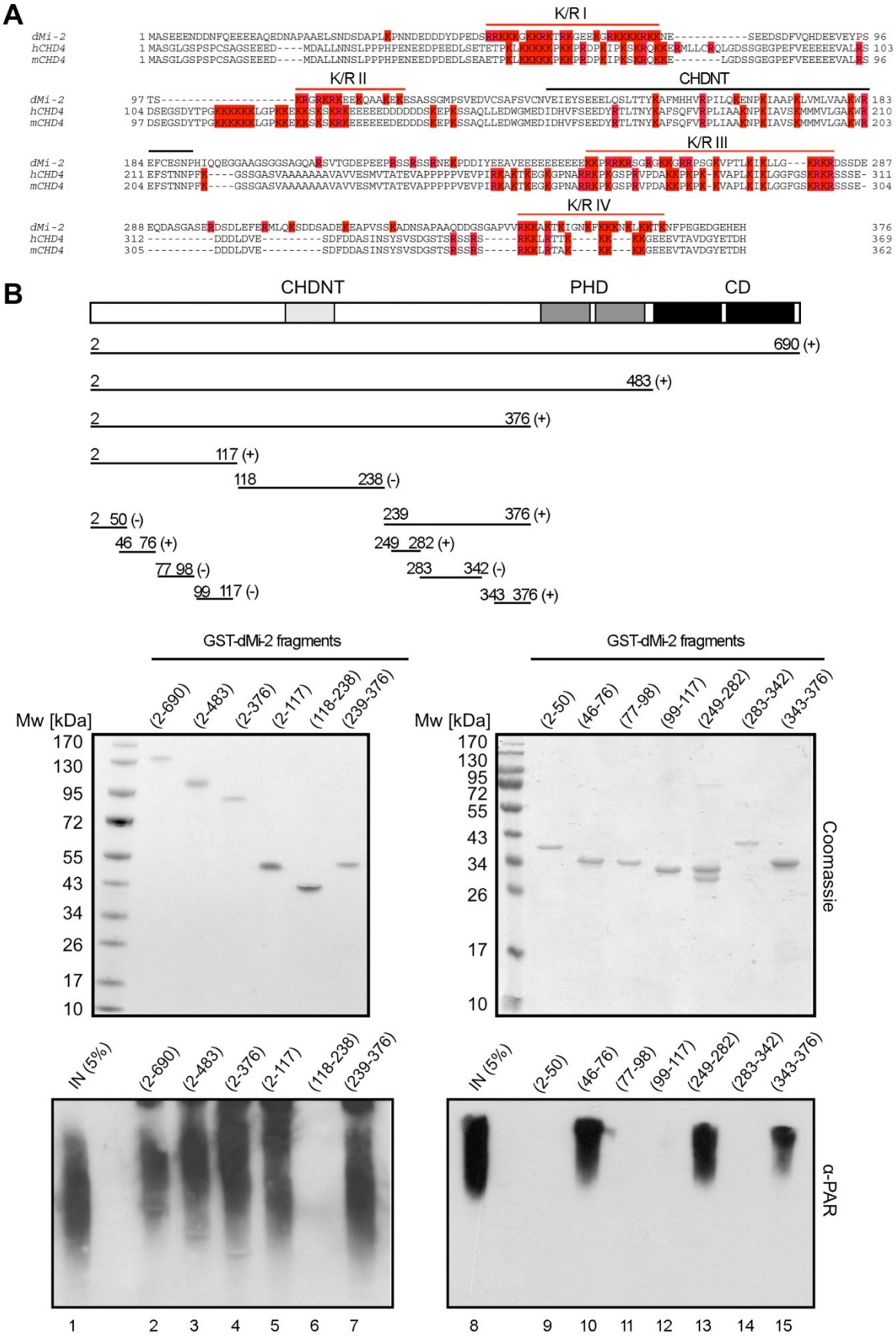
A
K/R I
K/R II
CHDNT
K/R III
K/R IV
dMi-2
hCHD4
mCHD4
B
CHDNT
PHD
CD
2 690 (+)
2 483 (+)
2 376 (+)
2 117 (+)
118 238 (-)
2 50 (-)
46 76 (+)
77 98 (-)
99 117 (-)
239 376 (+)
249 282 (+)
283 342 (-)
343 376 (+)
GST-dMi-2 fragments
(2-690)
(2-483)
(2-376)
(2-117)
(118-238)
(239-376)
Mw [kDa]
170
130
95
72
55
43
34
26
17
10
(2-50)
(46-76)
(77-98)
(99-117)
(249-282)
(283-342)
(343-376)
Coomassie
IN (5%)
α-PAR
1
2
3
4
5
6
7
8
9
10
11
12
13
14
15

Figure 5.35 PAR binding regions of dMi-2.
(**A**) Multiple sequence alignment of N-terminus of dMi-2 and human and mouse CHD4. All K and R amino acid residues are coloured in red. Red lines indicate the four K/R rich regions. The black line indicates the CHDNT domain. (**B**) Mapping of PAR binding regions in the N-terminal part of dMi-2. Upper panel: Schematic representation of dMi-2 constructs used. Numbers indicate the amino acid borders of the constructs. (+) and (-) indicate binding to PAR. Middle panel: Coomassie stained SDS-Page gels with purified GST-dMi-2 fragments used for PARP pulldown assays. Lower panel: PAR binding assays with GST-dMi-2 fragments were performed as in Figure 5.34. Bound material was analysed by anti-PAR Western blot. Lanes 1 and 8: inputs.

As *in vitro* binding analysis revealed that the N-terminal region of dMi-2 contains several regions important for PAR binding, it was plausible that this part plays also a role in dMi-2 recruitment to heat shock genes *in vivo*. If this is the case, the dMi-2 mutant lacking the entire N-terminus should not be recruited to heat shock puffs. To monitor dMi-2 binding to heat shock loci *in vivo*, transgenic fly lines carried GFP-tagged dMi-2WT and dMi-2ΔN variant were generated. As the predicted nuclear localization signal of dMi-2 localizes to the N-terminal part of the protein, to assure correct nuclear localization of the dMi-2ΔN mutant, a GFP tag with an independent NLS was utilized. GFP fluorescence in the whole salivary glands confirmed proper nuclear localization of both constructs (Fig. 5.36, lower left panel). In addition, Western blot analysis of whole cell extracts from larval brains confirmed equal expression of both proteins (Fig. 5.36 lower right panel).

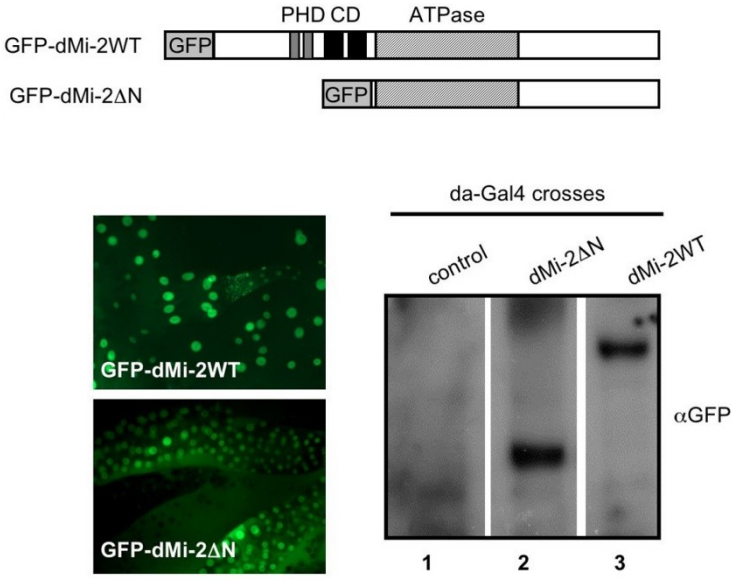

Figure 5.36 Verification of transgene expression in GFP-dMi-2WT and GFP-dMi-2ΔN flies
Upper panel: Scheme of GFP-tagged dMi-2 variants used for transgenic flies generation. PHD, PHD fingers; CD, chromodomains; ATPase, ATPase domain. Lower panel, left: GFP fluorescence in whole salivary glands in GFP-dMi-2WT and GFP-dMi-2ΔN expressing flies. To induce

transgene expression, flies were crossed with a salivary gland specific Gal4-driver, 58AB-Gal4. Lower panel, right: verification of dMi-2 transgene expression in larvae. Control flies and flies carrying a GFP-dMi-2WT and GFP-dMi-2ΔN transgenes were crossed with a da-GAL4 driver strain. Whole cell larval brain extract were subjected to Western blot analysis with anti-GFP antibodies, as indicated.

To assess the localization of GFP-tagged dMi-2 transgenes on polytene chromosomes, a 58ABGal4-driver, which specifically drives transgene expression in salivary glands, was used. Polytene chromosomes were isolated upon heat shock and the localization of dMi-2WT and dMi-2ΔN was monitored by indirect immunofluorescence with anti-GFP antibody. The staining revealed a strong signal for GFP-dMi-2WT on heat shock puffs, which suggests that the tagged, full length protein is recruited correctly to the *hsp70* loci. By contrast, the N-terminal mutant failed to stain the *hsp70* puffs (Fig. 5.37). This result demonstrates that the PAR binding, N-terminal part of dMi-2 is important for the remodeler recruitment to heat shock genes *in vivo*. Interestingly, dMi-2 mutant with internal deletion of chromodomains was still binding to the heat shock loci (data not shown). This indicates that the region containing chromodomains is dispensable or redundant with the N-terminal (1-485 aa) region for the recruitment of dMi-2 to activated heat shock genes. Altogether, these results support the notion that dMi-2 binding to PAR makes an important contribution to the recruitment of this chromatin remodeler to stress-activated *hsp70* genes.

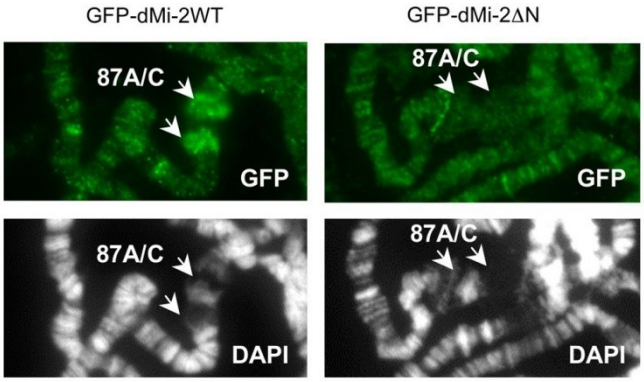

Figure 5.37 N-terminal region of dMi-2 is essential for dMi-2 recruitment to *hsp70* loci
Polytene chromosomes from transgenic larvae expressing GFP-dMi-2 transgenes (dMi-2WT and dMi-2ΔN) were analysed by immunofluorescence using anti-GFP antibody (green) and DAPI (grey). To induce transgene expression, flies were crossed with a salivary gland specific 58AB-Gal4 driver. 3rd instar larvae were heat shocked at 37°C for 20 min before squash preparation.

Pictures show magnified chromosome sections with the *hsp70* 87A and 87C loci indicated by arrows.

5.4.7 Comparison of dMi-2 binding to PAR and nucleic acids

dMi-2 recruitment to *hsp*70 loci by interaction with PAR and its subsequent binding to RNA of heat shock genes, suggests that dMi-2 switches binding from negatively charged PAR polymer to nascent RNA, once it is recruited to the activated genes. This also suggests that dMi-2 should possess different affinities to different nucleic acids and the PAR polymer. To gain insight into the relative affinities of dMi-2 for DNA, RNA and PAR, and to determine if dMi-2 can bind to several types of nucleic acid simultaneously or if binding is competitive, several competition assays have been performed. First, dMi-2 binding to RNA and DNA was tested in the presence of increasing amounts of PAR (mass ratios 1:1, 1:2 and 1:4) in electrophoretic mobility shift assays (Fig. 5.38 A). In this assay, PAR was able to compete with RNA and DNA for dMi-2 binding. However, whereas dMi-2 no longer bound to DNA at a DNA:PAR mass ratio of 1:2, residual dMi-2/RNA complexes were still detectable at an RNA:PAR mass ratio of 1:4. This suggests that dMi-2 has a higher binding affinity for RNA than for DNA. To test his hypothesis, dMi-2 was incubated with different mass ratios of RNA and DNA (Fig. 5.38 B). This experiment showed that, at a DNA:RNA mass ratio of 1:1, dMi-2/RNA complexes formed readily but dMi-2/DNA complexes were not detected (Fig. 5.38 B, left and right panel, line 3). Moreover, dMi-2/RNA complexes formed even at DNA:RNA mass ratios of 4:1, while dMi-2/DNA complexes were still not detected (Fig. 5.38 B, left panel, line 5).

To test if RNA or DNA can compete with dMi-2 for binding to the PAR polymer, a dot blot assay was performed. dMi-2 was preincubated with increasing amount of RNA or DNA, followed by incubation with PAR. In this system, RNA competed with immobilised PAR for binding to dMi-2 whereas DNA failed to do so (data not shown).

Taken together, the competition assays suggest that dMi-2 has a higher affinity for binding to RNA and PAR than for binding to DNA. In addition, dMi-2 appears to bind RNA and PAR in a mutually exclusive manner. Thus, these results are consistent with the hypothesis that dMi-2 is first recruited to HS loci by interaction with PAR (which is produced prior to and independent of transcription) and, once RNA synthesis has been strongly activated, the remodeler switches to binding the nascent RNA.

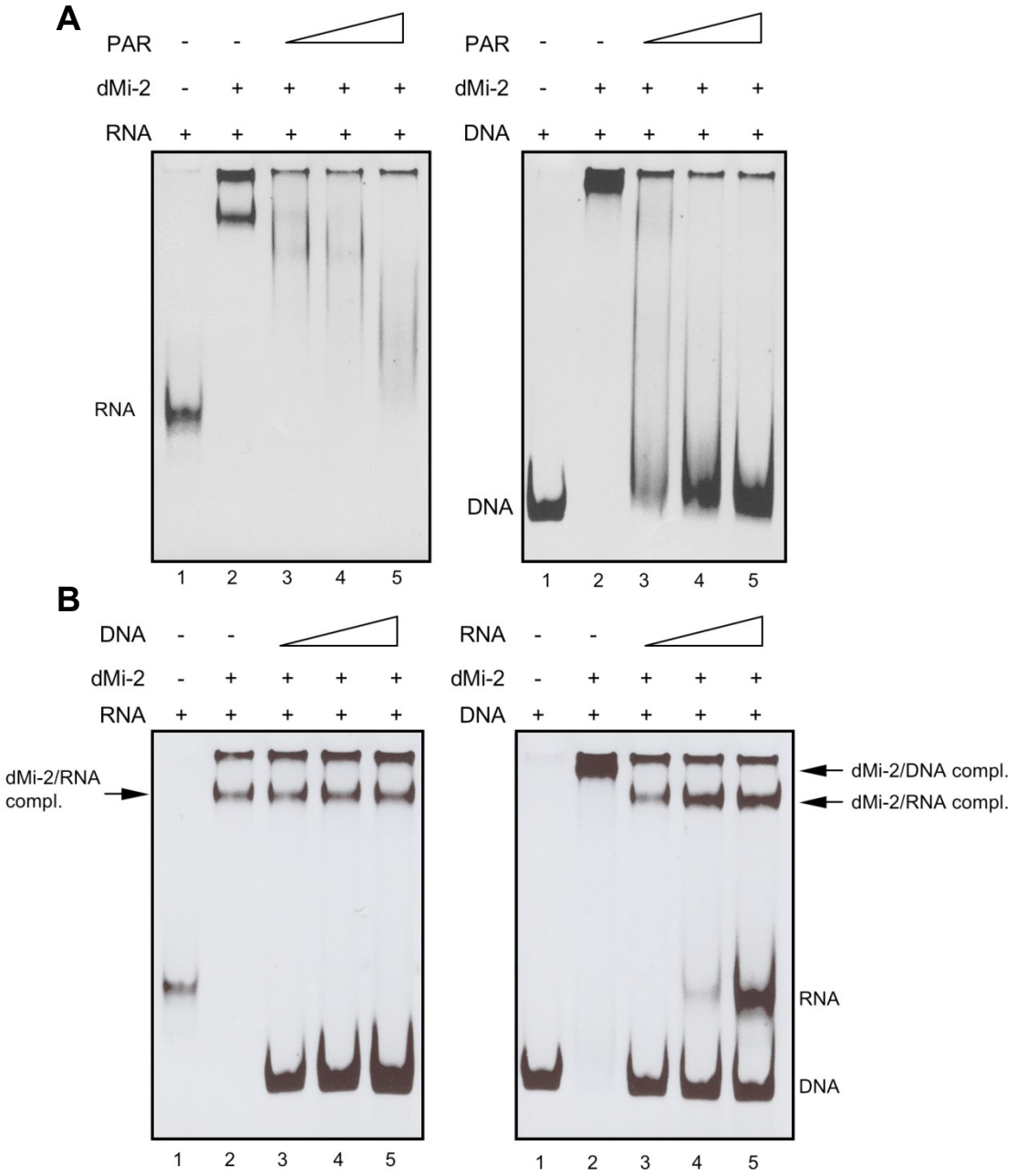

Figure 5.38 dMi-2 binding to PAR, RNA and DNA

(**A**) Competition mobility shift assays. Left panel: 80 ng of single stranded *hsp70* RNA was incubated with 0,2 μg of recombinant dMi-2 in the absence or in the presence of increasing amounts of PAR polymer, as indicated. Right panel: 80 ng of hsp70 DNA was incubated with 0,2 μg of recombinant dMi-2 in the absence or in the presence of increasing amounts of PAR polymer, as indicated. The following mass ratios of RNA to PAR or DNA to PAR were used: lane 3 - 1:1, lane 4 -1:2, lane 5 -1:4. Positions of unbound RNA and DNA probes are indicated on the left.

(**B**) Left panel: 80 ng of single stranded *hsp70* RNA was incubated with 0,2 μg of recombinant dMi-2 in the absence or in the presence of increasing amounts of DNA, as indicated. Right panel: 80 ng of *hsp70* DNA was incubated with 0,2 μg of recombinant dMi-2 in the absence or in the presence of increasing amounts of RNA, as indicated. The following weight ratios of RNA to DNA or DNA to RNA were used: line 3 - 1:1, lane 4 -1:2, lane 5 -1:4. Positions of unbound RNA and DNA probes and dMi-2/DNA and dMi-2/RNA complexes are shown on the right.

6. Discussion

This doctoral thesis consists of two major parts. In the first part, a novel CHD chromatin remodeler, dCHD3 has been characterized biochemically and functionally. These results contribute to the current knowledge of ATP-dependent chromatin remodeling by the CHD family of remodelers. In the second part, a role of dMi-2 in active heat shock gene expression and its recruitment mechanism therein have been investigated. The results from this part revealed a novel function of this remodeler in transcription and the recruitment mechanism of dMi-2 to a set of inducible genes. These results constitute foundations to study dMi-2 in a broader context of active transcription.

6.1 dCHD3 is a novel nucleosome stimulated ATPase

dCHD3 is the only member of the CHD family in *Drosophila* which has not been studied to date. Phylogenetic analysis of the *dChd3* gene has revealed that it is present not in all *Drosophila* species but only in the *D. melanogaster* subgroup (Fig. 5.1). The similarity to *dMi-2* suggests that the *dChd3* gene originated from integration of a truncated, reverse-transcribed *dMi-2* mRNA. This hypothesis is supported by the fact that the *dCHD3* gene lacks introns.

In order to characterize dCHD3, I have cloned it and studied enzymatic activities of the recombinant protein. These experiments showed that, similarly to dMi-2, dCHD3 is a nucleosome stimulated ATPase and it does not require histone tails for this activity (Fig. 5.2 and Fig. 5.3). Nucleosome stimulation of dCHD3 activity is shared by other members of CHD family, such as Mi-2 and CHD1. Remodelers belonging to the same family may differ in the ATPase activation. This might be the consequence of differences in their substrate recognition, domain structure or the presence of other subunits in the complex. For instance, it has been shown that yeast Chd1 requires the H4 tail for efficient ATPase activation, whereas removal of histone tails has no effect on dCHD3 and dMi-2 ATPase activity (Fig. 5.3) (Brehm et al. 2000; Ferreira et al. 2007). In this regard, partial activation of dCHD3 by naked DNA seems to be a specific feature of this remodeler (Fig. 5.2). Interestingly, it has been demonstrated that a dMi-2 mutant lacking the entire C-terminal domain is stimulated by free DNA as well as by nucleosomes (Bouazoune et al. 2002). This suggests that the C-terminal domain of dMi-2 might play a regulatory role in the ATPase activity by defining substrate recognition. As dCHD3 lacks most of the C-terminal

domain, consequently it becomes more prone for activation by free DNA. The C-terminal domain of dMi-2 and to a lesser extent, dCHD3, might inhibit stimulation of the ATPase activity in the presence of the wrong substrate. In agreement with this, removal of the last 92 aa from dCHD3 activates its ATPase even more in the presence of DNA without changing its DNA and nucleosome binding (Fig. 5.8). These results are reminiscent of the studies on yChd1 which have revealed that yChd1 tandem chromodomains inhibit activation of this remodeler by DNA (Hauk et al. 2010). Crystallographic studies showed that this is due to a special positioning of chromodomains which block the ATPase domain in the absence of nucleosomes (chapter 2.3.3.1) (Hauk et al. 2010). Hence, it is plausible that the C-terminus of dCHD3 and especially of dMi-2 acquires a similar position. Crystallographic studies will be required to test this hypothesis.

6.2 Substrate binding and nucleosome remodeling by dCHD3

dCHD3 binds both nucleosomes and DNA *in vitro* and its chromodomains are important for this (Fig. 5.8). In contrast to dMi-2, dCHD3 creates up to four products on the gel in nucleosome and DNA binding assays (Fig. 5.4). This indicates that more than one dCHD3 molecule is binding to these substrates and could be due to more than one binding sites on the substrates. However, this also suggests a possibility of a cooperative binding of dCHD3 to the substrates. Indeed, it has been demonstrated that some helicases dimerize on DNA substrate (Maluf et al. 2003a; Maluf et al. 2003b). Moreover, it has been shown recently, that ACF dimerizes upon nucleosome binding and works as a dimeric ATPase (Racki et al. 2009). It would be interesting to test whether the same applies to dCHD3. Interestingly, truncated dMi-2 mutants also generate several products in band shift assays and this requires the presence of chromodomains (Bouazoune et al. 2002). Thus, it is plausible that chromodomains of dMi-2 and dCHD3 might play a role in cooperative binding to the substrate.

It has been shown previously, that dMi-2 binds to mononucleosomes assembled on 146 bp and 248 bp DNA fragments, which indicates that it does not require flanking DNA for binding (Brehm et al. 2000). In the experiments made in the course of this thesis, mononucleosomes assembled on 200 bp DNA fragments containing a positioning sequence have been used. Thus, it cannot be excluded that dCHD3 needs free DNA ends for nucleosome binding. However, one result speaks against this. dCHD3 remodels both end

positioned and middle positioned nucleosomes equally well (Fig. 5.5). This suggests that dCHD3 does not require free DNA on both sides of the nucleosome and it is plausible that dCHD3 acts primarily through contacts with the nucleosomal DNA.

Mononucleosome mobilization assays have revealed that dCHD3 is a potent nucleosome remodeling enzyme. In the remodeling reactions used in these studies, both dMi-2 and dCHD3 mobilize end- and middle-positioned mononucleosomes (Fig. 5.5 and Fig. 6.1). This is in contrast to previous studies on dMi-2 which showed that it remodels preferentially nucleosomes from the end to the middle (Brehm et al. 2000). This discrepancy may come from different DNA fragments used for mononucleosome assembly. In the studies mentioned above, a 248 bp mouse 5S rDNA promoter was used for nucleosome assembly, whereas in the assay used in this thesis, a 200 bp DNA fragment containing a high nucleosome affinity '601' positioning sequence was utilized (Lowary and Widom 1998). Indeed, it has been demonstrated that DNA sequence might determine the nucleosome translocation direction and controls nucleosome destination. For instance, the nucleosome positions after enzymatic remodeling have been changed by inserting DNA fragments into the '601' positioning element (van Vugt et al. 2009). This demonstrates that direction preference is not an invariant property of the remodeling machine but is influenced by the underlying DNA sequence (Murawska et al. 2008).

dCHD3, similarly to dMi-2, moves end positioned mononucleosomes to the middle (Fig. 5.5). However, lower concentrations of dCHD3 than dMi-2 are required to show a nucleosome mobilization effect, which suggests that dCHD3 is more active remodeler than dMi-2 *in vitro*. It would be interesting to make more quantitative ATPase assays in order to determine and compare the enzymatic parameters of dMi-2 and dCHD3.

Strikingly, dCHD3 seems to differ from dMi-2 when middle positioned nucleosomes are used as a substrate. In this reaction, free DNA accumulates which likely reflects nucleosome disassembly. Moreover, dCHD3 generates a nucleosome product that migrates quicker than the end-positioned nucleosome (Fig. 5.5, lower panel). This reflects probably the movement of the histone octamer beyond the DNA ends, a phenomenon previously observed for SWI/SNF remodeling complexes (Jaskelioff et al. 2000; Flaus and Owen-Hughes 2003; Kassabov et al. 2003; Fan et al. 2005; Gutiérrez et al. 2007). It has been demonstrated that sliding beyond the DNA ends on mononucleosome templates leads to nucleosome destabilization and histone displacement (Flaus and Owen-Hughes 2003). The kinetics of the mobilization reaction by dCHD3 are in agreement with this view as

mobilized nucleosomes are produced within five seconds, whereas free DNA becomes detectable only after 10 min, when most nucleosomes have already been relocalized (Fig. 5.6).

However, this result also raises the question, whether dCHD3 is capable of nucleosome disassembly. This activity has been described for the SWI/SNF and RSC complexes and it has been suggested that the nucleosome disassembly is accompanied by histone octamer transfer to DNA in trans. Interestingly, the RSC complex cooperates with histone chaperone Nap1 for this activity, whereas the SWI/SNF complex needs the activation domain of a transcription factor (Lorch et al. 1999; Gutiérrez et al. 2007). In the case of SWI/SNF the presence of an oligonucleosome probe is required for mononucleosome dissociation, suggesting that evicted histones are transferred in trans to this oligonucleosome probe (Walter et al. 1995; Owen-Hughes and Workman 1996; Gutiérrez et al. 2007). In fact, in the remodeling experiments used in this thesis, in addition to the mononucleosomes, a nucleosomal array derived from the plasmid backbone is still present (Fig. 3.3). In order to test whether observed nucleosome disassembly in dCHD3 reaction requires histone octamer transfer, the remodeling assay should be performed in the presence of mononucleosomes only. The plasmid backbone should be therefore removed before mononucleosome assembly is set up.

There is also another possibility of nucleosome disassembly. The generation of a quicker migrating nucleosomal particle by movement of the histone octamer beyond the DNA ends, potentially creates an opportunity to disassemble nucleosome by invading the region of DNA inhabited by a neighbor nucleosome. Indeed, such mechanism of nucleosome disassembly has been suggested (Engeholm et al. 2009). To address this question a di- or trinucleosome templates should be utilized for the remodeling reaction. Recently, a quantitative double-label technique has been used to demonstrate the nucleosome disassembly reaction by SWI/SNF from di- and trinucleosomes (Dechassa et al. 2010). Using this method, it has been shown that SWI/SNF remodels the nucleosome and translocates in one direction along the DNA. Upon encountering the downstream nucleosome, an H2A dimer is first displaced, followed by eviction of the entire neighboring nucleosome from the DNA template. Notably, in this experimental set up, histone displacement occurs in the absence of histone chaperones or naked DNA as acceptors (Dechassa et al. 2010). In the light of these experiments, in order to figure out

whether dCHD3 activity can disassemble nucleosomes, more elaborate experimental approaches than mononucleosome mobility assays, are needed.

Noteworthy, free DNA accumulation in the remodeling reaction was previously observed also for dMi-2, but only when it was added in huge excess to the end positioned mononucleosomes (Bouazoune and Brehm 2005). The nucleosome destabilization was more pronounce upon dMi-2 dephosphorylation and it has been suggested that dMi-2 phosphorylation by the CK2 kinase plays a role in regulation of dMi-2 enzymatic activity (Bouazoune et al. 2002; Bouazoune and Brehm 2005). Thus it is plausible, that also dMi-2 possesses nucleosome dissociation activity under certain conditions.

In addition to mononucleosome mobilization assays, the ability of recombinant dCHD3 and dMi-2 to remodel polynucleosomal substrates *in vitro* followed by restriction enzyme digestion has been tested (data not shown). Both remodelers increased the accessibility of nucleosomal restriction sites. Interestingly, this effect was observed when the restriction enzyme was present during the remodeling reaction as well as when it was added after remodeling took place. This result demonstrates that both factors can create stably remodeled polynucleosomes *in vitro* (Murawska et al. 2008).

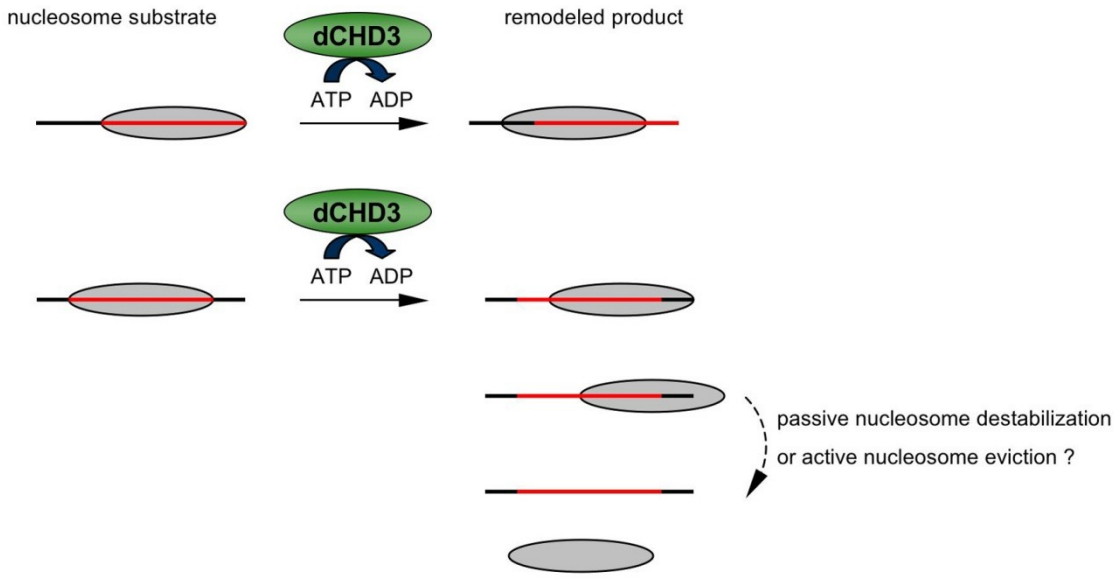

Figure 6.1 Model of mononucleosome remodeling by dCHD3
End positioned or middle positioned nucleosome substrate is depicted on the left and the remodeling products are depicted on the right. Grey oval represents histone octamer, red line indicates '601' positioning sequence, black line indicates flanking DNA, green oval represents dCHD3. Dashed arrow points towards nucleosome disassembly which can occur either by passive

destabilization caused by the movement of the histone octamer beyond the DNA ends or alternatively dCHD3 can evict nucleosomes in the course of the remodeling reaction (see text for details).

6.3 Chromodomains of dCHD3 as DNA binding modules

Studies on dCHD3 truncation mutants have revealed that the chromodomains of dCHD3 are critical for the ATP-dependent nucleosome mobilization. Removal of the part containing chromodomains and PHD finger, impairs the nucleosome remodeling, as well as nucleosome and DNA binding of dCHD3 (Fig. 5.8 and 5.9). By contrast, removal of PHD finger has no effect on substrate binding and remodeling by dCHD3 (Fig. 5.8 and 5.9). These results suggest that chromodomains of dCHD3 are involved in nucleosome remodeling by providing an interaction surface for nucleosomal DNA. However, because the dCHD3 truncation mutant impaired in nucleosome mobility lacks both the PHD finger and chromodomains, it cannot be formally excluded that PHD finger and chromodomains of dCHD3 carry out redundant functions. To address this issue, a mutant with an internal deletion of chromodomains should be tested for nucleosome remodeling activity. Nevertheless, the findings that chromodomains are involved in nucleosome remodeling are in agreement with the results previously reported for the chromodomains of dMi-2 (Bouazoune et al. 2002). It has been suggested that the dMi-2 chromodomains mediate the interaction between the enzyme and its nucleosomal DNA and thus they function at an early step of the chromatin remodeling reaction. Hence, it is plausible that chromodomains of both dMi-2 and dCHD3 have evolved as DNA rather than modified histone binding modules. Based on sequence differences between chromodomains of CHD3/CHD4 and CHD1, it has been suggested that CHD3/CHD4-type chromodomains do not bind methylated histone tails (Okuda et al. 2007). Indeed, histone peptide pulldowns as well as histone peptide arrays performed in our laboratory with dMi-2 chromodomains have not identified any specific histone modification to which these chromodomains bind (P. Steffen, diploma thesis, and this study, unpublished data). However, it still remains possible that a specific tail modification not tested so far is recognized by chromodomains or PHD fingers of these chromatin remodelers.

6.4 dCHD3 and dMi-2 differ *in vivo*

Despite a significant sequence similarity between dCHD3 and dMi-2, *in vivo* analysis revealed that both factors differ from each other significantly. Whereas dMi-2 is present throughout embryogenesis, dCHD3 is strongly detected in early embryos and then dCHD3 levels decrease until it becomes undetectable at late embryo stages (Fig. 5.10 A). Differences are also observed in adult flies, as dMi-2 is detected in both male and female animals, whereas dCHD3 is detected only in female flies. However, it cannot be excluded that due to the Western blot detection limitations, dCHD3 expression in the tested developmental stages is underestimated. Indeed, although there is no dCHD3 detected at larval stages by Western blot, dCHD3 is clearly detectable in salivary glands of 3rd instar larvae with indirect immunofluorescence (Fig. 5.15). In addition, dCHD3 seems to be at least five times less abundant in cells than dMi-2 as revealed by quantitative Western blot (M. Groh, data not shown). This strongly suggests that the level and expression of dCHD3 are restricted to early developmental stages and perhaps certain tissues at later stages of development. Thus, dCHD3 might play specific roles on chromatin rather than be involved in global chromatin remodeling or maintenance.

Apart from expression and abundance differences, dCHD3 differs from dMi-2 significantly with respect to interactions with other proteins. It does not interact with histone deacetylase dRPD3 or dMep1 (Fig. 5.12 and data no shown) which makes it unlikely to be a component of the dNuRD or dMec-like complexes. Moreover, in contrast to most known chromatin remodelers, dCHD3 does not form a stable multiprotein complex *in vivo* but it rather exists as a monomer in cells and embryos (Fig. 5.13). Thus, dCHD3 resembles *S. cerevisiae* or *D. melanogaster* CHD1 which were also shown to predominantly exist as monomers (Tran et al. 2000; Lusser et al. 2005). This finding does not exclude the possibility that dCHD3 forms transient interactions with other factors or that it is a part of larger complexes at later developmental stages. To test this possibility, it would be interesting to perform immunopurification of dCHD3 from cells and different developmentally staged extracts and try to identify the interacting proteins by Mass Spectrometry.

Another striking difference between dCHD3 and dMi-2 concerns their requirement for cell viability. The depletion of dMi-2 has a significant effect on cell growth and viability, suggesting that dMi-2 is essential for cell survival (Fig. 5.14 B). In line with this, dMi-2-

deficient flies are generally nonviable and die during larval stages (Kehle et al. 1998). Their survival to larval stage is probably due to the maternal contribution of dMi-2. Indeed, Western blot analysis and indirect immunofluorescence show a high level of dMi-2 protein in embryos prior to the onset of zygotic transcription (Fig. 5.10 and 5.11). By contrast, the depletion of dCHD3 has no significant effect on cell growth and viability. This is in agreement with a recent report on dCHD3 mutant flies which has shown that dCHD3 is not essential for adult fly viability and fertility (Cooper et al. 2010). These results also suggest that dCHD3 and dMi-2 are not fully redundant and that dCHD3 is not able to compensate for the loss of dMi-2.

Further evidence for *in vivo* differences between dCHD3 and dMi-2 comes from overexpression studies in flies (data not shown). Overexpression of a catalytically inactive mutant of dMi-2 impairs larvae development as they arrest as 3rd instar larvae and fail to develop further to the pupal stage. This phenotype is similar to the dMi-2 null mutant flies suggesting that ectopic expression of catalytically inactive mutant of dMi-2 efficiently replaces the endogenous enzyme and results in a dominant-negative phenotype.

Overexpression of a catalytically inactive mutant of dCHD3 in whole animals has no apparent effect on their survival or development. Remarkably, overexpression of wild type dCHD3 with the same Gal4 driver causes lethality at the first and second instar larvae stage. This phenotype could result from the overexpression effect of dCHD3. It has been shown that high overexpression of certain proteins causes lethality. For instance, overexpression of CP190, a component of chromatin insulator complexes, leads to lethality and severe developmental defects. It has been demonstated that this is due to high expression levels obtained with UAS Gal4 system. Decreasing expression levels of CP190 by using the *Ubi-63E* promoter, which can drive the expression of transgenes in many tissues at low levels, allowed to avoid the lethality problems (Akbari et al. 2009). Therefore, it might be necessary to change the expression system of dCHD3 transgene in order to prevent dCHD3 overexpression. However, expression levels of wild type and mutant dCHD3 are comparable due to the same chromosome integration site of the two transgenes. This strongly suggests that the phenotypes observed in wild type dCHD3 expressing animals cannot be explained solely by protein levels but they rather depend on the catalytic activity of the enzyme. Given that the dCHD3 abundance is very low in comparison to dMi-2, and given that dCHD3 is a more active remodeler than dMi-2 *in vitro*, it is plausible that dCHD3 has to be kept at low levels in order to prevent undesirable

chromatin alterations. To test this hypothesis, a polytene chromosome structure analysis in a transgenic line overexpressing dCHD3 to tolerable levels, could be performed.

Finally, there is also evidence that dCHD3 and dMi-2 could be regulated in a different way. It has been shown that dMi-2 is constitutively phosphorylated *in vivo* by dCK2. Dephosphorylation of recombinant dMi-2 plays a regulatory role as it increases its affinity for the nucleosomes, nucleosome-stimulated ATPase, and ATP-dependent nucleosome mobilization activities (Bouazoune and Brehm 2005). *In vitro* kinase experiment performed with SL2 whole cell extracts has revealed that in contrast to dMi-2, dCHD3 is not phosphorylated *in vitro* (data not shown). Although several phosphorylation sites are predicted in the dCHD3 sequence, dCHD3 lacks the N-terminal domain which is the main part of dMi-2 that is phosphorylated *in vivo*. This result suggests that phosphorylation by dCK2 is not a common regulatory mechanism for CHD chromatin remodelers. It is plausible that phosphorylation might play a role in a tight control of ATPase activity regulation of highly expressed remodelers. In this regard, a constitutive phosphorylation of an abundant dMi-2 would ensure its proper activity at its genomic targets, whereas much less abundant dCHD3 might not need to be regulated by phosphorylation. It is possible that dCHD3 is phosphorylated only under certain conditions or at specific cell cycle stages. It also remains to be determined if and how dCHD3 activity is regulated *in vivo*.

6.5 dCHD3 associates with mitotic chromosomes

Indirect immunofluorescence on *Drosophila* embryos has revealed that dCHD3 associates with condensed chromosomes in mitotic nuclei whereas dMi-2 displays a more diffuse nuclear staining (Fig. 5.11). Binding of dCHD3 to mitotic chromosomes is unusual as many transcription factors, RNAP II, histone modifying enzymes and cofactors are displaced from chromosomes at the onset of mitosis (reviewed in (Zaidi et al. 2010)). The proteins that remain associated with mitotic chromosomes include chromosome scaffold proteins (Hagstrom and Meyer 2003), the chromosomal passenger proteins (Adams et al. 2001), nuclear matrix proteins (Bérubé et al. 2000) and components of the basal transcription machinery (Michelotti et al. 1997; Chen et al. 2002; Christova and Oelgeschläger 2002). Proteins associated with mitotic chromosomes are thought to be either structural components of condensed chromosomes or they mark genes for specific gene expression pattern reestablishment upon mitosis exit. Therefore any potential dCHD3

function on mitotic chromosomes has to be further investigated. It would be important to determine the exact localization of dCHD3 at different stages of mitosis. For this, one could express GFP-tagged dCHD3 in *Drosophila* SL2 cells and analyse its chromosomal distribution by confocal microscopy. This approach has been used before to determine protein distribution during cell cycle in *Drosophila* cells (Clarke et al. 2005). In addition, it is important to confirm the staining with antibodies against endogenous dCHD3 with second independent antibodies to exclude any immunofluorescence staining artefacts.

What could be the function of an ATP-dependent chromatin remodeler in mitosis? Some chromatin remodelers, as human Brahma and BRG1, are excluded from mitotic chromosomes due to their phosphorylation. It has been suggested that this contributes to mitotic silencing (Muchardt et al. 1996). Not much is known about functions of chromatin remodelers during mitosis. For instance, ATRX, a human SWI/SNF remodeler, is enriched at condensed chromosomes during mitosis and plays a role in chromosome cohesion and segregation (Bérubé et al. 2000; Ritchie et al. 2008). A recent study on the ISWI remodeler has revealed its role in spindle microtubule stabilization during anaphase in *Xenopus* and *Drosophila* (Yokoyama et al. 2009). Thus, chromatin remodelers can have transcription independent functions during mitosis and contribute to proper chromosome segregation. Whether similar functions are acquired by dCHD3 remains to be determined.

A second interesting possibility is an involvement of dCHD3 in gene bookmarking during mitosis. It has been demonstrated that promoters of genes, which expression has to be inherited in daughter cells upon cell division, are bound by specific transcription factors during mitosis (Zaidi et al. 2010). This includes *Myc* and *Hsp70i* promoters, promoters of genes involved in cell growth or lineage commitment (Martínez-Balbás et al. 1995; Michelotti et al. 1997; Xin et al. 2007). Moreover, a recent genome wide study on human mitotic chromosomes has shown a mitotic shift of histone H2A.Z containing +1 nucleosome of active genes, resulting in the nucleosome occupancy at transcription start sites (Kelly et al. 2010). It remains to be determined whether a similar gene marking mechanism occurs in *Drosophila*. Nevertheless, it is tempting to speculate that ATP-dependent chromatin remodeling activities might be involved in regulation of this nucleosome shift. Thus, dCHD3 could be a candidate remodeler for gene bookmarking during mitosis.

6.6 Potential role of dCHD3 in transcription

Despite all the differences between dCHD3 and dMi-2, strikingly, they stain the same regions on polytene chromosomes of 3rd instar larvae (Fig. 5.15). The test for antibody specificity (Fig. 3.1) clearly showed that the antibodies against dCHD3 and dMi-2 do not cross-react which gives a strong indication that the observed staining pattern is specific for dCHD3. However, to exclude any cross-reactivity within the cell, one should use different antibodies against dCHD3 or ectopically express a tagged-version of dCHD3 at a very low level in order to observe the chromosomal binding sites of this remodeler.

The identical binding pattern of dCHD3 and dMi-2 suggests a common recruitment mechanism for both factors. Several targeting mechanisms have been proposed before for dMi-2. First, dMi-2 binds to DNA bound transcriptional repressors via a C-terminal domain (Kehle et al. 1998; Murawsky et al. 2001; Reddy et al. 2010). Second, dNuRD complexes could be guided to regions of methylated DNA via MBD-domain-containing subunits (Marhold et al. 2004b). However, the targeting mechanisms that have been proposed for dMi-2 do not seem to be applicable to dCHD3 as it lacks the C-terminal domain and does not interact with subunits of the dNuRD complex. Given that dCHD3 binds to interbands and given that it colocalizes with dMi-2, it most likely similarly to dMi-2, also localizes with actively transcribed genes (Fig. 5.16 and data not shown). This raises the possibility that dCHD3 could be recruited to active genes via binding to the transcription machinery. Indeed, coimmunoprecipitation experiments revealed a weak but significant association of dCHD3 with hypophosphorylated RNAP II (data not shown). Whether this interaction plays a role in recruitment mechanism, remains to be determined. Polytene chromosome staining upon heat shock has also revealed a strong recruitment of dCHD3 to *hsp70* loci (data not shown). However, no recruitment has been observed when the same antibodies have been used for ChIP (data not shown). By contrast, ChIP with polyclonal antibodies against dCHD3 has shown a promoter-associated peak which disappeared upon heat shock and no recruitment to the transcribed region of *hsp70* gene. Due to these discrepancies between immunofluorescence staining and ChIP analysis, to determine, if dCHD3 indeed is recruited to heat shock genes, it would be necessary to generate new polyclonal antibodies. Analysis of dCHD3´s role in *hsp70* gene transcription has been also performed. dCHD3 knockdown in flies had no effect on heat shock gene transcription (data not shown). However, it cannot be excluded that this is due to the

inefficient depletion of dCHD3 from larvae. Altogether, although polytene chromosome staining suggests a role of dCHD3 in active gene transcription, it is too early at this point to speculate on its possible functions therein. One possibility to address this question would be to perform transcriptome analysis upon dCHD3 knockdown or genome wide ChIP analysis in order to determine dCHD3 binding sites and correlate them to RNAP II binding, transcription factors and histone marks associated with transcription. In order to do this it would be necessary to generate new, ChIP grade antibodies for dCHD3.

6.7 dCHD3 – perspectives and further experiments

The lack of any obvious phenotype upon dCHD3 knockdown in cells, dCHD3 deletion or overexpression of catalytically inactive mutant in flies, suggests that perhaps this remodeler is specialized for very specific functions and further detailed analysis of these mutants will be required. One possibility would be to study dCHD3 using the eye as a model organ. The fly eye provides a useful system for studying cell proliferation and differentiation, cell cycle progression and it is dispensable for viability (Huang et al. 1999; Hirose et al. 2001). An eye-specific GMR-Gal4 driver induces transgene expression in the eye imaginal disc in differentiated cells. Interestingly, overexpression of dCHD3 wild type but not the catalytic mutant with this driver causes a rough eye phenotype (data not shown). This suggests that cells overexpressing dCHD3 undergo apoptosis. To test whether the rough eye phenotype is caused by cell apoptosis, it would be necessary to suppress this phenotype by coexpressing a baculovirus protein p35 or DIAP1 (p35 homolog in *Drosophila*). These proteins are caspase inhibitors, thus their overexpression blocks apoptosis. This strategy is commonly used to demonstrate apoptosis in the differentiated cells of the eye (Hirose et al. 2001). In addition, staining with acridine orange for apoptotic cells in the eye discs should also indicate whether the cells overexpressing dCHD3 undergo apoptosis. These experiments should clarify any potential link of dCHD3 to apoptosis.

Overexpression of dCHD3 with the ey-Gal4 driver, which first induces transgene expression in the eye and antenna anlagen in the embryo and then in proliferating cells in the eye imaginal disc, causes severe abnormalities, for instance: lack of eye or the whole head, antenna-like structures, ectopic antennas (data not shown). Similar phenotypes have been observed with ectopic eye expression of dACF1, a subunit of the ISWI complex

(Chioda et al. 2010). The defects in eye morphogenesis upon ectopic expression of dCHD3 might be caused by an altered cell cycle progression. To test this, a number of experiments should be performed. For instance, cell cycle could be observed by monitoring S-phase progression by BrdU incorporation in imaginal discs of larvae overexpressing dCHD3.
Finally, the presence of rough eye phenotype upon dCHD3 overexpression in the eye by the GMR-Gal4 driver, allows to design a genetic screen for enhancers or suppressors of this phenotype and thus, to identify factors which genetically interact with dCHD3. This approach has been used extensively to identify downstream transcriptional targets or potential factor binding partners for number of proteins (Therrien et al. 2000; Hirose et al. 2001; Park and Song 2008). Hence, this approach might shed light on *in vivo* functions of dCHD3.

6.8 dMi-2 in active transcription

Mi-2 is strongly linked to transcriptional repression in both vertebrate and invertebrate organisms (chapter 2.5.4.1). Many reports have shown that it contributes to the repression of lineage-specific genes as a subunit of the NuRD or dMec complexes (Kim et al. 1999; Fujita et al. 2004; Kunert et al. 2009; Reddy et al. 2010). Thus, significant colocalization of dMi-2 with active forms of RNAP II and elongation factors on polytene chromosomes (Fig. 5.16) is surprising and suggests that dMi-2 might be involved in active transcription. Indeed, several studies have implicated Mi-2 in gene activation before. First, Mi-2β contributes to the *CD4* gene expression via recruitment of transcription factor HEB and histone acetyltransferase p300 to the gene enhancer element during T-cell development (Naito et al. 2007). Second, NuRD is present at active FOG-1-regulated genes in erythroid cells and is directly required for transcriptional activation of GATA-1/FOG-1-dependent genes (Gregory et al. 2010). Third, Mi-2α enhances c-Myb-dependent reporter activation in a helicase-independent fashion (Saether et al. 2007). Finally, one report has suggested that Mi-2β is involved in rDNA activation in the nucleolus (Shimono et al. 2005). Altogether these results suggest that at least in some gene contexts, Mi-2 might be involved in gene activation. Currently it is unclear whether activating Mi-2 exists within the NuRD complex or whether it is a part of different complexes. It also remains to be determined how Mi-2 influences gene activation.

The results obtained in this study clearly demonstrate that dMi-2 is involved in transcription of induced heat shock genes. This is the first example in *Drosophila* that this remodeler has been shown to play a role in active transcription. Several pieces of evidence support this hypothesis. First, dMi-2 is rapidly recruited to the *hsp70* locus on polytene chromosomes upon heat shock (Fig. 5.17). Second, chromatin immunoprecipitation experiments show enrichment of dMi-2 in the transcribed regions of *hsp* genes upon heat shock (Fig. 5.20 and data not shown). Finally, both depletion and overexpression of a catalytically inactive mutant of dMi-2 significantly impair expression of *hsp70*, *hsp26* and *hsp83* (Fig. 5.22 and 5.24).

Interestingly, SWI/SNF and ISWI remodelers seem not to be recruited to heat shock genes. For instance, Brahma (BRM) is not enriched at *hsp70* puffs and heat shock gene activation is independent of BRM function (Fig. 5.18) (Armstrong et al. 2002). Notably, this differs from the human system, where the Brahma homolog, BRG1, is recruited to the *hsp70* gene promoter and transcribed regions and contributes to transcription elongation of this gene (Corey et al. 2003). Moreover, although the *Drosophila* ISWI complex, dNURF, is important for *hsp* gene transcription, ISWI does not accumulate at active *hsp70* loci (Fig. 5.18) (Badenhorst et al. 2002). Conversely, recruitment to heat shock puffs has previously been reported for *Drosophila* CHD1 (Kelley et al. 1999; Morettini et al. 2011). Thus, association with active *hsp* genes is shared by at least two members of the CHD family of nucleosome remodelers, dMi-2 and dCHD1, but not by SWI/SNF and ISWI proteins.

It has to be mentioned, that depletion of dMi-2 does not significantly perturb *hsp* gene transcription in Kc cells and, therefore, dMi-2 is dispensable for heat shock gene activation in this system (data not shown). It is believed that many factors contributing to *hsp* gene activation, for instance, FACT and Spt6, are highly abundant or redundant in Kc cells but more limiting in other contexts (Saunders et al. 2003).

6.9 dMi-2 plays a role in RNA processing and splicing of *hsp* genes

Expression of several *hsp* genes is strongly abrogated in flies with depleted levels of dMi-2 or flies expressing its inactive form. This raises the possibility that dMi-2 might be involved in chromatin remodeling on these genes and thus facilitate their expression. However, several results do not support this hypothesis. First, heat shock genes undergo rapid nucleosome disruption across the entire locus within two minutes after gene

activation and this requires at least three factors: HSF1, GAF factor and PARP1 enzyme (Petesch and Lis 2008). However, the first signal for dMi-2 is observed earliest at two minutes of heat shock and it increases in time (Fig. 5.29). Second, no significant differences in histone H3 removal on *hsp* genes in dMi-2 knockdown flies were observed (data not shown). Thus, it is unlikely that dMi-2 plays a role in nucleosome removal at heat shock loci.

The low transcript levels of *hsp* genes in dMi-2 depleted or mutant overexpressing flies may reflect disturbances in RNA processing. Indeed, the ratio of unprocessed or unspliced forms of *hsp70* and *hsp83* to total RNA levels of these transcripts are significantly increased in both, dMi-2 depleted and catalytic mutant overexpressing flies (Fig. 5.25). Similar defects have been reported previously for several factors involved in RNA processing. For instance, depletion of THO complex subunits in SL2 cells increases the ratio of unprocessed transcripts to total *hsp70* RNA while decreasing the heat shock gene response (Rehwinkel et al. 2004; Kopytova et al. 2010). Another report has shown that pharmacological inhibition of P-TEFb, a kinase that phosphorylates CTD of RNAP II at Ser2, leads to reduction of *hsp* transcripts and significant increase of unprocessed *hsp* RNA species. The authors postulated that inhibition of CTD phosphorylation at Ser2 abrogates recruitment of RNA processing factors which in turn leads to inefficient RNA processing and rapid degradation of *hsp* transcripts (Ni et al. 2004).

Several other experiments suggest dMi-2´s role in mRNA 3'end processing. First, it crosslinks throughout the entire transcribed *hsp70* gene and it is associated with the 3' end of the gene, where the cleavage and polyadenylation site is present (Fig. 5.21). Second, a recent ChIP deep sequencing on heat shocked cells performed in our laboratory has confirmed the binding of dMi-2 downstream of the transcription termination sites at most of *hsp* genes (Eve-Lyne. Mathieu, data not published). It has been reported that factors involved in transcription elongation and RNA processing display different crosslinking patterns at coding regions and downstream of the polyadenylation site. Some of them bind through the entire transcribed regions, others drop downstream of the polyadenylation site or conversely crosslink just downstream of the polyadenylation site (Kim et al. 2004; Mayer et al. 2010). Thus, there is an evidence for a transition of the elongation and processing factors at 3' ends of transcribed genes. Finally, dMi-2 interacts with nascent unprocessed *hsp70* and *hsp83* transcripts, which suggests that it can be involved in RNA processing more directly (Fig. 5.26). For example, dMi-2 might facilitate proper substrate

formation or access of processing factors to pre-mRNA 3' end. In this context, it would be important to determine whether any interactions between processing factors and dMi-2 occur *in vivo*.

mRNA 3' end processing is functionally coupled to transcription termination downstream of protein coding genes. This interplay between mRNA 3' end processing and transcription termination, makes it difficult to distinguish in which of these two processes dMi-2 plays a direct role. Despite extensive studies, still little is known about the mechanism of transcription termination and mRNA 3' end processing. There are currently two models which explain how transcription is terminated. The first model, known as the "anti-terminator model", suggests that the appearance of the polyadenylation sequence on the mRNA triggers an exchange in factors associated with elongating RNAP II which would decrease its processivity and eventually lead to transcription termination. The second scenario, called the "torpedo model" proposes that the mRNA cleavage at polyadenylation site could act as an entry point for an enzyme (helicase or exonuclease) that would track along the RNA and dissociate the RNAP II. Recent discoveries provide a support for both models (reviewed in (Buratowski 2005; Kuehner et al. 2011)). In addition, pausing of RNAP II downstream of the polyadenylation site facilitates transcription termination (Gromak et al. 2006).

Studies in yeast suggest a link between chromatin remodeling and transcription termination. yChd1 and Hrp1 have been implicated in transcription termination regulation at several genes via regulation of the chromatin structure at the 3' end of these genes. It has been proposed that chromatin structure at 3' end of the gene may enhance RNAP II pausing and thus facilitate the switch of RNAP II mode from elongation to termination (chapter 2.5.4.4) (Alén et al. 2002). In order to determine the role of dMi-2 in transcription termination, it would be interesting to test how far RNAP II transcribes beyond the polyadenylation site at the *hsp70* gene upon dMi-2 depletion. This question can be addressed by performing RNAP II ChIP experiments and compare its association with downstream regions of the polyadenylation site between dMi-2 depleted and wild type flies. Additionally, analysis of the transcription readthrough at the 3' end of *hsp70* gene could be also performed in wild type and mutant flies. Moreover, it would be interesting to monitor the chromatin structure at the 3' end of heat shock genes upon dMi-2 depletion by histone H3 and micrococcal nuclease accessibility assay. It has been reported that there is a nucleosomal free region at the 3' end of *hsp70* (Petesch and Lis 2008). Thus, it is plausible

that chromatin remodeling activities are involved in proper chromatin structure maintenance at the 3' end and consequently proper transcription termination.
Finally, it has been reported that defective transcription termination at the 3' end of a gene leads to decreased splicing and is required for optimal gene transcription (West and Proudfoot 2009). In this respect, the transcription and splicing defects of *hsp* genes could be an indirect effect of affected transcription termination. It has been shown that transcription termination involves protein components that bind to DNA and/or RNA polymerase and employ ATPase activity to dissociate polymerase complexes from the DNA template (Deng and Shuman 1998; Liu et al. 1998). Thus, it is plausible that ATPase activity of dMi-2 contributes to coupling ATP hydrolysis to transcription termination. Undoubtedly, the fascinating link between chromatin remodeling and RNA processing has to be elucidated in future experiments.

Recent years have also revealed interplay between splicing and chromatin remodeling. Two chromatin remodelers, hCHD1 and Brahma, have been implicated in pre-mRNA splicing, although the role of their ATPase activity is not clear in this context. First, hCHD1 is involved in regulation of pre-mRNA splicing by recruiting components of the splicing machinery to the transcribed RNA via recognition of the H3K4me3 mark (chapter 2.5.4.5) (Sims et al. 2007). Second, human Brahma associates with components of the spliceosome and favours inclusion of variant exons in the mRNA of several genes independent of its enzymatic activity. It has been found that Brahma decreases RNAP II elongation rate and thus facilitates recruitment of the splicing machinery to variant exons with suboptimal splice sites (Batsché et al. 2006). Moreover, Brahma is incorporated into nascent pre-mRNPs co-transcriptionally in *Chironomus tentans*. Depletion of SWI/SNF complex subunits in *Drosophila* SL2 cells changes the relative abundance of alternative transcripts from a subset of genes (Tyagi et al. 2009). Altogether, these results suggest that Brahma is involved in splicing regulation in different species. However, the molecular mechanism still remains to be determined.
The role of dMi-2 in splicing also has to be elucidated in further studies. It would be important to figure out whether dMi-2 plays a direct role in this process. One possibility would be to test if dMi-2 interacts with splicing machinery by making immunoprecipitation experiments followed by mass spectrometry. Although dMi-2 complex purification with classic chromatography did not show association of any splicing

factors, it is plausible that such associations exist in only substoichiometric amounts or are transient and become lost during traditional purification steps. Therefore it would be worth to try to perform coimmunoprecipitation experiments directly from crude nuclear extracts using milder purification conditions. Interestingly, in the recent release of The *Drosophila* Protein Interaction Mapping (DPiM) project that applied purification of transiently expressed tagged proteins followed by identification of associated peptides by mass spectrometry, an association of a splicing factor U2af50 with dMi-2 has been identified (https://interfly.med.harvard.edu). It would be interesting to test whether this interaction occurs between endogenous proteins. Another experiment, which would allow to study dMi-2 involvement in splicing, could be *in vitro* splicing assay in the presence of extracts containing or depleted of dMi-2. Similar experiments have been applied to test hCHD1 role in splicing (Sims et al. 2007). In addition a splice reporter minigene could be also adapted to *Drosophila* cell lines in order to study dMi-2 function in splicing *in vivo* (Lallena et al. 2002; Batsché et al. 2006).

Hsp genes usually do not possess introns, but *hsp83* is an exception. The role of dMi-2 in splicing regulation of this gene raises the question whether dMi-2 is involved in splicing regulation on a more global, genome wide scale. Currently there is no microarray platform designed for splicing analysis in *Drosophila*, thus in order to address this question other methods should be utilized. For instance, a recent development of next-generation deep sequencing technology is extensively used to study splicing events on a genome wide scale (Pan et al. 2008; Fox et al. 2009; Filichkin et al. 2010). Comparison of transcriptomes at high resolution between wild type and dMi-2 depleted cells or flies, could shed light onto its potential role in splicing genome-wide.

What could be the role of dMi-2 in splicing? dMi-2 might similarly to hCHD1 link or recruit splicing machinery to RNA via binding to nascent transcripts. However, the role of the enzymatic activity of dMi-2 for splicing suggests a more active role of this remodeler. In one possible scenario, dMi-2 might function as an RNP remodeling factor to modulate interactions between RNA splicing factors and their target RNA. It is also plausible that dMi-2 influences splicing less directly, for instance by remodeling chromatin structure during transcription. Indeed, recently, chromatin structure and histone modifications have been linked to splicing regulation. Mapping nucleosome positions at a genome-wide scale from various organisms has shown that nucleosomes are particularly enriched at intron-exon junctions (Andersson et al. 2009; Nahkuri et al. 2009; Schwartz et al. 2009; Dhami et

al. 2010). Nucleosomes can act as barriers that modulate RNAP II density by inducing its pausing (Hodges et al. 2009). Thus, nucleosome positioning might affect splicing efficiency. It is possible that chromatin remodelers, like dMi-2, might influence splicing by remodeling nucleosomes in the way of RNAP II. Although nucleosomes are severely disrupted at *hsp* genes upon gene induction there are still some histones left, besides histone variant H3.3 is deposited in the body of *hsp* genes which indicates that chromatin remodeling might occur to some extent on these genes upon their activation (Schwartz and Ahmad 2005). Whether dMi-2 plays any of these roles in splicing, remains to be determined in the future.

Finally, one reason for inefficient transcription of *hsp* genes in dMi-2 depleted flies could be that transcription elongation by RNAP II is affected. This possibility cannot be formally excluded and demands further investigation. Western blot analysis revealed no differences in the level of RNAP II phosphorylation at Ser2 in wild type and dominant negative mutant overexpressing flies (data not shown). This suggests that at least at the global scale dMi-2 depletion does not affect RNAP II elongation. One experiment to test this more directly on *hsp* genes would be to probe for elongating RNAP II occupancy at *hsp* genes upon gene induction by ChIP in dMi-2 depleted flies.

To sum up, the results presented in this doctoral thesis provide a first link of a catalytic activity of the ATP dependent chromatin remodeler in RNA processing and splicing. Many experiments remain to be done in order to clarify the function of dMi-2 in this context.

6.10 Recruitment mechanism of dMi-2 to *hsp* genes

6.10.1 Recruitment mechanism of dMi-2 to *hsp* genes is PAR dependent

One of the goals of this PhD thesis was to determine the recruitment mechanism of dMi-2 to activated heat shock genes. The binding of dMi-2 to the entire transcribed regions of *hsp* genes raised the possibility that dMi-2 is recruited by the transcription machinery. However, several lines of evidence do not agree with this hypothesis. First, dMi-2 binding profile and kinetics differ from RNAP II (Fig. 5.29). dMi-2 is detected at two minutes at *hsp70* gene whereas RNAP II is detected as early as one minute after gene activation. The highest level of RNAP II is detected at *hsp70* after five minutes of heat shock, by contrast dMi-2 signal increases significantly until the 20 minutes time point. Second, dMi-2 is not interacting with elongating forms of RNAP II or elongation factors (Fig. 5.28 and data not

shown). Finally, dMi-2 recruitment is transcription independent as blocking transcription by DRB treatment has no effect on dMi-2 binding to the *hsp70* gene (Fig. 5.30). Another possibility is that dMi-2 is recruited to induced heat shock genes via recognition of specific histone marks associated with active transcription. However, peptide pulldown experiments performed with isolated chromodomains or the full length dMi-2 show that the remodeler displays no specificity for H3K4me3 or H3K36me3 histone tails (Fig. 5.27 and P. Steffen, unpublished data). Thus, it is unlikely that dMi-2 is recruited to *hsp* genes via binding to these histone marks.

It has been shown that heat shock genes are extensively poly(ADP-ribosylated) (PARylated) upon gene activation in a transcription independent mode (Tulin and Spradling 2003; Petesch and Lis 2008). Moreover, recently a number of papers have reported PAR dependent recruitment of a human homolog of dMi-2, CHD4, to the sites of DSBs (Chou et al. 2010; Larsen et al. 2010; Polo et al. 2010; Smeenk et al. 2010). Hence, it is plausible that dMi-2 recruitment to *hsp* genes is PAR dependent. Indeed, pharmacological inhibition of PARP by PJ34 treatment strongly decreases dMi-2 recruitment to heat shock genes. Notably, the reduction of dMi-2 recruitment is significant even though the inhibition of PARP is not complete (Fig. 5.31). Several other experiments support the idea that PARP activity and PAR binding play a role in dMi-2 recruitment to *hsp* genes. First, the broad distribution of dMi-2 over the entire transcribed region correlates with the distribution of PAR polymer (Tulin and Spradling 2003). Second, dMi-2 binds to PARylated PARP and PAR polymers *in vitro* (Fig. 5.32 and 5.33). Third, deletion of the N-terminal region, which binds to PAR, abolishes dMi-2 recruitment to *hsp70* locus *in vivo* (5.34 and 5.37). Finally, dMi-2, ectopically expressed in human cells, similarly to CHD4 is recruited to laser induced DSBs (data not shown). Thus, there is a strong evidence that dMi-2 is recruited to activated *hsp* genes via PAR binding.

How might PAR polymers contribute to dMi-2 recruitment? During cellular stress, such as DNA strand breaks or heat shock, the cell has to respond quickly and efficiently. A number of factors are rapidly recruited to coordinate the DNA repair or immense transcription activation upon heat shock. Rapid PARP activation and synthesis of PAR at sites of DNA damage or heat shock genes transcription might provide an efficient mechanism to recruit chromatin remodelers and other factors involved in response to these processes.

6.10.2 PAR binding domains of dMi-2

Mapping experiments suggest that dMi-2 harbours several PAR-binding motifs in its N-terminal region (Fig. 5.34 and 5.35). To date, two structural protein modules directly and specifically interacting with PAR have been described: the macrodomain and the PAR-binding zinc finger domain (PBZ) (Karras et al. 2005; Ahel et al. 2008; Timinszky et al. 2009; Eustermann et al. 2010). In addition, motifs that contain several basic residues interspersed with hydrophobic residues have been identified in many proteins that bind the PAR polymer. These motifs share amino acid composition but they do not show extensive sequence homology (Pleschke et al. 2000; Gagné et al. 2008).

In this study, PARP pulldown assays have identified three K/R-rich regions with PAR binding activity near the N-terminus of dMi-2. Two of these three K/R-rich regions (III and IV) in dMi-2 consist of interspersed basic and hydrophobic residues and are thus reminiscent of the previously described PAR binding motifs (Figure 5.35 A) (Pleschke et al. 2000; Gagné et al. 2008). However, the first K/R motif lacks hydrophobic residues. Moreover, none of the three K/R regions matches the consensus PAR binding motifs reported previously. It is plausible that a high content of positively charged K and R-residues in these regions is sufficient to provide PAR binding activity *in vitro*. Moreover, mammalian CHD4 proteins also contain N-terminal K/R regions but they do not share sequence similarity with those of dMi-2 (Fig. 5.35 A).

Currently, the way how PAR interacts with PAR motifs is not clear. An alanine scan in the PAR binding motif showed that hydrophobic amino acids are important for PAR binding (Pleschke et al. 2000). However, there are also reports showing that positively charged K residues are important for binding to the PAR polymer (Zhang et al. 2011). Further characterization of the K/R regions in dMi-2 will be required to resolve this issue. Also, it remains to be determined whether all PAR binding regions mapped *in vitro,* are required for dMi-2 targeting to *hsp* loci *in vivo*. In addition to the K/R regions, the tandem chromodomains of dMi-2 bind PAR *in vitro* (Figure 5.34 and data not shown). It has been previously demonstrated that the chromodomains of dMi-2 are required for interacting with nucleosomal DNA *in vitro* (Bouazoune et al. 2002). Thus, these chromodomains can interact with different nucleic acids. Interestingly, dMi-2 chromodomains do not possess K/R reach motifs which suggests that the interaction with PAR might occur in a different manner.

6.10.3 Model of dMi-2 recruitment to *hsp* genes

The results obtained in this thesis support the following, two-step model of dMi-2 recruitment to *hsp* genes (Fig. 6.2). Upon heat shock, PARP1 is activated and PARylates the *hsp* locus. This activity leads to rapid nucleosome disruption, caused probably by PARylation of histones within the first two minutes of heat shock (Petesch and Lis 2008). In addition, PARylation serves as a scaffold for recruitment of factors with strong nucleic acid affinity, like dMi-2. dMi-2 is targeted to *hsp* genes via binding to PAR polymers. Finally, once transcription has been strongly activated, dMi-2 switches to transcribed nascent transcripts and contributes to efficient *hsp* gene processing (Figure 6.2).

This model is consistent with the *in vitro* competition assays, which suggest that RNA, but not DNA can compete for PAR binding to dMi-2 (Fig. 5.38 A). Thus, in the physiological situation, during robust transcription, RNA might be bound by dMi-2 in the presence of PAR. Interestingly, direct comparison of dMi-2 binding to DNA and RNA, has revealed that dMi-2 binds RNA much better than DNA (Fig. 5.38 B). This suggests that at least at some gene context, like strongly transcribed heat shock genes, the favourable substrate for dMi-2 might be RNA not the nucleosomal DNA. Consequently, dMi-2 might preferentially play a role in RNA on these genes. More quantitative experiments should be performed in order to characterize dMi-2 binding to RNA and DNA.

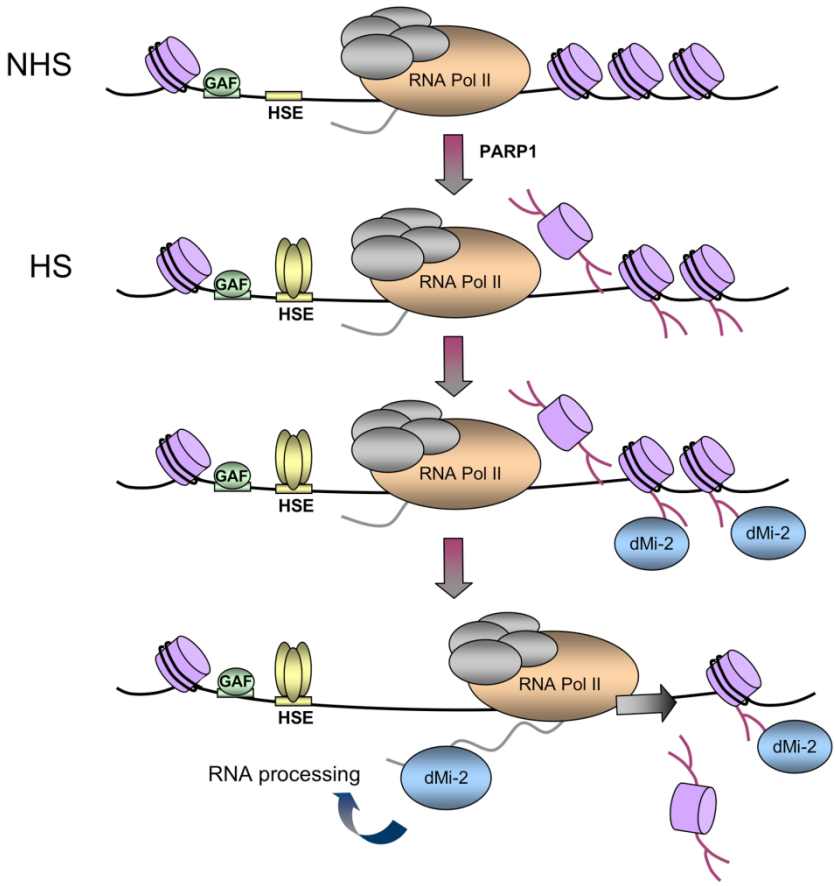

Figure 6.3 Model of dMi-2 recruitment to heat shock genes
Upon heat shock (HS), PARylation of the locus by PARP1 creates binding sites for PAR-sensing regions of dMi-2. dMi-2 is recruited and, subsequently, interacts with nascent transcripts to support transcription and processing, possibly by direct involvement in RNA processing events. See text for details. GAF: GAGA Factor, HSE: HS elements, yellow ovals: Heat Shock Factor.

Several issues concerning dMi-2 recruitment remain to be determined. It is not known whether dMi-2 binds to PARylated histones, PARP1 itself or other PARylated proteins at *hsp* locus. Although nucleosomes are disrupted upon heat shock, FRAP experiments on salivary glands have shown that histone H2B remains associated with *hsp70* locus (Zobeck et al. 2010). Thus, PARylation of histones might not only disrupt nucleosomes but also contribute to histone retention in the close proximity of transcribed genes. Consequently, PARylated histones might serve as a recruitment platform for factors such as dMi-2. It would be interesting to see whether PARylation of nucleosomes has any effect on the binding affinity of dMi-2. Secondly, it is currently unknown whether this mechanism of dMi-2 recruitment is applied outside of the heat shock gene context. Polytene chromosome staining suggests that dMi-2 also binds to ecdysone regulated puffs. Based on immunofluorescence staining, it has been reported that these genes are also PARylated *in*

vivo (Tulin and Spradling 2003). Thus it is plausible that dMi-2 recruitment to ecdysone regulated genes is also PAR dependent. Other genes, which expression seems to be PARP dependent, are immune response genes (Tulin and Spradling 2003). Further analysis is required to resolve whether dMi-2 is recruited to these genes and whether it plays any role in their transcriptional regulation.

6.10.4 Novel role of poly(ADP-ribosylation) in *hsp* gene transcription

So far, several molecular functions of PARylation at *hsp* genes have been proposed. First, PARP enzymatic activity is required for rapid, transcription independent nucleosomal loss at *hsp70* within the first two minutes after heat shock (Petesch and Lis 2008). Second, PARP has been shown to be important for establishment of a transcription compartment, which constrains the diffusion of RNAP II and elongation factors, thus promoting their efficient recycling during transcription. This function of PARP was observed at later stages of the heat shock response, 20-60 minutes after heat shock (Zobeck et al. 2010). The results of this thesis suggest a third function of PARP at activated *hsp* genes. PAR polymers might serve as a recruiting platform for factors which have affinity to nucleic acids, like dMi-2. The earliest time point when dMi-2 binding to *hsp70* is detected is between two and five minutes after heat shock (Fig. 5.29). This places dMi-2 recruitment between the early PARP dependent nucleosome removal (first two minutes after heat shock) and transcription compartment formation (20-60 minutes after heat shock). This also suggests a PARP dependent order of events that follow after each other on *hsp* genes after heat shock. First, at early time point nucleosomes are disassembled before RNAP II initiates transcription. Next, the accumulation of PAR polymers allows for recruitment of factors which are not recruited via transcription machinery and which possess nucleic acid binding affinity (like dMi-2). Finally, increasing concentration of PAR polymers creates a transcription compartment that facilitates transcription by spacial factor retention.

Rapid synthesis of PAR polymers might be used as an efficient mechanism for factor recruitment not only in the context of transcriptional stress response, but also at DNA strand brakes. Indeed, it has recently been shown that PARylation at DNA breaks is instrumental in recruiting chromatin remodelers, including mammalian ALC1 and dMi-2 homologs, to damaged sites (Ahel et al. 2009; Gottschalk et al. 2009; Polo et al. 2010). The high local concentration of PAR polymers at DNA breaks and *hsp* genes might exploit the

general affinity of some factors for nucleic acids. In this manner, PAR polymers might act as a scaffold to redirect chromatin remodelers to chromatin regions where they are required, thus acting as a stress-dependent, transient affinity site for chromatin remodeling and probably RNA processing activities.

6.11 dMi-2 on active genes – outlook

Apart from experiments described in the previous chapters, there are some additional questions which remind to be addressed in the future studies. The finding that dMi-2 is recruited to *hsp* genes by binding to PAR polymer raises the question whether there is any regulatory effect of PARP on the enzymatic activity of dMi-2. Indeed, it has been reported that poly(ADP-ribosylation) of nucleosomes can stimulate the ATPase activity of the ALC1 remodeler, which is recruited to sites of DSBs (Ahel et al. 2009). Whether the same applies to dMi-2 could be tested in an ATPase assay. The assays could be performed in the presence of PARP and/or PARylated nucleosomes. Another chromatin remodeler shown to be affected by PARP is ISWI. In this case PARylation of ISWI itself inhibits its enzymatic activity by reducing the affinity of ISWI for its nucleosomal substrate. The authors argue that PARylation of ISWI might serve as a mechanism to dissociate ISWI from chromatin. Indeed, ISWI and PAR occupy different chromatin domains on polytene chromosomes (Sala et al. 2008). Thus, PARP activity might have different consequences for different chromatin remodeling enzymes.

One issue, also not addressed in this study, concerns the dMi-2 complex, which is involved in the regulation of heat shock genes. Polytene chromosome staining with dMep1 and dp66 antibodies suggests that both subunits of the dMec and dNuRD complexes can be recruited to *hsp70* loci (data not shown). However, lack of good antibodies for these proteins does not allow to perform ChIP experiments on *hsp* genes. Moreover, it is not clear whether the same complexes, as the one purified from Kc cells, exist at larvae stages. The differences with complex composition between different material source might suggest that chromatin remodeling complexes change their composition during animal development (Kunert et al. 2009; Reddy et al. 2010). Thus, it should be determined which dMi-2 complex is involved in the regulation of heat shock genes.

Mi-2-like chromatin remodelers have been shown to play an essential role in the transcriptional repression programs of different organisms. This study, for the first time,

implicates the role of dMi-2 in active gene regulation and suggests its possible role in RNA processing. Further studies will be important to dissect the mechanism of dMi-2 activity on transcribed genes. Moreover, the recruitment of dMi-2 via PAR, suggests that other mechanisms than transcription factor binding, are employed by this remodeler to reach the proper chromosomal sites. Finally, this study also highlights the role of PARP and PARylation in the integration and coordination of stress-dependent nuclear activities.

7. References

Adams RR, Carmena M, Earnshaw WC. 2001. Chromosomal passengers and the (aurora) ABCs of mitosis. *Trends Cell Biol* **11**: 49-54.

Agalioti T, Chen G, Thanos D. 2002. Deciphering the transcriptional histone acetylation code for a human gene. *Cell* **111**: 381-392.

Ahel D, Horejsí Z, Wiechens N, Polo SE, Garcia-Wilson E, Ahel I, Flynn H, Skehel M, West SC, Jackson SP et al. 2009. Poly(ADP-ribose)-dependent regulation of DNA repair by the chromatin remodeling enzyme ALC1. *Science* **325**: 1240-1243.

Ahel I, Ahel D, Matsusaka T, Clark AJ, Pines J, Boulton SJ, West SC. 2008. Poly(ADP-ribose)-binding zinc finger motifs in DNA repair/checkpoint proteins. *Nature* **451**: 81-85.

Ahmad K, Henikoff S. 2002. The histone variant H3.3 marks active chromatin by replication-independent nucleosome assembly. *Mol Cell* **9**: 1191-1200.

Ahringer J. 2000. NuRD and SIN3 histone deacetylase complexes in development. *Trends Genet* **16**: 351-356.

Akbari OS, Oliver D, Eyer K, Pai CY. 2009. An Entry/Gateway cloning system for general expression of genes with molecular tags in Drosophila melanogaster. *BMC Cell Biol* **10**: 8.

Alén C, Kent NA, Jones HS, O'Sullivan J, Aranda A, Proudfoot NJ. 2002. A role for chromatin remodeling in transcriptional termination by RNA polymerase II. *Mol Cell* **10**: 1441-1452.

Andersson R, Enroth S, Rada-Iglesias A, Wadelius C, Komorowski J. 2009. Nucleosomes are well positioned in exons and carry characteristic histone modifications. *Genome Res* **19**: 1732-1741.

Andrulis ED, Werner J, Nazarian A, Erdjument-Bromage H, Tempst P, Lis JT. 2002. The RNA processing exosome is linked to elongating RNA polymerase II in Drosophila. *Nature* **420**: 837-841.

Aoyagi S, Hayes JJ. 2002. hSWI/SNF-catalyzed nucleosome sliding does not occur solely via a twist-diffusion mechanism. *Mol Cell Biol* **22**: 7484-7490.

Arents G, Moudrianakis EN. 1995. The histone fold: a ubiquitous architectural motif utilized in DNA compaction and protein dimerization. *Proc Natl Acad Sci U S A* **92**: 11170-11174.

Armstrong JA. 2007. Negotiating the nucleosome: factors that allow RNA polymerase II to elongate through chromatin. *Biochem Cell Biol* **85**: 426-434.

Armstrong JA, Bieker JJ, Emerson BM. 1998. A SWI/SNF-related chromatin remodeling complex, E-RC1, is required for tissue-specific transcriptional regulation by EKLF in vitro. *Cell* **95**: 93-104.

Armstrong JA, Papoulas O, Daubresse G, Sperling AS, Lis JT, Scott MP, Tamkun JW. 2002. The Drosophila BRM complex facilitates global transcription by RNA polymerase II. *EMBO J* **21**: 5245-5254.

Avvakumov N, Nourani A, Côté J. 2011. Histone chaperones: modulators of chromatin marks. *Mol Cell* **41**: 502-514.

Axel R. 1975. Cleavage of DNA in nuclei and chromatin with staphylococcal nuclease. *Biochemistry* **14**: 2921-2925.

Ayyanathan K, Lechner MS, Bell P, Maul GG, Schultz DC, Yamada Y, Tanaka K, Torigoe K, Rauscher FJ. 2003. Regulated recruitment of HP1 to a euchromatic gene induces

mitotically heritable, epigenetic gene silencing: a mammalian cell culture model of gene variegation. *Genes Dev* **17**: 1855-1869.

Badenhorst P, Voas M, Rebay I, Wu C. 2002. Biological functions of the ISWI chromatin remodeling complex NURF. *Genes Dev* **16**: 3186-3198.

Badenhorst P, Xiao H, Cherbas L, Kwon SY, Voas M, Rebay I, Cherbas P, Wu C. 2005. The Drosophila nucleosome remodeling factor NURF is required for Ecdysteroid signaling and metamorphosis. *Genes Dev* **19**: 2540-2545.

Baetz KK, Krogan NJ, Emili A, Greenblatt J, Hieter P. 2004. The ctf13-30/CTF13 genomic haploinsufficiency modifier screen identifies the yeast chromatin remodeling complex RSC, which is required for the establishment of sister chromatid cohesion. *Mol Cell Biol* **24**: 1232-1244.

Bajpai R, Chen DA, Rada-Iglesias A, Zhang J, Xiong Y, Helms J, Chang CP, Zhao Y, Swigut T, Wysocka J. 2010. CHD7 cooperates with PBAF to control multipotent neural crest formation. *Nature* **463**: 958-962.

Ball LJ, Murzina NV, Broadhurst RW, Raine AR, Archer SJ, Stott FJ, Murzin AG, Singh PB, Domaille PJ, Laue ED. 1997. Structure of the chromatin binding (chromo) domain from mouse modifier protein 1. *EMBO J* **16**: 2473-2481.

Ballestar E, Pile LA, Wassarman DA, Wolffe AP, Wade PA. 2001. A Drosophila MBD family member is a transcriptional corepressor associated with specific genes. *Eur J Biochem* **268**: 5397-5406.

Bao X, Cai W, Deng H, Zhang W, Krencik R, Girton J, Johansen J, Johansen KM. 2008. The COOH-terminal domain of the JIL-1 histone H3S10 kinase interacts with histone H3 and is required for correct targeting to chromatin. *J Biol Chem* **283**: 32741-32750.

Barker N, Hurlstone A, Musisi H, Miles A, Bienz M, Clevers H. 2001. The chromatin remodelling factor Brg-1 interacts with beta-catenin to promote target gene activation. *EMBO J* **20**: 4935-4943.

Batsché E, Yaniv M, Muchardt C. 2006. The human SWI/SNF subunit Brm is a regulator of alternative splicing. *Nat Struct Mol Biol* **13**: 22-29.

Baylin SB, Esteller M, Rountree MR, Bachman KE, Schuebel K, Herman JG. 2001. Aberrant patterns of DNA methylation, chromatin formation and gene expression in cancer. *Hum Mol Genet* **10**: 687-692.

Beisel C, Buness A, Roustan-Espinosa IM, Koch B, Schmitt S, Haas SA, Hild M, Katsuyama T, Paro R. 2007. Comparing active and repressed expression states of genes controlled by the Polycomb/Trithorax group proteins. *Proc Natl Acad Sci U S A* **104**: 16615-16620.

Beisel C, Paro R. 2011. Silencing chromatin: comparing modes and mechanisms. *Nat Rev Genet* **12**: 123-135.

Bentley DL. 1995. Regulation of transcriptional elongation by RNA polymerase II. *Curr Opin Genet Dev* **5**: 210-216.

Berger SL. 2007. The complex language of chromatin regulation during transcription. *Nature* **447**: 407-412.

Bernstein BE, Meissner A, Lander ES. 2007. The mammalian epigenome. *Cell* **128**: 669-681.

Bird A. 2002. DNA methylation patterns and epigenetic memory. *Genes Dev* **16**: 6-21.

Bischof J, Maeda RK, Hediger M, Karch F, Basler K. 2007. An optimized transgenesis system for Drosophila using germ-line-specific phiC31 integrases. *Proc Natl Acad Sci U S A* **104**: 3312-3317.

Boehm AK, Saunders A, Werner J, Lis JT. 2003. Transcription factor and polymerase recruitment, modification, and movement on dhsp70 in vivo in the minutes following heat shock. *Mol Cell Biol* **23**: 7628-7637.

Bouazoune K, Brehm A. 2005. dMi-2 chromatin binding and remodeling activities are regulated by dCK2 phosphorylation. *J Biol Chem* **280**: 41912-41920.

Bouazoune K, Mitterweger A, Längst G, Imhof A, Akhtar A, Becker PB, Brehm A. 2002. The dMi-2 chromodomains are DNA binding modules important for ATP-dependent nucleosome mobilization. *EMBO J* **21**: 2430-2440.

Bowman GD. 2010. Mechanisms of ATP-dependent nucleosome sliding. *Curr Opin Struct Biol* **20**: 73-81.

Brackertz M, Boeke J, Zhang R, Renkawitz R. 2002. Two highly related p66 proteins comprise a new family of potent transcriptional repressors interacting with MBD2 and MBD3. *J Biol Chem* **277**: 40958-40966.

Brackertz M, Gong Z, Leers J, Renkawitz R. 2006. p66alpha and p66beta of the Mi-2/NuRD complex mediate MBD2 and histone interaction. *Nucleic Acids Res* **34**: 397-406.

Bradford MM. 1976. A rapid and sensitive method for the quantitation of microgram quantities of protein utilizing the principle of protein-dye binding. *Anal Biochem* **72**: 248-254.

Brehm A, Längst G, Kehle J, Clapier CR, Imhof A, Eberharter A, Müller J, Becker PB. 2000. dMi-2 and ISWI chromatin remodelling factors have distinct nucleosome binding and mobilization properties. *EMBO J* **19**: 4332-4341.

Brehm A, Tufteland KR, Aasland R, Becker PB. 2004. The many colours of chromodomains. *Bioessays* **26**: 133-140.

Brower-Toland BD, Smith CL, Yeh RC, Lis JT, Peterson CL, Wang MD. 2002. Mechanical disruption of individual nucleosomes reveals a reversible multistage release of DNA. *Proc Natl Acad Sci U S A* **99**: 1960-1965.

Bruno M, Flaus A, Stockdale C, Rencurel C, Ferreira H, Owen-Hughes T. 2003. Histone H2A/H2B dimer exchange by ATP-dependent chromatin remodeling activities. *Mol Cell* **12**: 1599-1606.

Bryant GO, Prabhu V, Floer M, Wang X, Spagna D, Schreiber D, Ptashne M. 2008. Activator control of nucleosome occupancy in activation and repression of transcription. *PLoS Biol* **6**: 2928-2939.

Buratowski S. 2005. Connections between mRNA 3' end processing and transcription termination. *Curr Opin Cell Biol* **17**: 257-261.

Burma S, Chen BP, Murphy M, Kurimasa A, Chen DJ. 2001. ATM phosphorylates histone H2AX in response to DNA double-strand breaks. *J Biol Chem* **276**: 42462-42467.

Bérubé NG, Smeenk CA, Picketts DJ. 2000. Cell cycle-dependent phosphorylation of the ATRX protein correlates with changes in nuclear matrix and chromatin association. *Hum Mol Genet* **9**: 539-547.

Cai Y, Jin J, Yao T, Gottschalk AJ, Swanson SK, Wu S, Shi Y, Washburn MP, Florens L, Conaway RC et al. 2007. YY1 functions with INO80 to activate transcription. *Nat Struct Mol Biol* **14**: 872-874.

Cairns BR. 2007. Chromatin remodeling: insights and intrigue from single-molecule studies. *Nat Struct Mol Biol* **14**: 989-996.

Cairns BR, Kim YJ, Sayre MH, Laurent BC, Kornberg RD. 1994. A multisubunit complex containing the SWI1/ADR6, SWI2/SNF2, SWI3, SNF5, and SNF6 gene products isolated from yeast. *Proc Natl Acad Sci U S A* **91**: 1950-1954.

Cairns BR, Lorch Y, Li Y, Zhang M, Lacomis L, Erdjument-Bromage H, Tempst P, Du J, Laurent B, Kornberg RD. 1996. RSC, an essential, abundant chromatin-remodeling complex. *Cell* **87**: 1249-1260.

Cairns BR, Schlichter A, Erdjument-Bromage H, Tempst P, Kornberg RD, Winston F. 1999. Two functionally distinct forms of the RSC nucleosome-remodeling complex, containing essential AT hook, BAH, and bromodomains. *Mol Cell* **4**: 715-723.

Campos EI, Reinberg D. 2009. Histones: annotating chromatin. *Annu Rev Genet* **43**: 559-599.

Cao Y, Cairns BR, Kornberg RD, Laurent BC. 1997. Sfh1p, a component of a novel chromatin-remodeling complex, is required for cell cycle progression. *Mol Cell Biol* **17**: 3323-3334.

Capelson M, Liang Y, Schulte R, Mair W, Wagner U, Hetzer MW. 2010. Chromatin-bound nuclear pore components regulate gene expression in higher eukaryotes. *Cell* **140**: 372-383.

Carlson M, Osmond BC, Neigeborn L, Botstein D. 1984. A suppressor of SNF1 mutations causes constitutive high-level invertase synthesis in yeast. *Genetics* **107**: 19-32.

Carrozza MJ, Li B, Florens L, Suganuma T, Swanson SK, Lee KK, Shia WJ, Anderson S, Yates J, Washburn MP et al. 2005. Histone H3 methylation by Set2 directs deacetylation of coding regions by Rpd3S to suppress spurious intragenic transcription. *Cell* **123**: 581-592.

Champagne KS, Kutateladze TG. 2009. Structural insight into histone recognition by the ING PHD fingers. *Curr Drug Targets* **10**: 432-441.

Chen D, Hinkley CS, Henry RW, Huang S. 2002. TBP dynamics in living human cells: constitutive association of TBP with mitotic chromosomes. *Mol Biol Cell* **13**: 276-284.

Cheng SW, Davies KP, Yung E, Beltran RJ, Yu J, Kalpana GV. 1999. c-MYC interacts with INI1/hSNF5 and requires the SWI/SNF complex for transactivation function. *Nat Genet* **22**: 102-105.

Cheung V, Chua G, Batada N, Landry C, Michnick S, Hughes T, Winston F. 2008. Chromatin- and transcription-related factors repress transcription from within coding regions throughout the Saccharomyces cerevisiae genome. *PLoS Biol* **6**: e277.

Chi TH, Wan M, Zhao K, Taniuchi I, Chen L, Littman DR, Crabtree GR. 2002. Reciprocal regulation of CD4/CD8 expression by SWI/SNF-like BAF complexes. *Nature* **418**: 195-199.

Chioda M, Vengadasalam S, Kremmer E, Eberharter A, Becker PB. 2010. Developmental role for ACF1-containing nucleosome remodellers in chromatin organisation. *Development* **137**: 3513-3522.

Chou DM, Adamson B, Dephoure NE, Tan X, Nottke AC, Hurov KE, Gygi SP, Colaiácovo MP, Elledge SJ. 2010. A chromatin localization screen reveals poly (ADP ribose)-regulated recruitment of the repressive polycomb and NuRD complexes to sites of DNA damage. *Proc Natl Acad Sci U S A* **107**: 18475-18480.

Christova R, Oelgeschläger T. 2002. Association of human TFIID-promoter complexes with silenced mitotic chromatin in vivo. *Nat Cell Biol* **4**: 79-82.

Cismasiu VB, Paskaleva E, Suman Daya S, Canki M, Duus K, Avram D. 2008. BCL11B is a general transcriptional repressor of the HIV-1 long terminal repeat in T lymphocytes through recruitment of the NuRD complex. *Virology* **380**: 173-181.

Clapier CR, Cairns BR. 2009. The biology of chromatin remodeling complexes. *Annu Rev Biochem* **78**: 273-304.

Clapier CR, Längst G, Corona DF, Becker PB, Nightingale KP. 2001. Critical role for the histone H4 N terminus in nucleosome remodeling by ISWI. *Mol Cell Biol* **21**: 875-883.

Clapier CR, Nightingale KP, Becker PB. 2002. A critical epitope for substrate recognition by the nucleosome remodeling ATPase ISWI. *Nucleic Acids Res* **30**: 649-655.

Clarke AS, Tang TT, Ooi DL, Orr-Weaver TL. 2005. POLO kinase regulates the Drosophila centromere cohesion protein MEI-S332. *Dev Cell* **8**: 53-64.

Collas P. 2010. The current state of chromatin immunoprecipitation. *Mol Biotechnol* **45**: 87-100.

Collins N, Poot RA, Kukimoto I, García-Jiménez C, Dellaire G, Varga-Weisz PD. 2002. An ACF1-ISWI chromatin-remodeling complex is required for DNA replication through heterochromatin. *Nat Genet* **32**: 627-632.

Cooper MT, Conant AW, Kennison JA. 2010. Molecular genetic analysis of Chd3 and polytene chromosome region 76B-D in Drosophila melanogaster. *Genetics* **185**: 811-822.

Corey LL, Weirich CS, Benjamin IJ, Kingston RE. 2003. Localized recruitment of a chromatin-remodeling activity by an activator in vivo drives transcriptional elongation. *Genes Dev* **17**: 1392-1401.

Cosma MP, Tanaka T, Nasmyth K. 1999. Ordered recruitment of transcription and chromatin remodeling factors to a cell cycle- and developmentally regulated promoter. *Cell* **97**: 299-311.

Crosby MA, Miller C, Alon T, Watson KL, Verrijzer CP, Goldman-Levi R, Zak NB. 1999. The trithorax group gene moira encodes a brahma-associated putative chromatin-remodeling factor in Drosophila melanogaster. *Mol Cell Biol* **19**: 1159-1170.

Czermin B, Schotta G, Hülsmann BB, Brehm A, Becker PB, Reuter G, Imhof A. 2001. Physical and functional association of SU(VAR)3-9 and HDAC1 in Drosophila. *EMBO Rep* **2**: 915-919.

Côté J, Quinn J, Workman JL, Peterson CL. 1994. Stimulation of GAL4 derivative binding to nucleosomal DNA by the yeast SWI/SNF complex. *Science* **265**: 53-60.

Dahmus ME. 1994. The role of multisite phosphorylation in the regulation of RNA polymerase II activity. *Prog Nucleic Acid Res Mol Biol* **48**: 143-179.

Dang W, Bartholomew B. 2007. Domain architecture of the catalytic subunit in the ISW2-nucleosome complex. *Mol Cell Biol* **27**: 8306-8317.

Dang W, Kagalwala MN, Bartholomew B. 2006. Regulation of ISW2 by concerted action of histone H4 tail and extranucleosomal DNA. *Mol Cell Biol* **26**: 7388-7396.

Daubresse G, Deuring R, Moore L, Papoulas O, Zakrajsek I, Waldrip WR, Scott MP, Kennison JA, Tamkun JW. 1999. The Drosophila kismet gene is related to chromatin-remodeling factors and is required for both segmentation and segment identity. *Development* **126**: 1175-1187.

de la Serna IL, Ohkawa Y, Berkes CA, Bergstrom DA, Dacwag CS, Tapscott SJ, Imbalzano AN. 2005. MyoD targets chromatin remodeling complexes to the myogenin locus prior to forming a stable DNA-bound complex. *Mol Cell Biol* **25**: 3997-4009.

Dechassa ML, Sabri A, Pondugula S, Kassabov SR, Chatterjee N, Kladde MP, Bartholomew B. 2010. SWI/SNF has intrinsic nucleosome disassembly activity that is dependent on adjacent nucleosomes. *Mol Cell* **38**: 590-602.

Dechassa ML, Zhang B, Horowitz-Scherer R, Persinger J, Woodcock CL, Peterson CL, Bartholomew B. 2008. Architecture of the SWI/SNF-nucleosome complex. *Mol Cell Biol* **28**: 6010-6021.

Dedon PC, Soults JA, Allis CD, Gorovsky MA. 1991. A simplified formaldehyde fixation and immunoprecipitation technique for studying protein-DNA interactions. *Anal Biochem* **197**: 83-90.

Delmas V, Stokes DG, Perry RP. 1993. A mammalian DNA-binding protein that contains a chromodomain and an SNF2/SWI2-like helicase domain. *Proc Natl Acad Sci U S A* **90**: 2414-2418.

Deng L, Shuman S. 1998. Vaccinia NPH-I, a DExH-box ATPase, is the energy coupling factor for mRNA transcription termination. *Genes Dev* **12**: 538-546.

Denslow SA, Wade PA. 2007. The human Mi-2/NuRD complex and gene regulation. *Oncogene* **26**: 5433-5438.

Deuring R, Fanti L, Armstrong JA, Sarte M, Papoulas O, Prestel M, Daubresse G, Verardo M, Moseley SL, Berloco M et al. 2000. The ISWI chromatin-remodeling protein is required for gene expression and the maintenance of higher order chromatin structure in vivo. *Mol Cell* **5**: 355-365.

Dhami P, Saffrey P, Bruce AW, Dillon SC, Chiang K, Bonhoure N, Koch CM, Bye J, James K, Foad NS et al. 2010. Complex exon-intron marking by histone modifications is not determined solely by nucleosome distribution. *PLoS One* **5**: e12339.

Dimova D, Nackerdien Z, Furgeson S, Eguchi S, Osley MA. 1999. A role for transcriptional repressors in targeting the yeast Swi/Snf complex. *Mol Cell* **4**: 75-83.

Dingwall AK, Beek SJ, McCallum CM, Tamkun JW, Kalpana GV, Goff SP, Scott MP. 1995. The Drosophila snr1 and brm proteins are related to yeast SWI/SNF proteins and are components of a large protein complex. *Mol Biol Cell* **6**: 777-791.

DiRenzo J, Shang Y, Phelan M, Sif S, Myers M, Kingston R, Brown M. 2000. BRG-1 is recruited to estrogen-responsive promoters and cooperates with factors involved in histone acetylation. *Mol Cell Biol* **20**: 7541-7549.

Downs JA, Allard S, Jobin-Robitaille O, Javaheri A, Auger A, Bouchard N, Kron SJ, Jackson SP, Côté J. 2004. Binding of chromatin-modifying activities to phosphorylated histone H2A at DNA damage sites. *Mol Cell* **16**: 979-990.

Duffy JB. 2002. GAL4 system in Drosophila: a fly geneticist's Swiss army knife. *Genesis* **34**: 1-15.

Dunaief JL, Strober BE, Guha S, Khavari PA, Alin K, Luban J, Begemann M, Crabtree GR, Goff SP. 1994. The retinoblastoma protein and BRG1 form a complex and cooperate to induce cell cycle arrest. *Cell* **79**: 119-130.

Dürr H, Körner C, Müller M, Hickmann V, Hopfner KP. 2005. X-ray structures of the Sulfolobus solfataricus SWI2/SNF2 ATPase core and its complex with DNA. *Cell* **121**: 363-373.

Ebbert R, Birkmann A, Schüller HJ. 1999. The product of the SNF2/SWI2 paralogue INO80 of Saccharomyces cerevisiae required for efficient expression of various yeast structural genes is part of a high-molecular-weight protein complex. *Mol Microbiol* **32**: 741-751.

Echalier G, Ohanessian A. 1970. In vitro culture of Drosophila melanogaster embryonic cells. *In Vitro* **6**: 162-172.

Eisen JA, Sweder KS, Hanawalt PC. 1995. Evolution of the SNF2 family of proteins: subfamilies with distinct sequences and functions. *Nucleic Acids Res* **23**: 2715-2723.

Eissenberg JC. 2001. Molecular biology of the chromo domain: an ancient chromatin module comes of age. *Gene* **275**: 19-29.

Elfring LK, Deuring R, McCallum CM, Peterson CL, Tamkun JW. 1994. Identification and characterization of Drosophila relatives of the yeast transcriptional activator SNF2/SWI2. *Mol Cell Biol* **14**: 2225-2234.

Emili A, Shales M, McCracken S, Xie W, Tucker PW, Kobayashi R, Blencowe BJ, Ingles CJ. 2002. Splicing and transcription-associated proteins PSF and p54nrb/nonO bind to the RNA polymerase II CTD. *RNA* **8**: 1102-1111.

Engeholm M, de Jager M, Flaus A, Brenk R, van Noort J, Owen-Hughes T. 2009. Nucleosomes can invade DNA territories occupied by their neighbors. *Nat Struct Mol Biol* **16**: 151-158.

Eustermann S, Brockmann C, Mehrotra PV, Yang JC, Loakes D, West SC, Ahel I, Neuhaus D. 2010. Solution structures of the two PBZ domains from human APLF and their interaction with poly(ADP-ribose). *Nat Struct Mol Biol* **17**: 241-243.

Fahrer J, Kranaster R, Altmeyer M, Marx A, Bürkle A. 2007. Quantitative analysis of the binding affinity of poly(ADP-ribose) to specific binding proteins as a function of chain length. *Nucleic Acids Res* **35**: e143.

Fan HY, Trotter KW, Archer TK, Kingston RE. 2005. Swapping function of two chromatin remodeling complexes. *Mol Cell* **17**: 805-815.

Fatemi M, Hermann A, Gowher H, Jeltsch A. 2002. Dnmt3a and Dnmt1 functionally cooperate during de novo methylation of DNA. *Eur J Biochem* **269**: 4981-4984.

Feng Q, Zhang Y. 2001. The MeCP1 complex represses transcription through preferential binding, remodeling, and deacetylating methylated nucleosomes. *Genes Dev* **15**: 827-832.

Ferreira H, Flaus A, Owen-Hughes T. 2007. Histone modifications influence the action of Snf2 family remodelling enzymes by different mechanisms. *J Mol Biol* **374**: 563-579.

Filichkin SA, Priest HD, Givan SA, Shen R, Bryant DW, Fox SE, Wong WK, Mockler TC. 2010. Genome-wide mapping of alternative splicing in Arabidopsis thaliana. *Genome Res* **20**: 45-58.

Fischle W, Wang Y, Allis CD. 2003. Histone and chromatin cross-talk. *Curr Opin Cell Biol* **15**: 172-183.

Flanagan JF, Mi LZ, Chruszcz M, Cymborowski M, Clines KL, Kim Y, Minor W, Rastinejad F, Khorasanizadeh S. 2005. Double chromodomains cooperate to recognize the methylated histone H3 tail. *Nature* **438**: 1181-1185.

Flanagan JF, Peterson CL. 1999. A role for the yeast SWI/SNF complex in DNA replication. *Nucleic Acids Res* **27**: 2022-2028.

Flaus A, Martin DM, Barton GJ, Owen-Hughes T. 2006. Identification of multiple distinct Snf2 subfamilies with conserved structural motifs. *Nucleic Acids Res* **34**: 2887-2905.

Flaus A, Owen-Hughes T. 2003. Dynamic properties of nucleosomes during thermal and ATP-driven mobilization. *Mol Cell Biol* **23**: 7767-7779.

Fox S, Filichkin S, Mockler TC. 2009. Applications of ultra-high-throughput sequencing. *Methods Mol Biol* **553**: 79-108.

Fryer CJ, Archer TK. 1998. Chromatin remodelling by the glucocorticoid receptor requires the BRG1 complex. *Nature* **393**: 88-91.

Fujita N, Jaye D, Geigerman C, Akyildiz A, Mooney M, Boss J, Wade P. 2004. MTA3 and the Mi-2/NuRD complex regulate cell fate during B lymphocyte differentiation. *Cell* **119**: 75-86.

Gagné JP, Isabelle M, Lo KS, Bourassa S, Hendzel MJ, Dawson VL, Dawson TM, Poirier GG. 2008. Proteome-wide identification of poly(ADP-ribose) binding proteins and poly(ADP-ribose)-associated protein complexes. *Nucleic Acids Res* **36**: 6959-6976.

Gaillard H, Fitzgerald DJ, Smith CL, Peterson CL, Richmond TJ, Thoma F. 2003. Chromatin remodeling activities act on UV-damaged nucleosomes and modulate DNA damage accessibility to photolyase. *J Biol Chem* **278**: 17655-17663.

Gangaraju VK, Prasad P, Srour A, Kagalwala MN, Bartholomew B. 2009. Conformational changes associated with template commitment in ATP-dependent chromatin remodeling by ISW2. *Mol Cell* **35**: 58-69.

Gao Z, Huang Z, Olivey HE, Gurbuxani S, Crispino JD, Svensson EC. 2010. FOG-1-mediated recruitment of NuRD is required for cell lineage re-enforcement during haematopoiesis. *EMBO J* **29**: 457-468.

Gaspar-Maia A, Alajem A, Polesso F, Sridharan R, Mason MJ, Heidersbach A, Ramalho-Santos J, McManus MT, Plath K, Meshorer E et al. 2009. Chd1 regulates open chromatin and pluripotency of embryonic stem cells. *Nature* **460**: 863-868.

Geng F, Laurent BC. 2004. Roles of SWI/SNF and HATs throughout the dynamic transcription of a yeast glucose-repressible gene. *EMBO J* **23**: 127-137.

Gerber M, Ma J, Dean K, Eissenberg JC, Shilatifard A. 2001. Drosophila ELL is associated with actively elongating RNA polymerase II on transcriptionally active sites in vivo. *EMBO J* **20**: 6104-6114.

Gilbert C, Svejstrup JQ. 2006. RNA immunoprecipitation for determining RNA-protein associations in vivo. *Curr Protoc Mol Biol* **Chapter 27**: Unit 27.24.

Gill G. 2004. SUMO and ubiquitin in the nucleus: different functions, similar mechanisms? *Genes Dev* **18**: 2046-2059.

Goldmark JP, Fazzio TG, Estep PW, Church GM, Tsukiyama T. 2000. The Isw2 chromatin remodeling complex represses early meiotic genes upon recruitment by Ume6p. *Cell* **103**: 423-433.

Gong Z, Brackertz M, Renkawitz R. 2006. SUMO modification enhances p66-mediated transcriptional repression of the Mi-2/NuRD complex. *Mol Cell Biol* **26**: 4519-4528.

Gottschalk AJ, Timinszky G, Kong SE, Jin J, Cai Y, Swanson SK, Washburn MP, Florens L, Ladurner AG, Conaway JW et al. 2009. Poly(ADP-ribosyl)ation directs recruitment and activation of an ATP-dependent chromatin remodeler. *Proc Natl Acad Sci U S A* **106**: 13770-13774.

Gregory G, Miccio A, Bersenev A, Wang Y, Hong W, Zhang Z, Poncz M, Tong W, Blobel G. 2010. FOG1 requires NuRD to promote hematopoiesis and maintain lineage fidelity within the megakaryocytic-erythroid compartment. *Blood* **115**: 2156-2166.

Gromak N, West S, Proudfoot NJ. 2006. Pause sites promote transcriptional termination of mammalian RNA polymerase II. *Mol Cell Biol* **26**: 3986-3996.

Guschin D, Wade PA, Kikyo N, Wolffe AP. 2000. ATP-Dependent histone octamer mobilization and histone deacetylation mediated by the Mi-2 chromatin remodeling complex. *Biochemistry* **39**: 5238-5245.

Gutiérrez JL, Chandy M, Carrozza MJ, Workman JL. 2007. Activation domains drive nucleosome eviction by SWI/SNF. *EMBO J* **26**: 730-740.

Guyon JR, Narlikar GJ, Sif S, Kingston RE. 1999. Stable remodeling of tailless nucleosomes by the human SWI-SNF complex. *Mol Cell Biol* **19**: 2088-2097.

Hagstrom KA, Meyer BJ. 2003. Condensin and cohesin: more than chromosome compactor and glue. *Nat Rev Genet* **4**: 520-534.

Hakimi MA, Bochar DA, Schmiesing JA, Dong Y, Barak OG, Speicher DW, Yokomori K, Shiekhattar R. 2002. A chromatin remodelling complex that loads cohesin onto human chromosomes. *Nature* **418**: 994-998.

Hakmé A, Wong HK, Dantzer F, Schreiber V. 2008. The expanding field of poly(ADP-ribosyl)ation reactions. 'Protein Modifications: Beyond the Usual Suspects' Review Series. *EMBO Rep* **9**: 1094-1100.

Hall JA, Georgel PT. 2007. CHD proteins: a diverse family with strong ties. *Biochem Cell Biol* **85**: 463-476.

Hall MA, Shundrovsky A, Bai L, Fulbright RM, Lis JT, Wang MD. 2009. High-resolution dynamic mapping of histone-DNA interactions in a nucleosome. *Nat Struct Mol Biol* **16**: 124-129.

Hamiche A, Sandaltzopoulos R, Gdula DA, Wu C. 1999. ATP-dependent histone octamer sliding mediated by the chromatin remodeling complex NURF. *Cell* **97**: 833-842.

Hara R, Sancar A. 2002. The SWI/SNF chromatin-remodeling factor stimulates repair by human excision nuclease in the mononucleosome core particle. *Mol Cell Biol* **22**: 6779-6787.

Hassan AH, Neely KE, Workman JL. 2001. Histone acetyltransferase complexes stabilize swi/snf binding to promoter nucleosomes. *Cell* **104**: 817-827.

Hauk G, McKnight JN, Nodelman IM, Bowman GD. 2010. The chromodomains of the Chd1 chromatin remodeler regulate DNA access to the ATPase motor. *Mol Cell* **39**: 711-723.

Havas K, Flaus A, Phelan M, Kingston R, Wade PA, Lilley DM, Owen-Hughes T. 2000. Generation of superhelical torsion by ATP-dependent chromatin remodeling activities. *Cell* **103**: 1133-1142.

Hay RT. 2005. SUMO: a history of modification. *Mol Cell* **18**: 1-12.

Henderson A, Holloway A, Reeves R, Tremethick DJ. 2004. Recruitment of SWI/SNF to the human immunodeficiency virus type 1 promoter. *Mol Cell Biol* **24**: 389-397.

Henry KW, Wyce A, Lo WS, Duggan LJ, Emre NC, Kao CF, Pillus L, Shilatifard A, Osley MA, Berger SL. 2003. Transcriptional activation via sequential histone H2B ubiquitylation and deubiquitylation, mediated by SAGA-associated Ubp8. *Genes Dev* **17**: 2648-2663.

Hirose F, Ohshima N, Shiraki M, Inoue YH, Taguchi O, Nishi Y, Matsukage A, Yamaguchi M. 2001. Ectopic expression of DREF induces DNA synthesis, apoptosis, and unusual morphogenesis in the Drosophila eye imaginal disc: possible interaction with Polycomb and trithorax group proteins. *Mol Cell Biol* **21**: 7231-7242.

Hirschhorn JN, Bortvin AL, Ricupero-Hovasse SL, Winston F. 1995. A new class of histone H2A mutations in Saccharomyces cerevisiae causes specific transcriptional defects in vivo. *Mol Cell Biol* **15**: 1999-2009.

Hirschhorn JN, Brown SA, Clark CD, Winston F. 1992. Evidence that SNF2/SWI2 and SNF5 activate transcription in yeast by altering chromatin structure. *Genes Dev* **6**: 2288-2298.

Ho L, Crabtree GR. 2010. Chromatin remodelling during development. *Nature* **463**: 474-484.

Hodges C, Bintu L, Lubkowska L, Kashlev M, Bustamante C. 2009. Nucleosomal fluctuations govern the transcription dynamics of RNA polymerase II. *Science* **325**: 626-628.

Holmstrom S, Van Antwerp ME, Iñiguez-Lluhi JA. 2003. Direct and distinguishable inhibitory roles for SUMO isoforms in the control of transcriptional synergy. *Proc Natl Acad Sci U S A* **100**: 15758-15763.

Holstege FC, Jennings EG, Wyrick JJ, Lee TI, Hengartner CJ, Green MR, Golub TR, Lander ES, Young RA. 1998. Dissecting the regulatory circuitry of a eukaryotic genome. *Cell* **95**: 717-728.

Hsu JM, Huang J, Meluh PB, Laurent BC. 2003. The yeast RSC chromatin-remodeling complex is required for kinetochore function in chromosome segregation. *Mol Cell Biol* **23**: 3202-3215.

Huang H, Potter CJ, Tao W, Li DM, Brogiolo W, Hafen E, Sun H, Xu T. 1999. PTEN affects cell size, cell proliferation and apoptosis during Drosophila eye development. *Development* **126**: 5365-5372.

Huang J, Hsu JM, Laurent BC. 2004. The RSC nucleosome-remodeling complex is required for Cohesin's association with chromosome arms. *Mol Cell* **13**: 739-750.

Huang ZQ, Li J, Sachs LM, Cole PA, Wong J. 2003. A role for cofactor-cofactor and cofactor-histone interactions in targeting p300, SWI/SNF and Mediator for transcription. *EMBO J* **22**: 2146-2155.

Ichinose H, Garnier JM, Chambon P, Losson R. 1997. Ligand-dependent interaction between the estrogen receptor and the human homologues of SWI2/SNF2. *Gene* **188**: 95-100.

Ito T, Bulger M, Pazin MJ, Kobayashi R, Kadonaga JT. 1997. ACF, an ISWI-containing and ATP-utilizing chromatin assembly and remodeling factor. *Cell* **90**: 145-155.

Ivanov AV, Peng H, Yurchenko V, Yap KL, Negorev DG, Schultz DC, Psulkowski E, Fredericks WJ, White DE, Maul GG et al. 2007. PHD domain-mediated E3 ligase activity directs intramolecular sumoylation of an adjacent bromodomain required for gene silencing. *Mol Cell* **28**: 823-837.

James TC, Elgin SC. 1986. Identification of a nonhistone chromosomal protein associated with heterochromatin in Drosophila melanogaster and its gene. *Mol Cell Biol* **6**: 3862-3872.

Jamrich M, Greenleaf AL, Bautz EK. 1977. Localization of RNA polymerase in polytene chromosomes of Drosophila melanogaster. *Proc Natl Acad Sci U S A* **74**: 2079-2083.

Jaskelioff M, Gavin IM, Peterson CL, Logie C. 2000. SWI-SNF-mediated nucleosome remodeling: role of histone octamer mobility in the persistence of the remodeled state. *Mol Cell Biol* **20**: 3058-3068.

Jin J, Cai Y, Yao T, Gottschalk AJ, Florens L, Swanson SK, Gutiérrez JL, Coleman MK, Workman JL, Mushegian A et al. 2005. A mammalian chromatin remodeling complex with similarities to the yeast INO80 complex. *J Biol Chem* **280**: 41207-41212.

Johnson ES. 2004. Protein modification by SUMO. *Annu Rev Biochem* **73**: 355-382.

Jones HS, Kawauchi J, Braglia P, Alen CM, Kent NA, Proudfoot NJ. 2007. RNA polymerase I in yeast transcribes dynamic nucleosomal rDNA. *Nat Struct Mol Biol* **14**: 123-130.

Jones PA, Laird PW. 1999. Cancer epigenetics comes of age. *Nat Genet* **21**: 163-167.

Jónsson ZO, Jha S, Wohlschlegel JA, Dutta A. 2004. Rvb1p/Rvb2p recruit Arp5p and assemble a functional Ino80 chromatin remodeling complex. *Mol Cell* **16**: 465-477.

Kal AJ, Mahmoudi T, Zak NB, Verrijzer CP. 2000. The Drosophila brahma complex is an essential coactivator for the trithorax group protein zeste. *Genes Dev* **14**: 1058-1071.

Kalocsay M, Hiller NJ, Jentsch S. 2009. Chromosome-wide Rad51 spreading and SUMO-H2A.Z-dependent chromosome fixation in response to a persistent DNA double-strand break. *Mol Cell* **33**: 335-343.

Kanemaki M, Kurokawa Y, Matsu-ura T, Makino Y, Masani A, Okazaki K, Morishita T, Tamura TA. 1999. TIP49b, a new RuvB-like DNA helicase, is included in a complex together with another RuvB-like DNA helicase, TIP49a. *J Biol Chem* **274**: 22437-22444.

Kaplan CD, Morris JR, Wu C, Winston F. 2000. Spt5 and spt6 are associated with active transcription and have characteristics of general elongation factors in D. melanogaster. *Genes Dev* **14**: 2623-2634.

Karras GI, Kustatscher G, Buhecha HR, Allen MD, Pugieux C, Sait F, Bycroft M, Ladurner AG. 2005. The macro domain is an ADP-ribose binding module. *EMBO J* **24**: 1911-1920.

Kassabov SR, Zhang B, Persinger J, Bartholomew B. 2003. SWI/SNF unwraps, slides, and rewraps the nucleosome. *Mol Cell* **11**: 391-403.

Kehle J, Beuchle D, Treuheit S, Christen B, Kennison JA, Bienz M, Müller J. 1998. dMi-2, a hunchback-interacting protein that functions in polycomb repression. *Science* **282**: 1897-1900.

Kelley DE, Stokes DG, Perry RP. 1999. CHD1 interacts with SSRP1 and depends on both its chromodomain and its ATPase/helicase-like domain for proper association with chromatin. *Chromosoma* **108**: 10-25.

Kelly TK, Miranda TB, Liang G, Berman BP, Lin JC, Tanay A, Jones PA. 2010. H2A.Z maintenance during mitosis reveals nucleosome shifting on mitotically silenced genes. *Mol Cell* **39**: 901-911.

Kennison JA, Vázquez M, Brizuela BJ. 1998. Regulation of the Sex combs reduced gene in Drosophila. *Ann N Y Acad Sci* **842**: 28-35.

Khalil AM, Guttman M, Huarte M, Garber M, Raj A, Rivea Morales D, Thomas K, Presser A, Bernstein BE, van Oudenaarden A et al. 2009. Many human large intergenic noncoding RNAs associate with chromatin-modifying complexes and affect gene expression. *Proc Natl Acad Sci U S A* **106**: 11667-11672.

Khavari PA, Peterson CL, Tamkun JW, Mendel DB, Crabtree GR. 1993. BRG1 contains a conserved domain of the SWI2/SNF2 family necessary for normal mitotic growth and transcription. *Nature* **366**: 170-174.

Khorasanizadeh S. 2004. The nucleosome: from genomic organization to genomic regulation. *Cell* **116**: 259-272.

Khorosjutina O, Wanrooij PH, Walfridsson J, Szilagyi Z, Zhu X, Baraznenok V, Ekwall K, Gustafsson CM. 2010. A chromatin-remodeling protein is a component of fission yeast mediator. *J Biol Chem* **285**: 29729-29737.

Kim H, Erickson B, Luo W, Seward D, Graber JH, Pollock DD, Megee PC, Bentley DL. 2010. Gene-specific RNA polymerase II phosphorylation and the CTD code. *Nat Struct Mol Biol* **17**: 1279-1286.

Kim J, Sif S, Jones B, Jackson A, Koipally J, Heller E, Winandy S, Viel A, Sawyer A, Ikeda T et al. 1999. Ikaros DNA-binding proteins direct formation of chromatin remodeling complexes in lymphocytes. *Immunity* **10**: 345-355.

Kim M, Ahn SH, Krogan NJ, Greenblatt JF, Buratowski S. 2004. Transitions in RNA polymerase II elongation complexes at the 3' ends of genes. *EMBO J* **23**: 354-364.

Klose RJ, Yamane K, Bae Y, Zhang D, Erdjument-Bromage H, Tempst P, Wong J, Zhang Y. 2006. The transcriptional repressor JHDM3A demethylates trimethyl histone H3 lysine 9 and lysine 36. *Nature* **442**: 312-316.

Klymenko T, Papp B, Fischle W, Köcher T, Schelder M, Fritsch C, Wild B, Wilm M, Müller J. 2006. A Polycomb group protein complex with sequence-specific DNA-binding and selective methyl-lysine-binding activities. *Genes Dev* **20**: 1110-1122.

Kobor MS, Venkatasubrahmanyam S, Meneghini MD, Gin JW, Jennings JL, Link AJ, Madhani HD, Rine J. 2004. A protein complex containing the conserved Swi2/Snf2-related ATPase Swr1p deposits histone variant H2A.Z into euchromatin. *PLoS Biol* **2**: E131.

Koipally J, Renold A, Kim J, Georgopoulos K. 1999. Repression by Ikaros and Aiolos is mediated through histone deacetylase complexes. *EMBO J* **18**: 3090-3100.

Komarnitsky P, Cho EJ, Buratowski S. 2000. Different phosphorylated forms of RNA polymerase II and associated mRNA processing factors during transcription. *Genes Dev* **14**: 2452-2460.

Kon C, Cadigan KM, da Silva SL, Nusse R. 2005. Developmental roles of the Mi-2/NURD-associated protein p66 in Drosophila. *Genetics* **169**: 2087-2100.

Konev AY, Tribus M, Park SY, Podhraski V, Lim CY, Emelyanov AV, Vershilova E, Pirrotta V, Kadonaga JT, Lusser A et al. 2007. CHD1 motor protein is required for deposition of histone variant H3.3 into chromatin in vivo. *Science* **317**: 1087-1090.

Kopytova DV, Orlova AV, Krasnov AN, Gurskiy DY, Nikolenko JV, Nabirochkina EN, Shidlovskii YV, Georgieva SG. 2010. Multifunctional factor ENY2 is associated with the THO complex and promotes its recruitment onto nascent mRNA. *Genes Dev* **24**: 86-96.

Korge G, Heide I, Sehnert M, Hofmann A. 1990. Promoter is an important determinant of developmentally regulated puffing at the Sgs-4 locus of Drosophila melanogaster. *Dev Biol* **138**: 324-337.

Kornberg RD. 1974. Chromatin structure: a repeating unit of histones and DNA. *Science* **184**: 868-871.

Kouzarides T. 2007. Chromatin modifications and their function. *Cell* **128**: 693-705.

Kowenz-Leutz E, Leutz A. 1999. A C/EBP beta isoform recruits the SWI/SNF complex to activate myeloid genes. *Mol Cell* **4**: 735-743.

Krauss V. 2008. Glimpses of evolution: heterochromatic histone H3K9 methyltransferases left its marks behind. *Genetica* **133**: 93-106.

Krebs JE, Kuo MH, Allis CD, Peterson CL. 1999. Cell cycle-regulated histone acetylation required for expression of the yeast HO gene. *Genes Dev* **13**: 1412-1421.

Krogan N, Kim M, Ahn S, Zhong G, Kobor M, Cagney G, Emili A, Shilatifard A, Buratowski S, Greenblatt J. 2002. RNA polymerase II elongation factors of Saccharomyces cerevisiae: a targeted proteomics approach. *Mol Cell Biol* **22**: 6979-6992.

Krogan NJ, Baetz K, Keogh MC, Datta N, Sawa C, Kwok TC, Thompson NJ, Davey MG, Pootoolal J, Hughes TR et al. 2004. Regulation of chromosome stability by the histone H2A variant Htz1, the Swr1 chromatin remodeling complex, and the histone acetyltransferase NuA4. *Proc Natl Acad Sci U S A* **101**: 13513-13518.

Krogan NJ, Keogh MC, Datta N, Sawa C, Ryan OW, Ding H, Haw RA, Pootoolal J, Tong A, Canadien V et al. 2003. A Snf2 family ATPase complex required for recruitment of the histone H2A variant Htz1. *Mol Cell* **12**: 1565-1576.

Kuehner JN, Pearson EL, Moore C. 2011. Unravelling the means to an end: RNA polymerase II transcription termination. *Nat Rev Mol Cell Biol* **12**: 283-294.

Kunert N, Brehm A. 2008. Mass production of Drosophila embryos and chromatographic purification of native protein complexes. *Methods Mol Biol* **420**: 359-371.

Kunert N, Brehm A. 2009. Novel Mi-2 related ATP-dependent chromatin remodelers. *Epigenetics* **4**: 209-211.

Kunert N, Wagner E, Murawska M, Klinker H, Kremmer E, Brehm A. 2009. dMec: a novel Mi-2 chromatin remodelling complex involved in transcriptional repression. *EMBO J* **28**: 533-544.

Kustatscher G, Hothorn M, Pugieux C, Scheffzek K, Ladurner AG. 2005. Splicing regulates NAD metabolite binding to histone macroH2A. *Nat Struct Mol Biol* **12**: 624-625.

Kwon H, Imbalzano AN, Khavari PA, Kingston RE, Green MR. 1994. Nucleosome disruption and enhancement of activator binding by a human SW1/SNF complex. *Nature* **370**: 477-481.

Lallena MJ, Chalmers KJ, Llamazares S, Lamond AI, Valcárcel J. 2002. Splicing regulation at the second catalytic step by Sex-lethal involves 3' splice site recognition by SPF45. *Cell* **109**: 285-296.

Larsen DH, Poinsignon C, Gudjonsson T, Dinant C, Payne MR, Hari FJ, Danielsen JM, Menard P, Sand JC, Stucki M et al. 2010. The chromatin-remodeling factor CHD4 coordinates signaling and repair after DNA damage. *J Cell Biol* **190**: 731-740.

Le Guezennec X, Vermeulen M, Brinkman AB, Hoeijmakers WA, Cohen A, Lasonder E, Stunnenberg HG. 2006. MBD2/NuRD and MBD3/NuRD, two distinct complexes with different biochemical and functional properties. *Mol Cell Biol* **26**: 843-851.

Leight ER, Glossip D, Kornfeld K. 2005. Sumoylation of LIN-1 promotes transcriptional repression and inhibition of vulval cell fates. *Development* **132**: 1047-1056.

Li G, Levitus M, Bustamante C, Widom J. 2005. Rapid spontaneous accessibility of nucleosomal DNA. *Nat Struct Mol Biol* **12**: 46-53.

Li H, Ilin S, Wang W, Duncan EM, Wysocka J, Allis CD, Patel DJ. 2006. Molecular basis for site-specific read-out of histone H3K4me3 by the BPTF PHD finger of NURF. *Nature* **442**: 91-95.

Li J, Lin Q, Wang W, Wade P, Wong J. 2002. Specific targeting and constitutive association of histone deacetylase complexes during transcriptional repression. *Genes Dev* **16**: 687-692.

Lia G, Praly E, Ferreira H, Stockdale C, Tse-Dinh YC, Dunlap D, Croquette V, Bensimon D, Owen-Hughes T. 2006. Direct observation of DNA distortion by the RSC complex. *Mol Cell* **21**: 417-425.

Lis JT. 2007. Imaging Drosophila gene activation and polymerase pausing in vivo. *Nature* **450**: 198-202.

Liu M, Xie Z, Price DH. 1998. A human RNA polymerase II transcription termination factor is a SWI2/SNF2 family member. *J Biol Chem* **273**: 25541-25544.

Livak KJ, Schmittgen TD. 2001. Analysis of relative gene expression data using real-time quantitative PCR and the 2(-Delta Delta C(T)) Method. *Methods* **25**: 402-408.

Loppin B, Bonnefoy E, Anselme C, Laurençon A, Karr TL, Couble P. 2005. The histone H3.3 chaperone HIRA is essential for chromatin assembly in the male pronucleus. *Nature* **437**: 1386-1390.

Lorch Y, Maier-Davis B, Kornberg RD. 2006. Chromatin remodeling by nucleosome disassembly in vitro. *Proc Natl Acad Sci U S A* **103**: 3090-3093.

Lorch Y, Zhang M, Kornberg RD. 1999. Histone octamer transfer by a chromatin-remodeling complex. *Cell* **96**: 389-392.

Lowary PT, Widom J. 1998. New DNA sequence rules for high affinity binding to histone octamer and sequence-directed nucleosome positioning. *J Mol Biol* **276**: 19-42.

Lu H, Flores O, Weinmann R, Reinberg D. 1991. The nonphosphorylated form of RNA polymerase II preferentially associates with the preinitiation complex. *Proc Natl Acad Sci U S A* **88**: 10004-10008.

Luco RF, Misteli T. 2011. More than a splicing code: integrating the role of RNA, chromatin and non-coding RNA in alternative splicing regulation. *Curr Opin Genet Dev*.

Luger K, Mäder AW, Richmond RK, Sargent DF, Richmond TJ. 1997. Crystal structure of the nucleosome core particle at 2.8 A resolution. *Nature* **389**: 251-260.

Luger K, Richmond TJ. 1998. DNA binding within the nucleosome core. *Curr Opin Struct Biol* **8**: 33-40.

Luk E, Ranjan A, Fitzgerald PC, Mizuguchi G, Huang Y, Wei D, Wu C. 2010. Stepwise histone replacement by SWR1 requires dual activation with histone H2A.Z and canonical nucleosome. *Cell* **143**: 725-736.

Luo J, Su F, Chen D, Shiloh A, Gu W. 2000. Deacetylation of p53 modulates its effect on cell growth and apoptosis. *Nature* **408**: 377-381.

Lusser A, Urwin DL, Kadonaga JT. 2005. Distinct activities of CHD1 and ACF in ATP-dependent chromatin assembly. *Nat Struct Mol Biol* **12**: 160-166.

Längst G, Becker PB. 2001. ISWI induces nucleosome sliding on nicked DNA. *Mol Cell* **8**: 1085-1092.

Längst G, Becker PB. 2004. Nucleosome remodeling: one mechanism, many phenomena? *Biochim Biophys Acta* **1677**: 58-63.

Längst G, Bonte EJ, Corona DF, Becker PB. 1999. Nucleosome movement by CHRAC and ISWI without disruption or trans-displacement of the histone octamer. *Cell* **97**: 843-852.

Malanga M, Althaus FR. 2005. The role of poly(ADP-ribose) in the DNA damage signaling network. *Biochem Cell Biol* **83**: 354-364.

Maluf NK, Ali JA, Lohman TM. 2003a. Kinetic mechanism for formation of the active, dimeric UvrD helicase-DNA complex. *J Biol Chem* **278**: 31930-31940.

Maluf NK, Fischer CJ, Lohman TM. 2003b. A Dimer of Escherichia coli UvrD is the active form of the helicase in vitro. *J Mol Biol* **325**: 913-935.

Mansfield RE, Musselman CA, Kwan AH, Oliver SS, Garske AL, Davrazou F, Denu JM, Kutateladze TG, Mackay JP. 2011. Plant homeodomain (PHD) fingers of CHD4 are histone H3-binding modules with preference for unmodified H3K4 and methylated H3K9. *J Biol Chem* **286**: 11779-11791.

Marcillac F, Bousquet F, Alabouvette J, Savarit F, Ferveur JF. 2005. A mutation with major effects on Drosophila melanogaster sex pheromones. *Genetics* **171**: 1617-1628.

Marfella CG, Imbalzano AN. 2007. The Chd family of chromatin remodelers. *Mutat Res* **618**: 30-40.

Margueron R, Reinberg D. 2011. The Polycomb complex PRC2 and its mark in life. *Nature* **469**: 343-349.

Marhold J, Brehm A, Kramer K. 2004a. The Drosophila methyl-DNA binding protein MBD2/3 interacts with the NuRD complex via p55 and MI-2. *BMC Mol Biol* **5**: 20.

Marhold J, Kramer K, Kremmer E, Lyko F. 2004b. The Drosophila MBD2/3 protein mediates interactions between the MI-2 chromatin complex and CpT/A-methylated DNA. *Development* **131**: 6033-6039.

Marmorstein R, Berger SL. 2001. Structure and function of bromodomains in chromatin-regulating complexes. *Gene* **272**: 1-9.

Martínez-Balbás MA, Dey A, Rabindran SK, Ozato K, Wu C. 1995. Displacement of sequence-specific transcription factors from mitotic chromatin. *Cell* **83**: 29-38.

Matsuoka S, Ballif BA, Smogorzewska A, McDonald ER, Hurov KE, Luo J, Bakalarski CE, Zhao Z, Solimini N, Lerenthal Y et al. 2007. ATM and ATR substrate analysis reveals extensive protein networks responsive to DNA damage. *Science* **316**: 1160-1166.

Mayer A, Lidschreiber M, Siebert M, Leike K, Söding J, Cramer P. 2010. Uniform transitions of the general RNA polymerase II transcription complex. *Nat Struct Mol Biol* **17**: 1272-1278.

Mayer C, Neubert M, Grummt I. 2008. The structure of NoRC-associated RNA is crucial for targeting the chromatin remodelling complex NoRC to the nucleolus. *EMBO Rep* **9**: 774-780.

Mayer C, Schmitz KM, Li J, Grummt I, Santoro R. 2006. Intergenic transcripts regulate the epigenetic state of rRNA genes. *Mol Cell* **22**: 351-361.

Mayer MP, Bukau B. 2005. Hsp70 chaperones: cellular functions and molecular mechanism. *Cell Mol Life Sci* **62**: 670-684.

Mazumdar A, Wang RA, Mishra SK, Adam L, Bagheri-Yarmand R, Mandal M, Vadlamudi RK, Kumar R. 2001. Transcriptional repression of oestrogen receptor by metastasis-associated protein 1 corepressor. *Nat Cell Biol* **3**: 30-37.

Mellor J. 2006. It takes a PHD to read the histone code. *Cell* **126**: 22-24.

Meneghini MD, Wu M, Madhani HD. 2003. Conserved histone variant H2A.Z protects euchromatin from the ectopic spread of silent heterochromatin. *Cell* **112**: 725-736.

Menon T, Yates JA, Bochar DA. 2010. Regulation of androgen-responsive transcription by the chromatin remodeling factor CHD8. *Mol Endocrinol* **24**: 1165-1174.

Michelotti EF, Sanford S, Levens D. 1997. Marking of active genes on mitotic chromosomes. *Nature* **388**: 895-899.

Mizuguchi G, Shen X, Landry J, Wu WH, Sen S, Wu C. 2004. ATP-driven exchange of histone H2AZ variant catalyzed by SWR1 chromatin remodeling complex. *Science* **303**: 343-348.

Mizuguchi G, Tsukiyama T, Wisniewski J, Wu C. 1997. Role of nucleosome remodeling factor NURF in transcriptional activation of chromatin. *Mol Cell* **1**: 141-150.

Mohrmann L, Verrijzer CP. 2005. Composition and functional specificity of SWI2/SNF2 class chromatin remodeling complexes. *Biochim Biophys Acta* **1681**: 59-73.

Morettini S, Tribus M, Zeilner A, Sebald J, Campo-Fernandez B, Scheran G, Wörle H, Podhraski V, Fyodorov DV, Lusser A. 2011. The chromodomains of CHD1 are critical for enzymatic activity but less important for chromatin localization. *Nucleic Acids Res* **39**: 3103-3115.

Morrison AJ, Highland J, Krogan NJ, Arbel-Eden A, Greenblatt JF, Haber JE, Shen X. 2004. INO80 and gamma-H2AX interaction links ATP-dependent chromatin remodeling to DNA damage repair. *Cell* **119**: 767-775.

Moss T, Boseley PG, Birnstiel ML. 1980. More ribosomal spacer sequences from Xenopus laevis. *Nucleic Acids Res* **8**: 467-485.

Muchardt C, Reyes JC, Bourachot B, Leguoy E, Yaniv M. 1996. The hbrm and BRG-1 proteins, components of the human SNF/SWI complex, are phosphorylated and excluded from the condensed chromosomes during mitosis. *EMBO J* **15**: 3394-3402.

Murawska M, Kunert N, van Vugt J, Längst G, Kremmer E, Logie C, Brehm A. 2008. dCHD3, a novel ATP-dependent chromatin remodeler associated with sites of active transcription. *Mol Cell Biol* **28**: 2745-2757.

Murawsky CM, Brehm A, Badenhorst P, Lowe N, Becker PB, Travers AA. 2001. Tramtrack69 interacts with the dMi-2 subunit of the Drosophila NuRD chromatin remodelling complex. *EMBO Rep* **2**: 1089-1094.

Musselman CA, Mansfield RE, Garske AL, Davrazou F, Kwan AH, Oliver SS, O'Leary H, Denu JM, Mackay JP, Kutateladze TG. 2009. Binding of the CHD4 PHD2 finger to histone H3 is modulated by covalent modifications. *Biochem J* **423**: 179-187.

Muthurajan UM, Park YJ, Edayathumangalam RS, Suto RK, Chakravarthy S, Dyer PN, Luger K. 2003. Structure and dynamics of nucleosomal DNA. *Biopolymers* **68**: 547-556.

Myers LC, Gustafsson CM, Bushnell DA, Lui M, Erdjument-Bromage H, Tempst P, Kornberg RD. 1998. The Med proteins of yeast and their function through the RNA polymerase II carboxy-terminal domain. *Genes Dev* **12**: 45-54.

Nahkuri S, Taft RJ, Mattick JS. 2009. Nucleosomes are preferentially positioned at exons in somatic and sperm cells. *Cell Cycle* **8**: 3420-3424.

Naito T, Gómez-Del Arco P, Williams CJ, Georgopoulos K. 2007. Antagonistic interactions between Ikaros and the chromatin remodeler Mi-2beta determine silencer activity and Cd4 gene expression. *Immunity* **27**: 723-734.

Nan X, Ng HH, Johnson CA, Laherty CD, Turner BM, Eisenman RN, Bird A. 1998. Transcriptional repression by the methyl-CpG-binding protein MeCP2 involves a histone deacetylase complex. *Nature* **393**: 386-389.

Narlikar GJ. 2010. A proposal for kinetic proof reading by ISWI family chromatin remodeling motors. *Curr Opin Chem Biol* **14**: 660-665.

Natarajan K, Jackson B, Zhou H, Winston F, Hinnebusch A. 1999. Transcriptional activation by Gcn4p involves independent interactions with the SWI/SNF complex and the SRB/mediator. *Mol Cell* **4**: 657-664.

Neely KE, Hassan AH, Wallberg AE, Steger DJ, Cairns BR, Wright AP, Workman JL. 1999. Activation domain-mediated targeting of the SWI/SNF complex to promoters stimulates transcription from nucleosome arrays. *Mol Cell* **4**: 649-655.

Ni Z, Schwartz BE, Werner J, Suarez JR, Lis JT. 2004. Coordination of transcription, RNA processing, and surveillance by P-TEFb kinase on heat shock genes. *Mol Cell* **13**: 55-65.

Nishida T, Yasuda H. 2002. PIAS1 and PIASxalpha function as SUMO-E3 ligases toward androgen receptor and repress androgen receptor-dependent transcription. *J Biol Chem* **277**: 41311-41317.

Nishioka K, Rice JC, Sarma K, Erdjument-Bromage H, Werner J, Wang Y, Chuikov S, Valenzuela P, Tempst P, Steward R et al. 2002. PR-Set7 is a nucleosome-specific methyltransferase that modifies lysine 20 of histone H4 and is associated with silent chromatin. *Mol Cell* **9**: 1201-1213.

Németh A, Strohner R, Grummt I, Längst G. 2004. The chromatin remodeling complex NoRC and TTF-I cooperate in the regulation of the mammalian rRNA genes in vivo. *Nucleic Acids Res* **32**: 4091-4099.

Ogawa H, Komatsu T, Hiraoka Y, Morohashi K. 2009. Transcriptional Suppression by Transient Recruitment of ARIP4 to Sumoylated nuclear receptor Ad4BP/SF-1. *Mol Biol Cell* **20**: 4235-4245.

Okada M, Okawa K, Isobe T, Fukagawa T. 2009. CENP-H-containing complex facilitates centromere deposition of CENP-A in cooperation with FACT and CHD1. *Mol Biol Cell* **20**: 3986-3995.

Okuda M, Horikoshi M, Nishimura Y. 2007. Structural polymorphism of chromodomains in Chd1. *J Mol Biol* **365**: 1047-1062.

Olave IA, Reck-Peterson SL, Crabtree GR. 2002. Nuclear actin and actin-related proteins in chromatin remodeling. *Annu Rev Biochem* **71**: 755-781.

Olins DE, Wright EB. 1973. Glutaraldehyde fixation of isolated eucaryotic nuclei. Evidence for histone-histone proximity. *J Cell Biol* **59**: 304-317.

Ooi L, Belyaev ND, Miyake K, Wood IC, Buckley NJ. 2006. BRG1 chromatin remodeling activity is required for efficient chromatin binding by repressor element 1-silencing transcription factor (REST) and facilitates REST-mediated repression. *J Biol Chem* **281**: 38974-38980.

Orlando V, Strutt H, Paro R. 1997. Analysis of chromatin structure by in vivo formaldehyde cross-linking. *Methods* **11**: 205-214.

Ostlund Farrants AK, Blomquist P, Kwon H, Wrange O. 1997. Glucocorticoid receptor-glucocorticoid response element binding stimulates nucleosome disruption by the SWI/SNF complex. *Mol Cell Biol* **17**: 895-905.

Oudet P, Gross-Bellard M, Chambon P. 1975. Electron microscopic and biochemical evidence that chromatin structure is a repeating unit. *Cell* **4**: 281-300.

Owen-Hughes T, Utley RT, Côté J, Peterson CL, Workman JL. 1996. Persistent site-specific remodeling of a nucleosome array by transient action of the SWI/SNF complex. *Science* **273**: 513-516.

Owen-Hughes T, Workman JL. 1996. Remodeling the chromatin structure of a nucleosome array by transcription factor-targeted trans-displacement of histones. *EMBO J* **15**: 4702-4712.

Pan Q, Shai O, Lee LJ, Frey BJ, Blencowe BJ. 2008. Deep surveying of alternative splicing complexity in the human transcriptome by high-throughput sequencing. *Nat Genet* **40**: 1413-1415.

Papamichos-Chronakis M, Krebs JE, Peterson CL. 2006. Interplay between Ino80 and Swr1 chromatin remodeling enzymes regulates cell cycle checkpoint adaptation in response to DNA damage. *Genes Dev* **20**: 2437-2449.

Park JH, Park EJ, Lee HS, Kim SJ, Hur SK, Imbalzano AN, Kwon J. 2006. Mammalian SWI/SNF complexes facilitate DNA double-strand break repair by promoting gamma-H2AX induction. *EMBO J* **25**: 3986-3997.

Park SY, Song YH. 2008. Genetic screen for genes involved in Chk2 signaling in Drosophila. *Mol Cells* **26**: 350-355.

Paro R, Hogness DS. 1991. The Polycomb protein shares a homologous domain with a heterochromatin-associated protein of Drosophila. *Proc Natl Acad Sci U S A* **88**: 263-267.

Passannante M, Marti CO, Pfefferli C, Moroni PS, Kaeser-Pebernard S, Puoti A, Hunziker P, Wicky C, Müller F. 2010. Different Mi-2 complexes for various developmental functions in Caenorhabditis elegans. *PLoS One* **5**: e13681.

Pearce JJ, Singh PB, Gaunt SJ. 1992. The mouse has a Polycomb-like chromobox gene. *Development* **114**: 921-929.

Pegoraro G, Kubben N, Wickert U, Göhler H, Hoffmann K, Misteli T. 2009. Ageing-related chromatin defects through loss of the NURD complex. *Nat Cell Biol* **11**: 1261-1267.

Peritz T, Zeng F, Kannanayakal TJ, Kilk K, Eiríksdóttir E, Langel U, Eberwine J. 2006. Immunoprecipitation of mRNA-protein complexes. *Nat Protoc* **1**: 577-580.

Peterson CL, Herskowitz I. 1992. Characterization of the yeast SWI1, SWI2, and SWI3 genes, which encode a global activator of transcription. *Cell* **68**: 573-583.

Peterson CL, Workman JL. 2000. Promoter targeting and chromatin remodeling by the SWI/SNF complex. *Curr Opin Genet Dev* **10**: 187-192.

Petesch S, Lis J. 2008. Rapid, transcription-independent loss of nucleosomes over a large chromatin domain at Hsp70 loci. *Cell* **134**: 74-84.

Phatnani HP, Greenleaf AL. 2006. Phosphorylation and functions of the RNA polymerase II CTD. *Genes Dev* **20**: 2922-2936.

Piacentini L, Fanti L, Berloco M, Perrini B, Pimpinelli S. 2003. Heterochromatin protein 1 (HP1) is associated with induced gene expression in Drosophila euchromatin. *J Cell Biol* **161**: 707-714.

Pleschke JM, Kleczkowska HE, Strohm M, Althaus FR. 2000. Poly(ADP-ribose) binds to specific domains in DNA damage checkpoint proteins. *J Biol Chem* **275**: 40974-40980.

Podhraski V, Campo-Fernandez B, Wörle H, Piatti P, Niederegger H, Böck G, Fyodorov DV, Lusser A. 2010. CenH3/CID incorporation is not dependent on the chromatin assembly factor CHD1 in Drosophila. *PLoS One* **5**: e10120.

Polo SE, Kaidi A, Baskcomb L, Galanty Y, Jackson SP. 2010. Regulation of DNA-damage responses and cell-cycle progression by the chromatin remodelling factor CHD4. *EMBO J* **29**: 3130-3139.

Pray-Grant MG, Daniel JA, Schieltz D, Yates JR, Grant PA. 2005. Chd1 chromodomain links histone H3 methylation with SAGA- and SLIK-dependent acetylation. *Nature* **433**: 434-438.

Qiu XB, Lin YL, Thome KC, Pian P, Schlegel BP, Weremowicz S, Parvin JD, Dutta A. 1998. An eukaryotic RuvB-like protein (RUVBL1) essential for growth. *J Biol Chem* **273**: 27786-27793.

Quan TK, Hartzog GA. 2010. Histone H3K4 and K36 methylation, Chd1 and Rpd3S oppose the functions of Saccharomyces cerevisiae Spt4-Spt5 in transcription. *Genetics* **184**: 321-334.

Racki LR, Yang JG, Naber N, Partensky PD, Acevedo A, Purcell TJ, Cooke R, Cheng Y, Narlikar GJ. 2009. The chromatin remodeller ACF acts as a dimeric motor to space nucleosomes. *Nature* **462**: 1016-1021.

Raisner RM, Hartley PD, Meneghini MD, Bao MZ, Liu CL, Schreiber SL, Rando OJ, Madhani HD. 2005. Histone variant H2A.Z marks the 5' ends of both active and inactive genes in euchromatin. *Cell* **123**: 233-248.

Ramírez J, Hagman J. 2009. The Mi-2/NuRD complex: a critical epigenetic regulator of hematopoietic development, differentiation and cancer. *Epigenetics* **4**: 532-536.

Rando OJ, Zhao K, Janmey P, Crabtree GR. 2002. Phosphatidylinositol-dependent actin filament binding by the SWI/SNF-like BAF chromatin remodeling complex. *Proc Natl Acad Sci U S A* **99**: 2824-2829.

Reddy BA, Bajpe PK, Bassett A, Moshkin YM, Kozhevnikova E, Bezstarosti K, Demmers JA, Travers AA, Verrijzer CP. 2010. Drosophila transcription factor Tramtrack69 binds MEP1 to recruit the chromatin remodeler NuRD. *Mol Cell Biol* **30**: 5234-5244.

Rehwinkel J, Herold A, Gari K, Köcher T, Rode M, Ciccarelli FL, Wilm M, Izaurralde E. 2004. Genome-wide analysis of mRNAs regulated by the THO complex in Drosophila melanogaster. *Nat Struct Mol Biol* **11**: 558-566.

Reinke H, Gregory PD, Hörz W. 2001. A transient histone hyperacetylation signal marks nucleosomes for remodeling at the PHO8 promoter in vivo. *Mol Cell* **7**: 529-538.

Rippe K, Schrader A, Riede P, Strohner R, Lehmann E, Längst G. 2007. DNA sequence- and conformation-directed positioning of nucleosomes by chromatin-remodeling complexes. *Proc Natl Acad Sci U S A* **104**: 15635-15640.

Ristic D, Wyman C, Paulusma C, Kanaar R. 2001. The architecture of the human Rad54-DNA complex provides evidence for protein translocation along DNA. *Proc Natl Acad Sci U S A* **98**: 8454-8460.

Ritchie K, Seah C, Moulin J, Isaac C, Dick F, Bérubé NG. 2008. Loss of ATRX leads to chromosome cohesion and congression defects. *J Cell Biol* **180**: 315-324.

Roberts S, Winston F. 1997. Essential functional interactions of SAGA, a Saccharomyces cerevisiae complex of Spt, Ada, and Gcn5 proteins, with the Snf/Swi and Srb/mediator complexes. *Genetics* **147**: 451-465.

Robertson KD. 2001. DNA methylation, methyltransferases, and cancer. *Oncogene* **20**: 3139-3155.

Robinson KM, Schultz MC. 2003. Replication-independent assembly of nucleosome arrays in a novel yeast chromatin reconstitution system involves antisilencing factor Asf1p and chromodomain protein Chd1p. *Mol Cell Biol* **23**: 7937-7946.

Rodríguez-Paredes M, Ceballos-Chávez M, Esteller M, García-Domínguez M, Reyes JC. 2009. The chromatin remodeling factor CHD8 interacts with elongating RNA polymerase II and controls expression of the cyclin E2 gene. *Nucleic Acids Res* **37**: 2449-2460.

Saether T, Berge T, Ledsaak M, Matre V, Alm-Kristiansen AH, Dahle O, Aubry F, Gabrielsen OS. 2007. The chromatin remodeling factor Mi-2alpha acts as a novel co-activator for human c-Myb. *J Biol Chem* **282**: 13994-14005.

Saha A, Wittmeyer J, Cairns BR. 2002. Chromatin remodeling by RSC involves ATP-dependent DNA translocation. *Genes Dev* **16**: 2120-2134.

Saha A, Wittmeyer J, Cairns BR. 2005. Chromatin remodeling through directional DNA translocation from an internal nucleosomal site. *Nat Struct Mol Biol* **12**: 747-755.

Sala A, La Rocca G, Burgio G, Kotova E, Di Gesù D, Collesano M, Ingrassia A, Tulin A, Corona D. 2008. The nucleosome-remodeling ATPase ISWI is regulated by poly-ADP-ribosylation. *PLoS Biol* **6**: e252.

Sambrook J, Russel, DW. 2001. *Molecular Cloning: A Laboratory Manual*. CSHL Press.

Santoro R, Grummt I. 2005. Epigenetic mechanism of rRNA gene silencing: temporal order of NoRC-mediated histone modification, chromatin remodeling, and DNA methylation. *Mol Cell Biol* **25**: 2539-2546.

Santoro R, Li J, Grummt I. 2002. The nucleolar remodeling complex NoRC mediates heterochromatin formation and silencing of ribosomal gene transcription. *Nat Genet* **32**: 393-396.

Santos-Rosa H, Schneider R, Bernstein BE, Karabetsou N, Morillon A, Weise C, Schreiber SL, Mellor J, Kouzarides T. 2003. Methylation of histone H3 K4 mediates association of the Isw1p ATPase with chromatin. *Mol Cell* **12**: 1325-1332.

Sarraf SA, Stancheva I. 2004. Methyl-CpG binding protein MBD1 couples histone H3 methylation at lysine 9 by SETDB1 to DNA replication and chromatin assembly. *Mol Cell* **15**: 595-605.

Saunders A, Core LJ, Lis JT. 2006. Breaking barriers to transcription elongation. *Nat Rev Mol Cell Biol* **7**: 557-567.

Saunders A, Werner J, Andrulis E, Nakayama T, Hirose S, Reinberg D, Lis J. 2003. Tracking FACT and the RNA polymerase II elongation complex through chromatin in vivo. *Science* **301**: 1094-1096.

Schiessel H, Widom J, Bruinsma RF, Gelbart WM. 2001. Polymer reptation and nucleosome repositioning. *Phys Rev Lett* **86**: 4414-4417.

Schmidt DR, Schreiber SL. 1999. Molecular association between ATR and two components of the nucleosome remodeling and deacetylating complex, HDAC2 and CHD4. *Biochemistry* **38**: 14711-14717.

Schneider I. 1972. Cell lines derived from late embryonic stages of Drosophila melanogaster. *J Embryol Exp Morphol* **27**: 353-365.

Schnetz MP, Bartels CF, Shastri K, Balasubramanian D, Zentner GE, Balaji R, Zhang X, Song L, Wang Z, Laframboise T et al. 2009. Genomic distribution of CHD7 on chromatin tracks H3K4 methylation patterns. *Genome Res* **19**: 590-601.

Schultz DC, Friedman JR, Rauscher FJ. 2001. Targeting histone deacetylase complexes via KRAB-zinc finger proteins: the PHD and bromodomains of KAP-1 form a cooperative unit that recruits a novel isoform of the Mi-2alpha subunit of NuRD. *Genes Dev* **15**: 428-443.

Schwanbeck R, Xiao H, Wu C. 2004. Spatial contacts and nucleosome step movements induced by the NURF chromatin remodeling complex. *J Biol Chem* **279**: 39933-39941.

Schwartz BE, Ahmad K. 2005. Transcriptional activation triggers deposition and removal of the histone variant H3.3. *Genes Dev* **19**: 804-814.

Schwartz BE, Werner JK, Lis JT. 2004. Indirect immunofluorescent labeling of Drosophila polytene chromosomes: visualizing protein interactions with chromatin in vivo. *Methods Enzymol* **376**: 393-404.

Schwartz S, Meshorer E, Ast G. 2009. Chromatin organization marks exon-intron structure. *Nat Struct Mol Biol* **16**: 990-995.

Seelig HP, Moosbrugger I, Ehrfeld H, Fink T, Renz M, Genth E. 1995. The major dermatomyositis-specific Mi-2 autoantigen is a presumed helicase involved in transcriptional activation. *Arthritis Rheum* **38**: 1389-1399.

Shakya A, Kang J, Chumley J, Williams MA, Tantin D. 2011. Oct1 is a switchable, bipotential stabilizer of repressed and inducible transcriptional states. *J Biol Chem* **286**: 450-459.

Shen X, Ranallo R, Choi E, Wu C. 2003. Involvement of actin-related proteins in ATP-dependent chromatin remodeling. *Mol Cell* **12**: 147-155.

Shi Y. 2007. Histone lysine demethylases: emerging roles in development, physiology and disease. *Nat Rev Genet* **8**: 829-833.

Shilatifard A. 2006. Chromatin modifications by methylation and ubiquitination: implications in the regulation of gene expression. *Annu Rev Biochem* **75**: 243-269.

Shimono K, Shimono Y, Shimokata K, Ishiguro N, Takahashi M. 2005. Microspherule protein 1, Mi-2beta, and RET finger protein associate in the nucleolus and up-regulate ribosomal gene transcription. *J Biol Chem* **280**: 39436-39447.

Siatecka M, Xue L, Bieker JJ. 2007. Sumoylation of EKLF promotes transcriptional repression and is involved in inhibition of megakaryopoiesis. *Mol Cell Biol* **27**: 8547-8560.

Simic R, Lindstrom DL, Tran HG, Roinick KL, Costa PJ, Johnson AD, Hartzog GA, Arndt KM. 2003. Chromatin remodeling protein Chd1 interacts with transcription elongation factors and localizes to transcribed genes. *EMBO J* **22**: 1846-1856.

Sims RJ, Chen CF, Santos-Rosa H, Kouzarides T, Patel SS, Reinberg D. 2005. Human but not yeast CHD1 binds directly and selectively to histone H3 methylated at lysine 4 via its tandem chromodomains. *J Biol Chem* **280**: 41789-41792.

Sims RJ, Millhouse S, Chen CF, Lewis BA, Erdjument-Bromage H, Tempst P, Manley JL, Reinberg D. 2007. Recognition of trimethylated histone H3 lysine 4 facilitates the

recruitment of transcription postinitiation factors and pre-mRNA splicing. *Mol Cell* **28**: 665-676.

Smeenk G, Wiegant W, Vrolijk H, Solari A, Pastink A, van Attikum H. 2010. The NuRD chromatin-remodeling complex regulates signaling and repair of DNA damage. *J Cell Biol* **190**: 741-749.

Smith S, Stillman B. 1989. Purification and characterization of CAF-I, a human cell factor required for chromatin assembly during DNA replication in vitro. *Cell* **58**: 15-25.

Solomon MJ, Larsen PL, Varshavsky A. 1988. Mapping protein-DNA interactions in vivo with formaldehyde: evidence that histone H4 is retained on a highly transcribed gene. *Cell* **53**: 937-947.

Song JJ, Garlick JD, Kingston RE. 2008. Structural basis of histone H4 recognition by p55. *Genes Dev* **22**: 1313-1318.

Srinivasan S, Armstrong JA, Deuring R, Dahlsveen IK, McNeill H, Tamkun JW. 2005. The Drosophila trithorax group protein Kismet facilitates an early step in transcriptional elongation by RNA Polymerase II. *Development* **132**: 1623-1635.

Srinivasan S, Dorighi K, Tamkun J. 2008. Drosophila Kismet regulates histone H3 lysine 27 methylation and early elongation by RNA polymerase II. *PLoS Genet* **4**: e1000217.

Stern M, Jensen R, Herskowitz I. 1984. Five SWI genes are required for expression of the HO gene in yeast. *J Mol Biol* **178**: 853-868.

Stevaux O, Dimova DK, Ji JY, Moon NS, Frolov MV, Dyson NJ. 2005. Retinoblastoma family 2 is required in vivo for the tissue-specific repression of dE2F2 target genes. *Cell Cycle* **4**: 1272-1280.

Stielow B, Sapetschnig A, Krüger I, Kunert N, Brehm A, Boutros M, Suske G. 2008. Identification of SUMO-dependent chromatin-associated transcriptional repression components by a genome-wide RNAi screen. *Mol Cell* **29**: 742-754.

Stockdale C, Flaus A, Ferreira H, Owen-Hughes T. 2006. Analysis of nucleosome repositioning by yeast ISWI and Chd1 chromatin remodeling complexes. *J Biol Chem* **281**: 16279-16288.

Stokes DG, Perry RP. 1995. DNA-binding and chromatin localization properties of CHD1. *Mol Cell Biol* **15**: 2745-2753.

Stokes DG, Tartof KD, Perry RP. 1996. CHD1 is concentrated in interbands and puffed regions of Drosophila polytene chromosomes. *Proc Natl Acad Sci U S A* **93**: 7137-7142.

Strohner R, Nemeth A, Jansa P, Hofmann-Rohrer U, Santoro R, Längst G, Grummt I. 2001. NoRC--a novel member of mammalian ISWI-containing chromatin remodeling machines. *EMBO J* **20**: 4892-4900.

Strohner R, Németh A, Nightingale KP, Grummt I, Becker PB, Längst G. 2004. Recruitment of the nucleolar remodeling complex NoRC establishes ribosomal DNA silencing in chromatin. *Mol Cell Biol* **24**: 1791-1798.

Studitsky VM, Clark DJ, Felsenfeld G. 1994. A histone octamer can step around a transcribing polymerase without leaving the template. *Cell* **76**: 371-382.

Sudarsanam P, Winston F. 2000. The Swi/Snf family nucleosome-remodeling complexes and transcriptional control. *Trends Genet* **16**: 345-351.

SullivanW, Ashburner M, Hawley RS. 2000. *Drosophila Protocols*. CSH Press.

Szerlong H, Hinata K, Viswanathan R, Erdjument-Bromage H, Tempst P, Cairns BR. 2008. The HSA domain binds nuclear actin-related proteins to regulate chromatin-remodeling ATPases. *Nat Struct Mol Biol* **15**: 469-476.

Szerlong H, Saha A, Cairns BR. 2003. The nuclear actin-related proteins Arp7 and Arp9: a dimeric module that cooperates with architectural proteins for chromatin remodeling. *EMBO J* **22**: 3175-3187.

Szutorisz H, Dillon N, Tora L. 2005. The role of enhancers as centres for general transcription factor recruitment. *Trends Biochem Sci* **30**: 593-599.

Tai HH, Geisterfer M, Bell JC, Moniwa M, Davie JR, Boucher L, McBurney MW. 2003. CHD1 associates with NCoR and histone deacetylase as well as with RNA splicing proteins. *Biochem Biophys Res Commun* **308**: 170-176.

Takada I, Mihara M, Suzawa M, Ohtake F, Kobayashi S, Igarashi M, Youn MY, Takeyama K, Nakamura T, Mezaki Y et al. 2007. A histone lysine methyltransferase activated by non-canonical Wnt signalling suppresses PPAR-gamma transactivation. *Nat Cell Biol* **9**: 1273-1285.

Talbert PB, Henikoff S. 2010. Histone variants--ancient wrap artists of the epigenome. *Nat Rev Mol Cell Biol* **11**: 264-275.

Therrien M, Morrison DK, Wong AM, Rubin GM. 2000. A genetic screen for modifiers of a kinase suppressor of Ras-dependent rough eye phenotype in Drosophila. *Genetics* **156**: 1231-1242.

Thompson BA, Tremblay V, Lin G, Bochar DA. 2008. CHD8 is an ATP-dependent chromatin remodeling factor that regulates beta-catenin target genes. *Mol Cell Biol* **28**: 3894-3904.

Thomä NH, Czyzewski BK, Alexeev AA, Mazin AV, Kowalczykowski SC, Pavletich NP. 2005. Structure of the SWI2/SNF2 chromatin-remodeling domain of eukaryotic Rad54. *Nat Struct Mol Biol* **12**: 350-356.

Timinszky G, Till S, Hassa PO, Hothorn M, Kustatscher G, Nijmeijer B, Colombelli J, Altmeyer M, Stelzer EH, Scheffzek K et al. 2009. A macrodomain-containing histone rearranges chromatin upon sensing PARP1 activation. *Nat Struct Mol Biol* **16**: 923-929.

Toh Y, Pencil SD, Nicolson GL. 1994. A novel candidate metastasis-associated gene, mta1, differentially expressed in highly metastatic mammary adenocarcinoma cell lines. cDNA cloning, expression, and protein analyses. *J Biol Chem* **269**: 22958-22963.

Tong JK, Hassig CA, Schnitzler GR, Kingston RE, Schreiber SL. 1998. Chromatin deacetylation by an ATP-dependent nucleosome remodelling complex. *Nature* **395**: 917-921.

Tran HG, Steger DJ, Iyer VR, Johnson AD. 2000. The chromo domain protein chd1p from budding yeast is an ATP-dependent chromatin-modifying factor. *EMBO J* **19**: 2323-2331.

Trouche D, Le Chalony C, Muchardt C, Yaniv M, Kouzarides T. 1997. RB and hbrm cooperate to repress the activation functions of E2F1. *Proc Natl Acad Sci U S A* **94**: 11268-11273.

Tsai MC, Manor O, Wan Y, Mosammaparast N, Wang JK, Lan F, Shi Y, Segal E, Chang HY. 2010. Long noncoding RNA as modular scaffold of histone modification complexes. *Science* **329**: 689-693.

Tsukiyama T, Becker PB, Wu C. 1994. ATP-dependent nucleosome disruption at a heat-shock promoter mediated by binding of GAGA transcription factor. *Nature* **367**: 525-532.

Tsukiyama T, Daniel C, Tamkun J, Wu C. 1995. ISWI, a member of the SWI2/SNF2 ATPase family, encodes the 140 kDa subunit of the nucleosome remodeling factor. *Cell* **83**: 1021-1026.

Tsukiyama T, Wu C. 1995. Purification and properties of an ATP-dependent nucleosome remodeling factor. *Cell* **83**: 1011-1020.

Tsukuda T, Fleming AB, Nickoloff JA, Osley MA. 2005. Chromatin remodelling at a DNA double-strand break site in Saccharomyces cerevisiae. *Nature* **438**: 379-383.

Tulin A, Spradling A. 2003. Chromatin loosening by poly(ADP)-ribose polymerase (PARP) at Drosophila puff loci. *Science* **299**: 560-562.

Tyagi A, Ryme J, Brodin D, Ostlund Farrants AK, Visa N. 2009. SWI/SNF associates with nascent pre-mRNPs and regulates alternative pre-mRNA processing. *PLoS Genet* **5**: e1000470.

Tyler JK, Bulger M, Kamakaka RT, Kobayashi R, Kadonaga JT. 1996. The p55 subunit of Drosophila chromatin assembly factor 1 is homologous to a histone deacetylase-associated protein. *Mol Cell Biol* **16**: 6149-6159.

Unhavaithaya Y, Shin TH, Miliaras N, Lee J, Oyama T, Mello CC. 2002. MEP-1 and a homolog of the NURD complex component Mi-2 act together to maintain germline-soma distinctions in C. elegans. *Cell* **111**: 991-1002.

Usheva A, Maldonado E, Goldring A, Lu H, Houbavi C, Reinberg D, Aloni Y. 1992. Specific interaction between the nonphosphorylated form of RNA polymerase II and the TATA-binding protein. *Cell* **69**: 871-881.

van Attikum H, Fritsch O, Gasser SM. 2007. Distinct roles for SWR1 and INO80 chromatin remodeling complexes at chromosomal double-strand breaks. *EMBO J* **26**: 4113-4125.

van Attikum H, Fritsch O, Hohn B, Gasser SM. 2004. Recruitment of the INO80 complex by H2A phosphorylation links ATP-dependent chromatin remodeling with DNA double-strand break repair. *Cell* **119**: 777-788.

van Attikum H, Gasser SM. 2005. The histone code at DNA breaks: a guide to repair? *Nat Rev Mol Cell Biol* **6**: 757-765.

van Vugt J, de Jager M, Murawska M, Brehm A, van Noort J, Logie C. 2009. Multiple aspects of ATP-dependent nucleosome translocation by RSC and Mi-2 are directed by the underlying DNA sequence. *PLoS One* **4**: e6345.

Varga-Weisz PD, Blank TA, Becker PB. 1995. Energy-dependent chromatin accessibility and nucleosome mobility in a cell-free system. *EMBO J* **14**: 2209-2216.

Varga-Weisz PD, Wilm M, Bonte E, Dumas K, Mann M, Becker PB. 1997. Chromatin-remodelling factor CHRAC contains the ATPases ISWI and topoisomerase II. *Nature* **388**: 598-602.

Vaughn JL, Goodwin RH, Tompkins GJ, McCawley P. 1977. The establishment of two cell lines from the insect Spodoptera frugiperda (Lepidoptera; Noctuidae). *In Vitro* **13**: 213-217.

Verreault A, Kaufman PD, Kobayashi R, Stillman B. 1996. Nucleosome assembly by a complex of CAF-1 and acetylated histones H3/H4. *Cell* **87**: 95-104.

Verreault A, Kaufman PD, Kobayashi R, Stillman B. 1998. Nucleosomal DNA regulates the core-histone-binding subunit of the human Hat1 acetyltransferase. *Curr Biol* **8**: 96-108.

Vincent JA, Kwong TJ, Tsukiyama T. 2008. ATP-dependent chromatin remodeling shapes the DNA replication landscape. *Nat Struct Mol Biol* **15**: 477-484.

Wade P, Jones P, Vermaak D, Wolffe A. 1998. A multiple subunit Mi-2 histone deacetylase from Xenopus laevis cofractionates with an associated Snf2 superfamily ATPase. *Curr Biol* **8**: 843-846.

Wade PA. 2001. Methyl CpG-binding proteins and transcriptional repression. *Bioessays* **23**: 1131-1137.

Wade PA, Gegonne A, Jones PL, Ballestar E, Aubry F, Wolffe AP. 1999. Mi-2 complex couples DNA methylation to chromatin remodelling and histone deacetylation. *Nat Genet* **23**: 62-66.

Walfridsson J, Khorosjutina O, Matikainen P, Gustafsson CM, Ekwall K. 2007. A genome-wide role for CHD remodelling factors and Nap1 in nucleosome disassembly. *EMBO J* **26**: 2868-2879.

Walter PP, Owen-Hughes TA, Côté J, Workman JL. 1995. Stimulation of transcription factor binding and histone displacement by nucleosome assembly protein 1 and nucleoplasmin requires disruption of the histone octamer. *Mol Cell Biol* **15**: 6178-6187.

Wan M, Zhang J, Lai D, Jani A, Prestone-Hurlburt P, Zhao L, Ramachandran A, Schnitzler GR, Chi T. 2009. Molecular basis of CD4 repression by the Swi/Snf-like BAF chromatin remodeling complex. *Eur J Immunol* **39**: 580-588.

Wang QE, Zhu Q, Wani G, Chen J, Wani AA. 2004. UV radiation-induced XPC translocation within chromatin is mediated by damaged-DNA binding protein, DDB2. *Carcinogenesis* **25**: 1033-1043.

Wang W, Côté J, Xue Y, Zhou S, Khavari PA, Biggar SR, Muchardt C, Kalpana GV, Goff SP, Yaniv M et al. 1996. Purification and biochemical heterogeneity of the mammalian SWI-SNF complex. *EMBO J* **15**: 5370-5382.

Wang Y, Zhang H, Chen Y, Sun Y, Yang F, Yu W, Liang J, Sun L, Yang X, Shi L et al. 2009. LSD1 is a subunit of the NuRD complex and targets the metastasis programs in breast cancer. *Cell* **138**: 660-672.

Warner MH, Roinick KL, Arndt KM. 2007. Rtf1 is a multifunctional component of the Paf1 complex that regulates gene expression by directing cotranscriptional histone modification. *Mol Cell Biol* **27**: 6103-6115.

Waterhouse AM, Procter JB, Martin DM, Clamp M, Barton GJ. 2009. Jalview Version 2--a multiple sequence alignment editor and analysis workbench. *Bioinformatics* **25**: 1189-1191.

Weake VM, Workman JL. 2008. Histone ubiquitination: triggering gene activity. *Mol Cell* **29**: 653-663.

Weake VM, Workman JL. 2010. Inducible gene expression: diverse regulatory mechanisms. *Nat Rev Genet* **11**: 426-437.

West S, Proudfoot NJ. 2009. Transcriptional termination enhances protein expression in human cells. *Mol Cell* **33**: 354-364.

Whitehouse I, Flaus A, Cairns BR, White MF, Workman JL, Owen-Hughes T. 1999. Nucleosome mobilization catalysed by the yeast SWI/SNF complex. *Nature* **400**: 784-787.

Whitehouse I, Rando OJ, Delrow J, Tsukiyama T. 2007. Chromatin remodelling at promoters suppresses antisense transcription. *Nature* **450**: 1031-1035.

Whitehouse I, Stockdale C, Flaus A, Szczelkun MD, Owen-Hughes T. 2003. Evidence for DNA translocation by the ISWI chromatin-remodeling enzyme. *Mol Cell Biol* **23**: 1935-1945.

Widom J. 1998. Structure, dynamics, and function of chromatin in vitro. *Annu Rev Biophys Biomol Struct* **27**: 285-327.

Widom J. 2001. Role of DNA sequence in nucleosome stability and dynamics. *Q Rev Biophys* **34**: 269-324.

Woodage T, Basrai MA, Baxevanis AD, Hieter P, Collins FS. 1997. Characterization of the CHD family of proteins. *Proc Natl Acad Sci U S A* **94**: 11472-11477.

Woodcock CL. 2006. Chromatin architecture. *Curr Opin Struct Biol* **16**: 213-220.

Workman JL, Kingston RE. 1998. Alteration of nucleosome structure as a mechanism of transcriptional regulation. *Annu Rev Biochem* **67**: 545-579.

Wu S, Shi Y, Mulligan P, Gay F, Landry J, Liu H, Lu J, Qi HH, Wang W, Nickoloff JA et al. 2007. A YY1-INO80 complex regulates genomic stability through homologous recombination-based repair. *Nat Struct Mol Biol* **14**: 1165-1172.

Wysocka J, Swigut T, Xiao H, Milne TA, Kwon SY, Landry J, Kauer M, Tackett AJ, Chait BT, Badenhorst P et al. 2006. A PHD finger of NURF couples histone H3 lysine 4 trimethylation with chromatin remodelling. *Nature* **442**: 86-90.

Xella B, Goding C, Agricola E, Di Mauro E, Caserta M. 2006. The ISWI and CHD1 chromatin remodelling activities influence ADH2 expression and chromatin organization. *Mol Microbiol* **59**: 1531-1541.

Xin L, Zhou GL, Song W, Wu XS, Wei GH, Hao DL, Lv X, Liu DP, Liang CC. 2007. Exploring cellular memory molecules marking competent and active transcriptions. *BMC Mol Biol* **8**: 31.

Xue Y, Wong J, Moreno G, Young M, Côté J, Wang W. 1998. NURD, a novel complex with both ATP-dependent chromatin-remodeling and histone deacetylase activities. *Mol Cell* **2**: 851-861.

Yadon AN, Tsukiyama T. 2011. SnapShot: Chromatin Remodeling: ISWI. *Cell* **144**: 453-453.e451.

Yamaguchi Y, Wada T, Watanabe D, Takagi T, Hasegawa J, Handa H. 1999. Structure and function of the human transcription elongation factor DSIF. *J Biol Chem* **274**: 8085-8092.

Yang JG, Madrid TS, Sevastopoulos E, Narlikar GJ. 2006. The chromatin-remodeling enzyme ACF is an ATP-dependent DNA length sensor that regulates nucleosome spacing. *Nat Struct Mol Biol* **13**: 1078-1083.

Yasui D, Miyano M, Cai S, Varga-Weisz P, Kohwi-Shigematsu T. 2002. SATB1 targets chromatin remodelling to regulate genes over long distances. *Nature* **419**: 641-645.

Yates JA, Menon T, Thompson BA, Bochar DA. 2010. Regulation of HOXA2 gene expression by the ATP-dependent chromatin remodeling enzyme CHD8. *FEBS Lett* **584**: 689-693.

Yoder JA, Soman NS, Verdine GL, Bestor TH. 1997. DNA (cytosine-5)-methyltransferases in mouse cells and tissues. Studies with a mechanism-based probe. *J Mol Biol* **270**: 385-395.

Yokoyama H, Rybina S, Santarella-Mellwig R, Mattaj IW, Karsenti E. 2009. ISWI is a RanGTP-dependent MAP required for chromosome segregation. *J Cell Biol* **187**: 813-829.

Yoon HG, Chan DW, Reynolds AB, Qin J, Wong J. 2003. N-CoR mediates DNA methylation-dependent repression through a methyl CpG binding protein Kaiso. *Mol Cell* **12**: 723-734.

Yoshinaga SK, Peterson CL, Herskowitz I, Yamamoto KR. 1992. Roles of SWI1, SWI2, and SWI3 proteins for transcriptional enhancement by steroid receptors. *Science* **258**: 1598-1604.

Yu EY, Steinberg-Neifach O, Dandjinou AT, Kang F, Morrison AJ, Shen X, Lue NF. 2007. Regulation of telomere structure and functions by subunits of the INO80 chromatin remodeling complex. *Mol Cell Biol* **27**: 5639-5649.

Yudkovsky N, Logie C, Hahn S, Peterson CL. 1999. Recruitment of the SWI/SNF chromatin remodeling complex by transcriptional activators. *Genes Dev* **13**: 2369-2374.

Zaidi SK, Young DW, Montecino MA, Lian JB, van Wijnen AJ, Stein JL, Stein GS. 2010. Mitotic bookmarking of genes: a novel dimension to epigenetic control. *Nat Rev Genet* **11**: 583-589.

Zegerman P, Canas B, Pappin D, Kouzarides T. 2002. Histone H3 lysine 4 methylation disrupts binding of nucleosome remodeling and deacetylase (NuRD) repressor complex. *J Biol Chem* **277**: 11621-11624.

Zhang Y, LeRoy G, Seelig HP, Lane WS, Reinberg D. 1998. The dermatomyositis-specific autoantigen Mi2 is a component of a complex containing histone deacetylase and nucleosome remodeling activities. *Cell* **95**: 279-289.

Zhang Y, Liu S, Mickanin C, Feng Y, Charlat O, Michaud GA, Schirle M, Shi X, Hild M, Bauer A et al. 2011. RNF146 is a poly(ADP-ribose)-directed E3 ligase that regulates axin degradation and Wnt signalling. *Nat Cell Biol* **13**: 623-629.

Zhang Y, Ng HH, Erdjument-Bromage H, Tempst P, Bird A, Reinberg D. 1999. Analysis of the NuRD subunits reveals a histone deacetylase core complex and a connection with DNA methylation. *Genes Dev* **13**: 1924-1935.

Zhou BO, Wang SS, Xu LX, Meng FL, Xuan YJ, Duan YM, Wang JY, Hu H, Dong X, Ding J et al. 2010. SWR1 complex poises heterochromatin boundaries for antisilencing activity propagation. *Mol Cell Biol* **30**: 2391-2400.

Zhou Y, Santoro R, Grummt I. 2002. The chromatin remodeling complex NoRC targets HDAC1 to the ribosomal gene promoter and represses RNA polymerase I transcription. *EMBO J* **21**: 4632-4640.

Zobeck KL, Buckley MS, Zipfel WR, Lis JT. 2010. Recruitment timing and dynamics of transcription factors at the Hsp70 loci in living cells. *Mol Cell* **40**: 965-975.

Zofall M, Persinger J, Bartholomew B. 2004. Functional role of extranucleosomal DNA and the entry site of the nucleosome in chromatin remodeling by ISW2. *Mol Cell Biol* **24**: 10047-10057.

Zofall M, Persinger J, Kassabov SR, Bartholomew B. 2006. Chromatin remodeling by ISW2 and SWI/SNF requires DNA translocation inside the nucleosome. *Nat Struct Mol Biol* **13**: 339-346.

8. Appendix

List of abbreviations and acronyms

α	anti
A	alanine
aa	amino acid
Abs	antibodies
ac	acetyl
ACF	ATP-utilizing chromatin assembly and remodeling factor
AcMNPV	Autographa californica nucleopolyhedrovirus
ADP	adenosindiphosphate
ADPr	ADP-ribose
ALC1	amplified in cancer 1
Arp	actin related protein
Ash	absent, small, or homeotic discs 1
ATM	ataxia telangiectasia mutated
ATP	adenosintriphosphate
ATR	ataxia telangiectasia and Rad3-related protein
ATRX	alpha thalassemia/mental retardation syndrome X-linked
BAF	BRG1-associated factors
BAP	Brahma-associated proteins
BLAST	basic local alignment search tool
bp	base pair
BPTF	bromodomain PHD finger transcription factor
BRG1	Brahma-associated gene 1
BRK	Brahma and Kismet domain
BRM	brahma
BSA	bovine serum albumine
C-	carboxy-
C/EBP	CCAAT/Enhancer-Binding Protein-β
CAF1	chromatin assembly factor 1
CBP	CREB binding protein
cdk	cyclin dependent kinase
cDNA	complementary DNA
CENP-A	centromere protein-A
CHD	chromodomain-helicase-DNA binding
ChIP	chromatin immunoprecipitation
CHRAC	chromatin assembly complex
CK2	casein kinase 2
CP190	centrosomal protein 190
CpG	cytosine-phospatidyl-guanosine

Cpm	counts per minute
Ct	cycle threshold
CTD	carboxy terminal domain
da	daughterless
Da	dalton
DAPI	4',6-diamidino-2-phenylindole
dATP	desoxyadenosintriphosphate
dCTP	desoxycytosinosintriphosphate
dGTP	desoxyguanidintriphosphate
dMec	drosophila MEP-1-containing complex
DMSO	dimethyl suloxide
DNA	desoxyribonucleic acid
DNMT	DNA methyltransferase
dNTP	desoxyribonucleotidetriphosphate
DOC1	deleted in oral cancer 1
DRB	5,6-dichloro-1-beta-D-ribofuranosylbenzimidazole
DSB	double strand break
dsRNA	double stranded RNA
DTT	dithiotreithol
dTTP	desoxythyminidintriphosphate
EcR	ecdyson receptor
EDTA	ethylenedioxy-diethylene-dinitrilo-tetraacetic acid
EGTA	ethylene glycol-bis-(2-aminoethyl)-N,N,N', N'-tetraacetic acid
EKLF	erythroid krüppel-like factor
ELL	eleven-nineteen lysine-rich leukemia protein
EMSA	electrophoretic mobility shift assay
ER	estrogen receptor
EtBr	ethidiumbromide
ey	eyless
FACT	facilitates chromatin transcription
FCS	fetal calf serum
FOG-1	cofactor friend of GATA-1
for	forward
FPLC	fast protein liquid chromatography
FRAP	fluorescence recovery after photobleaching
g	gram
G1	gap phase 1
GAF	GAGA tactor
GFP	green fluorescent protein
GMR	glass multimer reporter
GR	glucocorticoid receptor
GST	glutathione-S-transferase
H	histone

HAS	helicase-sant domain
HAT	histone acetyltransferase
HDAC	histone deacetylase
HEPES	N-(2-Hydroxyethyl)piperazine-N′-(2-ethanesulfonic acid)
HMG	high mobility group
HP1	heterochromatin protein 1
HPLC	high performance liquid chromatography
HRP	horseradish peroxidase
HS	heat shock
HSE	heat shock element
HSF	heat shock factor
hsp	heat shock protein
Ig	immunoglobuline
INO80	inositol requiring 80
IP	immunoprecipitation
IPTG	sopropyl β-D-1-thiogalactopyranoside
Isw1	imitation SWitch subfamily 1
ISWI	imitation switch
K	lysine
KAP-1	krüppel-associated box (KRAB) domain–associated protein 1
kDA	kilodalton
Kis	kismet
LB	Luria-Bertani
Lys	lysine
M	molar
MBP	methyl-CpG-binding protein
MDa	mega dalton
me	methyl
MEF	mouse embryonic fibroblast
Mep1	mog interacting ectopic P granulocytes 1
MEP50	methylosome protein 50
min	minute
MLL	mixed lineage leukemia
MNase	micrococcal nuclease
mRNA	messenger RNA
MS	mass spectrometry
MTA	metastasis associated protein
N-	amino-
NAD	nicotinamide adenine dinucleotide
Nap1	nucleosome assembly protein 1
ncRNA	non coding RNA
NELF	negative elongation factor
NLK	nemo like kinase

NHS	no heat shock
NoRC	nucleolar remodeling complex
NuRD	nucleosome remodeling and histone deacetylation
NURF	nucleosome remodeling factor
OD	optical density
PAA	polyacrylamide
PAGE	polyacrylamide gel electrophoresis
PAR	poly(ADP-ribose)
PARP	poly(ADP-robose) polymerase
PBAF	polybromo-associated BAF
PBAP	polybromo-associated BAP
PBS	phosphate buffered saline
PBZ	PAR-binding zinc finger
Pc	polycomb
PCR	polymerase chain reaction
PHD	plant homeo domain
PMSF	phenylmethane sulfonyl fluoride
PPAR	peroxisome proliferator-activated receptor
P-TEFb	positive transcription elongation factor b
PVDF	polyvinylidine difluoride
QPCR	quantitative PCR
R	arginine
RBF	retinoblastoma like factor
rDNA	ribosomal DNA
rev	reverse
RNA	ribonucleic acid
RNAi	RNA interference
RNAP II	RNA polymerase II
rp49	ribosomal protein 49
RpAp	retinoblastoma associated protein
RPD3	reduced potassium dependency 3
rpm	revoltations per minute
RSC	remodels the structure of chromatin
RT	room temperature
S	DNA synthesis phase
SAGA	Spt-Ada-Gcn5
SANT	ySWI3, yADA2, hNCoR, hTFIIIB
SCRAP	Snf2-related CBP activator protein
SDS	sodium dodecyl sulphate
sec	second
Ser	serine
SF2	superfamily 2
sgs	salivary gland specific

SHL	superhelical location
SLIDE	SANT-like ISWI domain
SLIK	SAGA like
Snf2	sucrose non-fermenting protein 2 homolog
snRNP	small nuclear ribonucleoprotein
Sp3	specificity protein 3
ssRNA	single stranded RNA
Sth1	SNF2 (Two) Homolog 1
suc	sucrose
SUMO	small ubiquitin-like modifier
SWI/SNF	switch/sucrose non-fermenting
Swr1	Swi2/Snf2-related 1
Tap	tandem affinity purification
Temed	N,N,N′,N′-Tetramethylethylenediamine
TFIIH	transcription factor II H
TIP5	TTF-I interacting protein 5
Tris	tris(hydroxymethyl)aminomethane
TRX	trithorax
TTF-I	transcription termination factor I
Ttk69	tramtrack69
v/v	volume per volume
w/v	weight per volume
WT	wild type
YY1	Yin-Yang-1
Zn	zinc

Curriculum vitae

Acknowledgements

Here, I would like to thank the people who supported me during this PhD thesis or contributed directly or indirectly to the results of this work.

List of academic teachers

My academic teachers at the University of Warsaw were the following professors: Baj, Bartnik, Bartosik, Bębas, Borsuk, Bryła, Cymborowski, Czubaj, Durka, Dzik, Garstka, Golik, Jagusztyn-Krynicka, Janiszowska, Jerzmanowski, Kaczanowska, Kaczanowski, Korczak-Kowalska, Maj-Żurawska, Mieczkowski, Moraczewski, Piekarowicz, Romanowska, Siedlecki, Spalik, Staroń, Stolarski, Szakiel, Szewczyk, Węgleński, Włodarczyk, Wolska, Wojciechowski, Zakryś, Zielenkiewicz.

Erklärung